ABSTRACT

Spectroscopic Probe Studies of Solvation
G. EATON

The major part of this Thesis concerns the use of relatively
simple compounds used in extremely dilute solution to study
solvation phenomena.  Use of many spectroscopic techniques
such as infrared, NMR, ultraviolet, etc., have made it
possible to follow the environment of the probe throughout
various mixed and pure solvent states.  Simple molecules such
as acetone, triethylphosphine oxide, small amides, etc., yield
similar results concerning the interaction of alcohol-base and
water-base systems and also provide information as to the
solvation state of the probes themselves.

A comparative study of the various solvent scales is included,
combining information obtained during the course of this
research with the various literature values.  The relative
merits and demerits of most of the widely-used scales such as
Gutmann's Donor and Acceptor numbers, Taft's $\alpha$ and $\beta$ scales,
Kosower's Z values and Dimroth's $E_T$ values, etc., are discussed
in the light of the various solvation parameters obtained.

Of particular interest was the formation of 'clathrate hydrate'
compounds, already well-established in the literature.  A
suitable technique was developed and is demonstrated herein
for following the formation of the acetone clathrate hydrate
using infrared spectroscopy.  Its relevance to some theories
of water structure and solvation are discussed with suggestions
as to acetone's solvation structure in liquid water.

A final chapter is included where techniques from the probe
studies are utilised in formulating a suggested mechanism for
the solvolysis of alkyl halides.  These reactions already
having been extensively studied by kinetic means previously
relied on simple mechanisms which gave adequate mathematical
results to the various rate laws.  The involvement of hydrogen
bonding to the solvent in no way alters the mathematics but is
highly relevant to the overall operating mechanism.

# Spectroscopic Probe Studies of Solvation

A Thesis submitted by

GRAHAM EATON

for the degree of

Doctor of Philosophy

in the

Faculty of Science

of the

University of Leicester

Department of Chemistry
The University
LEICESTER                                    AUGUST 1983

UMI Number: U346574

UMI

Dissertation Publishing

UMI U346574

ProQuest

ProQuest LLC
789 East Eisenhower Parkway
P.O. Box 1346
Ann Arbor, MI  48106-1346

Thesis

STATEMENT

The experimental work described in this thesis was carried out
solely by the author, except the work presented in Chapter 9
which was carried out in conjunction with Mr. N. G. M. Pay, in
the Department of Chemistry of the University of Leicester
during the period between July 1978 and July 1983.

The work in this thesis is not being concurrently presented
for any other degree.

All work recorded herein is original unless otherwise stated
in the text or by reference.


AUGUST 1983                    Signed: .....G. Eaton........

Dedicated to my children, Nicholas and Alison, for them the future is waiting

"It is not necessary to hope in order to try. nor to succeed in order to persevere"

~ William, The Silent

## ACKNOWLEDGEMENTS

## ABSTRACT

Spectroscopic Probe Studies of Solvation
### G. EATON

The major part of this Thesis concerns the use of relatively simple compounds used in extremely dilute solution to study solvation phenomena. Use of many spectroscopic techniques such as infrared, NMR, ultraviolet, etc., have made it possible to follow the environment of the probe throughout various mixed and pure solvent states. Simple molecules such as acetone, triethylphosphine oxide, small amides, etc., yield similar results concerning the interaction of alcohol-base and water-base systems and also provide information as to the solvation state of the probes themselves.

A comparative study of the various solvent scales is included, combining information obtained during the course of this research with the various literature values. The relative merits and demerits of most of the widely-used scales such as Gutmann's Donor and Acceptor numbers, Taft's $\alpha$ and $\beta$ scales, Kosower's Z values and Dimroth's $E_T$ values, etc., are discussed in the light of the various solvation parameters obtained.

Of particular interest was the formation of 'clathrate hydrate' compounds, already well-established in the literature. A suitable technique was developed and is demonstrated herein for following the formation of the acetone clathrate hydrate using infrared spectroscopy. Its relevance to some theories of water structure and solvation are discussed with suggestions as to acetone's solvation structure in liquid water.

A final chapter is included where techniques from the probe studies are utilised in formulating a suggested mechanism for the solvolysis of alkyl halides. These reactions already having been extensively studied by kinetic means previously relied on simple mechanisms which gave adequate mathematical results to the various rate laws. The involvement of hydrogen bonding to the solvent in no way alters the mathematics but is highly relevant to the overall operating mechanism.

# LIST OF CONTENTS

# CHAPTER 1

INTRODUCTION

INTRODUCTION

## 1.1  THE STRUCTURE OF WATER

The work presented in this thesis is concerned with the study of
solvation.  Water holds prime position in such a study and, therefore,
an outline of the structure and properties of this very important compound
is a necessary precursor to the work described herein.

### a  The Hydrogen Bond

The concept of hydrogen bonding, where a hydrogen atom is shared
between two electronegative atoms, has been accepted for many years.
Werner [1] in 1902 suggested the existence of such a bond for the
initial stages of the formation of Ammonium chloride from Ammonia and
Hydrogen chloride.  The first use of this idea in the interaction
between water molecules was by Latimer and Rodebush [2] in 1920.

The precise nature of hydrogen bonding is still open to debate.
Coulson and Danielsson [3] proposed that charge transfer was the mechanism
whereby the hydrogen bond was stabilised giving three resonance hybrid
structures.  Kollman and Allen [4], however, disagreed and suggested that
many of the phenomena associated with hydrogen bonding could be explained
without invoking charge transfer.  It seems reasonable to assume that the
true picture is some combination of electrostatic and covalent effects
depending upon circumstances.

### b  The Uniform Model

This model, sometimes called 'the continuum model', was defined by
Kell [5], "Water has essentially complete hydrogen bonding, at least at
low temperatures, and has a full distribution (or continuum) of bond
angles, distances and energies".  The first uniform model was proposed
by Bernal and Fowler [6] with later contributions from several other

authors [7-9].

## c   The Mixture Model

A definition of this model is again given by Kell [5] and describes water as "an equilibrium mixture of species each of which are distinguishable in an instantaneous picture".  Whilst there are many mixture models proposed [10-13] the most important is that suggested by Frank and Wen [14] as the "Flickering Cluster Model".  They proposed that liquid water consisted of clusters of ice-like material surrounded by disordered close-packed water molecules, the clusters and the 'free' molecules would be interchanging rapidly with the lifetime of the clusters estimated at approximately $10^{-11}$ seconds from dielectric relaxation measurements.  Nemethy and Scheraga [15] applying this approach calculated the size of the clusters to be between 25 and 91 water molecules.

## d   An Alternative Model

A model of water structure has been proposed by Symons [16];  this is neither 'continuum' nor 'mixture' but retains some characteristics of each.  One major disadvantage of the two preceding models is their inability to explain satisfactorily all the various anomalous properties of liquid water.  In particular it is difficult to decide when a hydrogen bond is so weak and long that it ceases to be a hydrogen bond.  This very dubious state is invoked by the continuum model in order to fully explain the OH overtone spectrum of liquid water.  Also judging by the obvious propensity of water to form a hydrogen bonded system it is difficult to envisage 'free' non-bonded water molecules having any measurable existence.

We can consider water as an equilibrium between bulk water, which is

ostensibly a fully hydrogen bonded 'uniform' state, and species designated (OH)$_{free}$ and (lp)$_{free}$ (lone pair free). These two species are not separate states (as for the mixture model), just the result of broken hydrogen bonds, breaking and re making at approximately $10^{-11}$ seconds, the rest of the molecule being still fully bound to the bulk system. This equilibrium can be written:-

$$H_2O_{(bulk)} \rightleftharpoons OH_{free} + lp_{free} \qquad \dots (1)$$
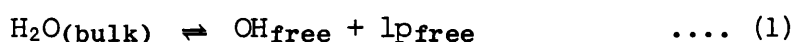
It follows that equal quantities of both (OH)$_{free}$ and (lp)$_{free}$ are present, the quantities of each have been calculated at approximately 8% [17]. The existence of (OH)$_{free}$ readily explains the features of the OH overtone spectra, however, (lp)$_{free}$ groups are much more difficult to identify by spectroscopic means.

The interaction of water with solutes can be regarded as a function of the properties of (lp)$_{free}$ and (OH)$_{free}$. Thus on adding a base (electron donor) (OH)$_{free}$ will be 'scavenged' hence increasing the relative concentration of (lp)$_{free}$ groups. Conversely, addition of an acid will scavenge (lp)$_{free}$ leading to an increase of (OH)$_{free}$. This model is used throughout the work of this thesis and, as will be seen, readily explains the various systems studied.

## 1.2  THE STRUCTURE OF ALCOHOLS

### a  Methanol

The structure of alcohols is much less controversial than that of water, a wide degree of general agreement existing. Methanol has been regarded as the ideal associated liquid [18] and can be considered as consisting of long chains of hydrogen bonded molecules spreading in two dimensions with a small quantity of branched chains, i.e.

```
----H——O----H——O----H——O——Me
       |        |        :
       Me       Me       H
                         |
      -----O——H---O——Me
           |       :
           Me      H
                   |
                   O——Me
                   :
```
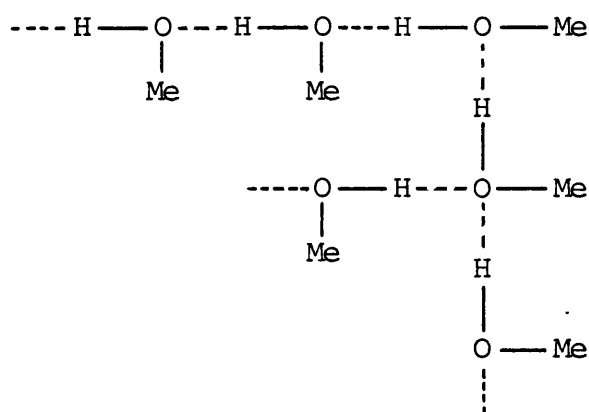
The extent of the chains is very large, with very few terminal OH groups [analogous to (OH)$_{free}$ as oscillators]. This is confirmed in the overtone OH spectrum where only a tiny shoulder is observed for free OH oscillators [19].

b  Other Alcohols

It is generally accepted that most alcohols have a similar structure to methanol.  However with those alcohols containing bulky alkyl groups, e.g. tert-Butanol and Fluoroalcohols, a larger amount of terminal groups seem to be present.  This is confirmed in the overtone OH spectra by the presence of a large narrow feature at the frequency for (OH)$_{free}$ oscillators.  [For spectra see Chapter 4.]

1.3  USE OF PROBES

a  The Concept

If a particular molecule possesses an observable property that is affected differently by the different components of its environment, then it may be used to probe that environment.  In an ideal situation a change from one state to another will produce a uniform change in the property being observed.  Any specific interactions between the various components, however, will produce deviations from ideality and hence allow some

measure of those interactions. This technique has been used previously to great advantage in this laboratory [20] by following an e.s.r. spin probe di-tert-Butyl-Nitroxide. It is possible to use almost any spectroscopic technique to study probes, although some care must be exercised in selecting the most suitable technique.

b  Criteria for Probe Studies

The various conditions required for a successful probe study may be listed as follows:-

(i)  The probe must be soluble in the various solvents studied.

(ii)  No chemical reaction should occur between the probe and solvents.

(iii)  Some suitable spectroscopic 'label' must be present on the probe, e.g. infrared band, electronic transition, magnetically active nucleus, etc.

1.4  THE INFRARED TECHNIQUE

a  Theory

The full theoretical basis for infrared spectroscopy is covered adequately by the many textbooks available on the subject. However, a brief outline of the method and its application to probe studies is given:-

Each bond in a molecule can be considered as a vibrating oscillator, having a vibration frequency within a narrow range of energies, specific to that bond. If that bond is irradiated with energy with a range of suitable frequencies then energy will be absorbed by the bond only within the range corresponding to its own vibration frequency. Thus when a molecule is irradiated through a range of suitable frequencies, various bonds will give rise to absorption bands, giving the characteristic 'spectrum' of that molecule. Vibrational frequencies correspond to what

is known as the infrared region of the electromagnetic spectrum (4000 to 200 $cm^{-1}$). If each vibration were harmonic then there would also be absorption of energy with frequencies corresponding to 2×, 3×, etc., the fundamental frequency of vibration. These absorptions are termed 'overtone' bands, but because in the real world the vibrations are anharmonic the overtones do not exactly correspond to multiples of the fundamental, in fact they tend to converge. These overtone regions have been particularly useful in the study of the OH oscillator of water and alcohols [21,22,23].

b  Advantages and Disadvantages of Infrared for the Study of Probes

The specific nature of the various infrared bands make it a very important technique. Some oscillators, e.g. OH, C=O, etc., are particularly susceptible to hydrogen bonding and also to dipolar inter-actions. Most interactions of this type lead to a weakening of the oscillator bond and hence a lowering of its absorption frequency. Samples for infrared spectroscopy are generally easily handled in specially designed cells with only small volumes of material required.

There are however some problems, sometimes insurmountable, when using infrared. As most probes are used in very dilute solution, the oscillator being observed must give rise to a reasonably strong absorption band. Solvents too have their own absorption spectrum in the infrared region and hence must be chosen so that their main absorption bands do not coincide with those of the probe under study.


1.5  THE N.M.R.  (NUCLEAR MAGNETIC RESONANCE)  TECHNIQUE

a  Theory

Many nuclei have magnetic moments and, if placed in a magnetic field, will line up with or against this external field. The population of these

two states can be described by the Boltzmann distribution. Energy can be absorbed so promoting nuclei from one state to the other. This energy may be provided by irradiation by radio frequency waves. The true magnetic environment of the nuclei is modified by the magnetic influence of the surrounding electrons and hence the chemical environments. Thus each proton in a suitable compound may absorb energy of a slightly different frequency giving rise to a characteristic n.m.r. spectrum. There are many textbooks giving full accounts of the theory and technique of n.m.r. spectroscopy [24,25] and only a brief account is given here.

The main n.m.r. measurements used in probe studies are chemical shifts and relaxation times. The former arise as described above by changes in the chemical environment of the nucleus in question. Chemical shifts are measured usually in dimensionless units 'parts per million' (ppm) relative to the position for the same nucleus in a suitable reference material. For protons, any hydrogen bonding generally induces a down-field shift relative to those chemical shift values of unassociated molecules and this has been studied extensively in this and other laboratories engaged in solvation work [17].

Relaxation times can be determined from measuring linewidths, however most work is now usually done using the 'Fourier Transform' technique. Relaxation times also give details about the environment of the nucleus but can also provide data as to the freedom of the molecules concerned, to rotate or move through liquid. This is of particular use when studying clathrate compounds.

N.m.r. tends to be much less affected by interference from the solvent, either the studied nucleus may not be present except in the probe or the resonance will occur at a completely different frequency and hence will

be still observable.

The time scale for n.m.r. to take place is in the order of $10^{-2}$ seconds whereas hydrogen bonding and exchange of such states is in the order of $10^{-11}$ seconds. This means that, in general, only one signal is seen by n.m.r. for several solvated states. Therefore any interpretations based on changes in chemical shift measurements are subject to difficulty unless the shifts are known for all the states involved.

REFERENCES FOR CHAPTER 1

1.  A. Werner, <u>Leibigs. Ann.</u>, <u>322</u>, (1902) 261.

2.  W. M. Latimer and W. H. Rodebush, <u>J. Am. Chem. Soc.</u>, <u>42</u>, (1920) 1419.

3.  C. A. Coulson and U. Danielsson, <u>Arkiv Fysik</u>, <u>8</u>, (1954) 239.

4.  P. A. Kollman and L. C. Allen, <u>Chem. Rev.</u>, <u>72</u>, (1972) 283.

5.  G. Kell, "Water and Aqueous Solutions", ed. R. A. Horne, Wiley Interscience, (1972).

6.  J. D. Bernal and R. H. Fowler, <u>J. Chem. Phys.</u>, <u>1</u>, (1933) 515.

7.  Morgan and Warren, <u>J. Chem. Phys.</u>, <u>6</u>, (1938) 666.

8.  J. A. Pople, <u>Proc. Roy. Soc.</u>, <u>A205</u>, (1951) 163.

9.  Rahman and Stillinger, <u>J. Chem. Phys.</u>, <u>55</u>, (1971) 3336.

10. W. K. Röntgen, <u>Ann. Phys.</u>, <u>45</u>, (1892) 91.

11. Grjothein and Krogh-Moe, <u>Acta Chem. Scand.</u>, <u>8</u>, (1954) 1193.

12. H. Eyring, T. Ree and N. Hirai, <u>Proc. Natl. Acad. Sci. USA</u>, <u>44</u>, (1958) 683.

13. G. Wada, <u>Bull. Chem. Soc. Japan</u>, <u>34</u>, (1961) 955.

14. H. S. Frank and W. Y. Wen, <u>Faraday Discuss. Chem. Soc.</u>, <u>24</u>, (1957) 133.

15. G. Nemethy and H. A. Scheraga, <u>J. Chem. Phys.</u>, <u>36</u>, (1962) 3382.

16. M. C. R. Symons, <u>Philos. Trans. R. Soc. London B</u>, (1975) 272.

17. V. K. Thomas, Ph.D. Thesis, Leicester University, (1980).

18. I. Prigogine and R. Defay, "Chemical Thermodynamics", Longmans Green & Co., (1954).

19. G. R. Choppin, <u>J. Mol. Struct.</u>, <u>45</u>, (1978) 39.

20. E. Smith, Ph.D. Thesis, Leicester University, (1979).

21. S. E. Jackson, Ph.D. Thesis, Leicester University, (1980).

22. W. A. P. Luck, <u>Angew. Chemie</u>, <u>19</u>, (1980) 28.

23. J. Paquette and C. Jolicoeur, <u>J. Soln. Chem.</u>, <u>6</u>, (1977) 403.

24. J. A. Pople, W. G. Schneider and H. J. Bernstein, "High Resolution Nuclear Magnetic Resonance", McGraw Hill, (1959).

25. J. W. Emsley, J. Feeney and L. H. Sutcliffe, "High Resolution Nuclear Magnetic Resonance Spectroscopy", Pergamon Press, (1965).

# CHAPTER 2

EXPERIMENTAL TECHNIQUES

## 2.1  PURIFICATION OF MATERIALS

Most organic solvents were purified and dried according to standard methods [1]. This in general required fractional distillation off some appropriate drying agent, e.g. calcium hydride, under an inert atmosphere. Water was purified by a preliminary deionisation followed by a secondary treatment using a Millipore Milli-Q system.

All materials and non aqueous solvents were stored in a dry box prior to use; light was excluded when necessary.

## 2.2  SAMPLE PREPARATION AND HANDLING

Samples were prepared by volume or weight, whichever was the most convenient for the materials being used. When necessary all mixing and transferring of materials was done in a dry box under an inert atmosphere (dry nitrogen). All spectra were recorded as soon as possible after preparation, to minimise any errors due to deterioration.

For the probe studies a simple standard procedure was followed for mixed solvent systems, i.e. A→B.

(a) A suitable concentration of probe (usually 1% $^V$/v) was prepared in 10 m$\ell$ of A and 10 m$\ell$ of B.

(b) These solutions·were then mixed to give a suitable range of concentrations (see Table 1).

TABLE 1

| Sample | Probe in A/m$\ell$ | Probe in B/m$\ell$ | Ratio |
|--------|--------------------|--------------------|-------|
| 1 | 1.0 | 0.0 | 1:0 |
| 2 | 1.0 | 0.1 | 10:1 |
| 3 | 1.0 | 0.2 | 5:1 |
| 4 | 1.0 | 0.5 | 2:1 |
| 5 | 1.0 | 1.0 | 1:1 |
| 6 | 0.5 | 1.0 | 1:2 |
| 7 | 0.2 | 1.0 | 1:5 |
| 8 | 0.1 | 1.0 | 1:10 |
| 9 | 0.0 | 1.0 | 0:1 |

(c) The same mixtures were prepared using pure A and pure B; these solutions were then used as references in the spectrophotometer.

(d) Mole fractions were calculated taking into account volume of mixing corrections, etc.

(e) Any obvious gaps in the data were then filled by making up suitable intermediate mixtures.

## 2.3  SPECTROSCOPIC TECHNIQUES

### (a)  Infrared spectroscopy

The instrument used throughout this work was a Perkin-Elmer 580 [2]. This is a double beam recording spectrophotometer with scale expansion facilities on ordinate and abscissa and pre-selectable modes for optimum resolution and/or noise level.  For many of the spectra an accuracy of $\pm 0.5$ cm$^{-1}$ was achieved for the peak position $(\nu_{max})$.

Cells were generally of the demountable type, having windows chosen for the spectral region and conditions encountered.  Usually calcium fluoride plates were used but silver chloride was utilised for measurements below 1000 cm$^{-1}$ and 'Irtran' or zinc selenide for variable temperature studies.  Path lengths were adjusted using PTFE spacers, a path of 0.025 cm being found suitable for most probe studies.

For dilute solutions in inert solvents as for the haloalkane work Infrasil cells having a fixed path length of 2 mm were used.  Variable temperatures were obtained using a 'Specac 20000' vacuum jacketed cell holder and proportional controller.  Temperatures could be held to $\pm 1°C$ in the range -200 to +250°C.  Cooling was by means of liquid nitrogen or solid $CO_2$ and heating by using the built-in cell heater blocks.

(b)  Near infrared, visible and ultraviolet spectroscopy

All the work in this region, 2600 to 190 nm, was carried out on a Perkin-Elmer – Hitachi 340 spectrophotometer [3]. This is a double beam, recording instrument with two spectral ranges determined by the type of detector and source required. 2600 to 800 nm is designated the near infrared region and uses a lead sulphide detector, all the O-H overtone studies were carried out in this region. 850 to 190 nm is the visible and ultraviolet region using a photomultiplier detector. The near infrared and visible (to approx. 380 nm) regions use a tungsten filament bulb as a source and the ultraviolet a deuterium lamp. Scale expansion facilities were available for both ordinate and abscissa and slit widths adjusted automatically by a servo system.

Cells were generally fixed path length "bottle" type of silica or glass. Usually 10 mm path was used but 2 or 1 mm were used when necessary.

A cell thermostat was installed around the cell block and this enabled variable temperatures to be utilised, however, for the work described here a constant 25°C was maintained.

(c)  Nuclear Magnetic Resonance Spectroscopy

Several spectrometers were used depending upon the type of work being undertaken. For proton ($^1$H) work a 'Jeol PS-100' was used. This is a 100 MHz spectrometer operating in the continuous wave mode and having variable temperature capability. 5 mm OD tubes were used with a coaxial insert, when necessary, for suitable referencing (see Appendix II) and an internal homonuclear lock system (usually on TMS).

For $^{13}$C and $^{31}$P work a 'Jeol FX-60' was used. This is a 60 MHz (proton) spectrometer operating in the pulsed Fourier transform mode and having variable temperature capability. 10 mm OD tubes were used with

coaxial inserts when necessary for referencing. This machine utilised a hetero-nuclear lock signal (deuterium) incorporated into the external reference solution.

$^{17}$O work was carried out at Warwick University Chemistry Department by courtesy of the SERC with assistance from Dr. O. Howarth. The spectrometer used was a 'Bruker WM-400', which is a 400 MHz (proton) Fourier transform instrument having a superconducting magnet and variable temperature facility. $^{17}$O measurements were made at natural abundance levels and so required several thousand pulses for production of a suitable spectrum. Referencing was by computer storage of $D_2^{17}O$ signal. 10 mm OD tubes were used for all samples.

(d) Electron Spin Resonance Spectroscopy

Two instruments were used, a 'Varian E109' and a 'Varian E3'; both gave satisfactory spectra for the determination of the $A_{iso}$ values.

The samples were placed in a small quartz flat cell and recorded over a ±25 Gauss scale. The $A(^{14}N)$ values were then read directly off the spectra. All samples were degassed using the freeze-thaw method on a vacuum line immediately prior to observation.

2.4 SPECTRAL BAND DECONVOLUTION

This technique is discussed in detail in Appendix I, however the instrumentation used throughout the work was as follows.

Preliminary curve analysis was done on a DuPont 310 curve resolver with the bands set to either fully gaussian or fully Lorentian.

For the use of the VIDCA program the spectra were first digitised using a 'Ferranti Freescan'. The data in this form was then processed and, using the VIDCA program, displayed on a DEC GT 42 graphics display. The whole operation was controlled through a PDP 11/45 minicomputer.

The final deconvoluted spectra and associated bands were plotted using a CalComp 1012 fast drum plotter in four colours.

## 2.5  GENERAL COMMENTS

All instruments were operated following standard procedures and according to manufacturers' instructions.  Care was taken over all aspects of the work in order to reduce experimental errors to a minimum, particularly in the preparation of samples and the cleanliness of equipment, cells, etc.  Most spectra recorded here were the result of several runs so reducing the chance of random errors.

REFERENCES FOR CHAPTER 2

1.  G. Riddick and E. R. Bunger, "Techniques of Chemistry, Vol. II, Organic Solvents", Wiley-Interscience, New York, 1970.

2.  Instruction Manual for Model 580 - Perkin-Elmer Ltd. (1975).

3.  Instruction Manual for Model 340 - Hitachi Ltd. (1977).

# CHAPTER 3

ACETONE PROBE STUDIES

## 3.1  INTRODUCTION

The carbonyl stretching frequency provides a very sensitive and useful way of following the behaviour of some probe molecules.  Many different carbonyl compounds have been investigated using infrared spectroscopy [1,2,3].  In particular, ketones and especially acetone, have been used in solvation studies [4].

The use of probe molecules has been described in Chapter 1.  However, acetone was chosen as a probe for study due to its similarity to dialkyl nitroxide radicals that have been used extensively as e.s.r. probes of mixed solvent systems [5,6].  The study of dialkyl nitroxide radicals by e.s.r. spectroscopy suffers from one serious drawback, that is, time averaging of information from several species.  This results in the loss of some information.  In this case we measure only the isotropic $^{14}$N hyperfine coupling constant.

Infrared spectra do not suffer from this 'averaging' problem, however the $N \!=\! O$ stretching frequency for di-tert-butyl nitroxide (the probe used in the previous studies) is difficult to assign and comes within a very congested region of the infrared spectrum [7].  Acetone being structurally similar but with a clear C=O stretching band should give more information about the differently solvated states that may exist in mixed solvent systems.

Most previous studies including acetone have taken one of several lines, i.e.

a  Study of the carbonyl frequencies of many different ketones in the pure state [2,3].

b  Study of the carbonyl frequency of selected ketones in several different pure solvents [1,8].

c  Study of the carbonyl frequency of selected ketones in mixed

solvents [4].

In this present study of acetone as a probe into aqueous and alcoholic solvation studies such as type $\underline{a}$ are of limited use, however types $\underline{b}$ and $\underline{c}$ should yield valuable information. Type $\underline{b}$ will give frequency shifts for interaction with solvents and should relate to similar scales for solvent strength such as those proposed by Guttmann [9]. Type $\underline{c}$ will give information as to the specific interactions between (i) the probe and water or alcohol, (ii) the mixed solvents, i.e. base and water or alcohol.

## 3.2   RESULTS AND DISCUSSION

### (a)   Pure solvent systems

Figure 1 shows the relationship between the $\nu_{max}$ $(>C=O)_{str}$ for acetone in different solvents, these values correlate well with values for $^{13}C$ chemical shift measurements [10], Figure 2 for the $>^{13}C=O$. In most cases, the infrared bands were symmetrical and single, in the case of methanol, however, a small shoulder was observed. This envelope was curve analysed into two bands, one small at 1715 $cm^{-1}$ and the main band at 1707.5 $cm^{-1}$. These bands were assigned to 'free' and 'bound' acetone respectively. The correlation with Gutmann acceptor numbers was very good as can be seen in Figure $1b$ of Chapter 7. This is probably due to the fact that any interaction between acetone and the solvent occurs mainly through the lone pairs on the carbonyl oxygen, i.e. the acetone is acting as an electron donor, the solvent as acceptor.

The plots of carbonyl stretch against $A(^{14}N)$ and $n \rightarrow \pi^*$ bands for di-tert-butyl nitroxide [5,11] show excellent correlation (Figure 3). This indicates the validity of using acetone as a similar probe to DTBN. However, one solvent is particularly off-line, i.e. DMSO (dimethyl-sulphoxide), it is suggested that this is due to the extreme degree of

# Figure  3.1



$\nu$ C=O stretch    cm$^{-1}$
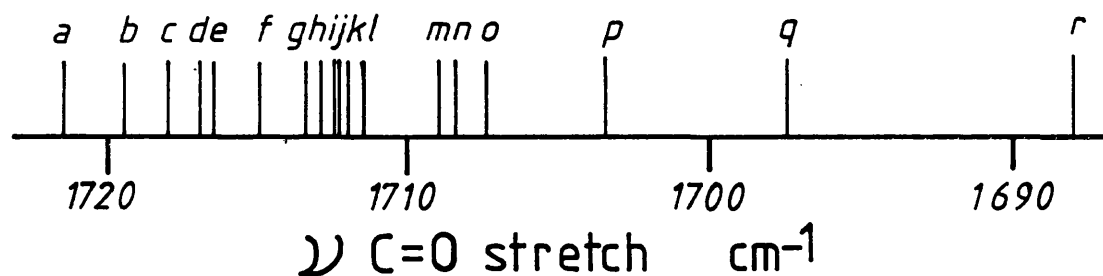
| KEY TO SOLVENTS | |
|---|---|
| a | Hexane |
| b | Triethylamine |
| c | Tetrachloromethane |
| d | Tetrahydrofuran |
| e | Acetone |
| f | Cyanomethane |
| g | Dimethylformamide |
| h | Dimethylacetamide |
| i | Hexamethylphosphoramide |
| j | t-Butanol |
| k | Dichloromethane |
| l | Nitromethane |
| m | Dimethylsulphoxide |
| n | Ethanol |
| o | Methanol |
| p | Ethane 1,2-diol |
| q | Water |
| r | Perfluoro-t-butanol |

Plot showing relative $\nu_{max}$ of Acetone $>$C=O str
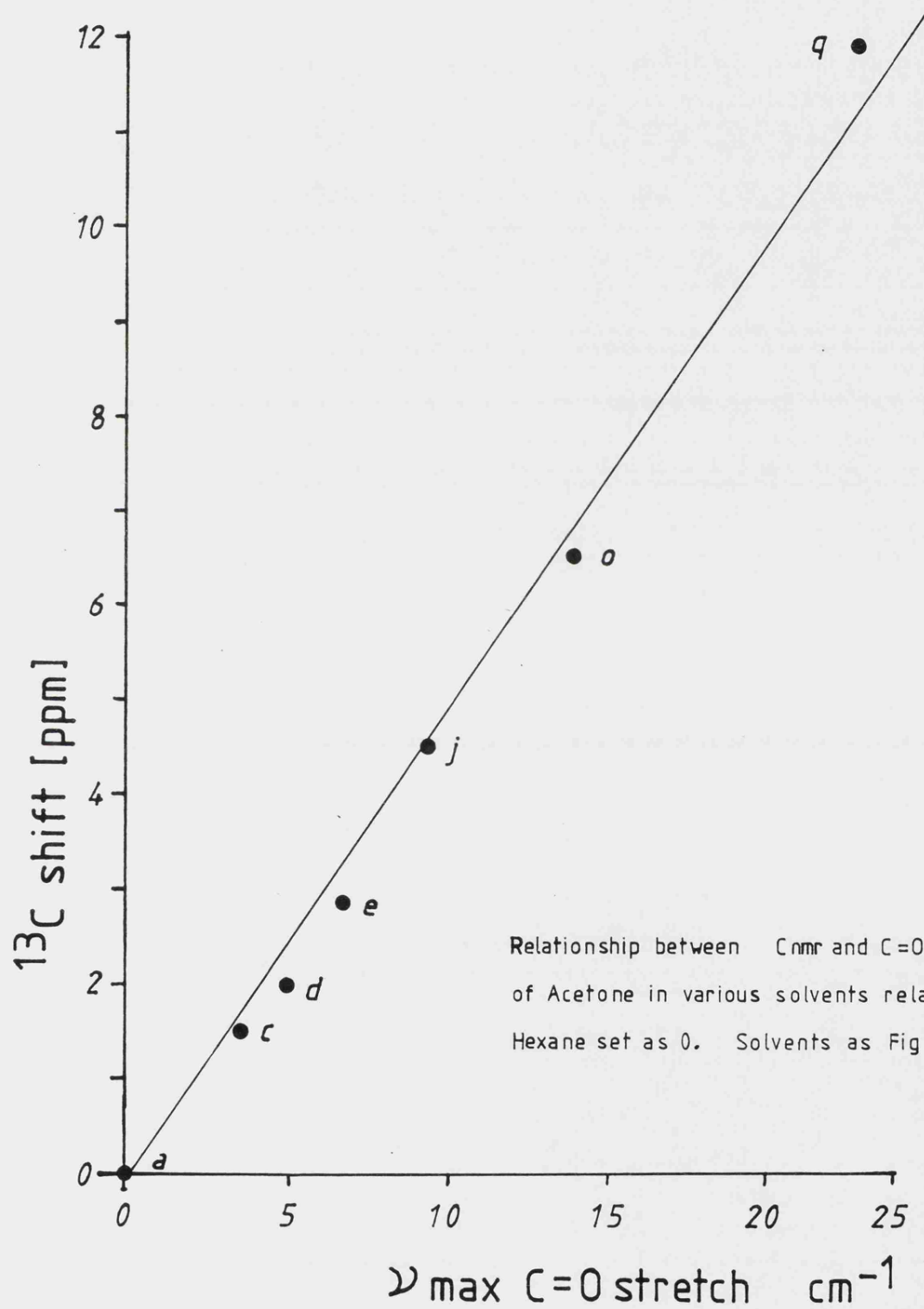in dilute solution in various solvents.

# Figure 3.2

Relationship between  Cnmr and C=O stretch of Acetone in various solvents relative to Hexane set as 0.   Solvents as Fig 3.1

# Figure 3.3



[a]

$A^{14}N$ [gauss]

Di-tert-butylnitroxide.
Relationship between a. $A^{14}N$ and
b. $n - \pi^*$, and $C = O$ stretch for
Acetone in various solvents.

$C = O$ stretch cm$^{-1}$

q, o, n, j, f, e, m

17·0  16·0  15·0
1720  1710  1700

[b]

$\times 10^3$

$n - \pi^*$ cm$^{-1}$

$C = O$ stretch cm$^{-1}$
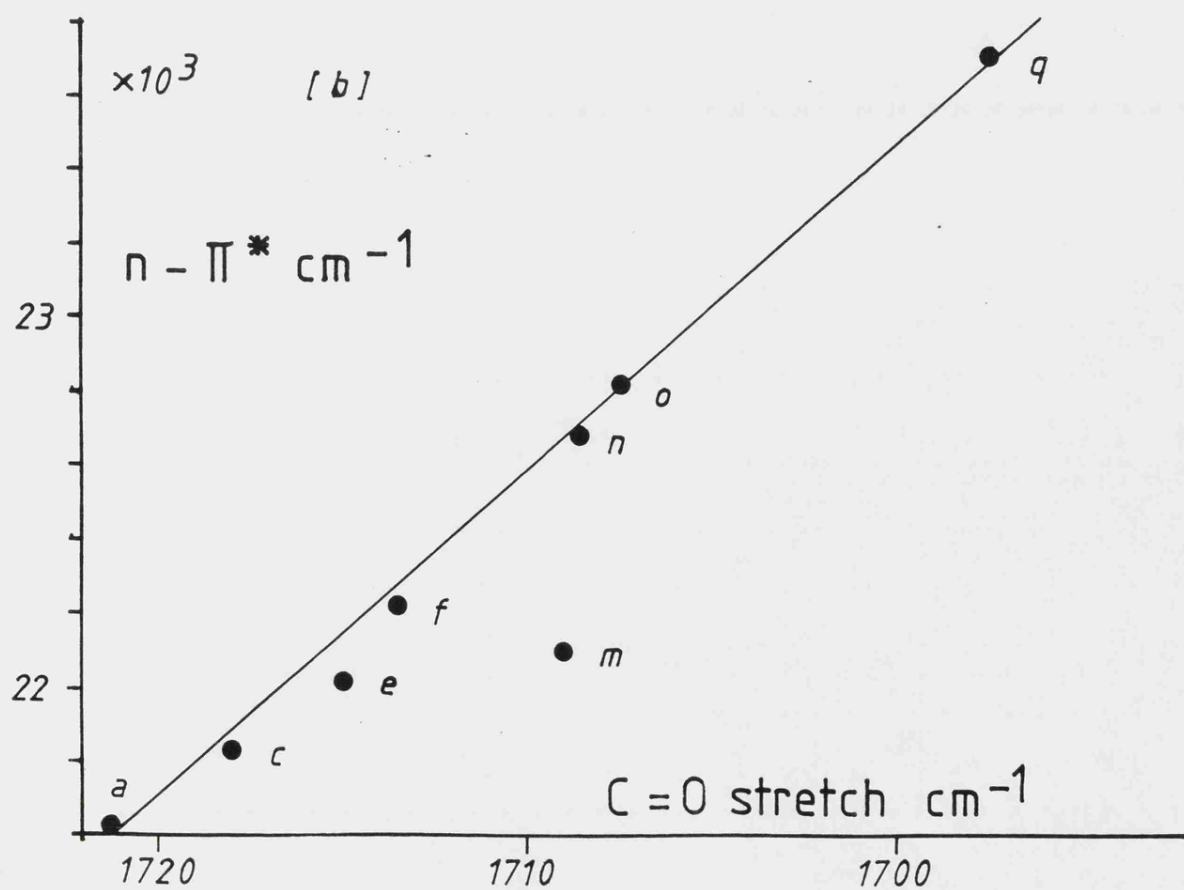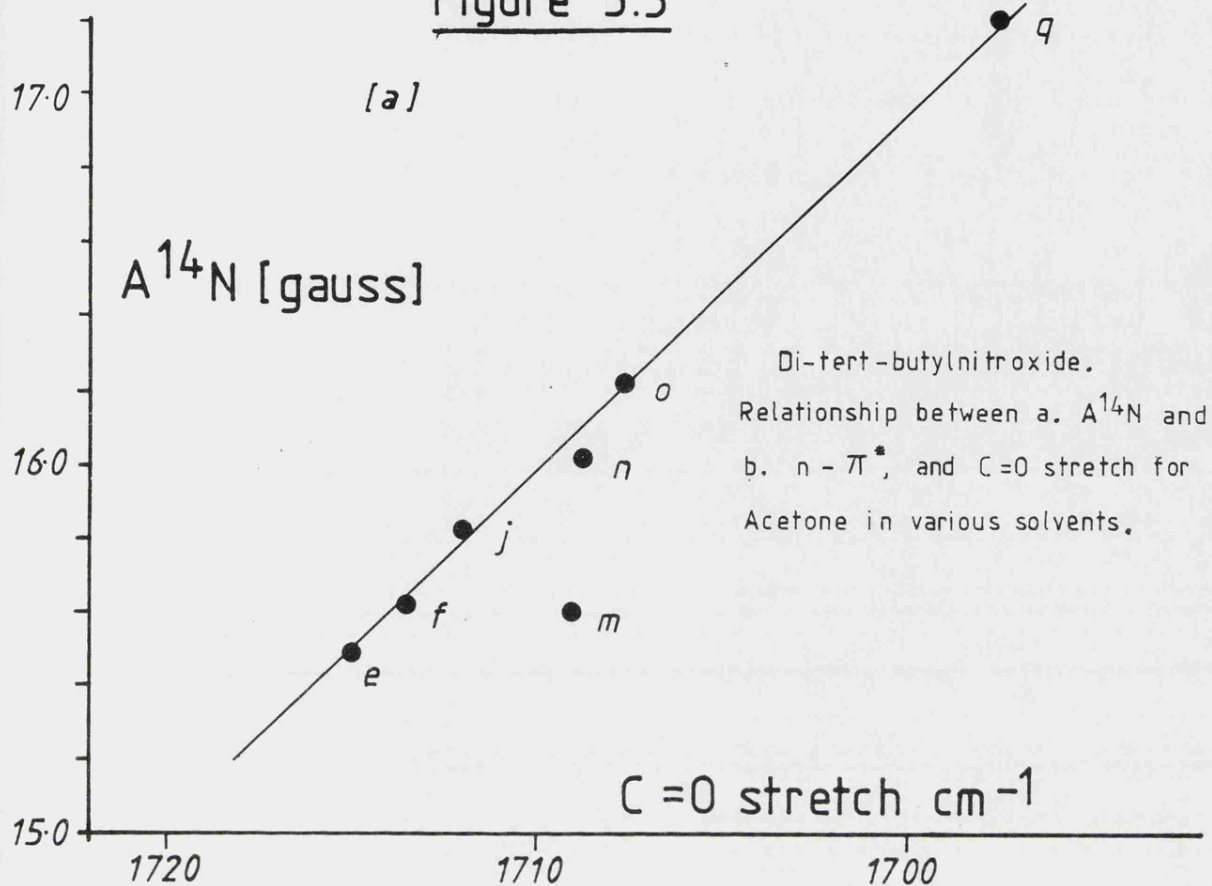
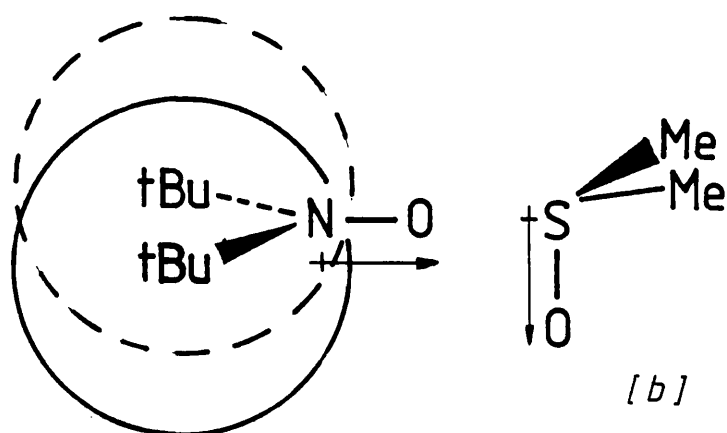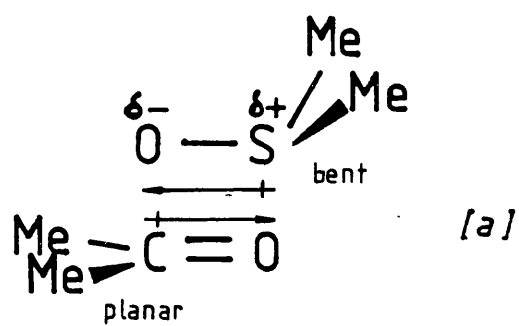q, o, n, f, m, e, c, a

23  22
1720  1710  1700

# Figure 3.4



[a]



[b]

Approach of S-O to
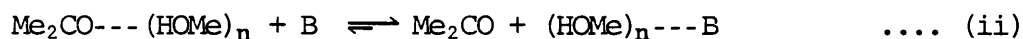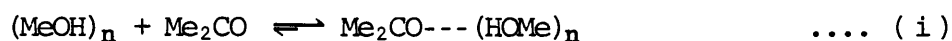N-O is hindered by bulky
tButyl groups.

Difference in dipolar interaction between Dimethyl Sulfoxide
and a.Acetone or b. D.T. B.N.

dipolar interaction between DMSO and acetone; this is shown diagram-matically in Figure 4, compared with the interaction with DTBN where the large tert-butyl groups will interfere. Further evidence is provided for this idea by the triethylphosphine oxide probe work, see Chapter 4, and HMPA probe, both correlate with DTBN in DMSO.

It should be noted that for all these correlation plots there are two distinct regions, (i) the aprotic region where dipole-dipole interactions dominate, and (ii) the protic region that is dominated by hydrogen bonding to the probe. It should, however, be borne in mind that these definitions are not rigid and that in the protic region some bulk effect is also apparent and in the aprotic region some weak H-bonding may be involved.

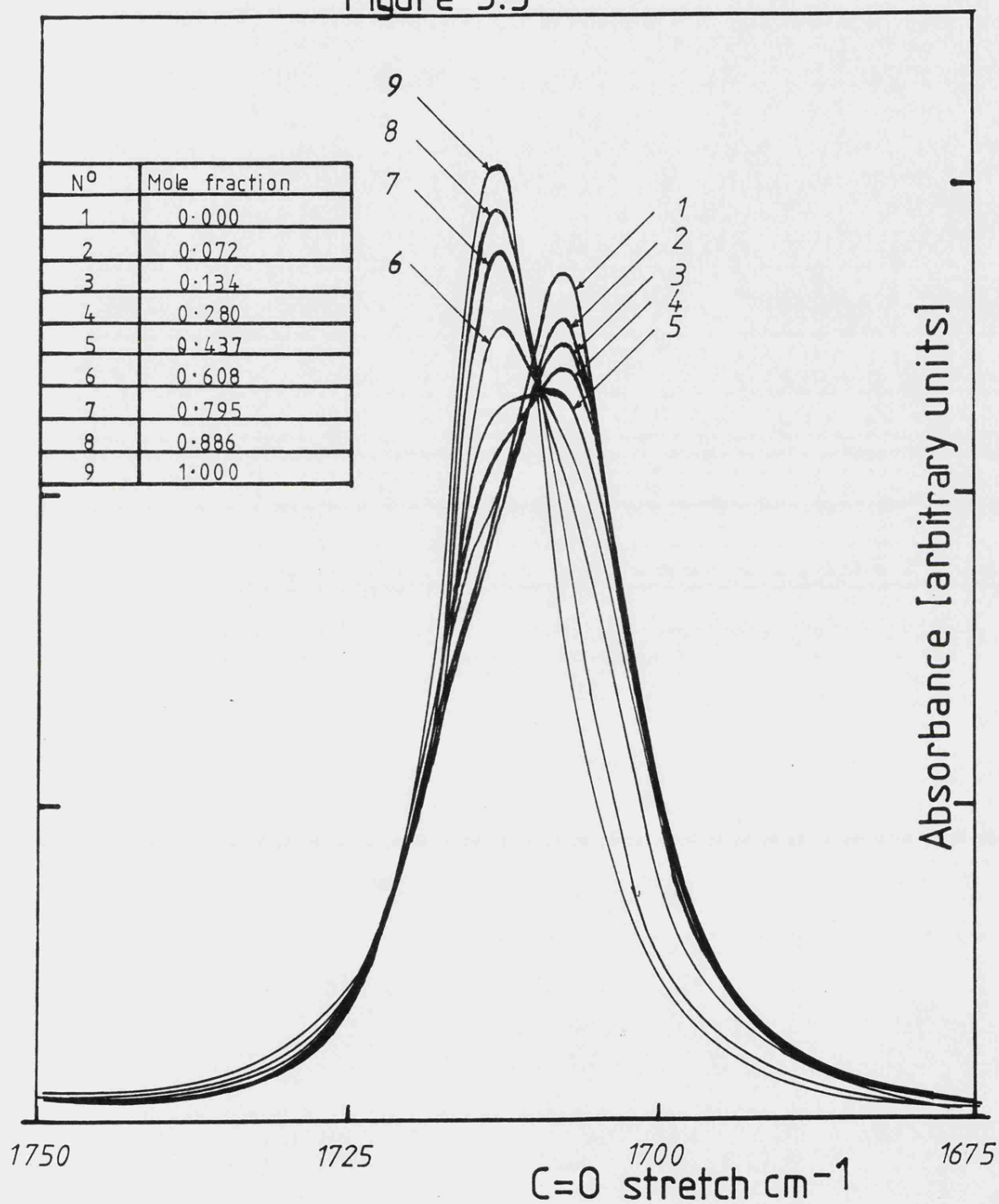(b)  Methanol with aprotic solvents

On taking acetone in methanol and titrating in some aprotic species such as MeCN (cyanomethane) a new band grows whilst the original band decreases. This is similar for all the aprotic solvents used. Examples are shown in Figures 5, 6 and 7. The position of the new band is ultimately determined by any interaction between the aprotic solvent and acetone (see Figure 1) but in the early stages it is at the same position as the small shoulder assigned to 'free' acetone in pure methanol. We can represent this by reactions (i) and (ii):

$$(MeOH)_n + Me_2CO \rightleftharpoons Me_2CO \text{---} (HOMe)_n \quad\quad \dots\text{( i )}$$
$$Me_2CO \text{---} (HOMe)_n + B \rightleftharpoons Me_2CO + (HOMe)_n \text{---} B \quad\quad \dots\text{(ii)}$$

This effect of 'free' acetone being produced initially and suitable bulk interactions occurring with increasing aprotic concentration is seen very effectively with DMSO.
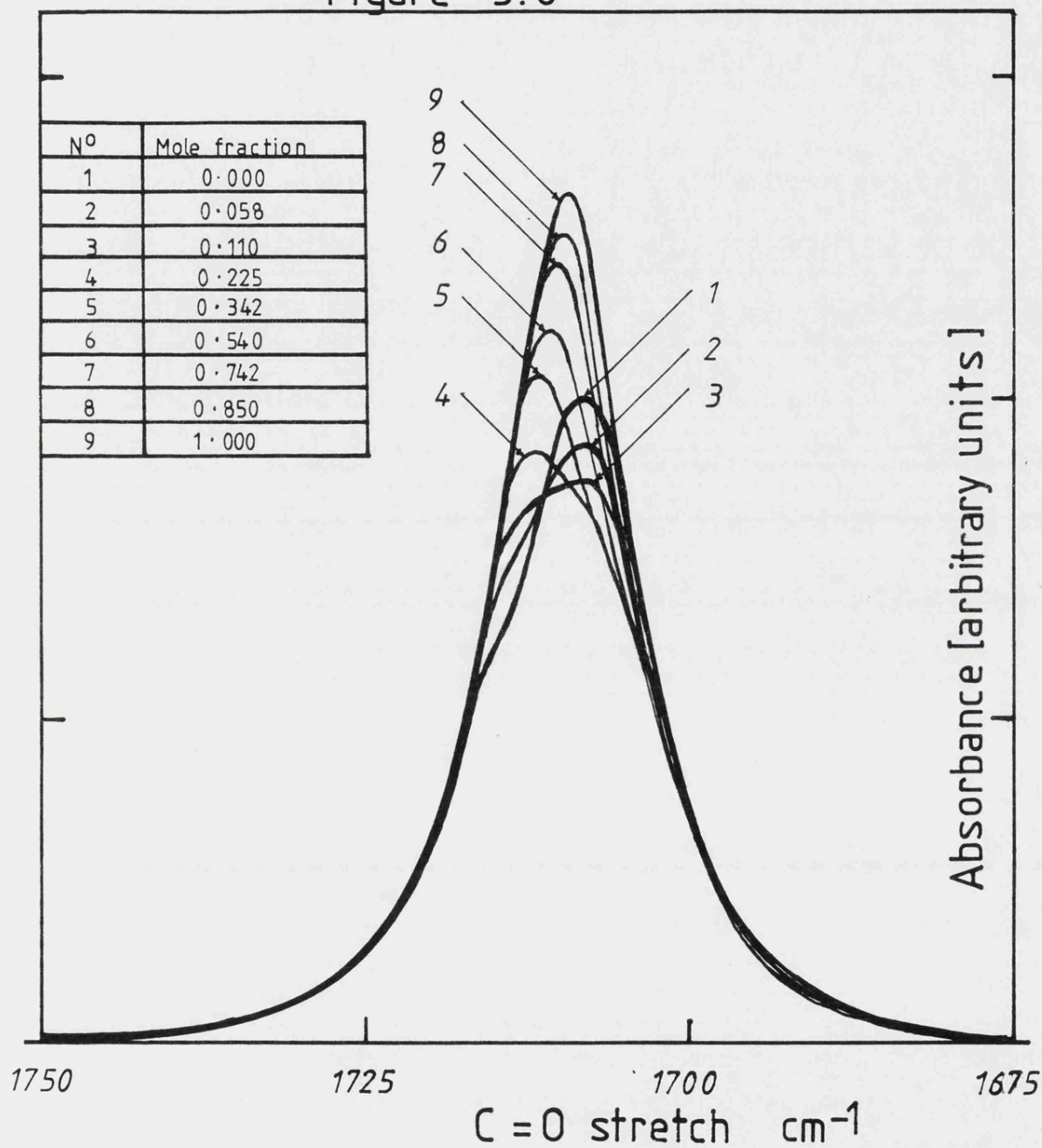
Here the new band initially grows at approximately 1715 $cm^{-1}$ then moves back to 1709 $cm^{-1}$ in keeping with the interaction with DMSO. This

# Figure 3.5



| N° | Mole fraction |
|----|---------------|
| 1  | 0·000 |
| 2  | 0·072 |
| 3  | 0·134 |
| 4  | 0·280 |
| 5  | 0·437 |
| 6  | 0·608 |
| 7  | 0·795 |
| 8  | 0·886 |
| 9  | 1·000 |

Absorbance [arbitrary units]

C=O stretch cm$^{-1}$

1750    1725    1700    1675

Change of C=O stretch band of acetone in a range of
mixtures, Methanol to Cyanomethane.

# Figure 3.6



| N° | Mole fraction |
|---|---|
| 1 | 0·000 |
| 2 | 0·058 |
| 3 | 0·110 |
| 4 | 0·225 |
| 5 | 0·342 |
| 6 | 0·540 |
| 7 | 0·742 |
| 8 | 0·850 |
| 9 | 1·000 |

Absorbance [arbitrary units]

1750     1725     1700     1675

C = O stretch   cm$^{-1}$

Change of C=O stretch band of Acetone in a range of
mixtures, Methanol to Dimethylsulphoxide.

# Figure 3.7



| Nº | Mole fraction |
|----|---------------|
| 1  | 0·000         |
| 2  | 0·030         |
| 3  | 0·050         |
| 4  | 0·130         |
| 5  | 0·230         |
| 6  | 0·370         |
| 7  | 0·570         |
| 8  | 0·740         |
| 9  | 1·000         |

Absorbance [arbitrary units]

C = O stretch cm$^{-1}$

1750  1725  1700  1675
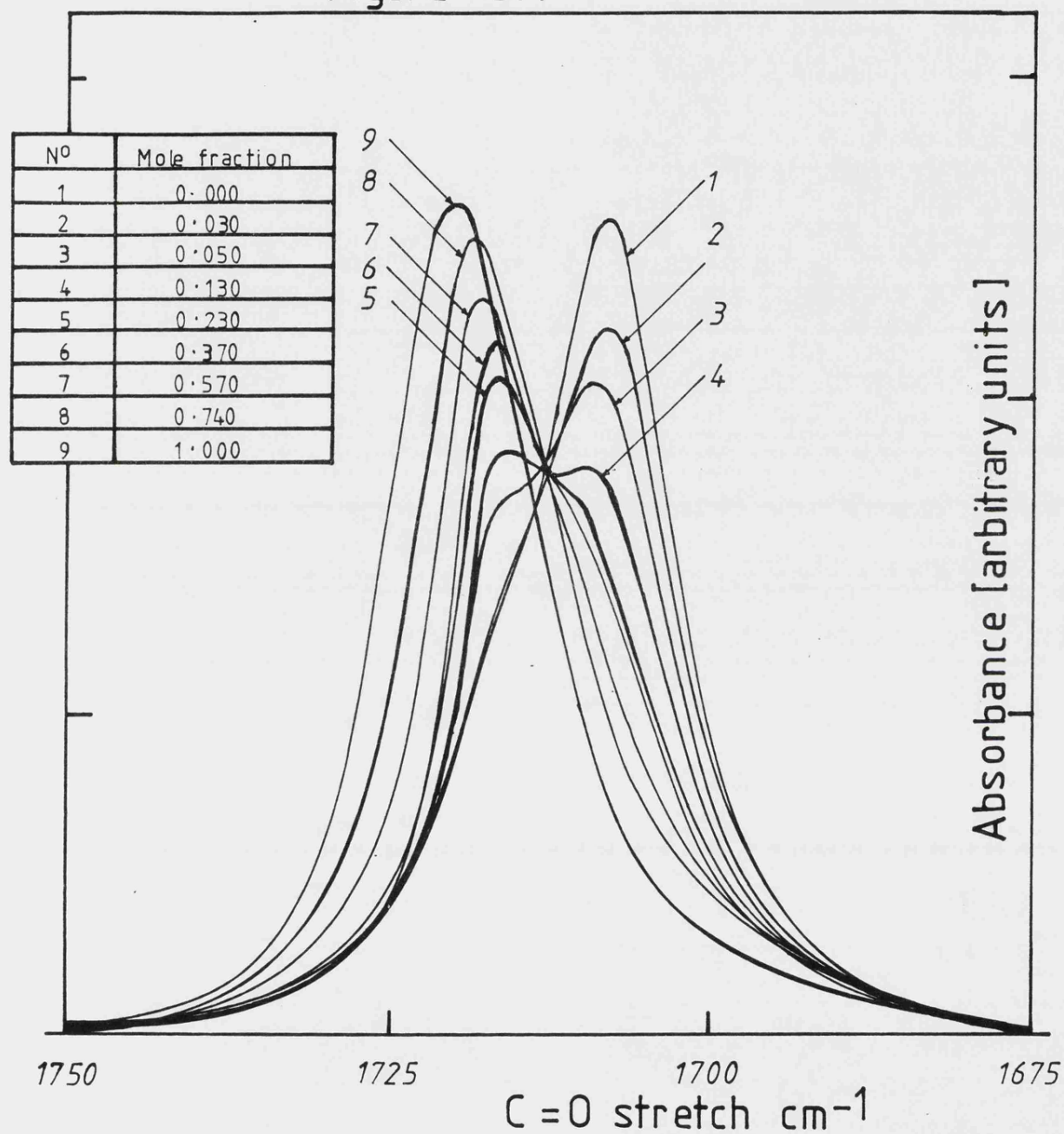
Change of C=O stretch band of Acetone in a range of
mixtures, Methanol to Triethylamine.

indicates that 'free' acetone in an environment of mainly bulk methanol
is less perturbed than by bulk DMSO. However, if totally 'free'
acetone, as in the case of an inert solvent system, were being formed
we should expect a band at around 1722 $cm^{-1}$. This is clearly not the
case and the difference can be accounted for by bulk interactions,
e.g. dipolar, etc., with the bulk methanol. In the previous argument
we have only considered 'free' and 'bound' acetone, however we can also
make some deductions as to the structure of the 'bound' species.

Acetone has two lone pairs of electrons on the oxygen that are avail-
able for hydrogen bonding to methanol. As we have seen in Chapter 1
methanol can be considered as having a chain-like structure and so it is
conceivable that two such chains may be bound to acetone or just one, as
shown by structures I and II:-

Disolvate          $Me_2CO$                                    I

Monosolvate   $Me_2CO$----H—O-----H—O-----          II
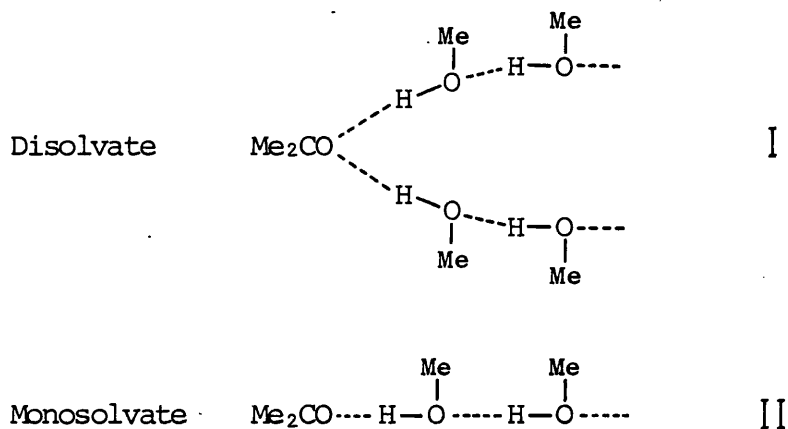
If we take a type I system and add a basic cosolvent two major events
may take place, (a) stripping off of parts of the methanol chain by
breaking MeOH----O—Me bonds or (b) desolvation of the acetone by breaking
the acetone-methanol bonds. Clearly (b) will have a greater effect on
the carbonyl stretching frequency and one would expect to see bands
corresponding to II, I and 'free' acetone as each methanol chain was
removed. Removal of methanol units from the chains would be expected to

-29-

produce only small changes in the carbonyl frequency, the result being seen as a progressive shift to higher values.

What we see is a single step, loss of one band with gain of another at higher frequency followed by a slight shift due to bulk interactions and overall we interpret this as being due to structure II in pure methanol being desolvated by added base with a bulk dipolar shift of 'free' acetone to its final position in pure aprotic base. We see no evidence for structure I in pure methanol.

By band deconvolution (see Appendix 1) it was possible to plot the loss and gain of various species over the mole fraction range (Figures 8, 9 and 10). It can be observed that the rate of loss of methanol from acetone is only partially affected by the base strength of the cosolvent. All the bases have roughly the same initial effect whereas their strengths are significantly different. This probably arises due to a buffering effect such as

$$(MeOH)_n + B \; \rightleftharpoons \; B\text{----}H\text{---}\overset{\overset{\displaystyle Me}{|}}{O}\text{----} \; + \; (lp)_{free} \qquad \ldots . \; (iii)$$
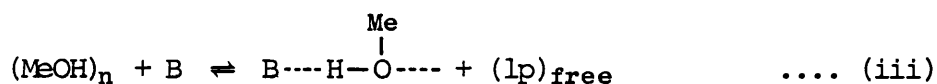
where $(lp)_{free}$ indicates a terminal methanol with a free lone-pair of electrons. This $(lp)_{free}$ will be the same for all bases and in the dynamic exchanging system of a methanol-rich mixture will be the controlling 'base' for desolvation of the acetone. However, on increasing the concentration of base, direct removal of the acetone becomes important. Hence the cross-over point where 50% of the acetone has become 'free' is related to base strength. The weaker base requiring a higher mole-fraction than the strong base to effect the same degree of removal.

(c) Ethane-1,2-diol with aprotic solvents

A single symmetrical band was observed for acetone in ethane-1,2-diol, the shift induced being greater than that for methanol (Figure 1). With
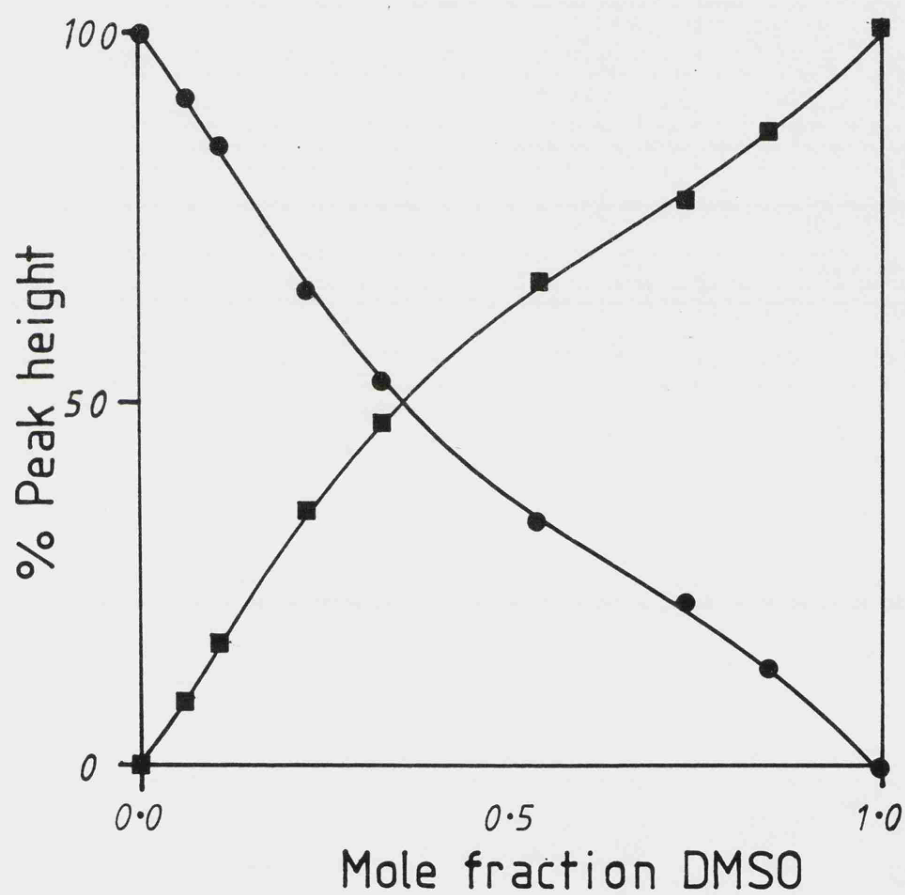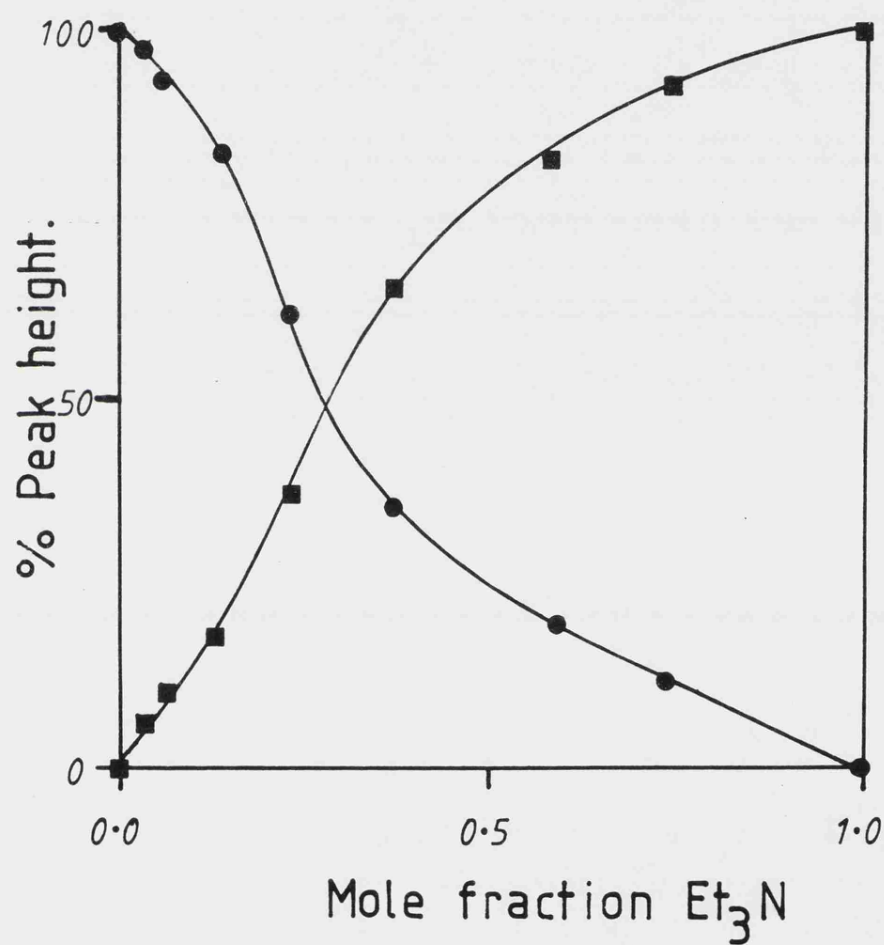
# Figure 3.8
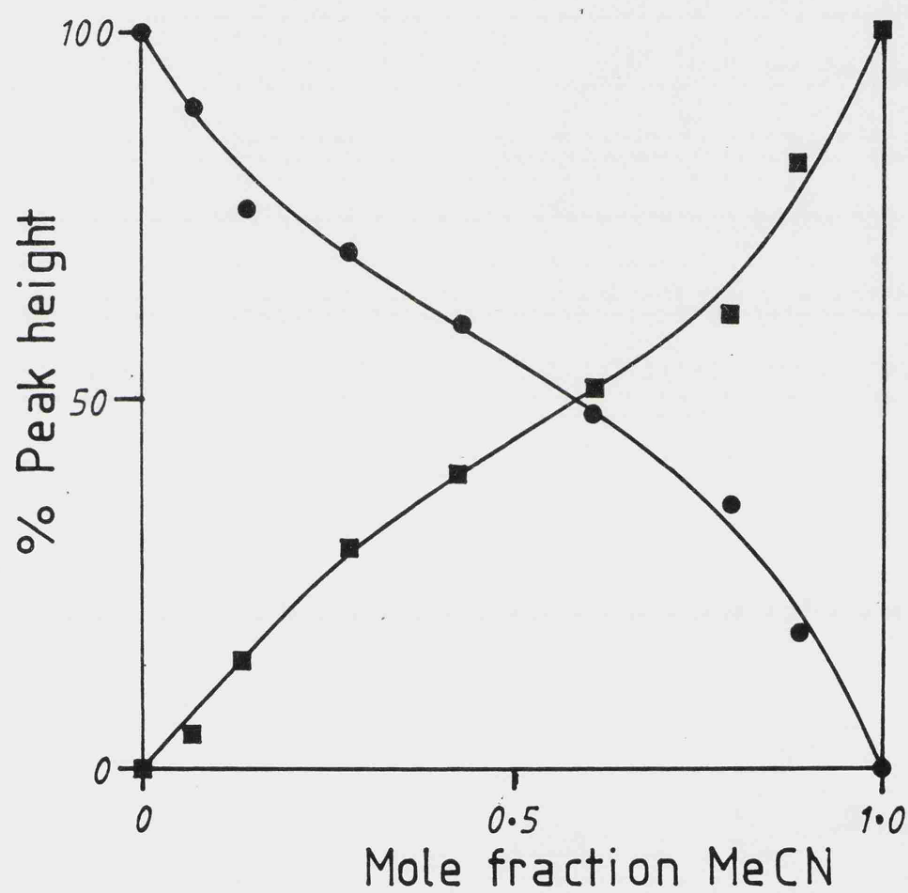


Deconvoluted bands, peak height shown as a
percentage of maximum. 𝒥 C=O Acetone in
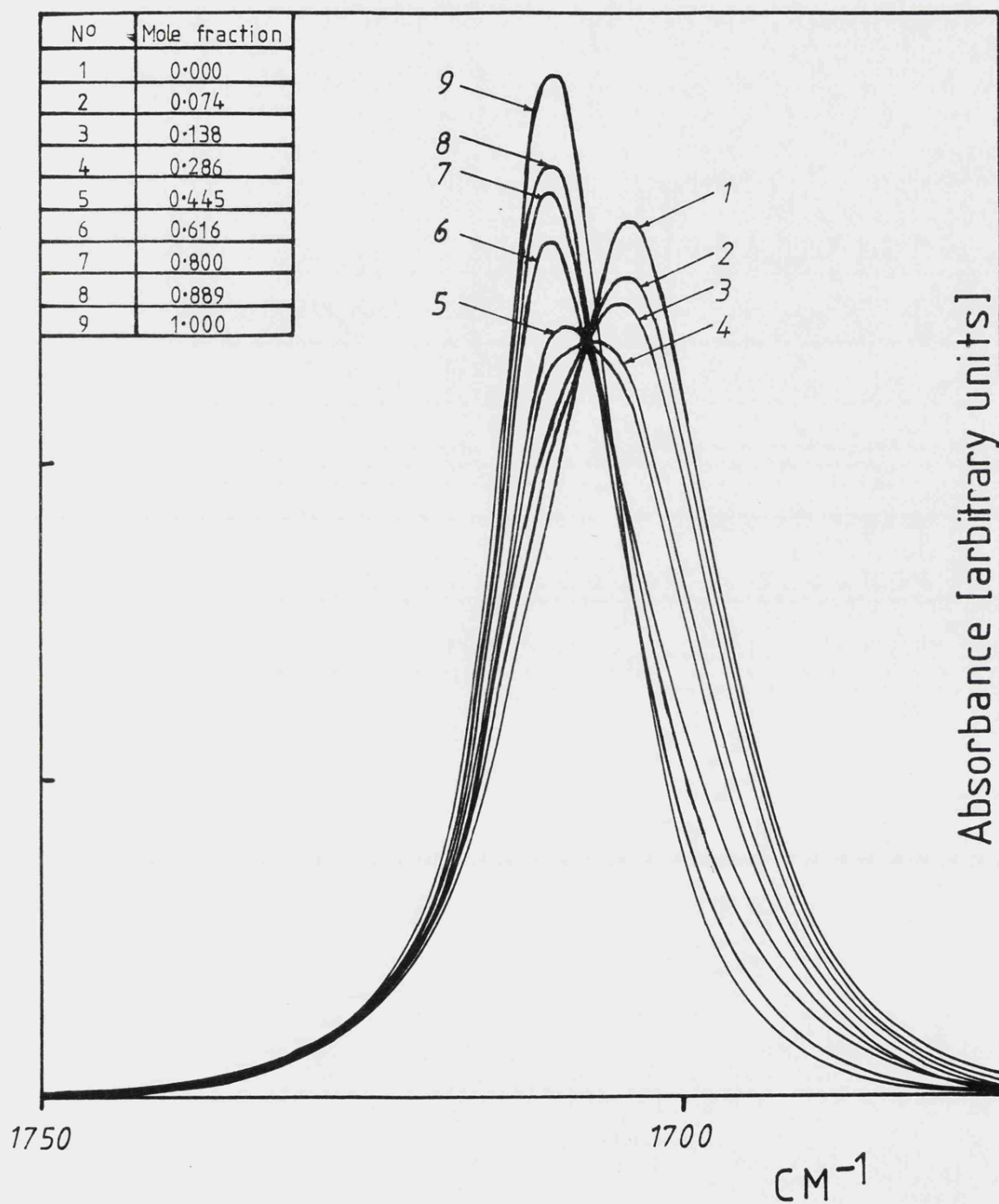mixture Methanol to Cyanomethane.

# Figure 3.9



Deconvoluted bands, peak height shown as a
percentage of maximum. ν C=O Acetone in a
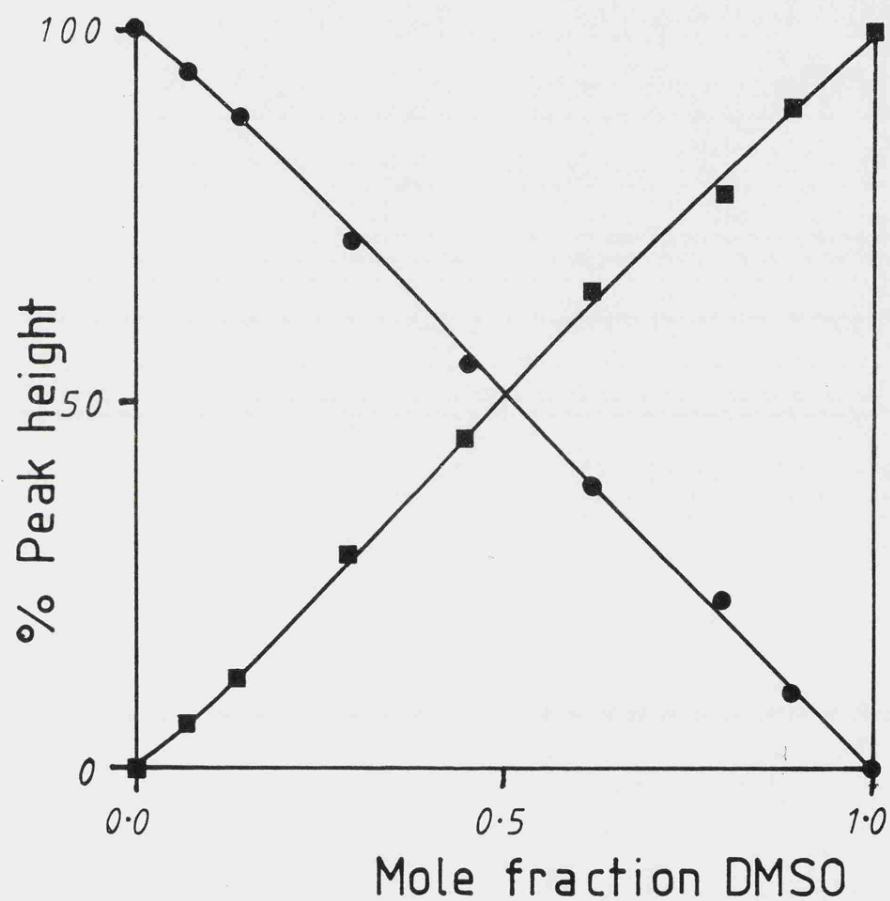mixture Methanol to Dimethylsulphoxide.

# Figure 3.10



Deconvoluted bands, peak height shown as a
percentage of maximum. $\nu$ C=O Acetone in a
mixture Methanol to Triethylamine.

# Figure 3.11

| Nº | Mole fraction |
|----|---------------|
| 1  | 0·000 |
| 2  | 0·074 |
| 3  | 0·138 |
| 4  | 0·286 |
| 5  | 0·445 |
| 6  | 0·616 |
| 7  | 0·800 |
| 8  | 0·889 |
| 9  | 1·000 |

9
8
7
6
5
1
2
3
4

Absorbance [arbitrary units]

1750

1700

$CM^{-1}$

Change of C=O stretch band of Acetone in a range
of mixtures, Ethane 1,2-diol to Dimethylsulphoxide.
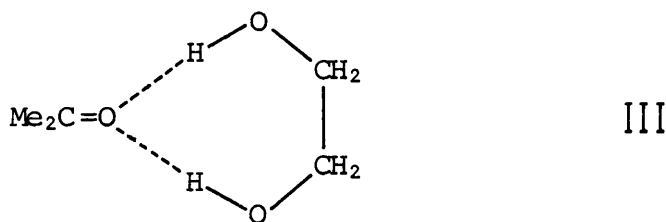
-34-

# Figure 3.12



Deconvoluted bands, peak height shown as a
percentage of maximum.  C=O Acetone in
mixture, Ethane 1,2-diol to Dimethylsulphoxide.

# Figure 3.13
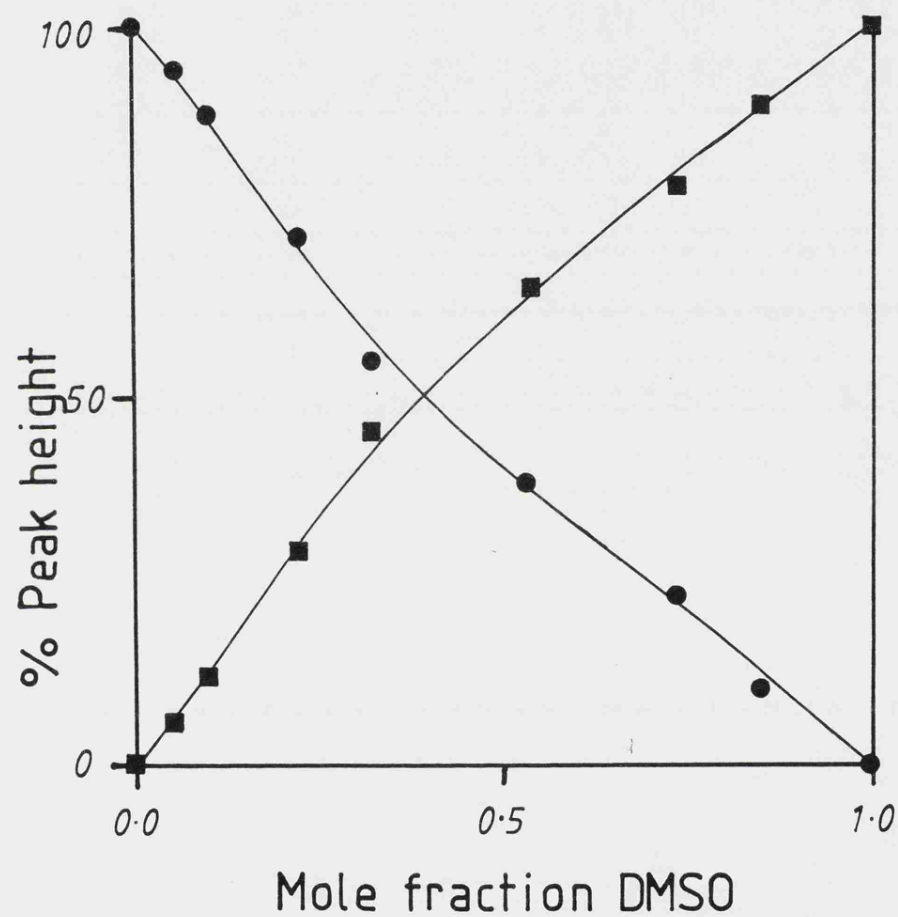


Deconvoluted bands, peak height shown as a percentage of maximum. $\nu C=O$ Acetone in mixture Ethane 1-2diol → Dimethylsulphoxide. Relative to [OH]

methanol structures I and II were the major possibilities but with ethane-diol there is a third, i.e. the cyclic structure.

$$Me_2C=O \begin{array}{c} \diagup H \diagup O \diagdown \\ \diagdown H \diagdown O \diagup \end{array} \begin{array}{c} CH_2 \\ | \\ CH_2 \end{array} \qquad III$$

However, on adding basic cosolvents as for methanol there are only two species seen, i.e. bound and free (Figure 11). After deconvolution and plotting the fall and rise against mole fraction diol a different picture to methanol appears (Figure 12) but if allowance is made for the excess OH groups by plotting against relative mole fraction OH groups the picture is very similar (Figure 13). It is concluded that ethane-diol is behaving in the same way as methanol and that only structure II is of any significance in the pure solvent case.
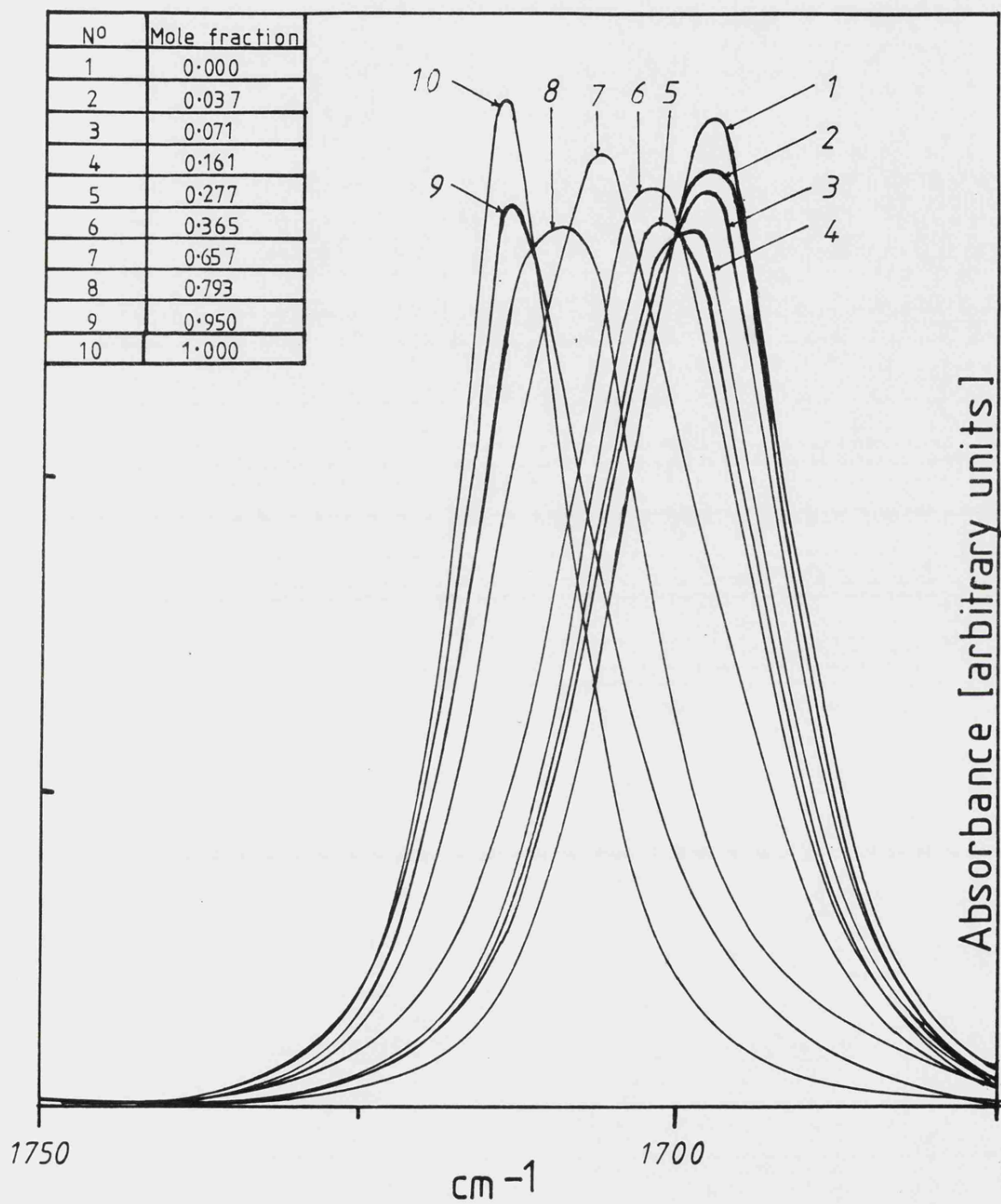
(d) Water with aprotic solvents

The carbonyl band for dilute aqueous acetone is a symmetrical single band indicating either all structure I or all structure II for the acetone. In view of the water equilibrium, viz.

$$(H_2O)_{bulk} \rightleftharpoons (OH)_{free} + (lp)_{free} \qquad \dots \text{(iv)}$$
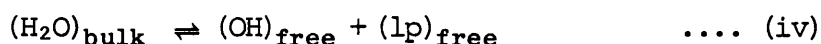
that has been discussed in Chapter 1, it would be reasonable to assume that small quantities of bases such as acetone will be solvated to their maximum extent. An inspection of Figure 1 reveals that the carbonyl band shifts in roughly equal steps: Aprotic $\rightarrow$ MeOH $\rightarrow$ H$_2$O which suggests a system 'Free' $\rightarrow$ Mono-bound $\rightarrow$ Di-bound. Other work (see Chapter 7) also indicates this sequence for acetone. Figures 14, 15 and 16 show the effect of adding aprotic cosolvents to aqueous acetone. It can be seen from these that three distinct regions exist in the spectrum, at 1697 cm$^{-1}$,
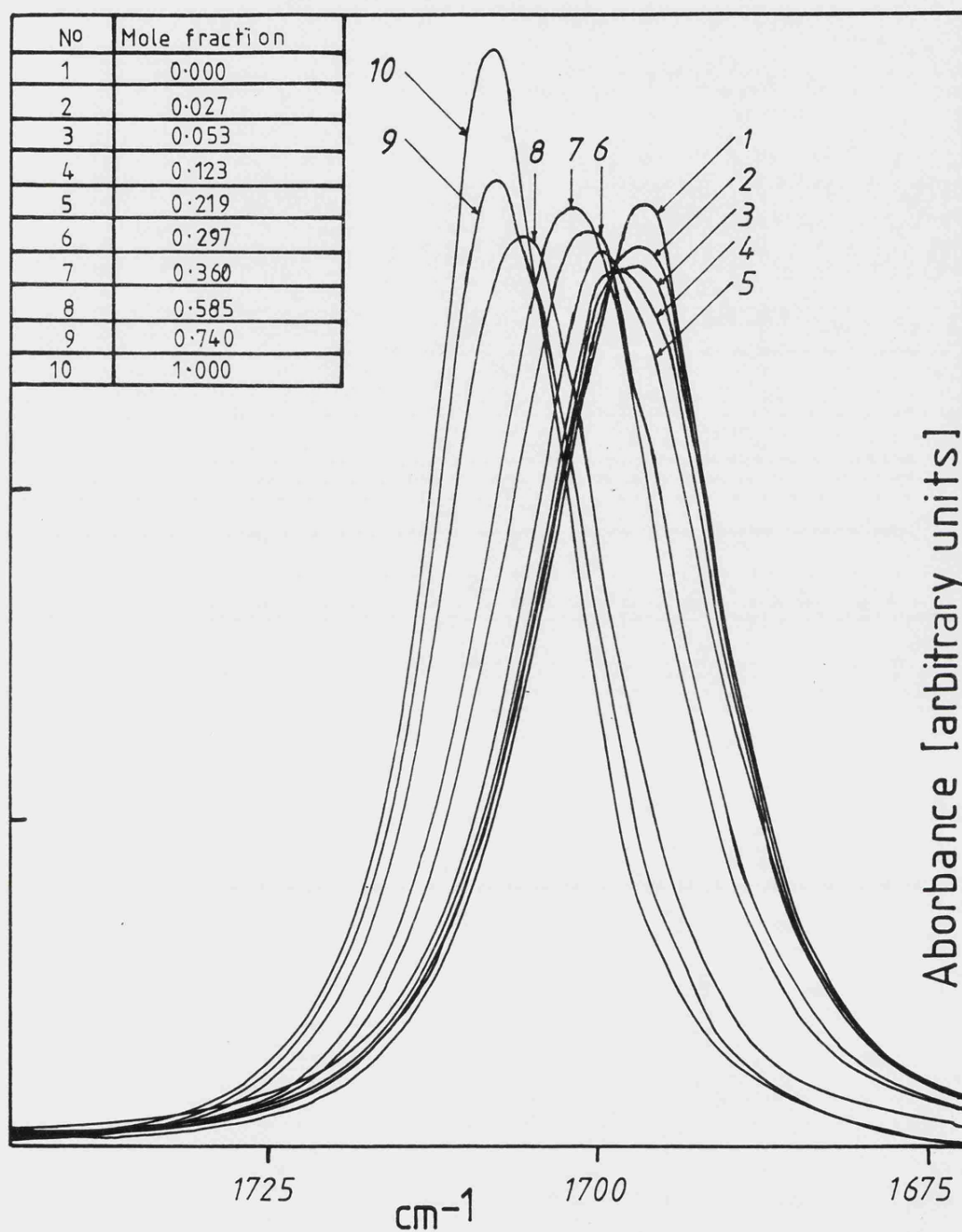
# Figure 3.14

| Nº | Mole fraction |
|----|---------------|
| 1 | 0·000 |
| 2 | 0·037 |
| 3 | 0·071 |
| 4 | 0·161 |
| 5 | 0·277 |
| 6 | 0·365 |
| 7 | 0·657 |
| 8 | 0·793 |
| 9 | 0·950 |
| 10 | 1·000 |



Change of C=O stretch of Acetone in range of
mixtures, Water($D_2O$) to Cyanomethane.

# Figure 3.15



| No | Mole fraction |
|----|---------------|
| 1  | 0·000         |
| 2  | 0·027         |
| 3  | 0·053         |
| 4  | 0·123         |
| 5  | 0·219         |
| 6  | 0·297         |
| 7  | 0·360         |
| 8  | 0·585         |
| 9  | 0·740         |
| 10 | 1·000         |

Change of C=O str band of Acetone in range of mixtures, Water ($D_2O$) → Dimethylsulphoxide.

# Figure 3.16



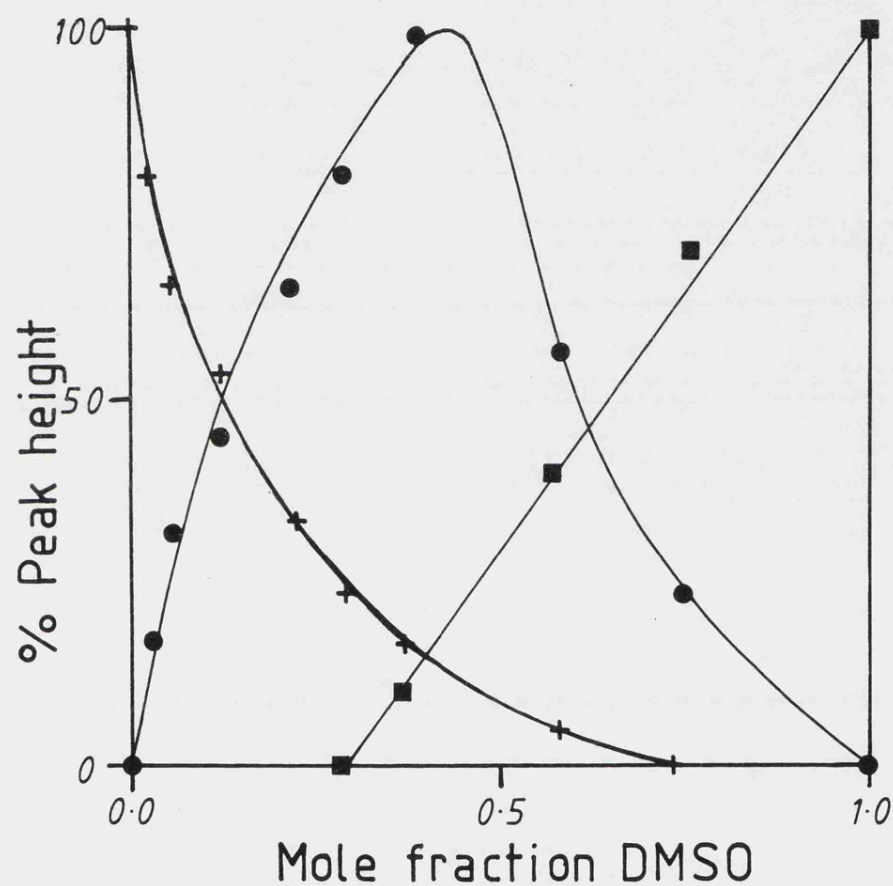| Nº | Mole fraction |
|----|---------------|
| 1  | 0·000         |
| 2  | 0·002         |
| 3  | 0·004         |
| 4  | 0·012         |
| 5  | 0·054         |
| 6  | 0·100         |
| 7  | 0·186         |
| 8  | 0·363         |
| 9  | 0·533         |
| 10 | 1·000         |
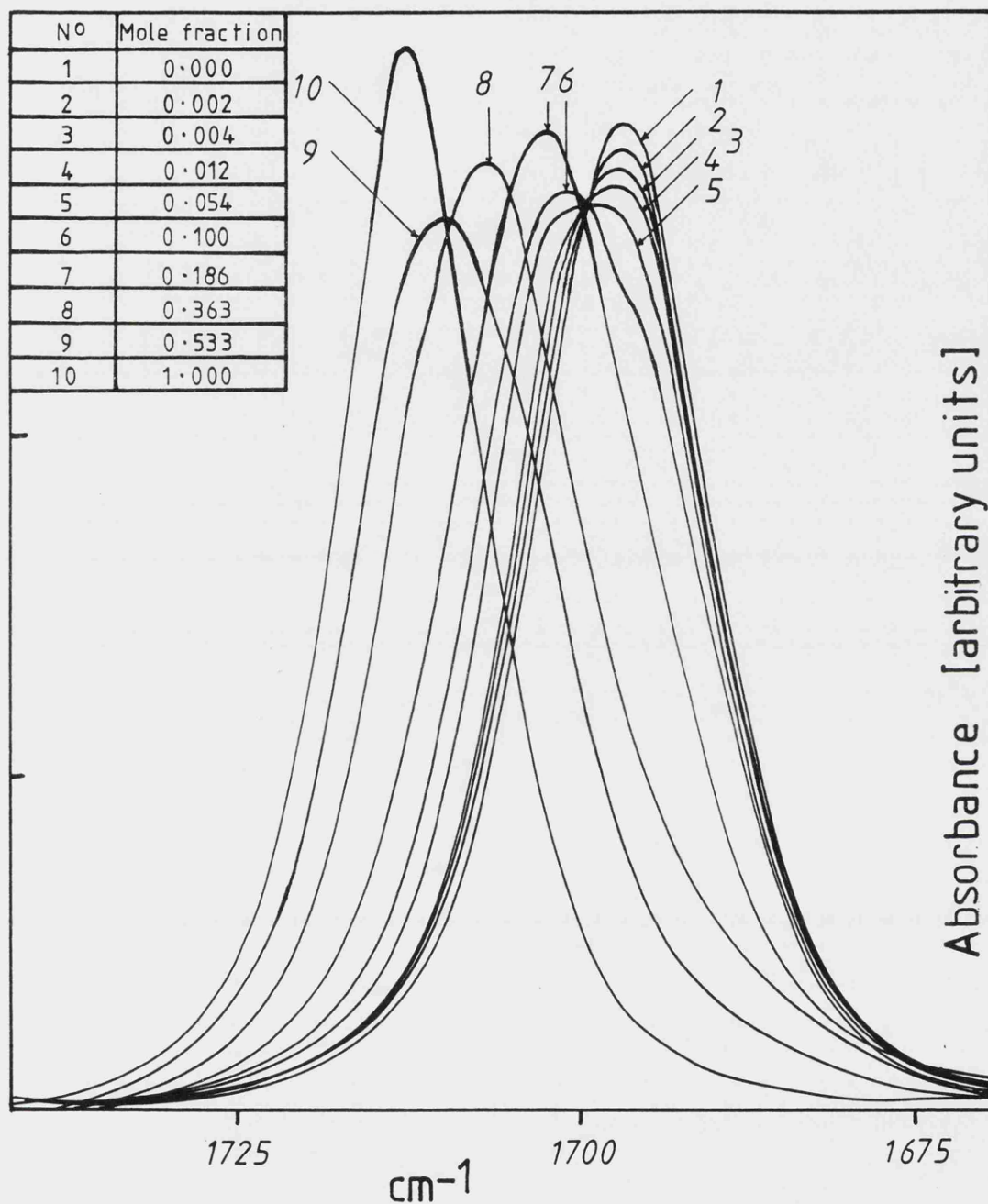
Change of C=O str band of Acetone in range of mixtures,
Water ($D_2O$) → Hexamethylphosphoramide.

# Figure 3.17
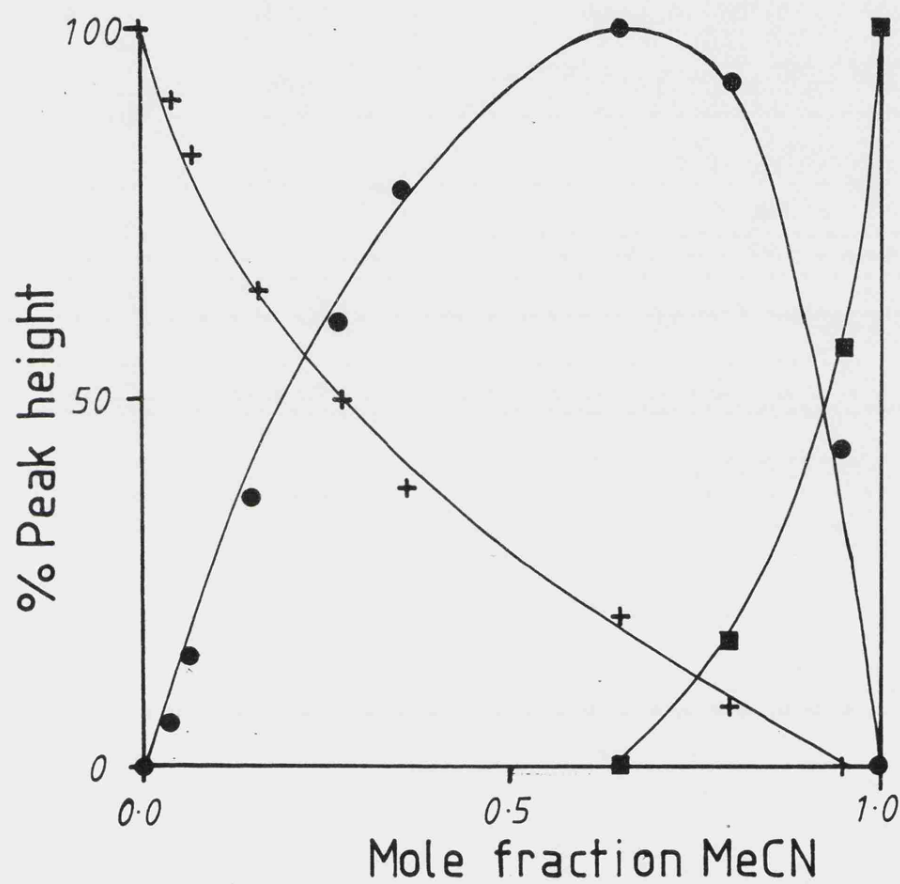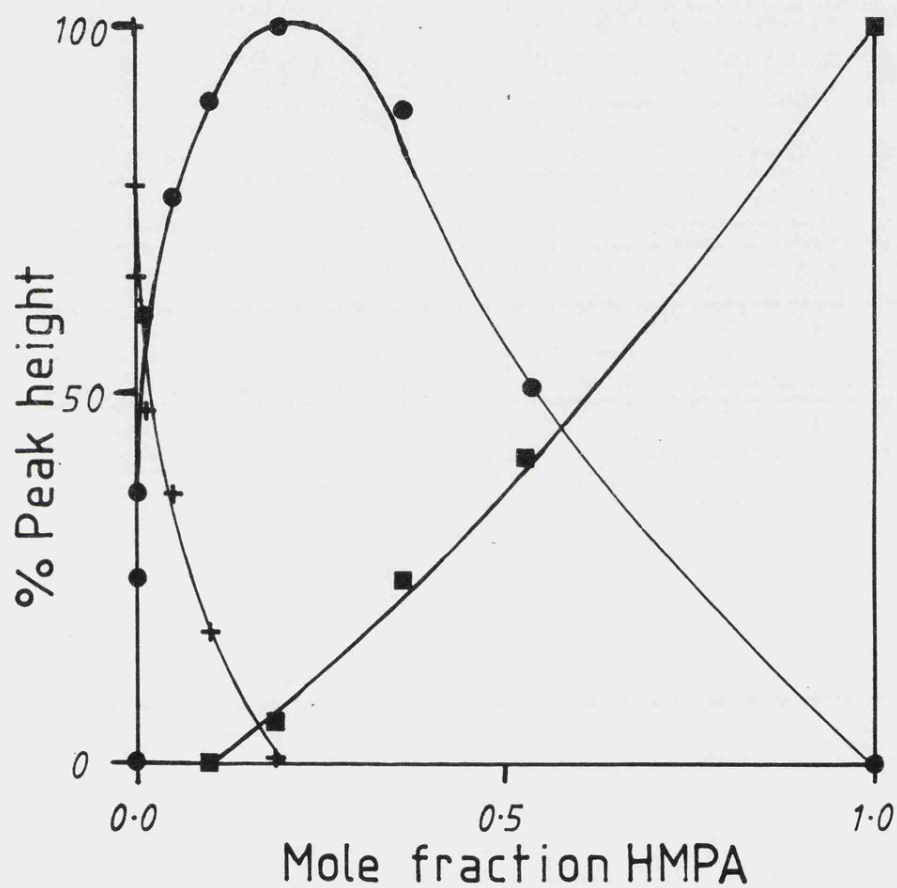


Deconvoluted bands, peak height shown as a percentage
of maximum.  $\nu C=O$ Acetone in mixture Water $(D_2O) \rightarrow$
Cyanomethane.

# Figure 3.18



Deconvoluted bands, peak height shown as a percentage of maximum. $\nu$ C=O Acetone in mixture Water ($D_2O$) → Dimethyl-sulphoxide.

# Figure 3.19



Deconvoluted bands, peak height shown as a
percentage of maximum.   $\nu C{=}O$ Acetone in mixture
Water $(D_2O) \rightarrow$ Hexamethylphosphoramide.

$1705\ cm^{-1}$ and the aprotic region.

If we interpret these changes in terms of structure II where the acetone is mono-basic, we have a situation similar to the methanol case. There is only one water-acetone hydrogen bond to break but many water-water bonds, a single loss/gain situation would be expected for the desolvation of the acetone but a slow shift for the progressive removal of water molecules from 3D chain structure. This is not what is observed.

However, if we consider structure I where acetone is di-basic, we can envisage two main desolvation steps for the acetone, i.e.

Structure I $\longrightarrow$ Structure II $\longrightarrow$ 'free'

or, possibly, a progressive shift due to loss of water from the 3D chain system. It is most likely that both situations will arise, the major steps being due to desolvation of the acetone with minor shifts due to the water structure being broken at higher aprotic mole fraction.

The deconvoluted bands plotted against mole fraction (Figures 17, 18 and 19) show the progress of the three bands clearly. The rate of desolvation of the disolvate appears to depend on the basicity of the aprotic base rather than base strength. This is interpreted as being due to the system in water(V).This will have the effect of shifting equation

$$(OH)_{free} + B \rightleftharpoons B---H-O \qquad \qquad .... \text{(v)}$$
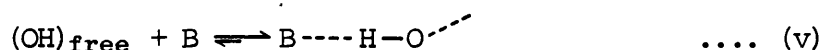
(iv) to the right so increasing the amount of $(lp)_{free}$, this and not the basic cosolvent (which is almost all bound to water) is the desolvating agent, even for fairly weak bases. Obviously the basicity of the aprotic cosolvent will determine how much excess $(lp)_{free}$ is formed and, therefore, the rate of desolvation. As the mole fraction of aprotic base increases, so the influence of base strength will increase and the effect of basicity will decrease. This can be seen in the way that the

monosolvated band is related to mole fraction. For a strong base the deconvoluted band height passes through a maximum at a low mole fraction of base. As the base strength decreases so the position of this maximum moves to higher mole fraction.
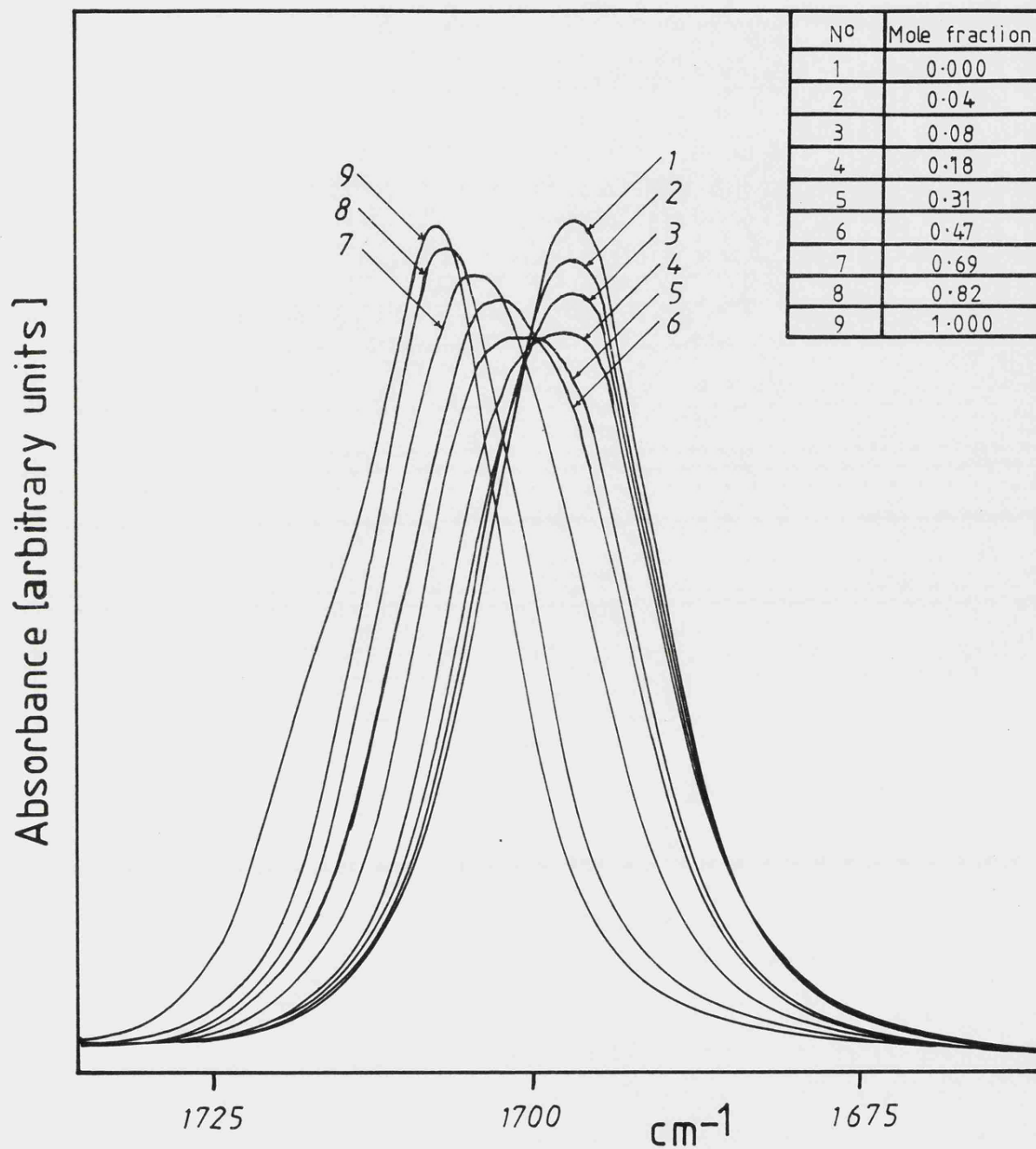
## (e) Water with methanol

Figure 20 shows the effect of adding methanol to water. We see only two main bands with a loss of the band at 1697 $cm^{-1}$ and a gain of the 1707 $cm^{-1}$ band. Small shifts are also observed throughout. If we suggest structure I type for acetone in water and structure II for acetone in methanol, a scheme as below indicates the various routes available for interconversion:-
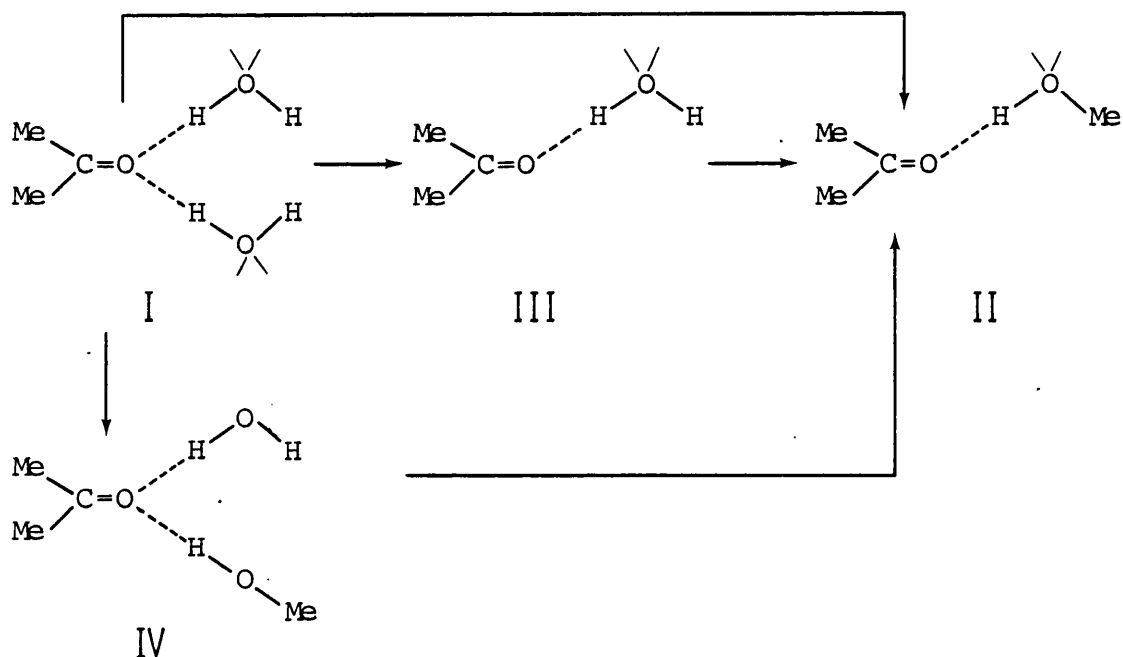


As structures I and IV are so similar no infrared spectroscopic technique could distinguish them - likewise III and II - there is therefore no evidence from this work for any of these routes to be preferred.

However, as water and methanol both have a tendency to form hydrogen bonds where possible, the direct route from I to II involving exchange

# Figure 3.20



| N° | Mole fraction |
|----|---------------|
| 1 | 0·000 |
| 2 | 0·04 |
| 3 | 0·08 |
| 4 | 0·18 |
| 5 | 0·31 |
| 6 | 0·47 |
| 7 | 0·69 |
| 8 | 0·82 |
| 9 | 1·000 |

Change of C=O str band of Acetone in range of mixtures
Water $(D_2O) \rightarrow$ Methanol.

and desolvation simultaneously would appear unlikely in any mixed solvent system. Also structure III would require desolvation before exchange and this would be unlikely in such a system.

## 3.3  CONCLUSIONS

From the work described in this Chapter and information from the literature, it can be seen that acetone is a useful probe into its own solvation and that of many other systems. It has been demonstrated that acetone is likely to be disolvated in water, mainly, monosolvated in methanol and other alcohols, this state of solvation being occasioned by hydrogen bonding. In solvents where no hydrogen bonding can take place, any interaction is with the bulk medium via dipolar coupling, etc. These bulk medium effects obviously have an effect within hydrogen bonded systems but only of minor importance.

The excellent correlation with nitroxide studies suggests that the information about solvated states is applicable and may be of use in the interpretation of the e.s.r. data. This will be discussed further in Chapter 6.

REFERENCES FOR CHAPTER 3

1.  K. B. Whetsel and R. E. Kagarise, Spectrochimica Acta, Vol. 18 (1962).

2.  L. J. Bellamy and R. J. Pace, Spectrochimica Acta, Vol. 19 (1963).

3.  C. Laurence, G. Guiheneuf and B. Wojtkowiak, J.A.C.S., 101:17 (1979).

4.  J. Lascombe, Ph.D. Thesis, University of Bordeaux (1960).

5.  Y. Y. Lim, E. A. Smith and M. C. R. Symons, J.C.S. Faraday I, 72 (1976).

6.  S. E. Jackson, E. A. Smith and M. C. R. Symons, Faraday Discussions, Chem. Soc., 64 (1978).

7.  D. A. C. Compton, C. Chatgillaloglu, H. H. Mantsch and K. U. Ingold, J. Phys. Chem., 85 (1981).

8.  L. B. Archibald and A. D. E. Pullin, Spectrochimica Acta, Vol. 12 (1958).

9.  V. Gutmann, "The Donor-Acceptor approach to Molecular Interactions", Plenum Press, New York/London, 1978.

10. G. E. Maciel and G. C. Ruben, J.A.C.S., Vol. 85 (1963).

11. A. S. Pena, unpublished results.

# CHAPTER 4

TRIETHYLPHOSPHINE OXIDE PROBE STUDIES

## 4.1  INTRODUCTION

[31]P chemical shifts for phosphine oxides have been shown to be very sensitive to solvent effects. This was utilised by Gutmann [1] for the determination of his acceptor numbers (AN) [for values see Table 1 in Chapter 7].

The P$\rightleftharpoons$O stretching frequency in the fundamental infrared (around 1150 cm$^{-1}$) was found also to be solvent sensitive [2] and a study of this together with [31]P n.m.r. shifts was undertaken as part of our studies of probes.

Triethyl phosphine oxide was chosen for several reasons, (a) this was the compound used by Gutmann, (b) it is stable and easily handled, (c) interaction occurs only via the oxygen lone pairs or by dipole-dipole effects. In Chapter 3 it was shown that the infrared work on acetone could be used to gain a greater understanding of previous nitroxide e.s.r. studies. N.m.r. studies usually suffer from time-averaging problems in the same way as e.s.r. It was therefore desirable to be able to interpret the n.m.r. results in the light of information about solvation states. In the case of acetone the infrared shifts correlate linearly with [13]C n.m.r. shifts for the carbonyl carbon. A similar correlation would be expected for ^{31}P shifts and P$\rightleftharpoons$O stretching frequency shifts for the phosphoryl group of triethyl phosphine oxide.

The P$\rightleftharpoons$O stretching frequency for phosphine oxides occurs at very low wavenumbers compared to most phosphoryl compounds, indicating a highly polar P$-$O bond [3]. Most authors use P = O without indicating any polarity, however in this thesis P$\rightleftharpoons$O will be used indicating only partial π bond character with a large degree of charge separation, such that the true picture is closer to $P^{\delta+} - O^{\delta-}$, and will be indicated by the dotted line.

## 4.2  RESULTS AND DISCUSSION

### 4.2.1  Pure Solvents

The band positions, $\nu_{max}$, for the P=O stretch of triethyl phosphine oxide in various solvents, are shown in Figure 1.  For most solvents a single band was observed, but for alcohols there were two bands.

The correlation of these values with the $^{31}$P chemical shifts shows a very good linear relationship (Figure 2).  However the alcohol data straddle the line.  If a value '$\alpha$' for the weighted mean infrared position is determined for each alcohol and plotted, it is found to lie directly on the line.  This is taken as evidence that the two states seen by infrared both contribute to the $^{31}$P shift value by fast averaging. The individual $^{31}$P shifts for the two species can be taken directly from the correlation and used to give AN values for each state.

As for previous probe studies, it can be seen that the solvents can be grouped into two separate classes, (a) aprotic, with degrees of dipolar interaction, and (b) protic H-bonding solvents.  The various shifts also form a pattern where:-

$$\text{Free} \xrightarrow{\text{i}} \text{Alcohol shoulder} \xrightarrow{\text{ii}} \text{Alcohol main band} \xrightarrow{\text{iii}} \text{Water band}$$

with intervals i, ii and iii being of similar magnitude.  This is inter-preted initially as 'free' $\longrightarrow$ 'mono-bound' $\longrightarrow$ 'di-bound' $\longrightarrow$ 'tri-bound'. The relatively large shifts of dimethyl sulphoxide (DMSO) and methyl cyanide (MeCN) are assigned to strong dipolar interaction.  However, the $\delta$+ve phosphorus is not exposed, being surrounded by three ethyl groups, so that specific 'side-by-side' dipole effects, as postulated for planar molecules such as acetone, etc., with DMSO, would not be expected, so placing it on the line for dipolar aprotic solvents.  Trichloromethane (CHCl$_3$) induced an exceptionally large shift compared to its effect on
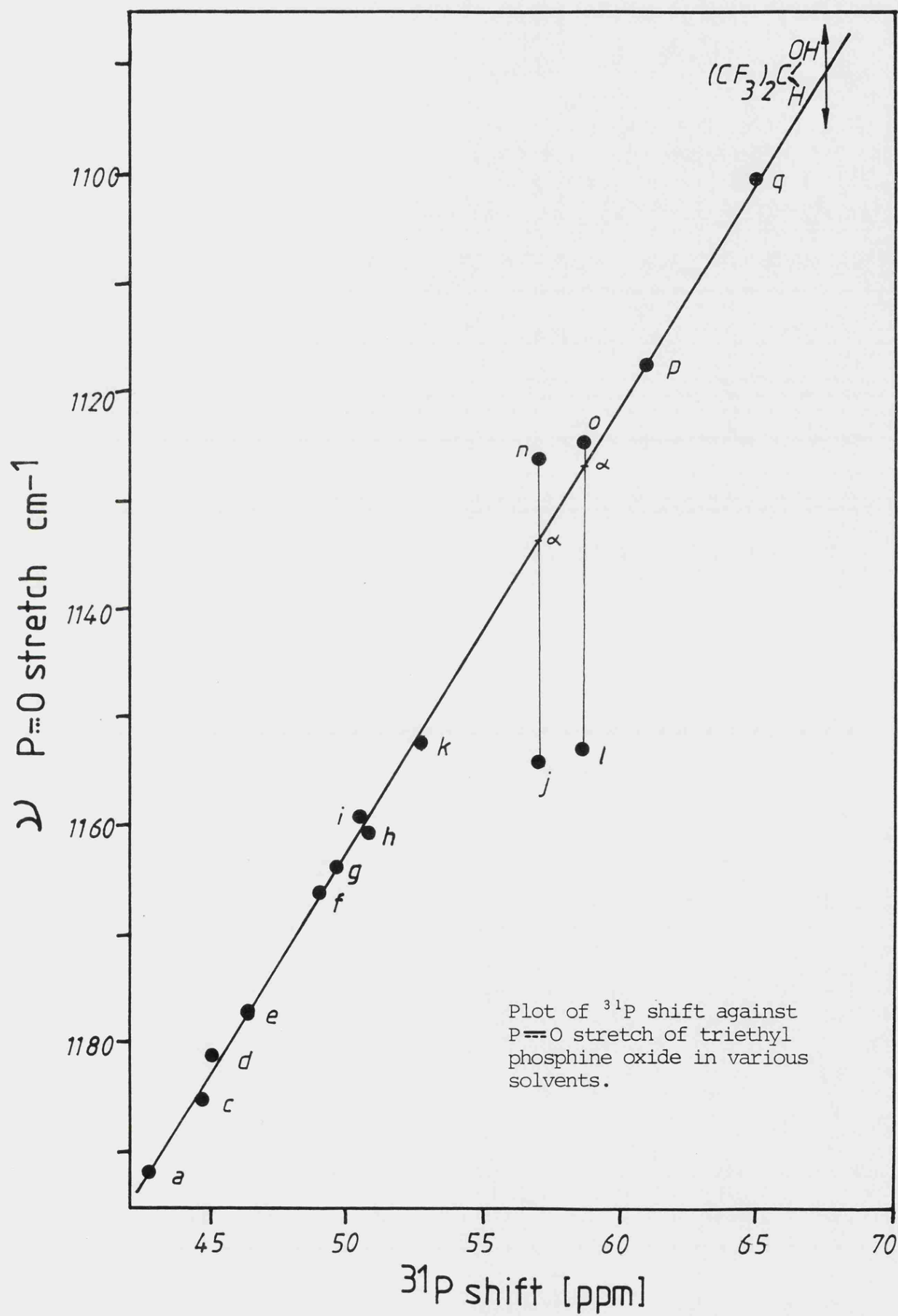
# Figure 4.1
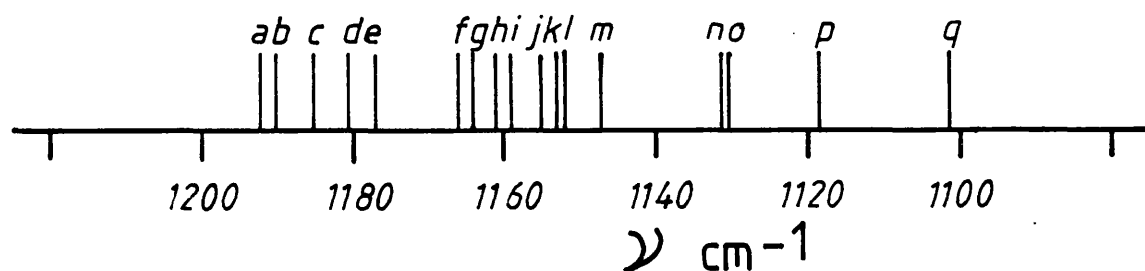


a    Hexane
b    Cyclohexane
c    Triethylamine
d    Tetrahydrofuran
e    Tetrachloromethane
f    Cyanomethane
g    Dimethylsulphoxide
h    Nitromethane
i    Dichloromethane
j    Ethanol [shoulder]
k    Trichloromethane
l    Methanol [shoulder]
m    Trichloromethane [shoulder]
n    Ethanol
o    Methanol
p    Ethane 1,2-diol
q    Water

Band positions of P$=$O stretch of triethyl phosphine oxide in different solvents.

# Figure 4.2



Plot of $^{31}P$ shift against P $=$ O stretch of triethyl phosphine oxide in various solvents.

x-axis: $^{31}P$ shift [ppm]

y-axis: $\nu$ P$=$O stretch cm$^{-1}$

$(CF_3)_2C\begin{smallmatrix}OH\\H\end{smallmatrix}$

other probes. This is interpreted as probably di-solvation. 1,2-Ethane-
diol gave a shift similar to the main alcohol band indicating a di-
solvate, whereas water induced a very large shift indicating tri-
solvation. The alternative possibility for water would be di- or mono-
solvation but with very high 'acidity' of water protons giving a much
stronger H-bond than the alcohols. However, work by other authors [4]
has shown similar bonding abilities by bulk water and bulk alcohol which
supports the idea of tri-solvation.

### 4.2.2 Mixed Solvent Systems

#### a  Methanol with aprotic bases

Figures 3, 4 and 5 show the effect on the $\nu P = O$ stretch of adding
various bases to methanolic solutions of $Et_3PO$ and Figure 6 shows the
effect on the $^{31}P$ shift of the same and other bases. It is observed that
initially the main infrared band diminishes whilst the minor band
increases, and that, subsequently, this band gives way to a third,
characteristic of $Et_3PO$ in the pure base. This is interpreted as
'Di' $\longrightarrow$ 'Mono' $\longrightarrow$ 'Free'. The shift in n.m.r. position follows the
apparent basicity of the added aprotic bases in the initial stages with
relative base strength becoming more prevalent in the later stages. This
is illustrated in Figures 7, 8 and 9 where the deconvoluted bands are
plotted; basicity is responsible for the 'di' $\longrightarrow$ 'mono' stage and base
strength more relevant to the 'mono' $\longrightarrow$ 'free' stage.
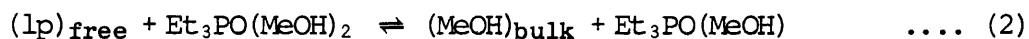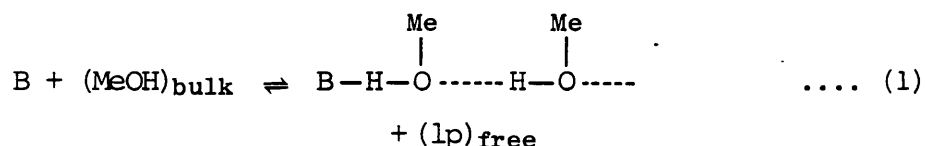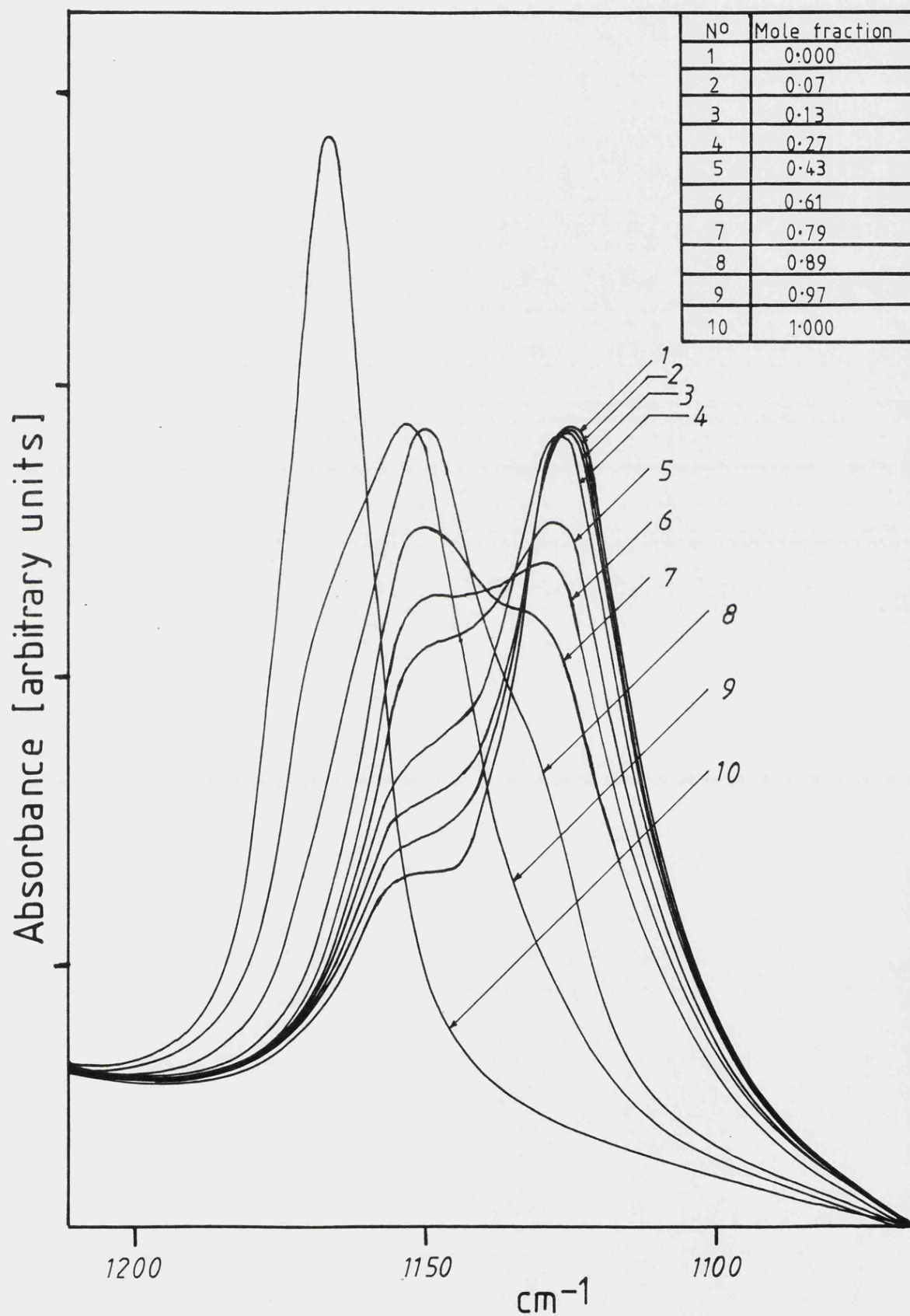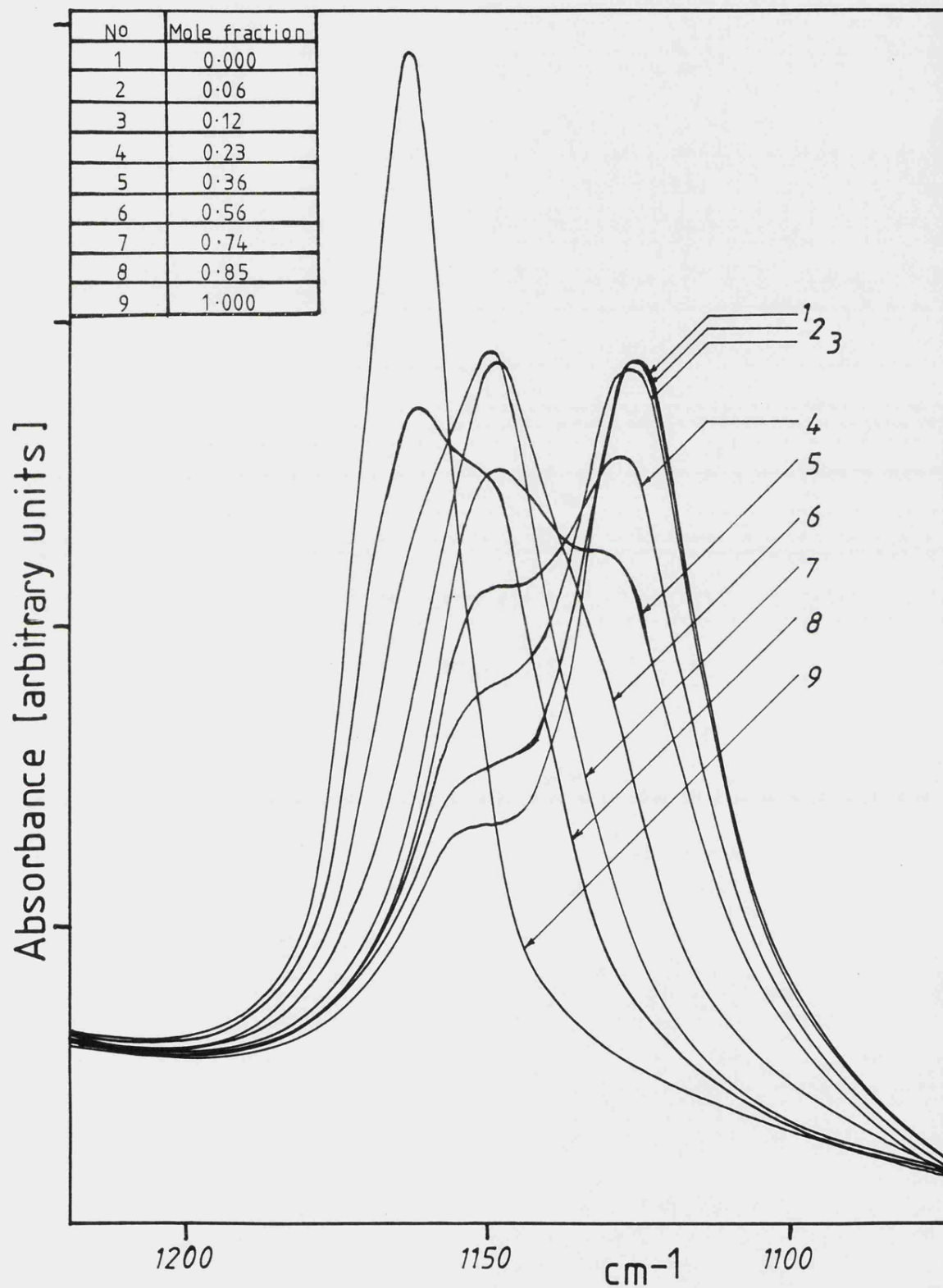
This situation arises due to the equilibria:-

$$B + (MeOH)_{bulk} \rightleftharpoons B - H - O \cdots\cdots H - O \cdots\cdots \qquad \cdots\cdots (1)$$
$$+ (lp)_{free}$$

$$(lp)_{free} + Et_3PO(MeOH)_2 \rightleftharpoons (MeOH)_{bulk} + Et_3PO(MeOH) \qquad \cdots\cdots (2)$$

# Figure 4.3



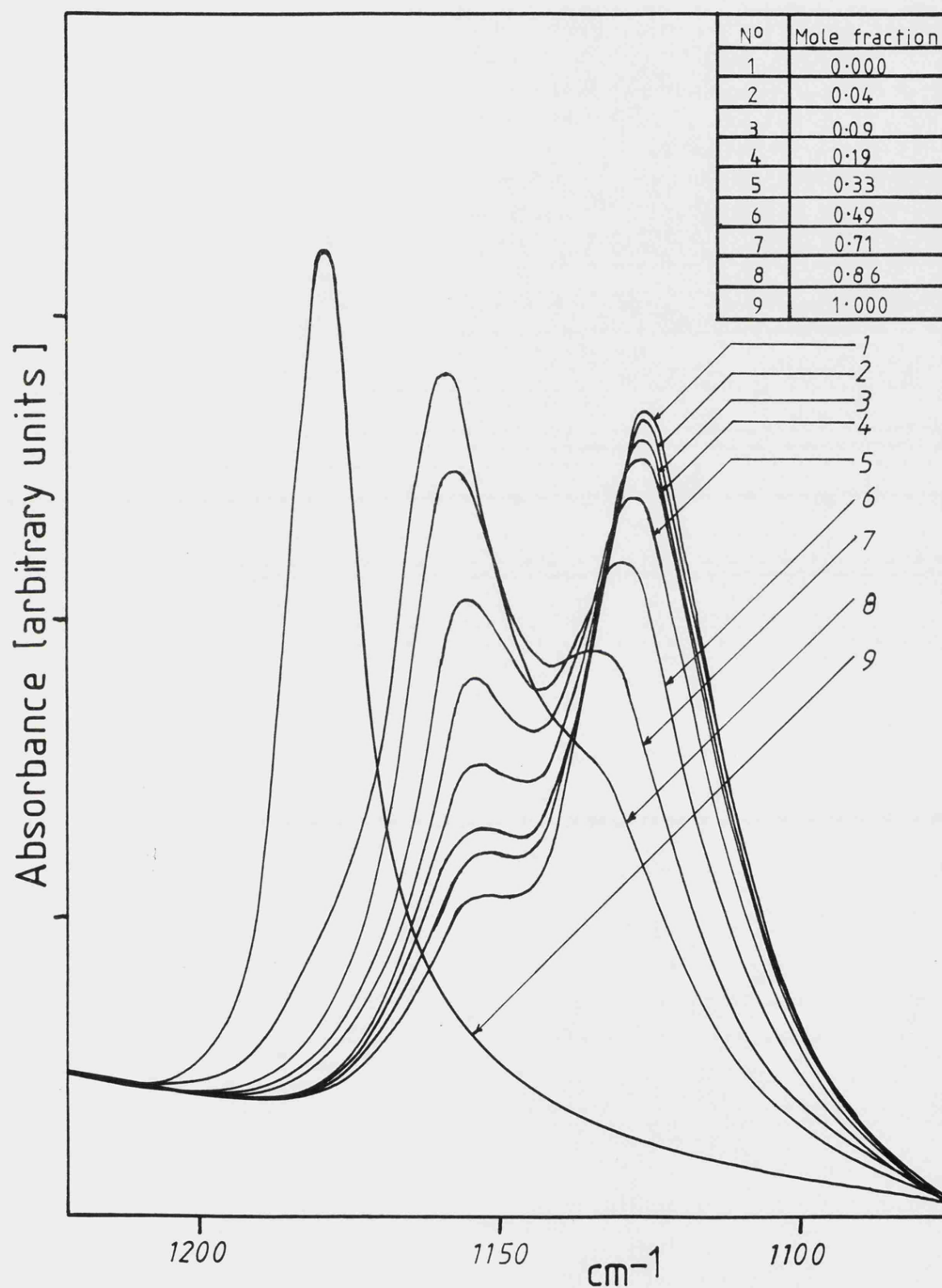| № | Mole fraction |
|---|---|
| 1 | 0:000 |
| 2 | 0·07 |
| 3 | 0·13 |
| 4 | 0·27 |
| 5 | 0·43 |
| 6 | 0·61 |
| 7 | 0·79 |
| 8 | 0·89 |
| 9 | 0·97 |
| 10 | 1·000 |

Spectra showing P=O stretch of triethylphosphine oxide
in various mixtures of Methanol to Cyanomethane.

# Figure 4.4



| No | Mole fraction |
|----|---------------|
| 1  | 0·000         |
| 2  | 0·06          |
| 3  | 0·12          |
| 4  | 0·23          |
| 5  | 0·36          |
| 6  | 0·56          |
| 7  | 0·74          |
| 8  | 0·85          |
| 9  | 1·000         |

Absorbance [arbitrary units]

1200    1150    cm−1    1100

Spectra showing P═O stretch of triethylphosphine oxide
in various mixtures of Methanol to Dimethylsulphoxide.

# Figure   4.5



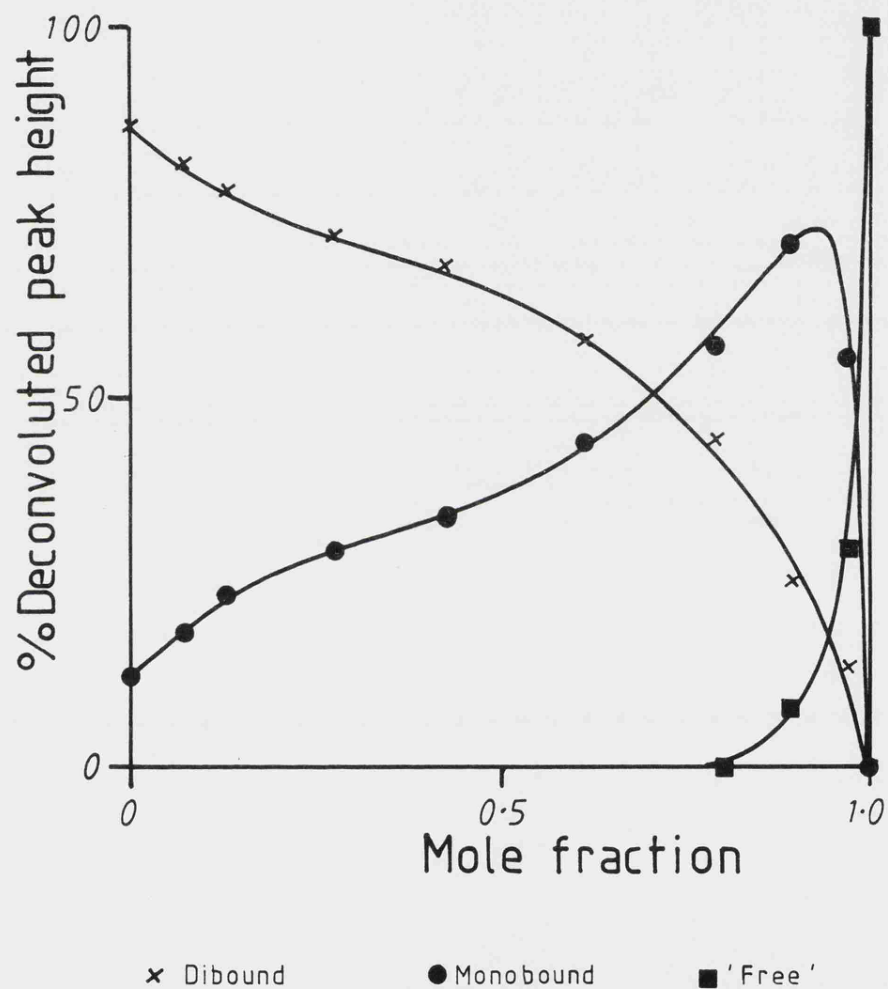| Nº | Mole fraction |
|----|---------------|
| 1  | 0·000 |
| 2  | 0·04 |
| 3  | 0·09 |
| 4  | 0·19 |
| 5  | 0·33 |
| 6  | 0·49 |
| 7  | 0·71 |
| 8  | 0·86 |
| 9  | 1·000 |

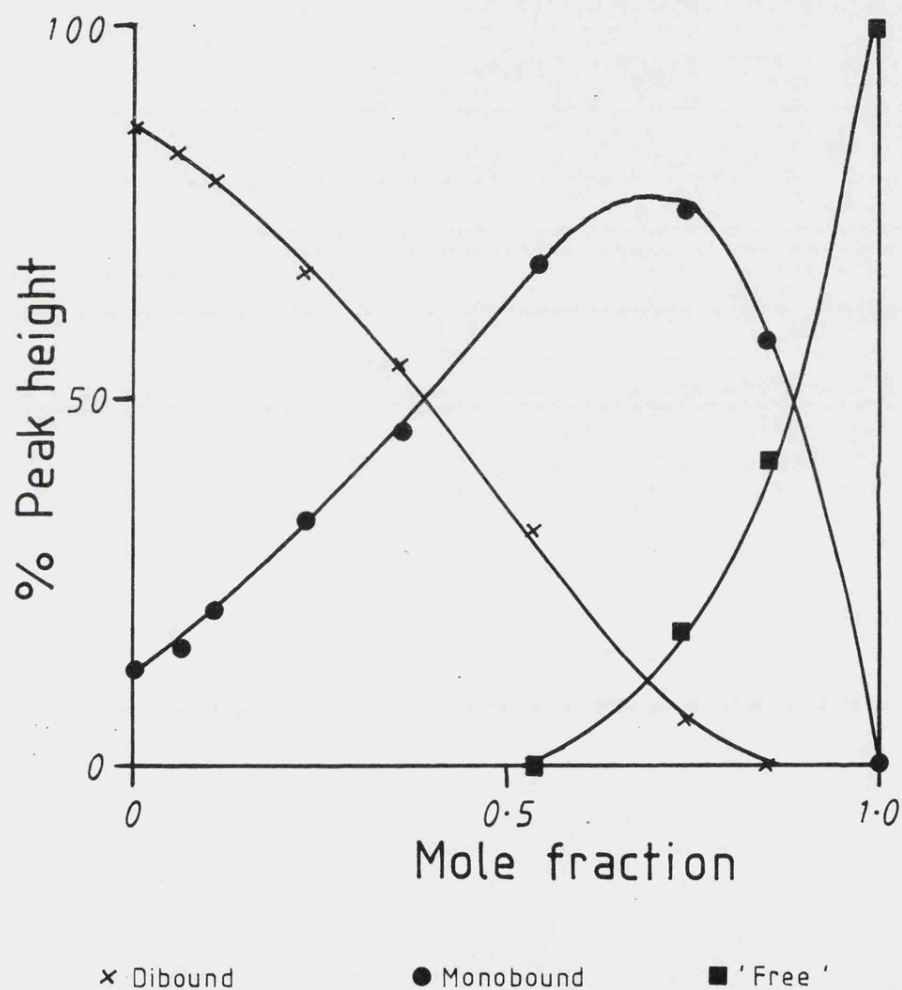Spectra showing P==O stretch of triethylphosphine oxide in various mixtures of Methanol to Tetrahydrofuran.

# Figure .4.6
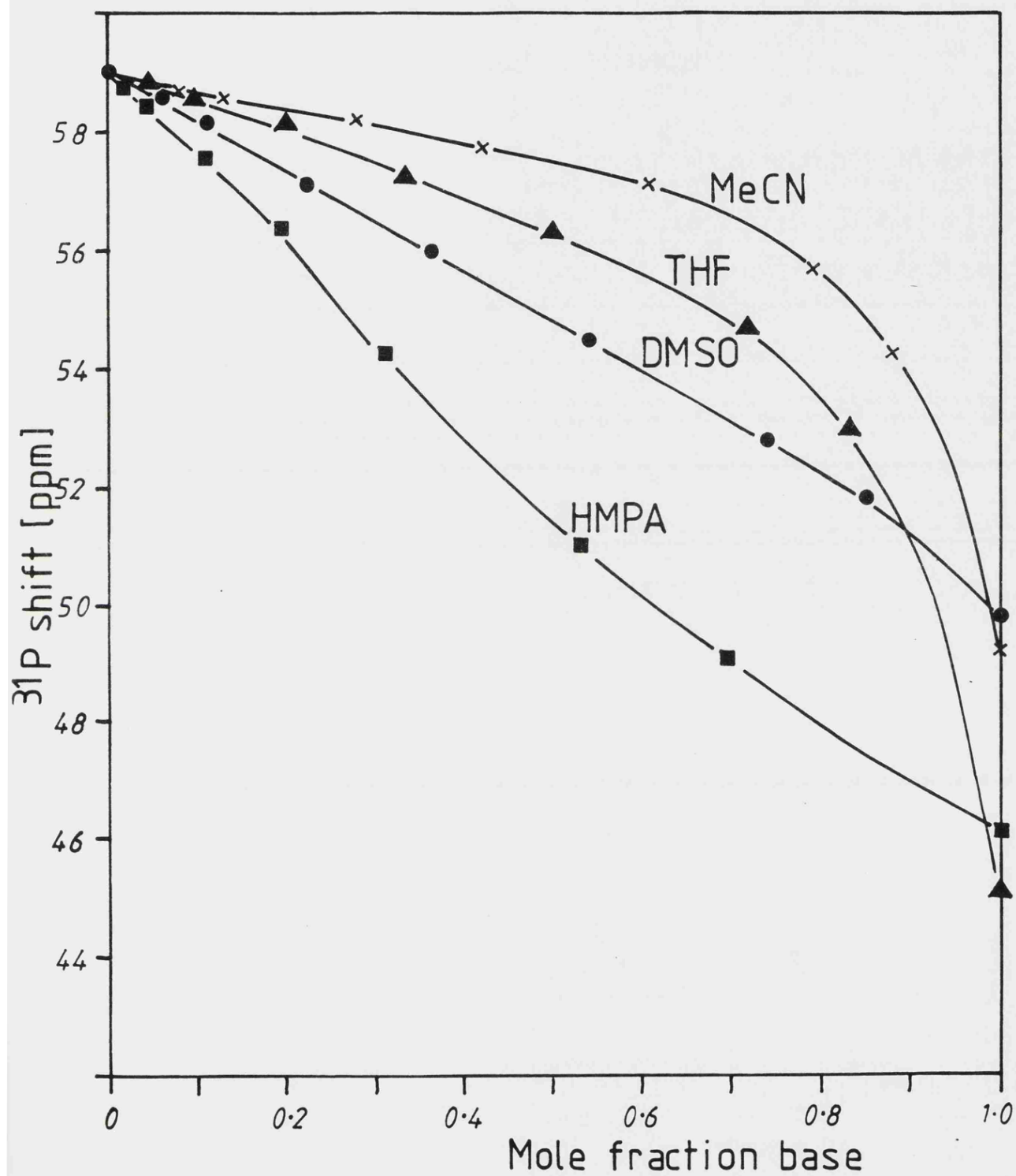


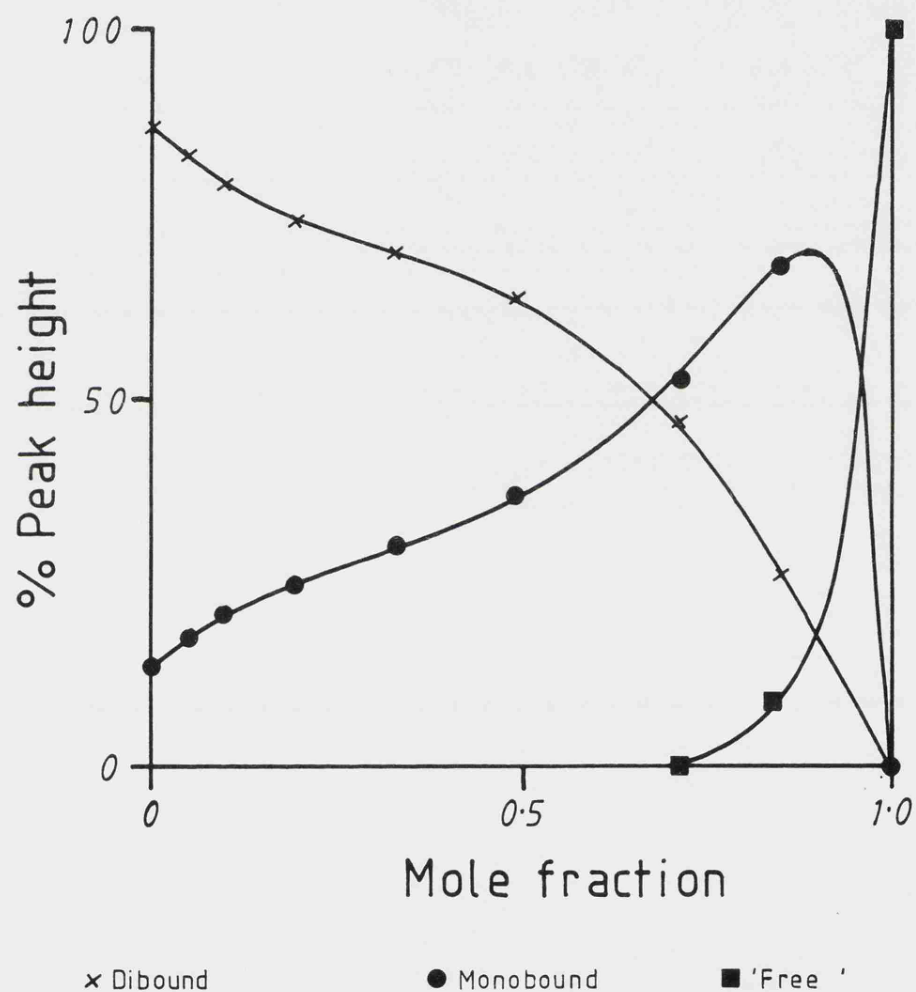$^{31}P$ shifts of triethylphosphine oxide in mixtures of methanol with base. $^{31}P$ relative to $H_3PO_4$.

# Figure 4.7



Deconvoluted bands, peak height shown as a percentage of maximum. $\nu_{max}$ P=O stretch of $Et_3PO$ in a mixture MeOH → MeCN.

# Figure 4.8



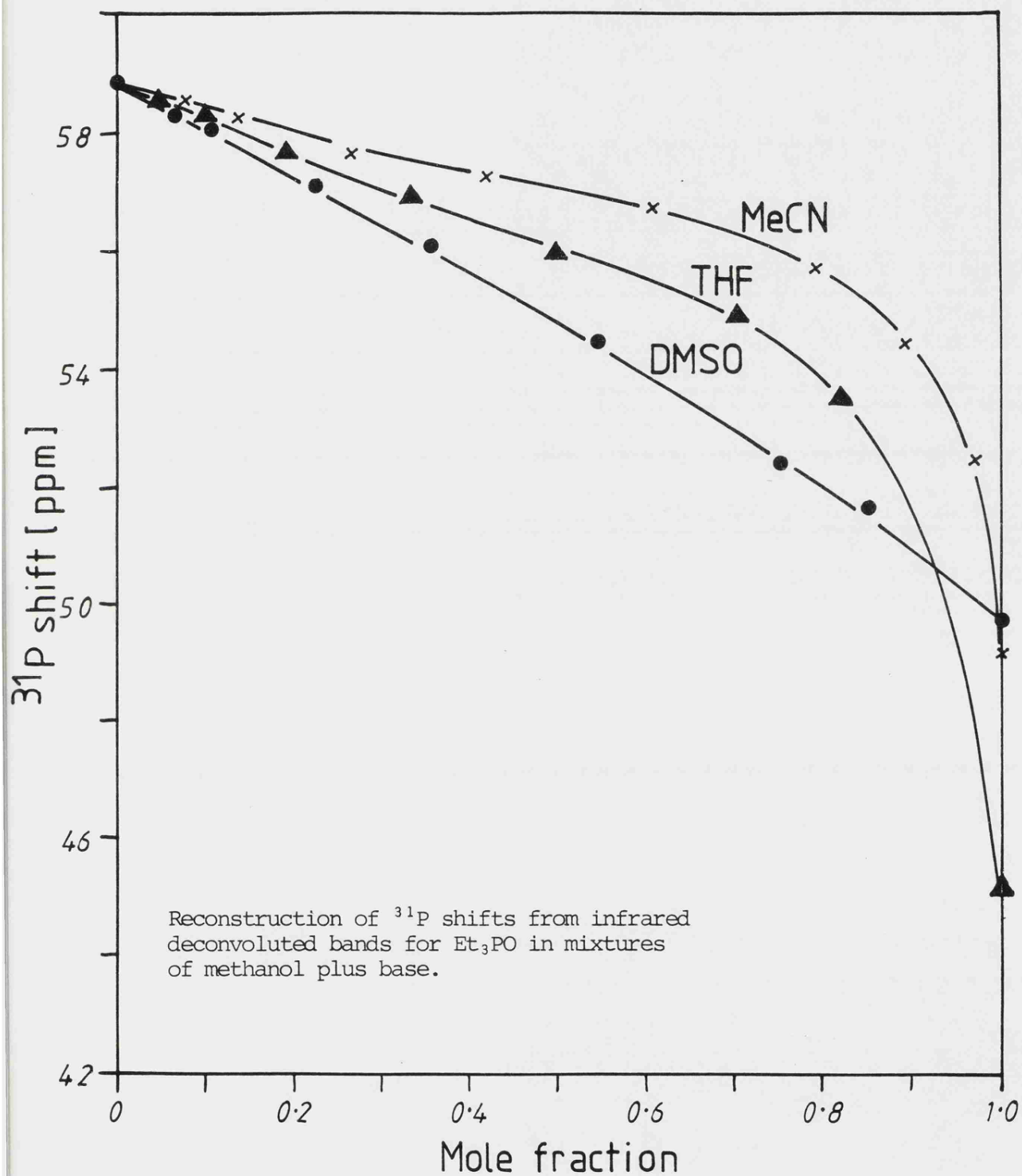Deconvoluted bands, peak height shown as a percentage of maximum. $\nu_{max}$P$\equiv$O stretch of Et$_3$PO in a mixture MeOH → DMSO.

# Figure 4.9



Deconvoluted bands, peak height shown as a percentage
of maximum. $\nu_{max}$P$=$O stretch of Et$_3$PO in a mixture
MeOH → THF.

# Figure   4 .10



Reconstruction of $^{31}P$ shifts from infrared
deconvoluted bands for $Et_3PO$ in mixtures
of methanol plus base.

-62-

$$B + Et_3PO(MeOH)_2 \rightleftharpoons B(MeOH) + Et_3PO(MeOH) \qquad \ldots. (3)$$
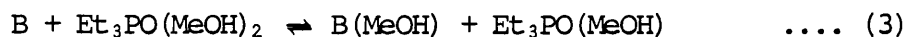
Because equation (1) is strongly to the right it is unlikely that in a methanol-rich system any base is free to participate in equation (3). Whereas $(lp)_{free}$ groups are readily available. Any initial removal of methanol from the probe would occur therefore as equation (2). The amount of $(lp)_{free}$ would be determined by the basicity of the base added.

However, as the mole fraction of added base increases direct attack by base will become more likely as in equation (3).

It must be realised, however, that basicity for a given base in water is different from that in alcohol. Water has an excess of OH free so allowing full solvation of the base. Alcohol, however, requires the base itself to break up the alcohol chains and so, depending upon the strength of the base, the solvation will be only partial. The basicity of DMSO, therefore, is 2 in water but probably only 1 in methanol.

By transposing the various bands corresponding to 'Di', 'Mono' and 'free', into $^{31}P$ shifts using Fig. 2, it was possible to reconstruct the n.m.r. shift vs mole fraction curves for each base (Fig. 10). A comparison of these curves with those of Figure 6 shows excellent quantitative agreement. This is believed to be the first time that infrared spectra have been used successfully to interpret n.m.r. results. Previous work at this laboratory [5] had been partially successful but agreement was only qualitative.

b  Water with aprotic bases

Figures 11, 12 and 13 show the effect on the P$=$O stretch of adding various bases to aqueous $Et_3PO$. Figure 14 shows the effect of the same and other bases on the $^{31}P$ shift. Unlike methanol, however, four distinct

bands are observed in the infrared through the mole fraction range, viz. band A observed in pure water, bands B and C that occur irrespective of the base and at positions similar to those for Di and Mono bound methanol, and band D for the pure base, position dependent upon the base. This is interpreted as Tri → Di → Mono → Free in terms of H-bonded species. Further evidence is provided by the deconvoluted infrared bands; over the full mole fraction range, each experimental band envelope can be constructed from combinations of four components which correspond with bands A, B, C and D. Plots of these various deconvoluted bands against mole fraction of added base, can be seen in Figures 15, 16 and 17.
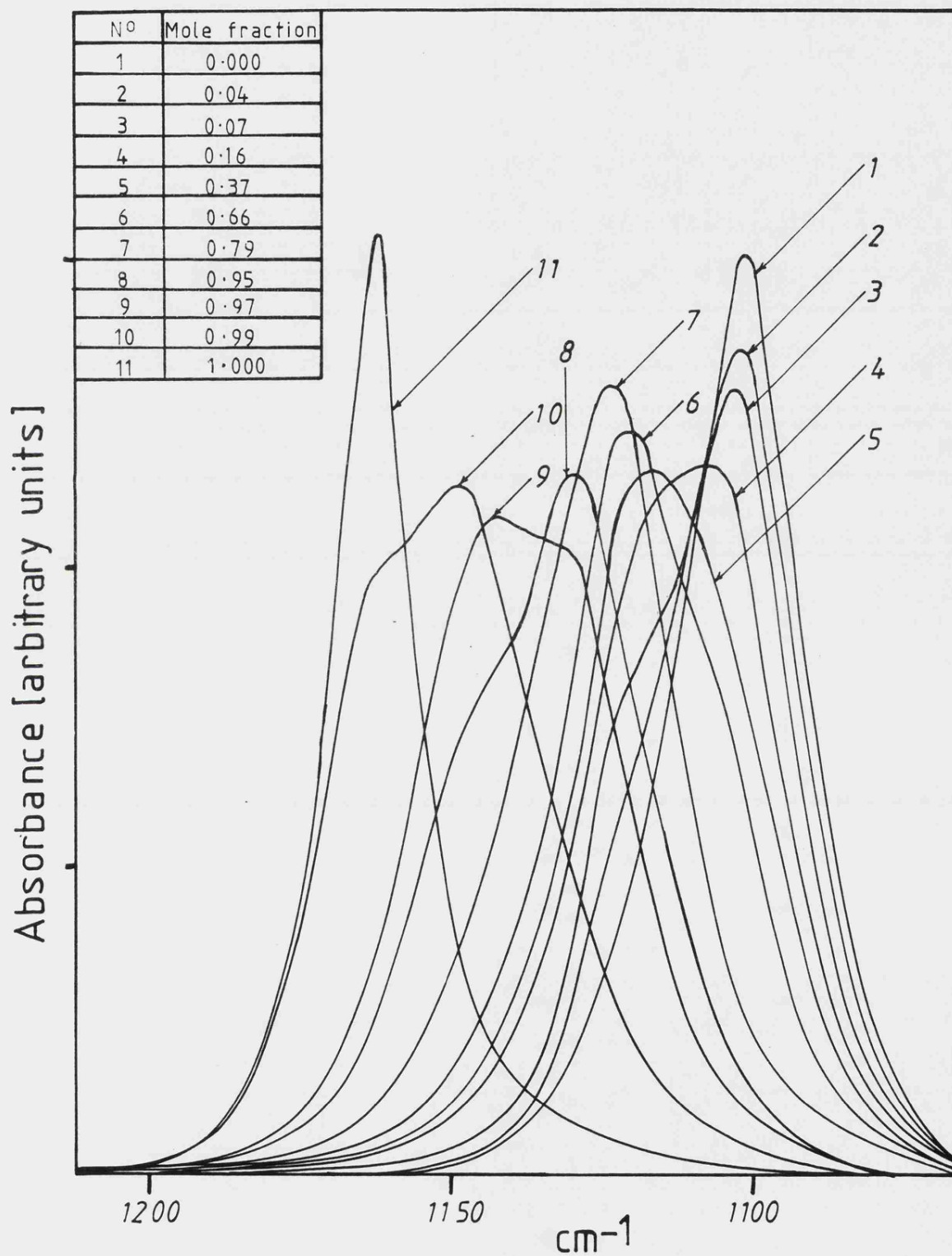
The rate of initial loss of tri-bound solvate with concurrent growth of di-bound solvate occurs to a very similar extent for each base studied. This indicates that desolvation is due to attack by $(lp)_{free}$ groups rather than base itself. We can write:-

$$(H_2O)_{bulk} \rightleftharpoons OH_{free} + lp_{free}$$

$$\Updownarrow + B$$

$$B\text{-----}H\text{—}O + lp_{free} \qquad \dots \text{(4)}$$
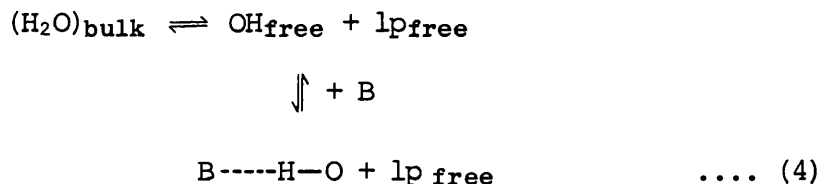
clearly the amount of $(lp)_{free}$ is dependent upon the basicity of B not upon base strength, but it is also buffered by the first part of the equilibrium. Unlike methanol, therefore, there is an excess of $(lp)_{free}$ available whatever the base, so it is not purely a 1:1 or 2:1 situation. The rates of desolvation of probe should therefore be expected to be similar whatever the base.
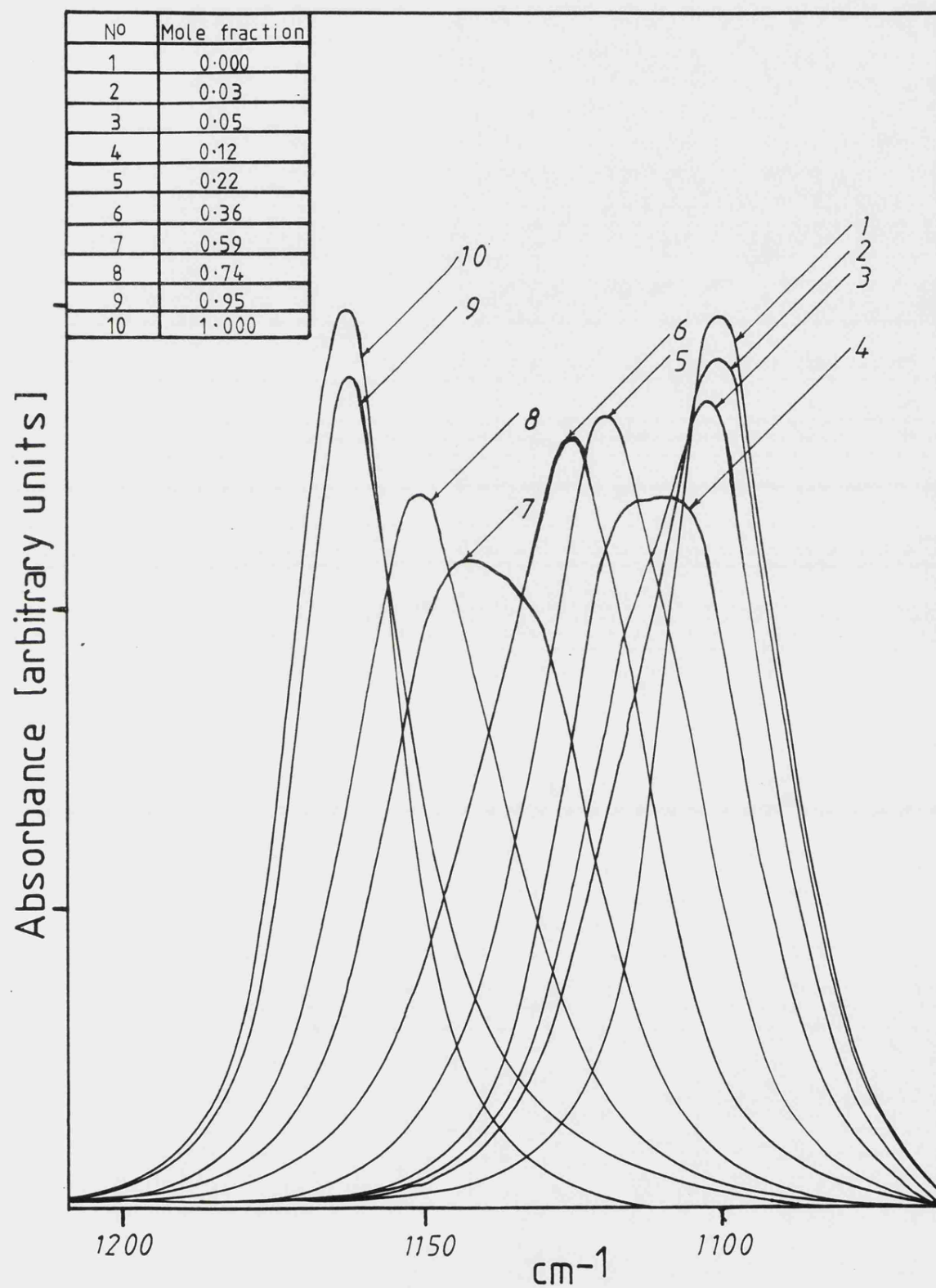
Base strength becomes apparent in the di-bound to mono to 'free' situation. It can be seen that a strong base such as DMSO desolvates the di-bound and produces mono and 'free' states at an earlier position on the mole fraction scale than the weaker bases. In fact for MeCN 'free'
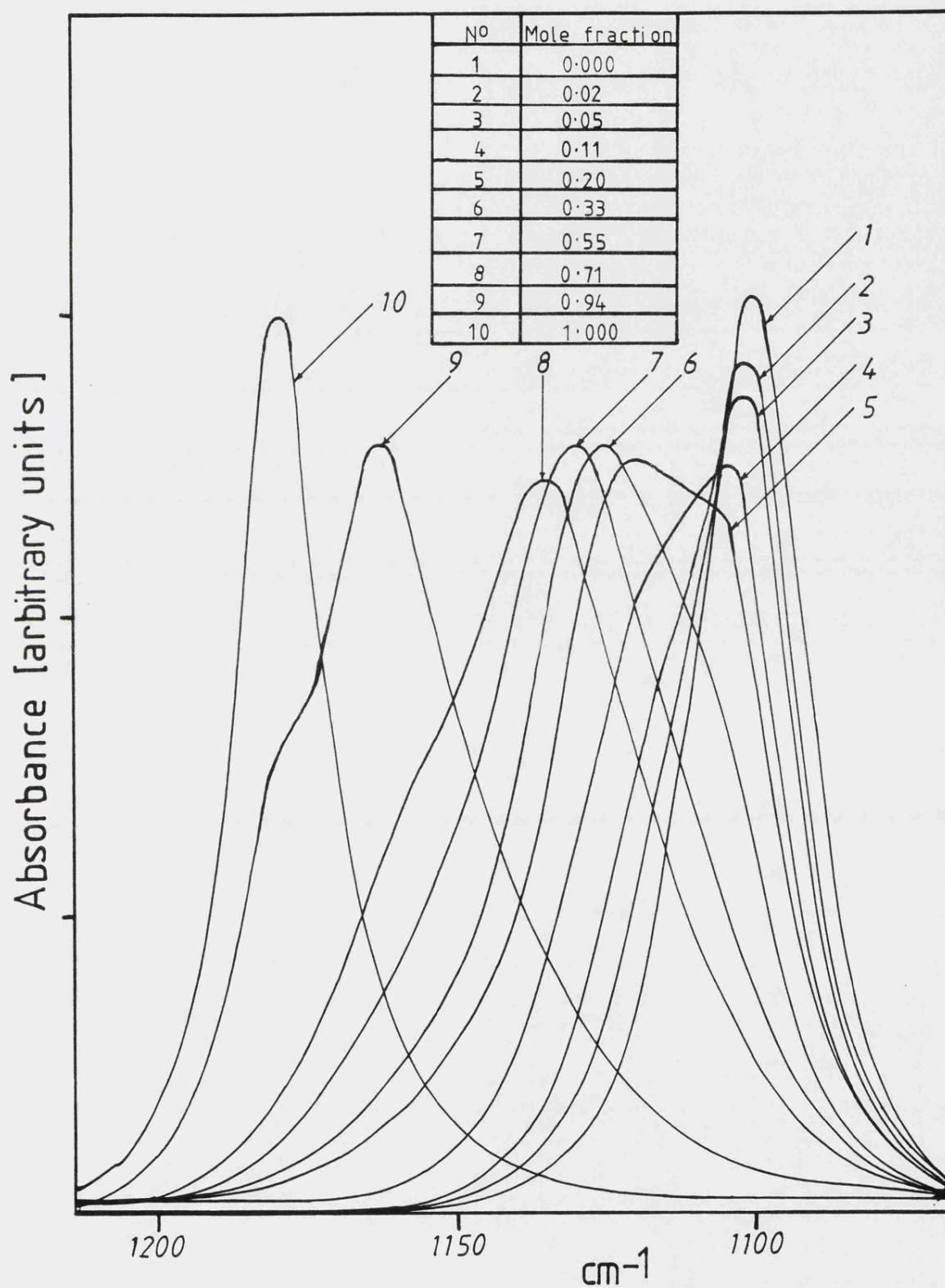
# Figure 4.11



| Nº | Mole fraction |
|----|---------------|
| 1  | 0·000 |
| 2  | 0·04  |
| 3  | 0·07  |
| 4  | 0·16  |
| 5  | 0·37  |
| 6  | 0·66  |
| 7  | 0·79  |
| 8  | 0·95  |
| 9  | 0·97  |
| 10 | 0·99  |
| 11 | 1·000 |

Absorbance [arbitrary units]

cm⁻¹

Spectra showing P═O stretch of triethylphosphine oxide
in various mixtures of Water to Cyanomethane.

# Figure  4.12

| No | Mole fraction |
|----|---------------|
| 1 | 0·000 |
| 2 | 0·03 |
| 3 | 0·05 |
| 4 | 0·12 |
| 5 | 0·22 |
| 6 | 0·36 |
| 7 | 0·59 |
| 8 | 0·74 |
| 9 | 0·95 |
| 10 | 1·000 |

Absorbance [arbitrary units]

1200          1150          1100

cm-1

Spectra showing P═O stretch of triethylphosphine oxide in various mixtures of Water to Dimethylsulphoxide.

**Figure 4.13**

| Nº | Mole fraction |
|----|---------------|
| 1  | 0·000         |
| 2  | 0·02          |
| 3  | 0·05          |
| 4  | 0·11          |
| 5  | 0·20          |
| 6  | 0·33          |
| 7  | 0·55          |
| 8  | 0·71          |
| 9  | 0·94          |
| 10 | 1·000         |

Spectra showing P$=$O stretch of triethylphosphine oxide in various mixtures of Water to Tetrahydrofuran.
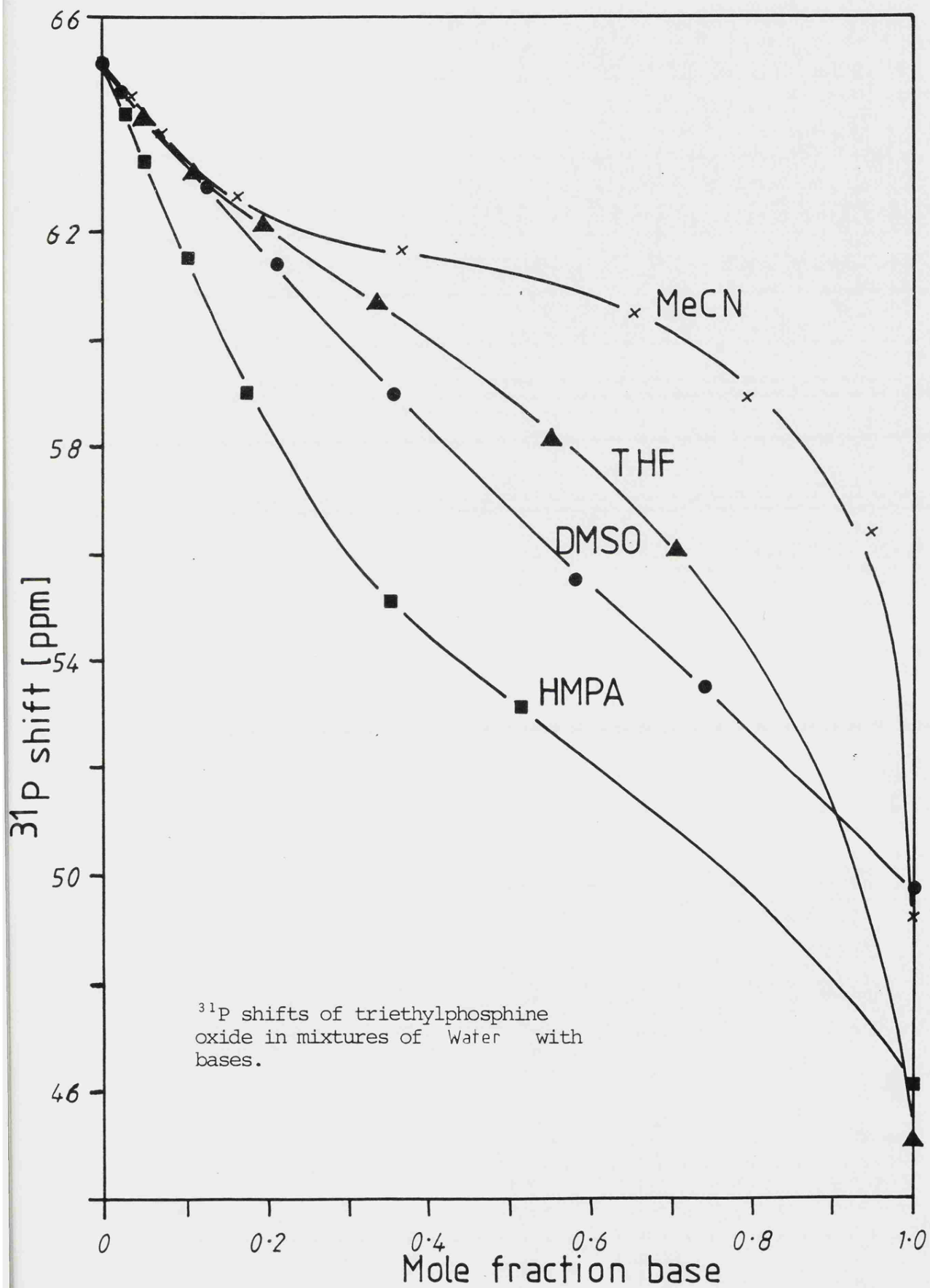
Figure 4.14
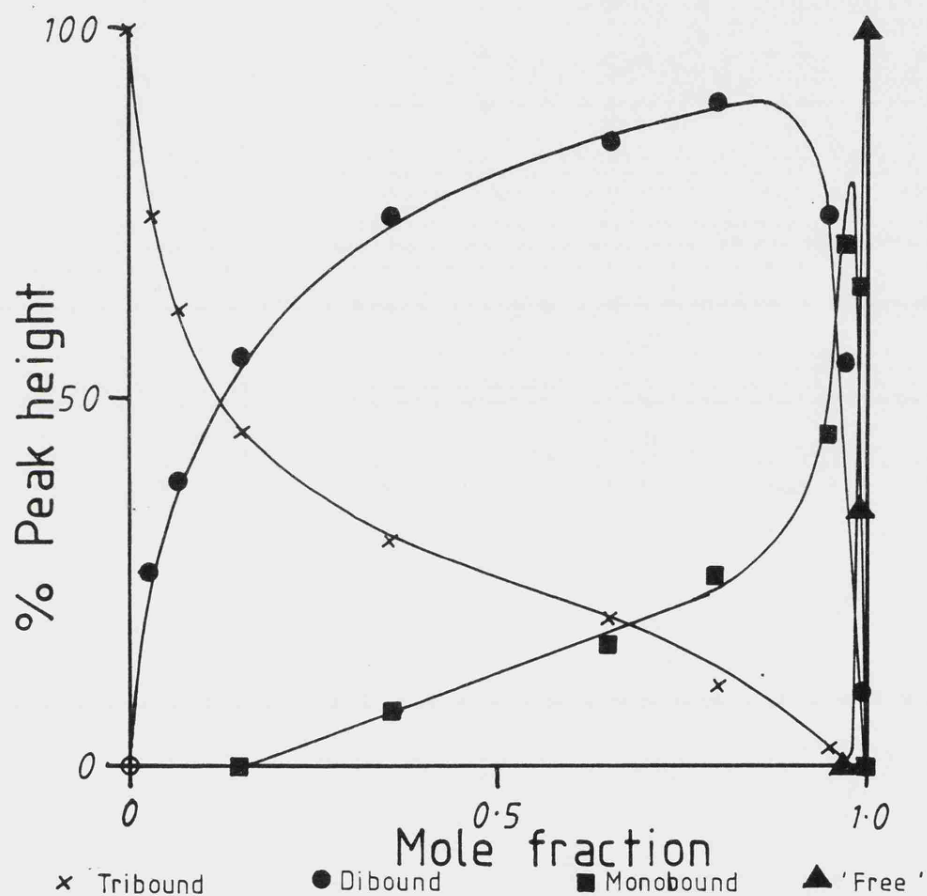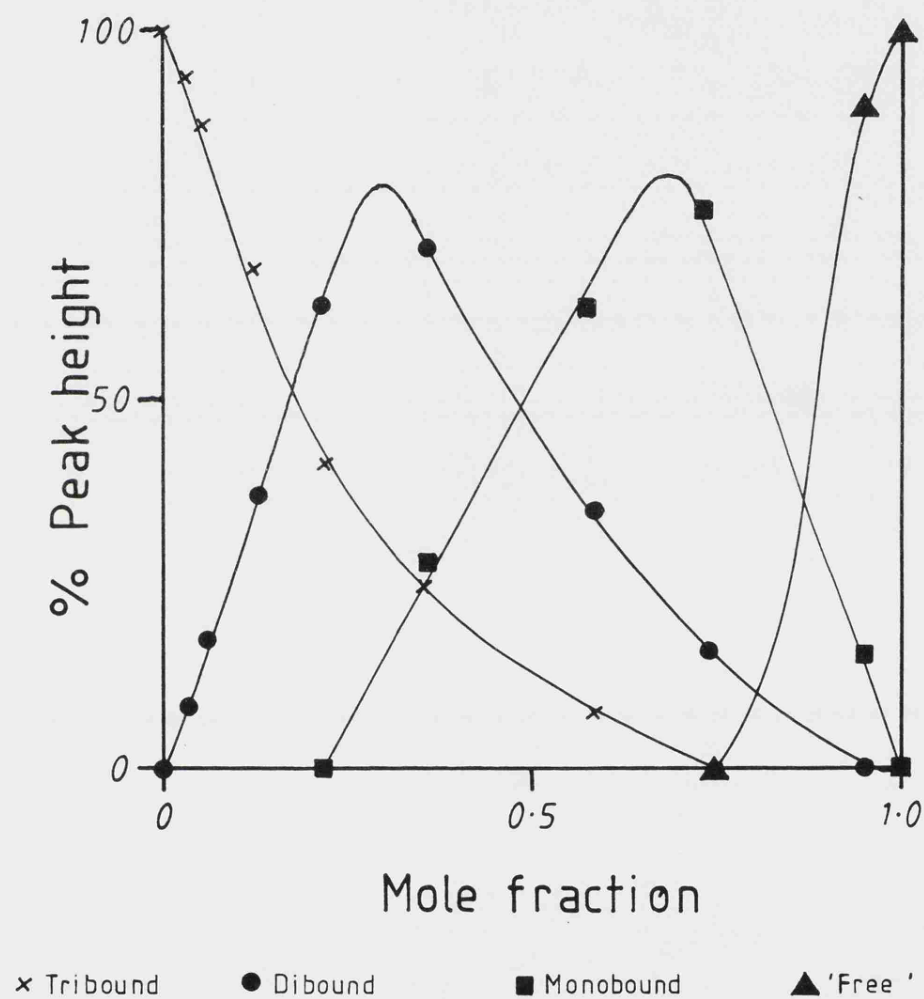
$^{31}$P shifts of triethylphosphine oxide in mixtures of Water with bases.

# Figure    4.15



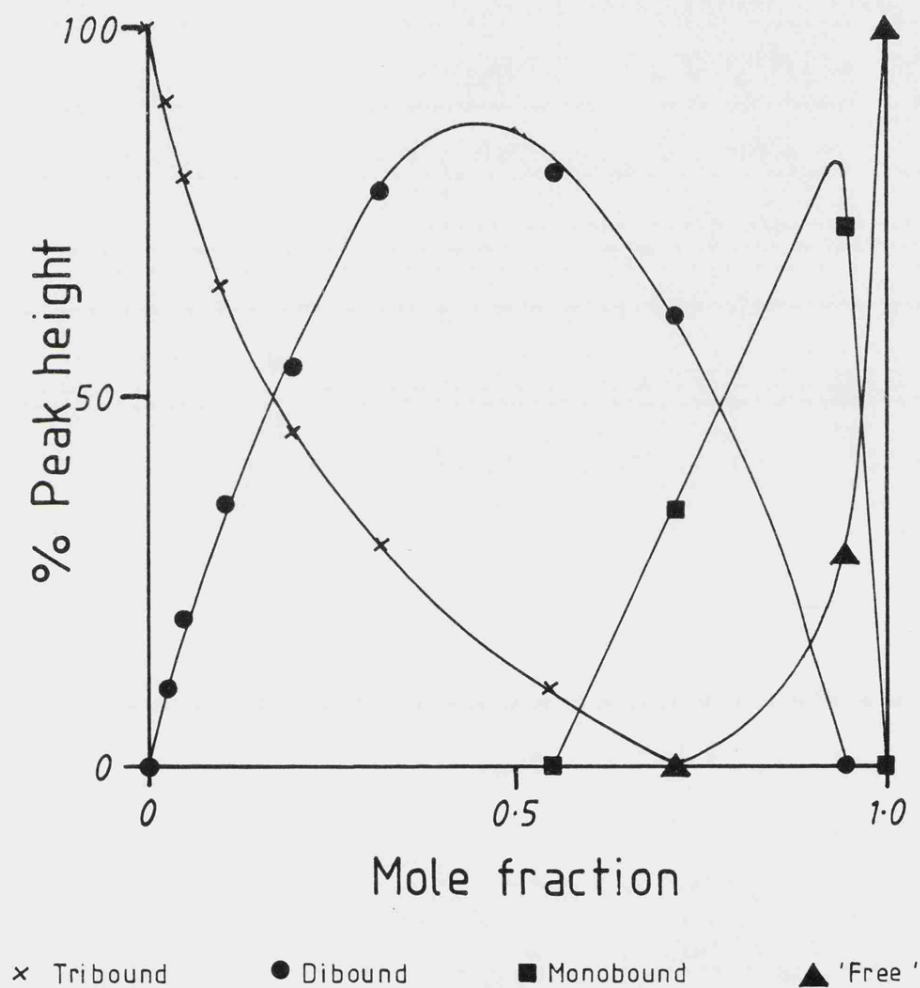Deconvoluted bands, peak height shown as a percentage of maximum. $\nu_{max}$ P≡O stretch of $Et_3PO$ in a mixture $H_2O \rightarrow MeCN$.

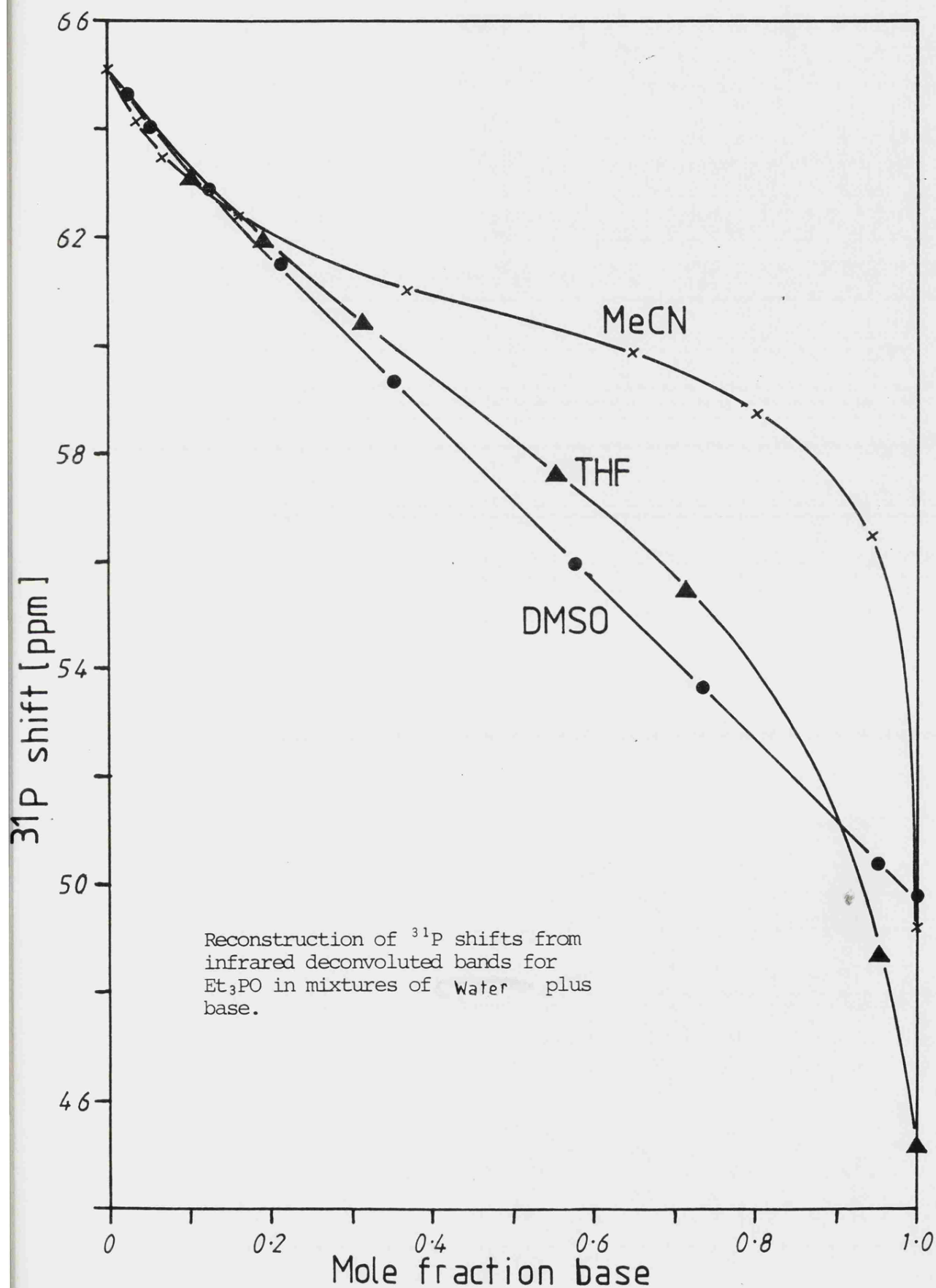# Figure     4.16



Deconvoluted bands, peak height shown as a percentage of maximum. $\nu_{max}$ P$=$O stretch of $Et_3PO$ in a mixture $H_2O \rightarrow$ DMSO.

# Figure 4.17



Deconvoluted bands, peak height shown as a percentage of maximum. $\nu_{max}$ P$\equiv$O stretch of $Et_3PO$ in a mixture $H_2O \rightarrow THF$.

# Figure 4.18



Reconstruction of $^{31}P$ shifts from infrared deconvoluted bands for $Et_3PO$ in mixtures of water plus base.

only becomes apparent at the extreme end of the mixture range with a

mole fraction >0.97 MeCN.

Following a similar procedure to the alcohol case and transposing

'Tri', 'Di', 'Mono' and 'free' states into $^{31}$P shifts, reconstructed

n.m.r./mole fraction curves were produced for each base (Fig. 18). A

comparison of this with Figure 14 shows the same excellent quantitative

agreement vindicating the interpretation used.

c  Trends in band positions

It can be observed from the infrared spectra of the mixed solvent

systems that in addition to the major loss/gain situation there are also

more subtle shifts of the various band maxima taking place. This occurs

in both the aqueous and methanolic systems and can be understood in

terms of loss of tertiary solvation. A series of structures I, II and

III for the methanol case help demonstrate the concept.
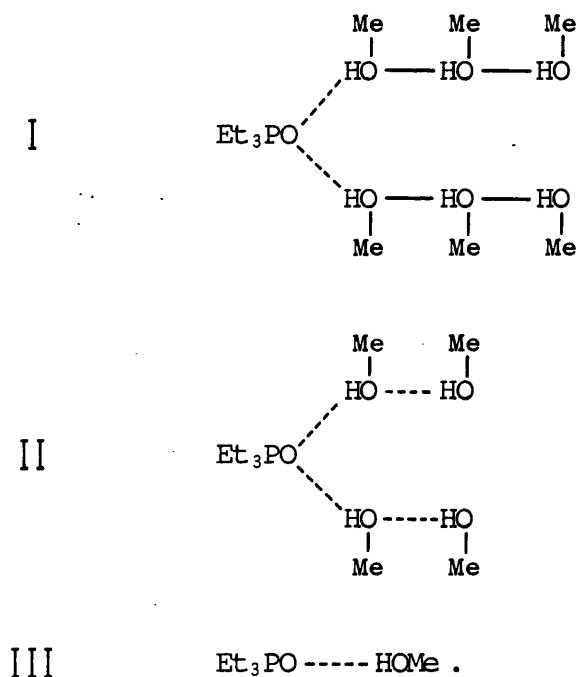


Structure I is the situation for dilute Et$_3$PO in methanol where there are

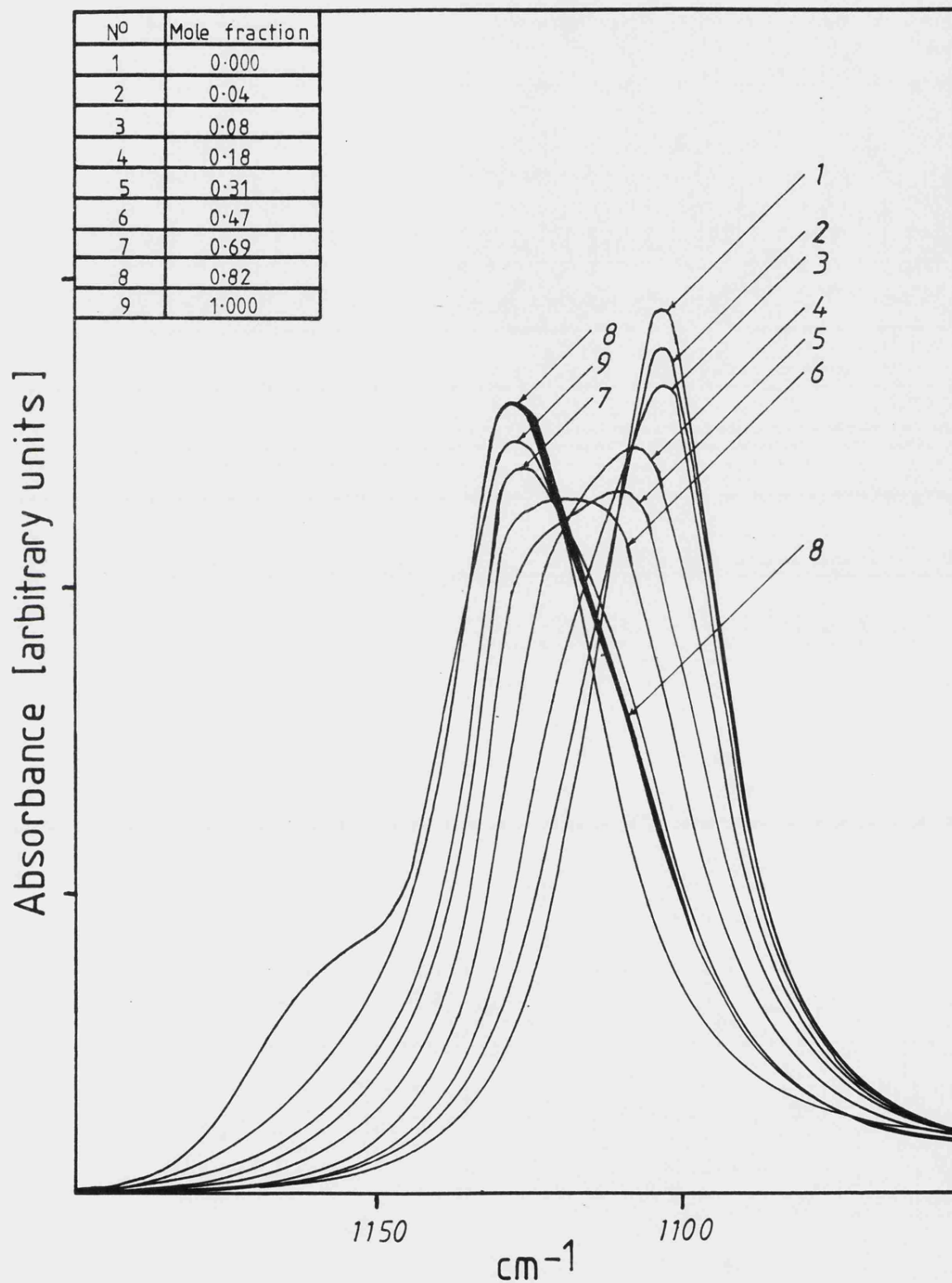mainly di-bound species. Long chains of methanol molecules ensure that

the probe to methanol H-bond is of maximum strength.  By increasing the

concentration of a basic cosolvent we will remove methanol molecules

from the chains so approaching structure II.  This will slightly weaken

the probe-alcohol H-bonds leading to a small shift to high frequency.

This shift will be small compared to that caused by loss of primary

solvation and is unlikely to be resolved.  This process will continue

for disolvate and monosolvate until the limiting solvated structure III

is reached.  The only step left is then to 'free'.  For water the

situation is more complex due to the 3D nature of bulk water H-bonding

but loss of tertiary waters will produce small high frequency shifts in

the same way.  These shifts were incorporated into the reconstruction of

the $^{31}$P shift plots.

d  Water with methanol and other alcohols

Figure 19 shows the change in the P=O stretch band on adding methanol

to aqueous phosphine oxide solution.  The change is uniform resulting in

the loss of the water band and growth of the methanol bands.  A similar

situation was observed for the water plus t-butanol system, Fig. 20.  If,

however, we compare the plots of deconvoluted bands against mole fraction

(Figs. 21, 22) we observe a much greater effect by t-butanol than

methanol in the low mole fraction region.  This is also observed in the

$^{31}$P n.m.r. against mole fraction plot (Fig. 23) where the effects of

ethanol and isopropanol are included.  Several explanations can be

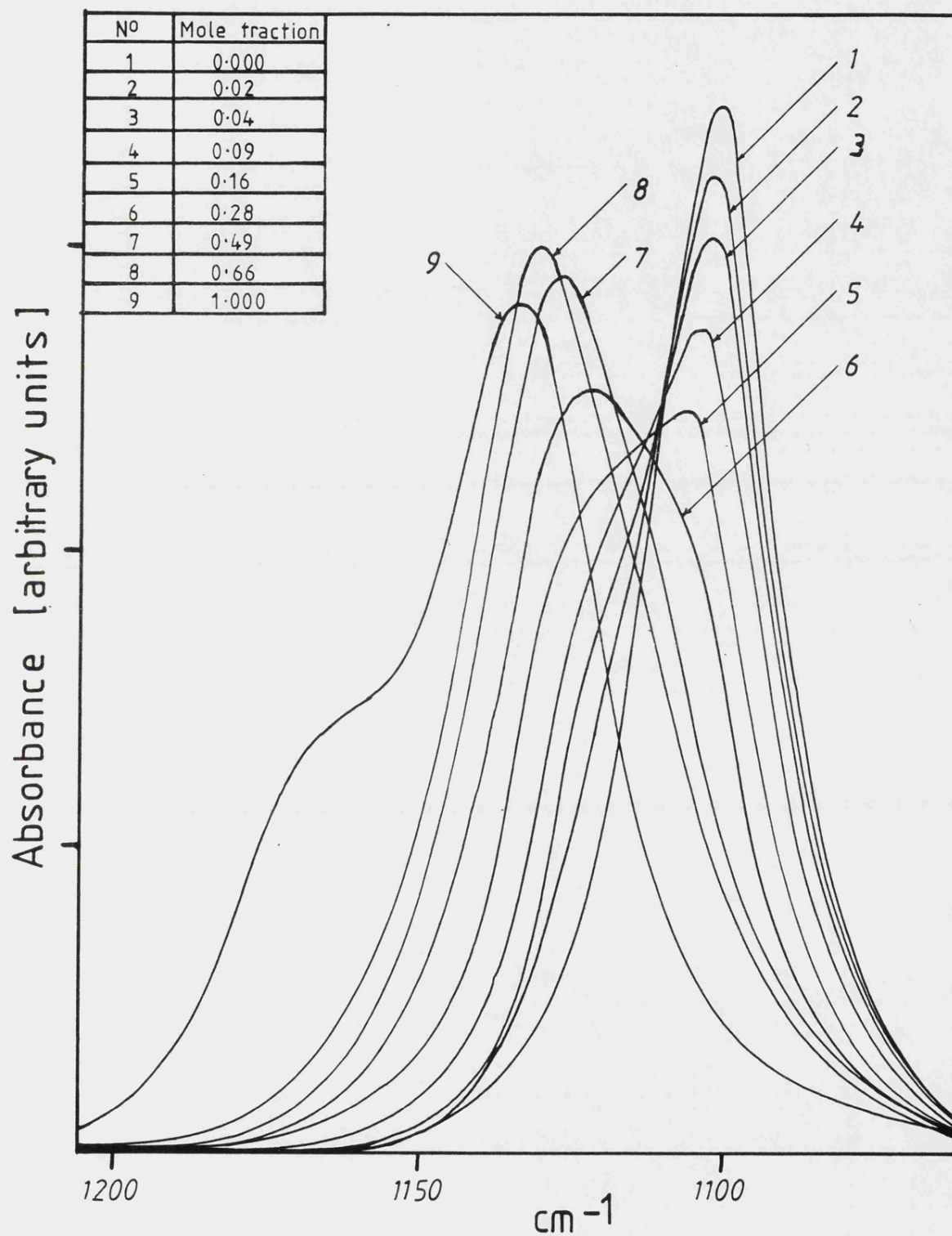proposed for the different rates observed.

A major consideration must be the size of the hydrophobic groups on

the alcohol molecules.  As alcohol is added to water any bulky hydrophobic

group must be accommodated into the water structure.  In the case of t-

butanol, a pseudo-clathrate structure has been previously proposed [6]

where the O-H group is involved in hydrogen bonding and the t-butyl group

# Figure 4.19



| Nº | Mole fraction |
|----|---------------|
| 1 | 0·000 |
| 2 | 0·04 |
| 3 | 0·08 |
| 4 | 0·18 |
| 5 | 0·31 |
| 6 | 0·47 |
| 7 | 0·69 |
| 8 | 0·82 |
| 9 | 1·000 |

Absorbance [arbitrary units]

1150       1100

$cm^{-1}$

Spectra showing $P \equiv O$ stretch of triethylphosphine oxide
in various mixtures of Water to Methanol.

# Figure 4.20



| Nº | Mole fraction |
|----|---------------|
| 1  | 0·000         |
| 2  | 0·02          |
| 3  | 0·04          |
| 4  | 0·09          |
| 5  | 0·16          |
| 6  | 0·28          |
| 7  | 0·49          |
| 8  | 0·66          |
| 9  | 1·000         |

Spectra showing P==O stretch of triethylphosphine oxide
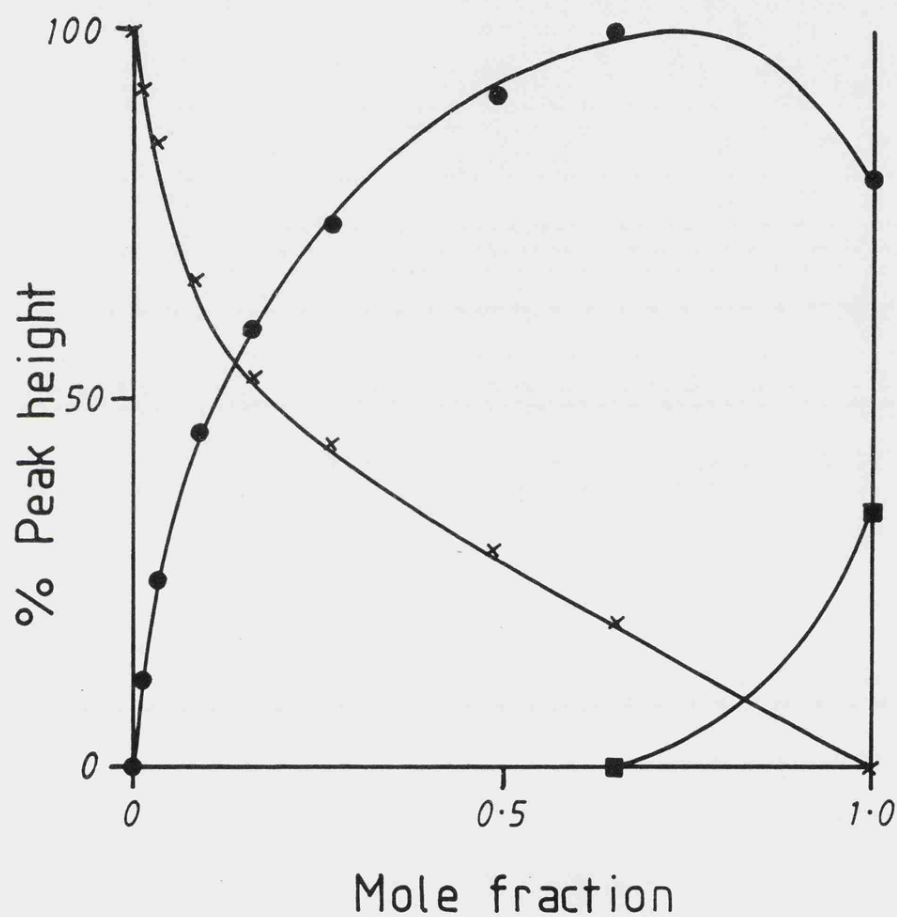in various mixtures of Water to tert. Butanol.

# Figure 4.21
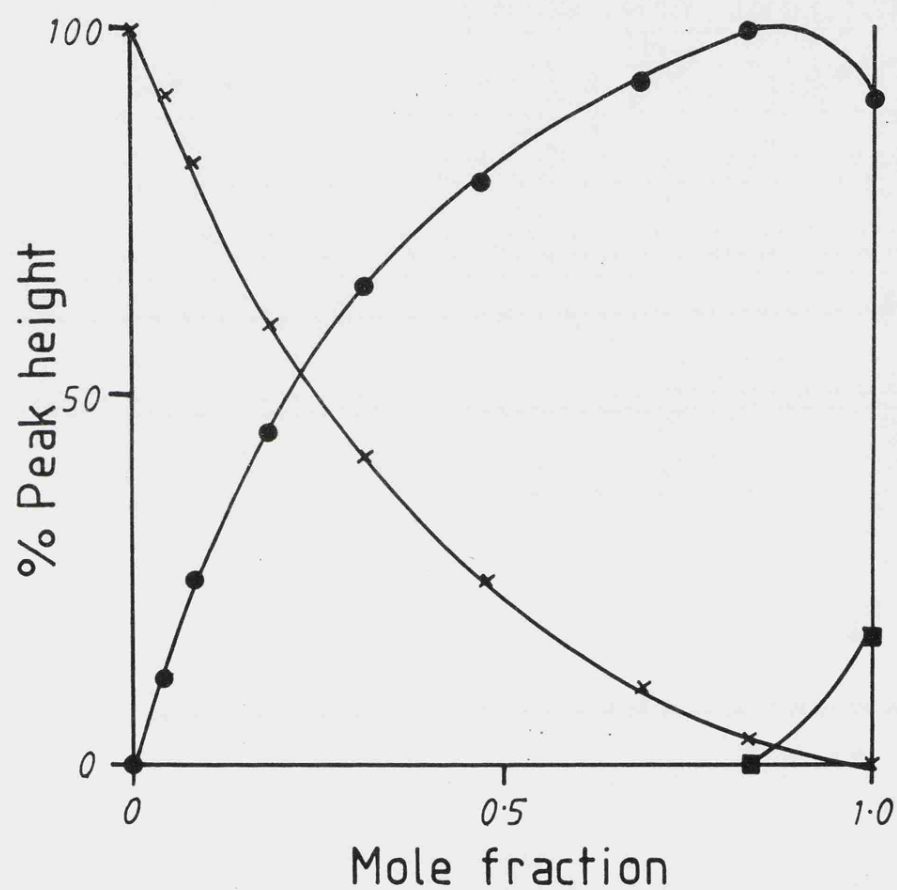


Deconvoluted bands, peak height shown as a percentage of maximum. $\nu P = O$ $Et_3PO$ in a mixture $H_2O \rightarrow MeOH$.

# Figure 4.22



Deconvoluted bands, peak height shown as a
percentage of maximum. $\nu P\!\!=\!\!\!=\!\!O$ $Et_3PO$ in a
mixture $H_2O \rightarrow tBuOH$.

# Figure  4.23



$^{31}P$ shifts of triethylphosphine oxide in mixtures of water with alcohols. $^{31}P$ relative to $H_3PO_4$.

# Figure     4.24



First overtone spectra of OH stretch for different alcohols.

Absorbance [arbitrary units]

MeOH

EtOH

iPrOH

tBuOH

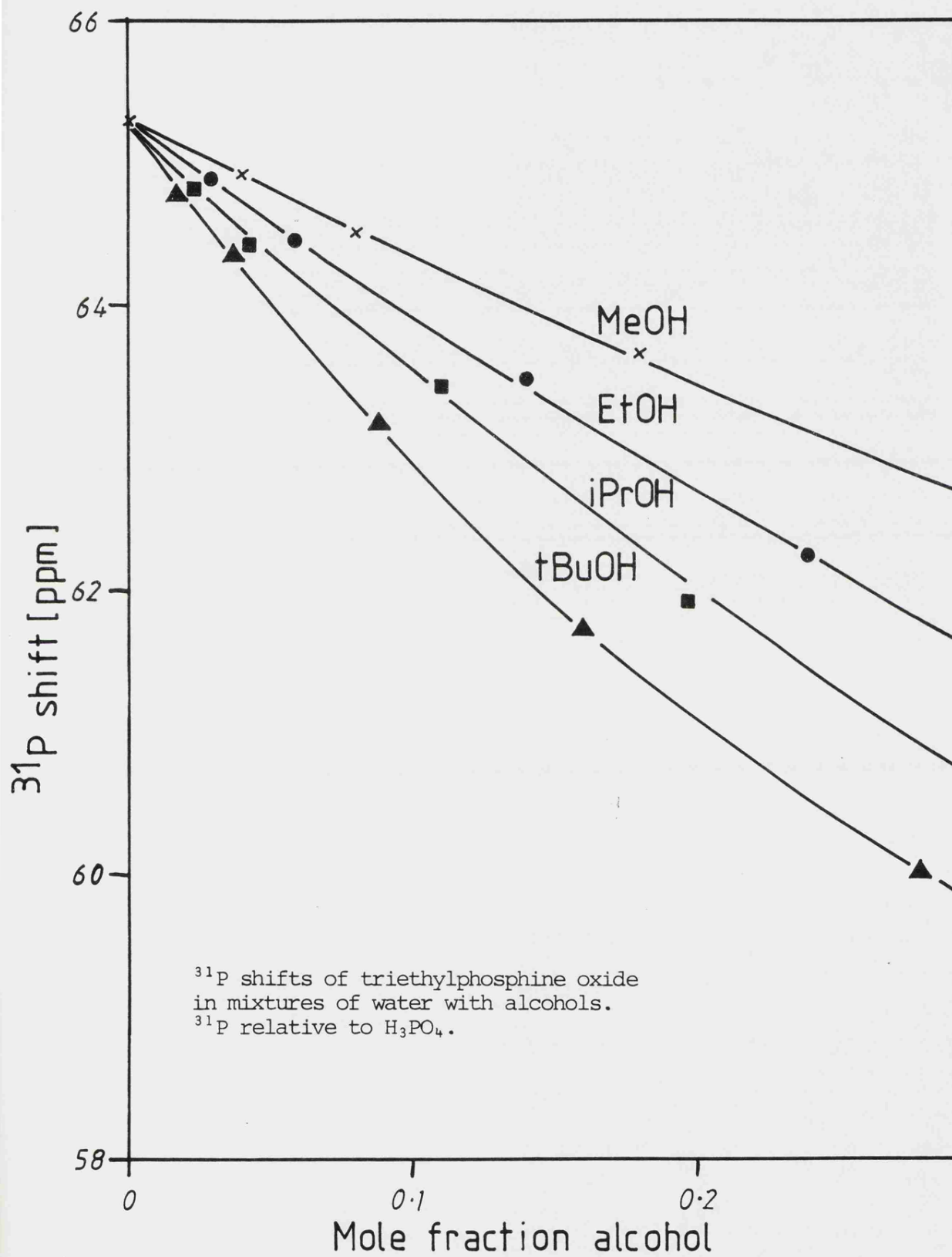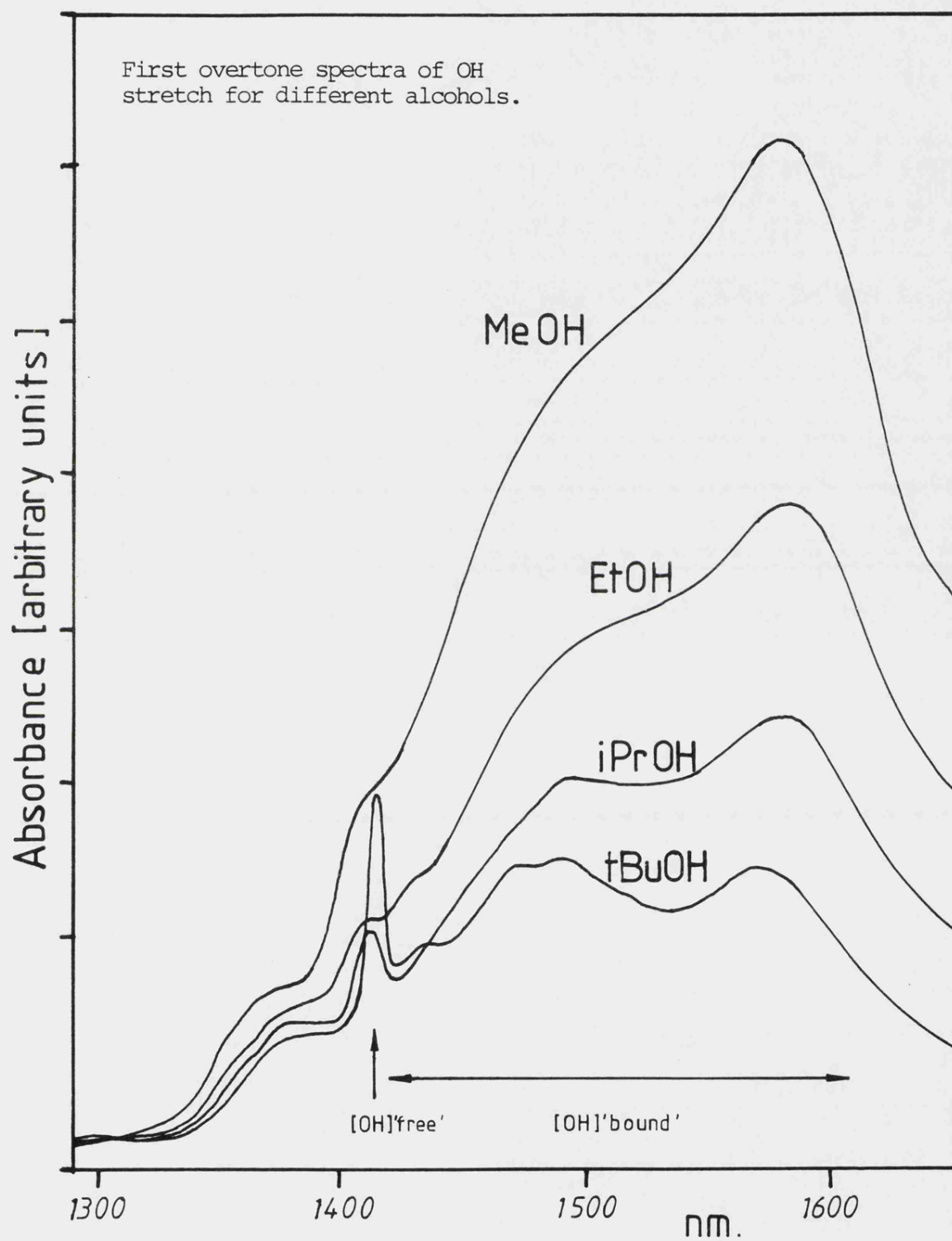[OH]'free'          [OH]'bound'

1300          1400          1500          1600

nm.

is surrounded by a 'cage' of water molecules. This 'structuring' of the water would lead to equilibrium (4) moving to the left and so 'de-solvating' the basic probe.

However, in general, clathrate structures in aqueous systems tend to be very temperature dependent, only being stable at lower temperatures. In the case of the probe system plus t-butanol raising the temperature by over 40.°C produced no effect on the apparent rate of de-solvation.

An alternative approach would be based on the possible difference in basicity/acidity of Methanol and t-Butanol. Any monohydric alcohol has three possible sites for hydrogen bonding, two lone pairs and one acidic proton. For the short chain alcohols in the pure bulk state one lone pair and the proton are involved in hydrogen bonding producing long chain-like structures. This leaves one 'free' lone pair per alcohol molecule, making it an effectively mono-base. On adding alcohol to water the two lone pairs would scavenge two OH (free)'s from the water and the OH from the alcohol would scavenge one lp (free) from the water giving the net effect of a mono-base. If, however, the basicity at the oxygen and/or the acidity of the proton were increased and/or decreased respectively, then the effect would be the same as for a multi-base. There is much evidence to show that for t-Butanol relative to Methanol this situation occurs. t-Butanol is classically a weaker acid than Methanol [e.g. less reactive with metallic sodium] also a spectrum of the first overtone band for O-H stretch of the alcohols (Fig. 24) indicates the large amount of OH (free) groups present in the pure t-Butanol relative to methanol. The trend is for increasing OH (free) Methanol ⟶ Ethanol ⟶ i-Propanol ⟶ t-Butanol. Subsequently, adding t-Butanol to water would result in a lesser scavenging of lp (free) water groups and, there-fore, a greater net increase of lp (free) water groups than for Methanol.

This would produce a greater de-solvating effect on the probe molecule. Temperature should, however, have little effect on this phenomenon, as is the case.

## 4.3  CONCLUDING REMARKS

Triethyl phosphine oxide has proved to be a remarkable probe for the study of solvation.  The relatively large spectroscopic shift of the $P=O$ stretching band have enabled a full comparison with n.m.r. data. The interpretation of the various solvated states of this probe in alcohols and water has given valuable insight into the respective structures.  This also allows a link to be made between solvent structure and the various scales of solvent polarity, etc.  This is discussed further in Chapter 7.

## REFERENCES FOR CHAPTER 4

1.  V. Gutmann, "The Donor-Acceptor approach to Molecular Interactions", Plenum Press, New York, 1978.

2.  M. C. R. Symons and G. Eaton, J. Chem. Soc., Faraday Trans. 1, (1982) 78.

3.  L. J. Bellamy, "The Infrared Spectra of Complex Molecules", Vol. II, Chapman & Hall, 1980.

4.  M. C. R. Symons, T. A. Shippey and P. P. Rastogi, J. Chem. Soc., Faraday Trans. 1, (1980) 76.

5.  V. K. Thomas, Ph.D. Thesis, University of Leicester (1980).

6.  M. C. R. Symons and M. J. Blandamer, "Hydrogen-Bonded Solvent Systems", (ed. A. K. Covington and P. Jones), Taylor & Francis, London, 1968.

# CHAPTER 5

SIMPLE AMIDES – PROBE STUDIES

## 5.1   INTRODUCTION

The use of a carbonyl compound (acetone) as a probe molecule was demonstrated in Chapter 3.   It was desirable to extend this use of probe molecules and amides offered several interesting features in the context of our solvation studies.

Amides as a class of compounds are very important in that they can be considered to constitute a large percentage of biological systems through the polypeptide chains.   The carbonyl group in amide compounds can be considered as a base and, as such, should be akin to ketones in their behaviour in solvent systems.   However, some modification would be expected due to the acidic proton sites found in secondary and primary amides.

Many studies of amides have been undertaken over the years [1-5], usually several amides have been compared with each other as regards to a particular property or a single amide studied within a particular interacting system by several different methods.

Of particular interest is the water-amide system having the greatest similarity to biological situations [6].   N.m.r. has been used extensively to study aqueous amide systems, the results however have generally been interpreted in terms of the 'making' or 'breaking' of water structure [5,7].   By making use of the probe technique using infrared spectroscopy a greater understanding of the solvation involved should be possible.

Work has previously been done within this laboratory both using amides as the acid site in the determination of halide-hydrogen bonded complex equilibrium constants [8] and also investigating the water/amide system directly in the light of $(OH)_{free}$ and $(lp)_{free}$ scavenging [9].   In this study three types of amide were used as probes, ternary, secondary and primary;   as a useful adjunct urea was also given a preliminary investiga-

tion, however the results of this will be mentioned in Chapter 6.


## 5.2  RESULTS AND DISCUSSION

## A  Pure Solvents

The infrared carbonyl stretching frequencies for the various amides studied in the range of solvents are depicted in Fig. 1.  In most cases, for a very dilute solution of the amide, a single symmetric carbonyl band is observed, however for methanolic solutions distinct shoulders are seen.  These bands are easily explained in terms of mono/di solvation as in previous chapters (3 and 4).  One very interesting feature of these schemes is the distinctly enhanced sensitivity of the substituted acetamides over the substituted formamides.  A possible explanation lies in the simple difference between the proton and the methyl group which lay adjacent to the carbonyl.  The methyl group has a significant inductive effect, potentially releasing electrons into the carbonyl, this will allow a greater degree of polarisability of the $>C=O$ bond, hence a more sensitive solvent effect relative to that of the formamides.  This effect is demonstrated very effectively by Figure 2.  The linearity of most of the amide carbonyl stretching frequencies when plotted against the carbonyl stretch for acetone in various solvents, as in Fig. 2, illustrates also that any effects on the $C=O$ stretch due to hydrogen bonding via the N-H protons may be minimal.  However, a truer test of this would be a plot of the carbonyl stretch for the protic amides against the carbonyl stretch for a non-protic amide such as Dimethyl acetamide, this is shown in Figure 3.  Whilst some general scatter is observed the linear trends are followed, further indicating the insensitivity of the carbonyl to any change in the N-H environment.
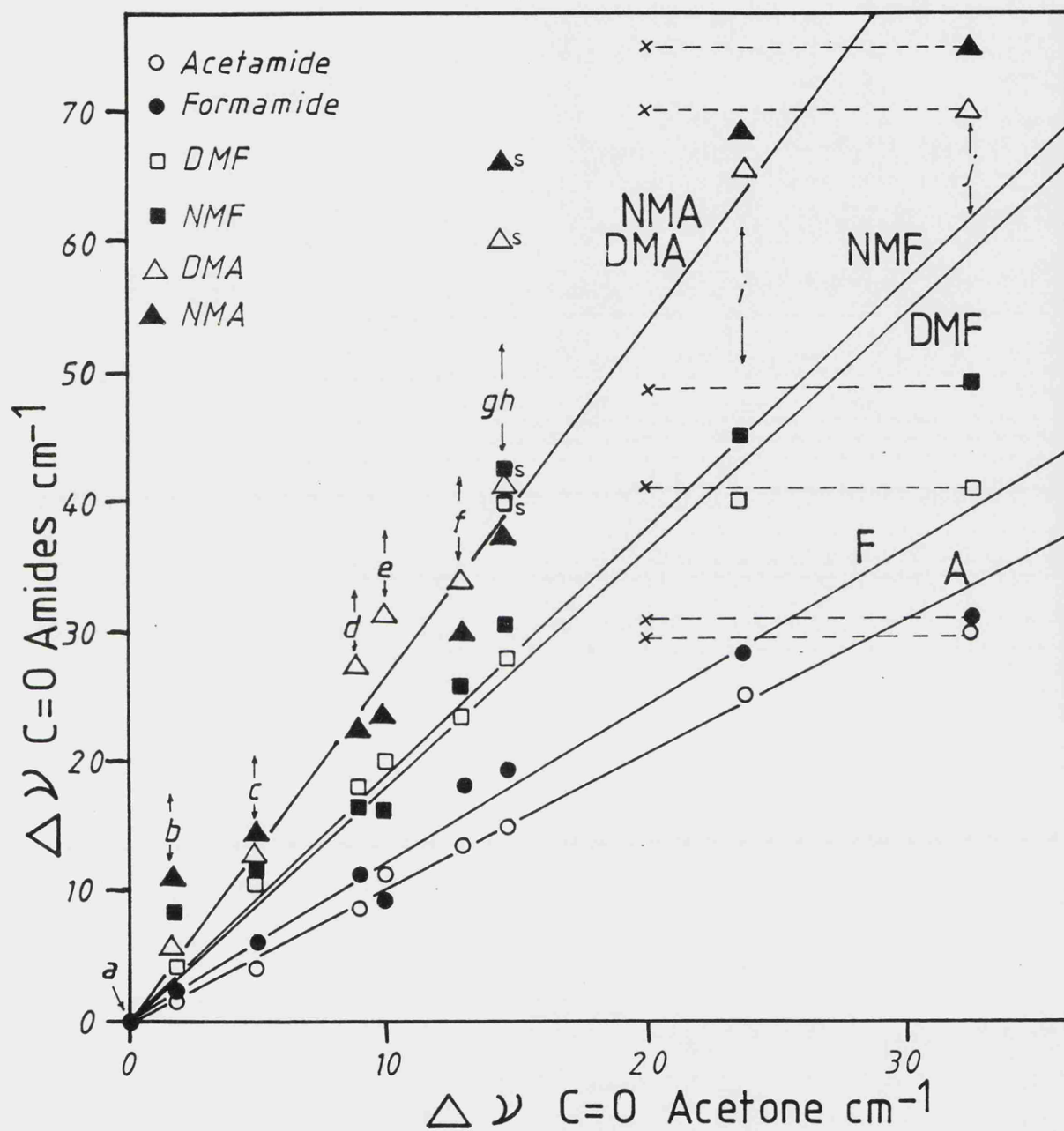
# Figure 5.1

Carbonyl band positions for various amides in solution.



KEY
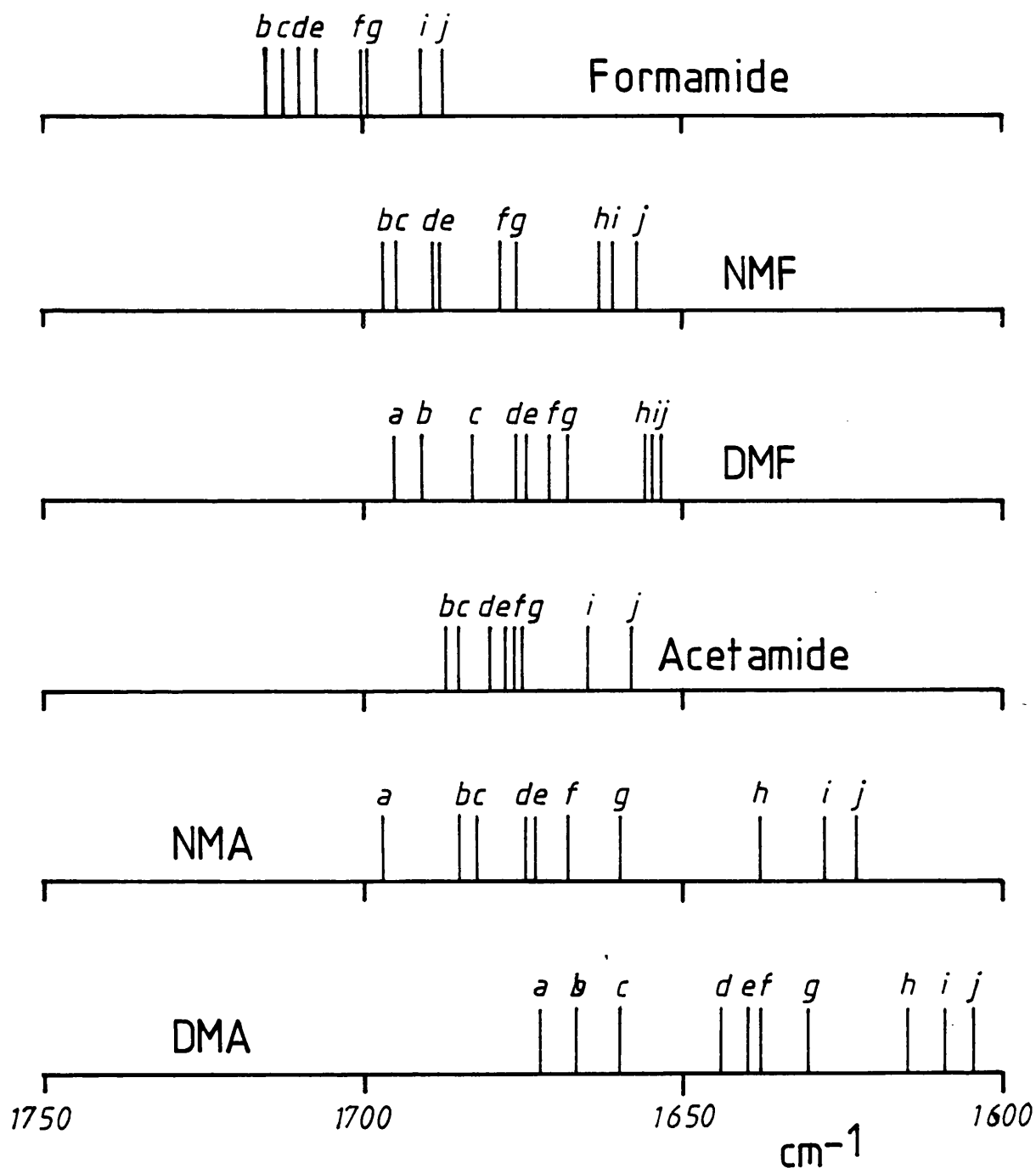
a. Hexane.   b. Triethylamine.   c. Tetrahydrofuran.   d. Cyanomethane.

e. Dichloromethane.   f. Dimethyl sulphoxide.   g/h. Methanol.

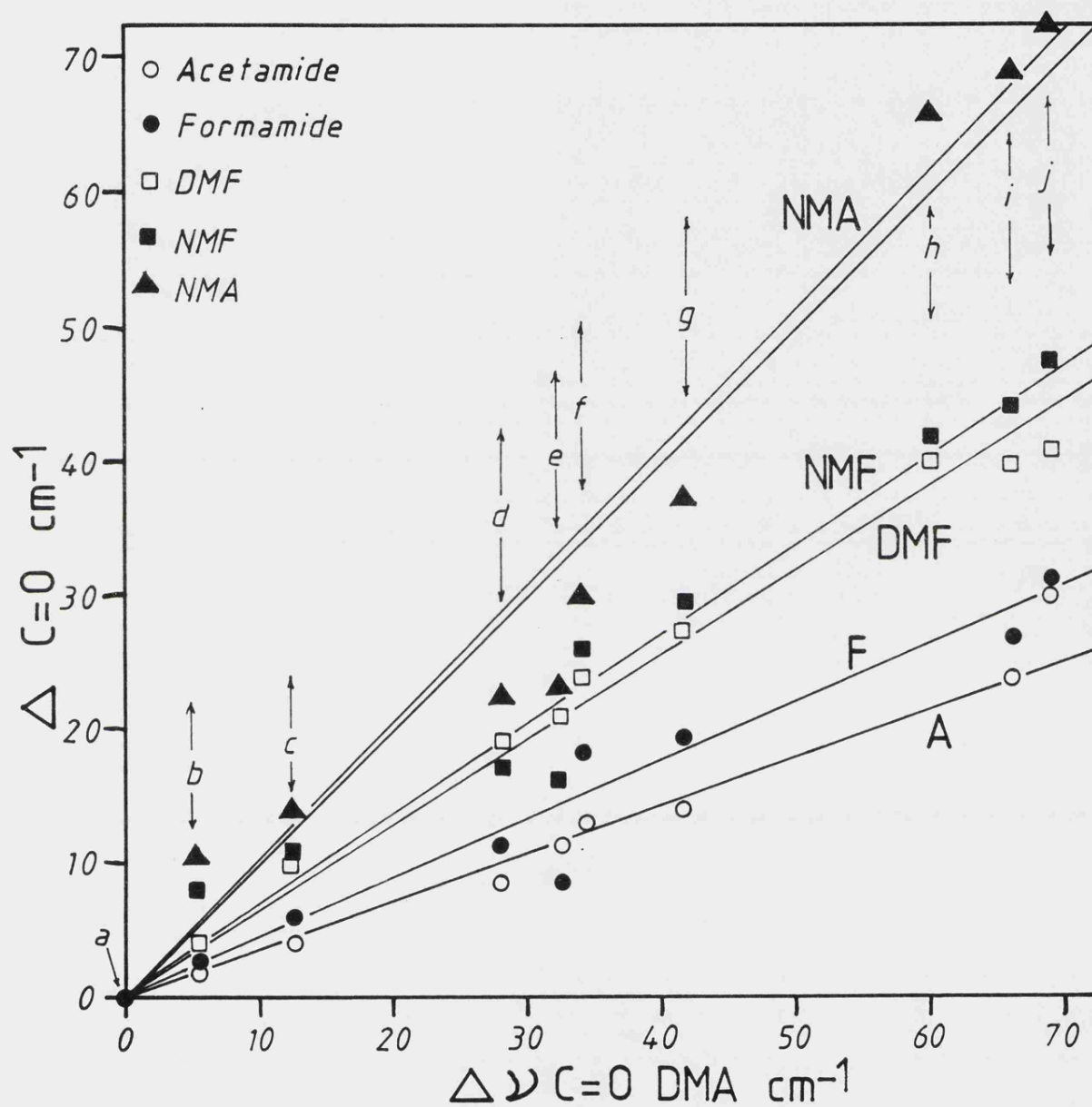i. Water.   j. Hexafluoroisopropanol.

# Figure 5.2



s    Amide shoulder in Methanol

✗--- Acetone   high $\nu$ band in $(CF_3)_2CHOH$

$\nu$ C=O stretch of amides versus $\nu$ C=O stretch
Acetone in various solvents. [Key as Figure
5.1]

# Figure    5.3



ν C=O stretch of various substituted amides
plotted against ν C=O stretch of Dimethyl
acetamide, for solution in various solvents.
[Key as Figure 5.1]

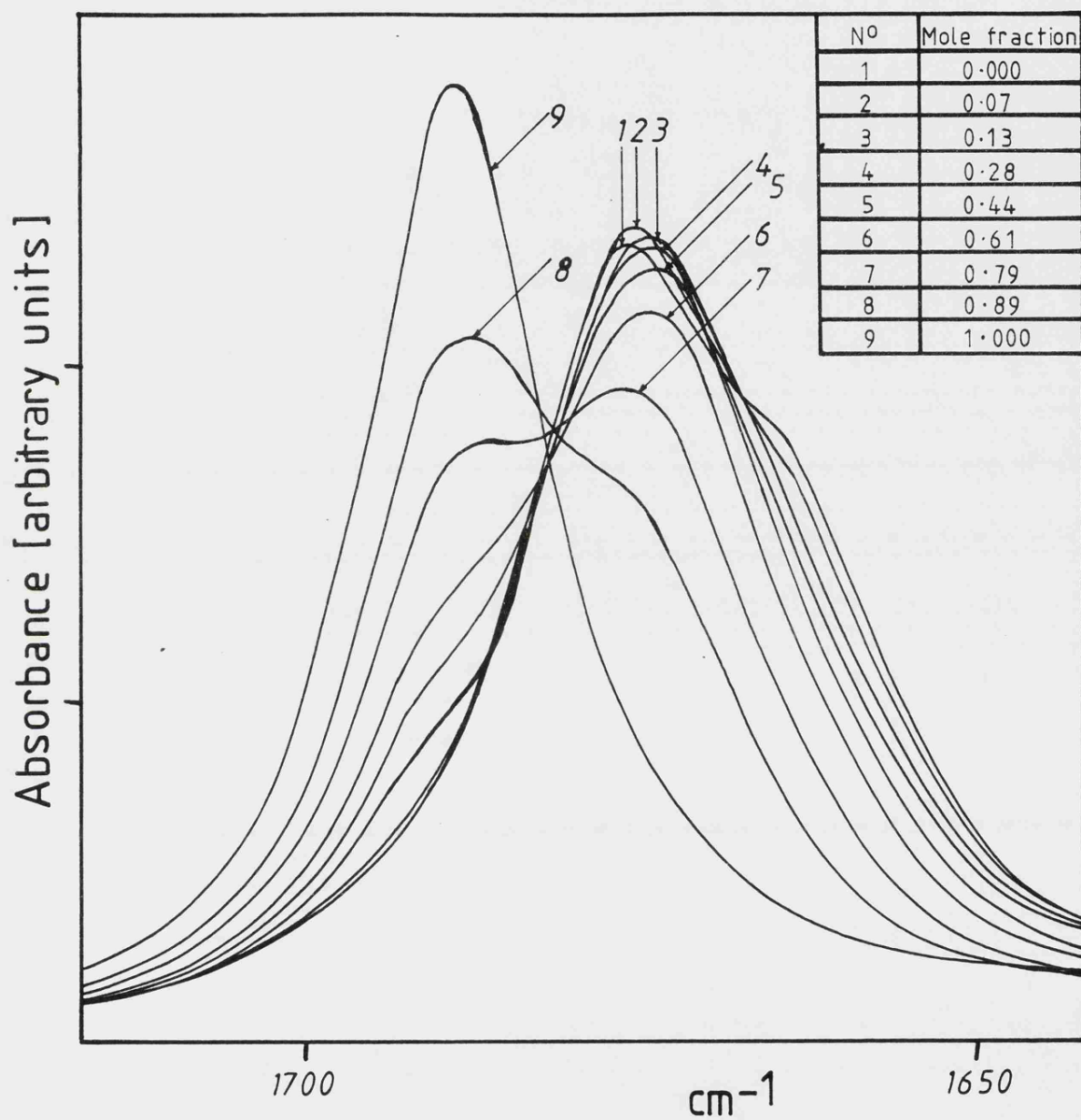## B  Methanol with Aprotic Base, Mixed Solvent Systems

Four different amides were used as probes in the mixed solvent
systems; Figures 4 to 7 illustrate the effect on each probe by methanol
and cyanomethane mixtures. The similarities between these systems is
apparent with an initial loss of the di-bound species, growth of the
mono-bound and a later loss of the mono-bound with gain of the 'free'
species for all the probes on going through a mole fraction range from
methanol to cyanomethane. The Figures 8 to 10 show the deconvoluted
spectral results for one of these probes in different methanol/base
systems. It can be seen that as in the previous probe work (Chapters 3
and 4) the removal of methanol from the hydrogen-bonded complex is
achieved by $(lp)_{free}$ groups, determined by the basicity of the aprotic
base added.

One interesting observation from the Figures 4 to 7 is that in the
initial stages of base addition a shift to lower wavenumbers is noted for
the mono-bound band. The explanation for this is unclear, however the
most likely suggestion stems from the fact that only strongly dipolar
bases show this effect. It would therefore be reasonable to assume that
the mono-bound complex throughout the initial stages of additions of
base are subject to a strong dipolar interaction in addition to their
normal hydrogen bonding interaction, this should cause a shift to lower
wavenumbers for the carbonyl band in the same way that it does for the
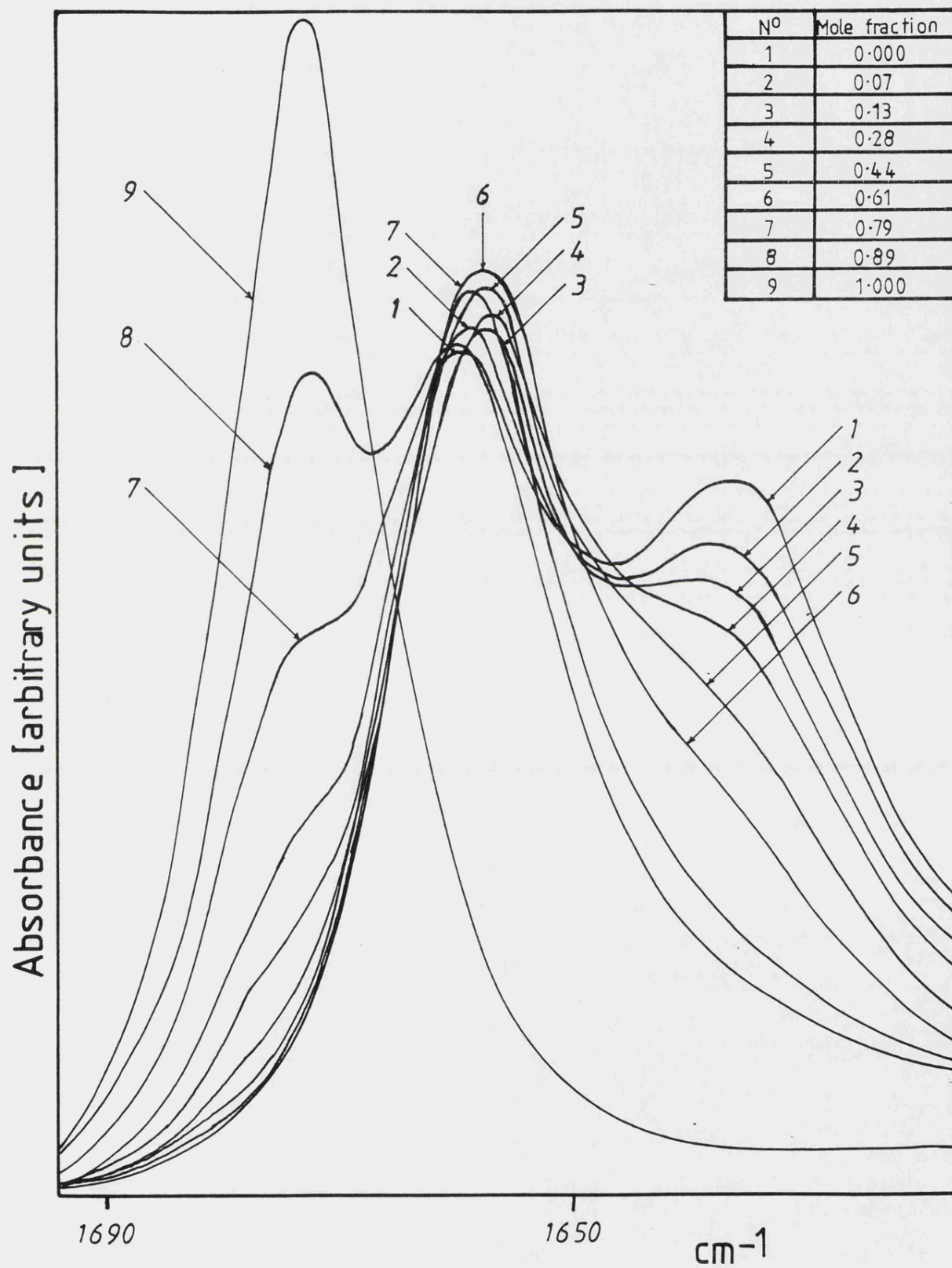'free' amide.

## C  Water with Aprotic Bases

Again the effect of the mixed solvent systems on the carbonyl stretch
of the selected probes can be demonstrated using a typical solvent
system. In Figures 11 to 14 this is shown for the water to cyanomethane
system using the same four amide probes as before. It can be observed

Figure 5.4

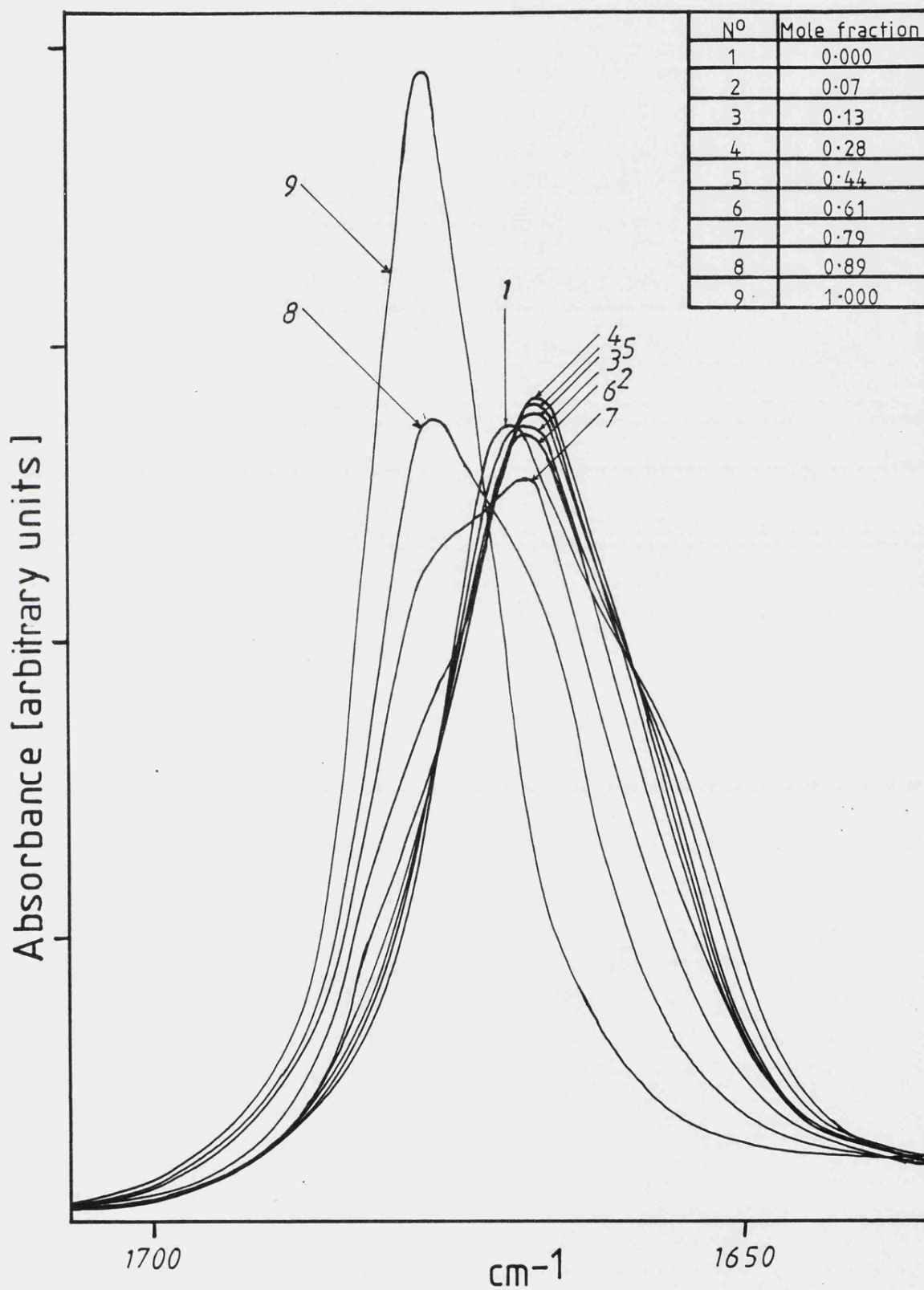| N° | Mole fraction |
|----|---------------|
| 1 | 0·000 |
| 2 | 0·07 |
| 3 | 0.13 |
| 4 | 0·28 |
| 5 | 0·44 |
| 6 | 0·61 |
| 7 | 0·79 |
| 8 | 0·89 |
| 9 | 1·000 |

Spectra showing the change in C=O stretch of
N-Methyl Formamide in mixed solvents Methanol
to Cyanomethane.

# Figure 5.5

| Nº | Mole fraction |
|---|---|
| 1 | 0·000 |
| 2 | 0·07 |
| 3 | 0·13 |
| 4 | 0·28 |
| 5 | 0·44 |
| 6 | 0·61 |
| 7 | 0·79 |
| 8 | 0·89 |
| 9 | 1·000 |

Spectra showing the change in C=O stretch of
N-Methyl Acetamide in mixed solvents, Methanol
to Cyanomethane.

# Figure 5.6



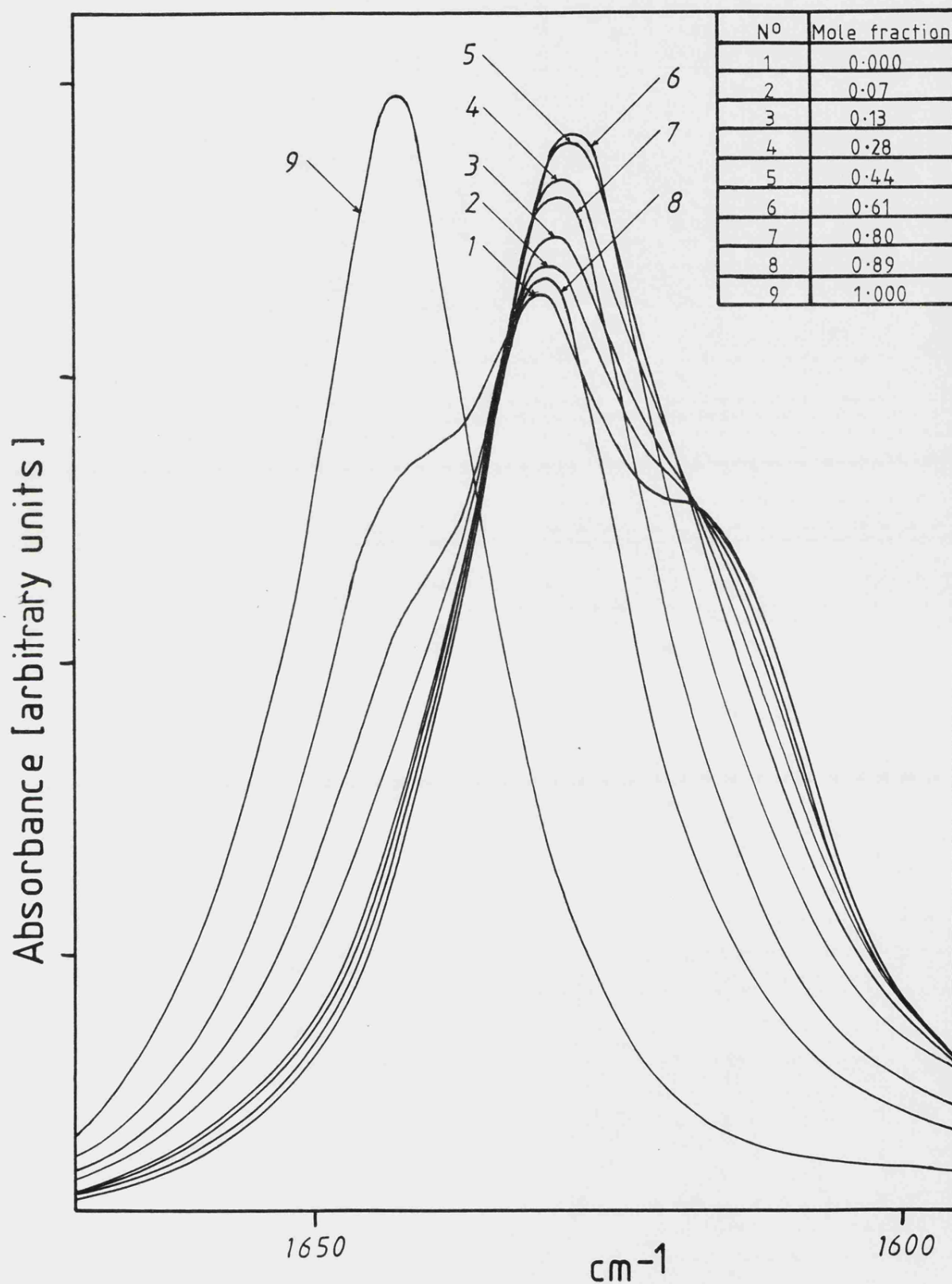| N° | Mole fraction |
|----|---------------|
| 1  | 0·000         |
| 2  | 0·07          |
| 3  | 0·13          |
| 4  | 0·28          |
| 5  | 0·44          |
| 6  | 0·61          |
| 7  | 0·79          |
| 8  | 0·89          |
| 9  | 1·000         |

Spectra showing the change in C=O stretch of N,N'-Dimethyl Formamide in mixed solvents, Methanol to Cyanomethane.

# Figure   5.7



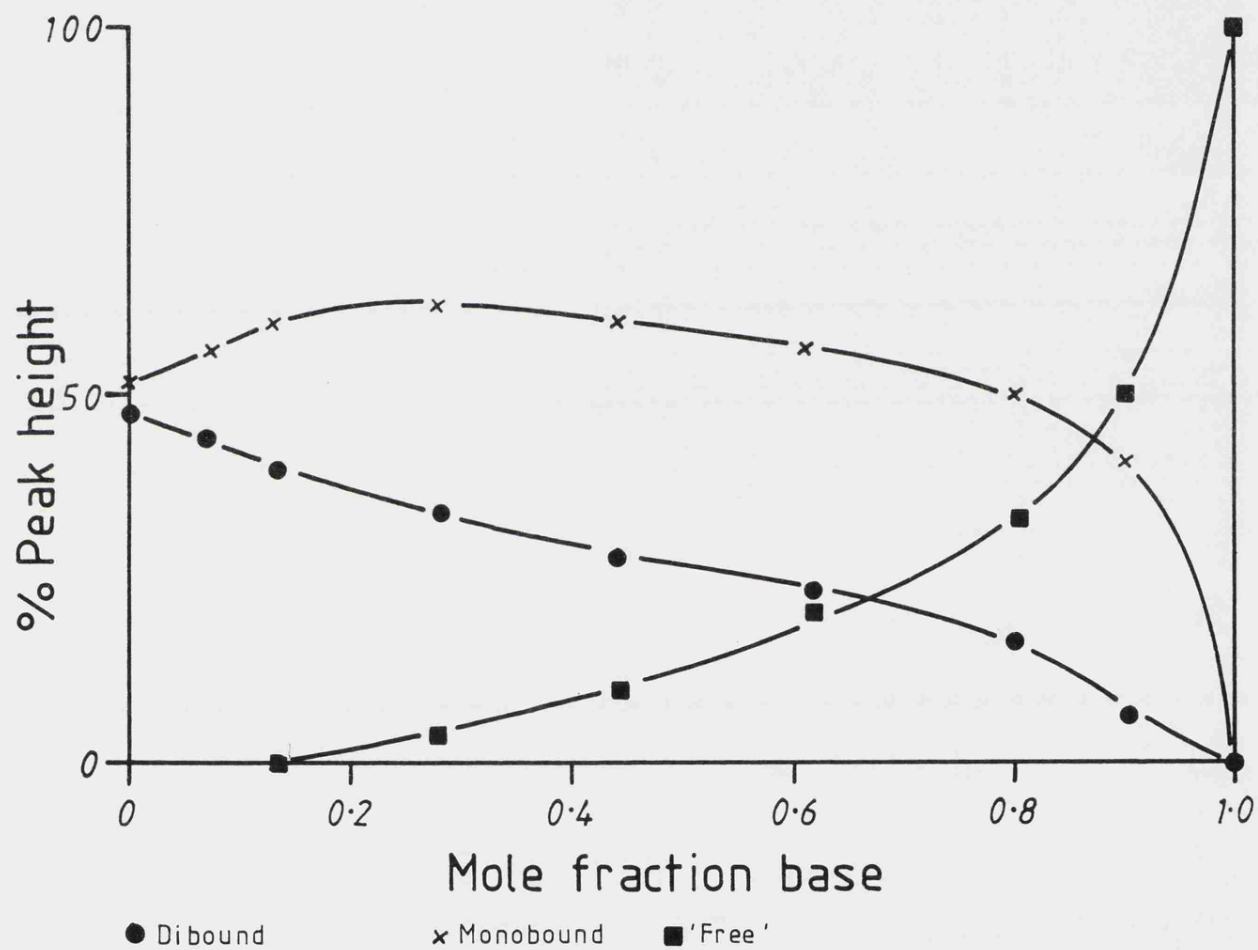| Nº | Mole fraction |
|----|---------------|
| 1 | 0·000 |
| 2 | 0·07 |
| 3 | 0·13 |
| 4 | 0·28 |
| 5 | 0·44 |
| 6 | 0·61 |
| 7 | 0·80 |
| 8 | 0·89 |
| 9 | 1·000 |

Spectra showing the change in C=O stretch of N,N'-Dimethyl Acetamide in mixed solvents, Methanol to Cyanomethane.
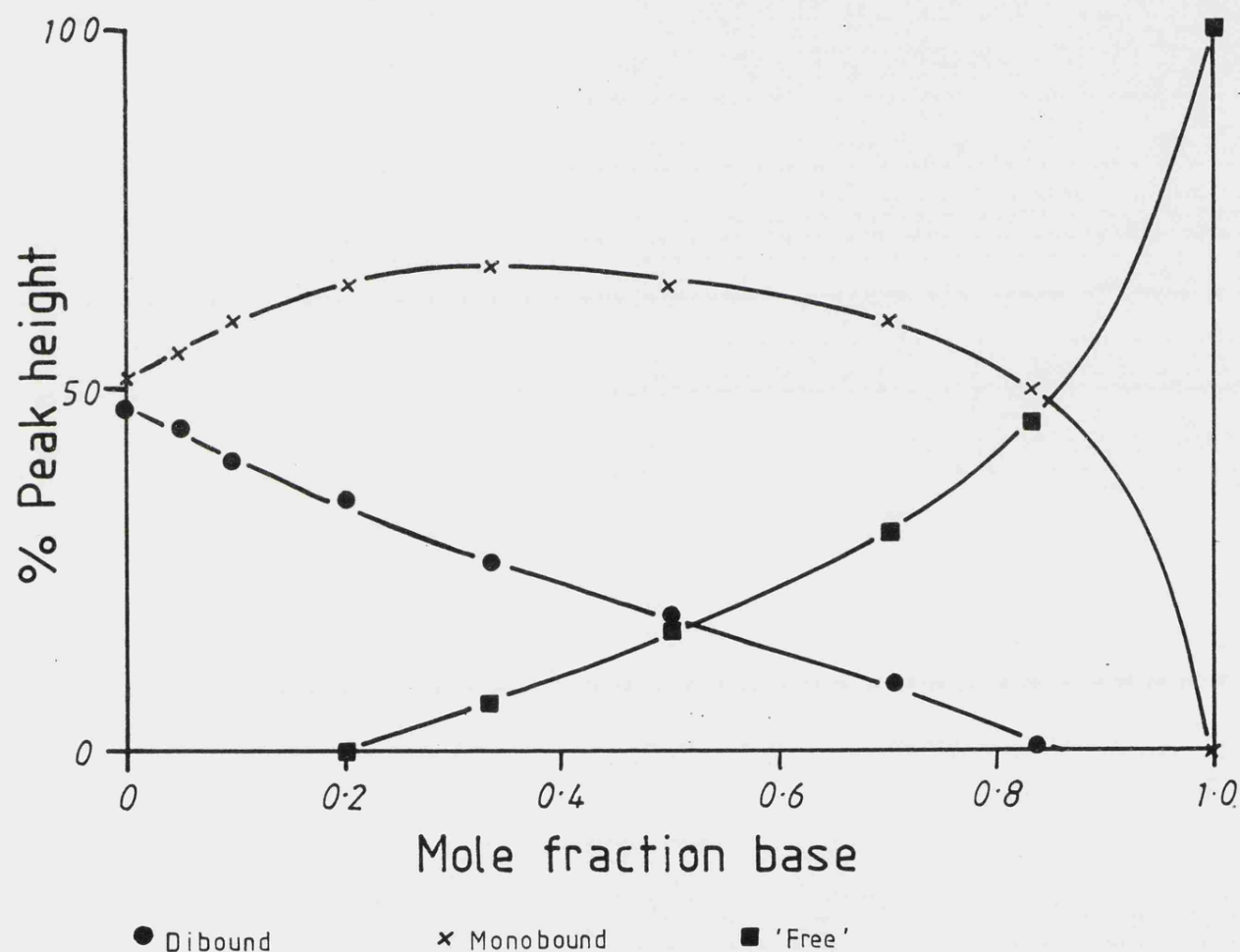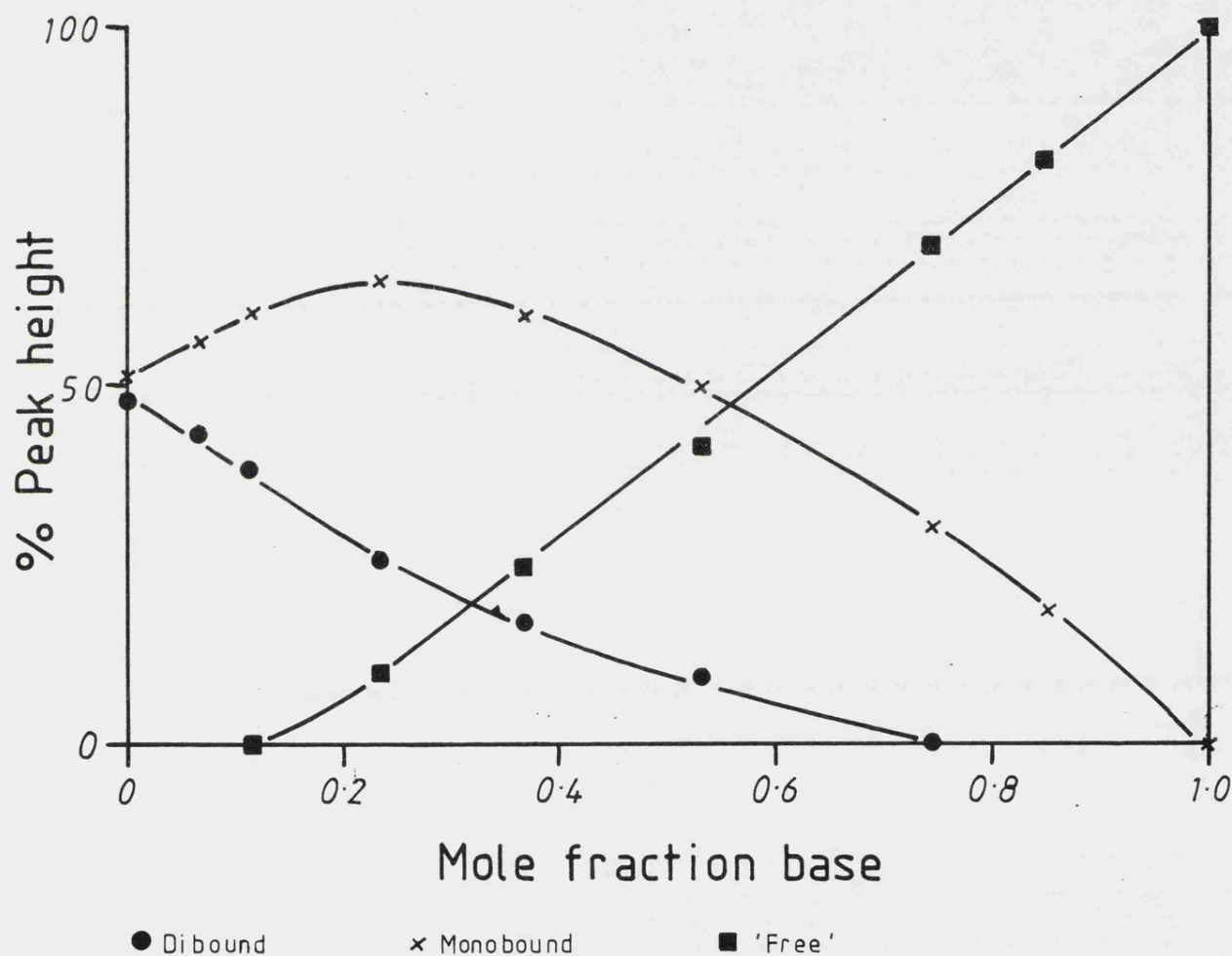
# Figure   5.8

Deconvoluted bands shown as a percentage peak
height of maximum value.   N-Methyl Acetamide
probe in mixture Methanol to Cyanomethane.
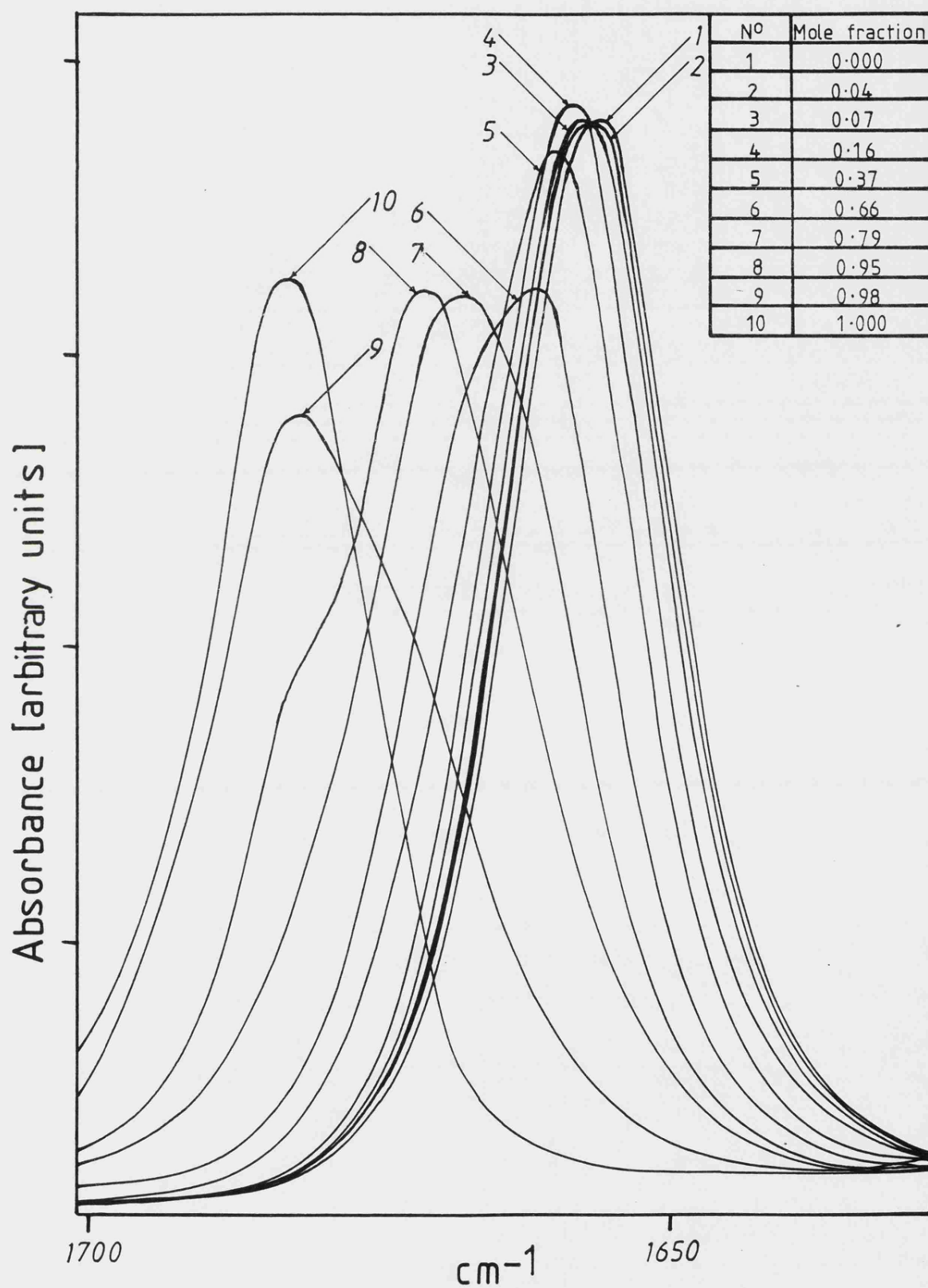
# Figure   5.9



Deconvoluted bands shown as a percentage peak
height of maximum value.  N-Methyl Acetamide
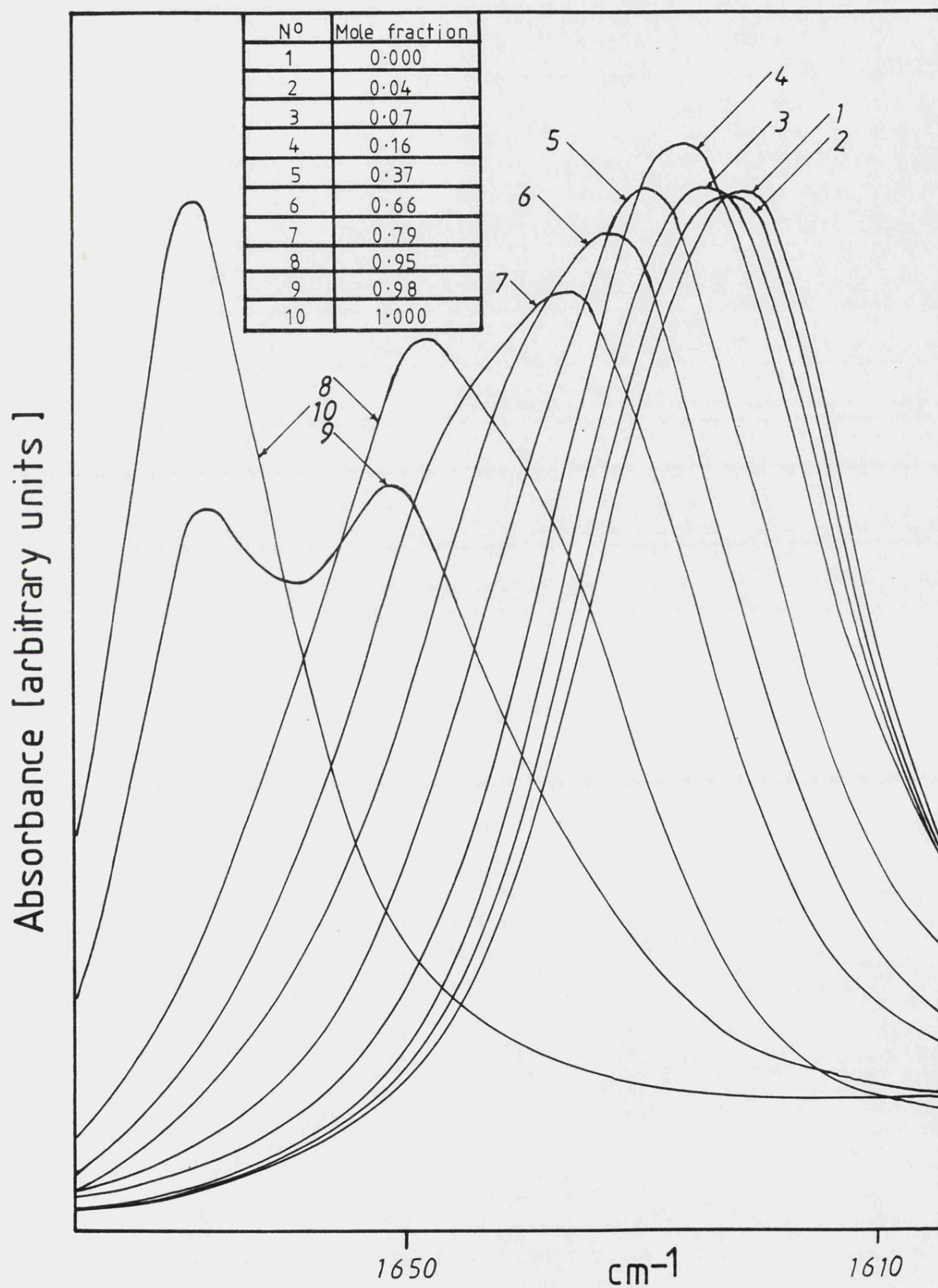probe in mixture Methanol to Tetrahydrofuran.

# Figure 5.10



Deconvoluted bands shown as a percentage peak height of maximum value. N-Methyl Acetamide probe in mixture Methanol to Dimethyl Sulphoxide.

# Figure 5.11



| Nº | Mole fraction |
|----|---------------|
| 1  | 0·000 |
| 2  | 0·04 |
| 3  | 0·07 |
| 4  | 0·16 |
| 5  | 0·37 |
| 6  | 0·66 |
| 7  | 0·79 |
| 8  | 0·95 |
| 9  | 0·98 |
| 10 | 1·000 |

Spectra showing the change in the C=O stretch of $d_1$ N-Methyl Formamide in a mixture, Water ($D_2O$) to Cyano-methane.

# Figure 5.12



| Nº | Mole fraction |
|----|---------------|
| 1  | 0·000         |
| 2  | 0·04          |
| 3  | 0·07          |
| 4  | 0·16          |
| 5  | 0·37          |
| 6  | 0·66          |
| 7  | 0·79          |
| 8  | 0·95          |
| 9  | 0·98          |
| 10 | 1·000         |

Absorbance [arbitrary units]

1650    cm⁻¹    1610
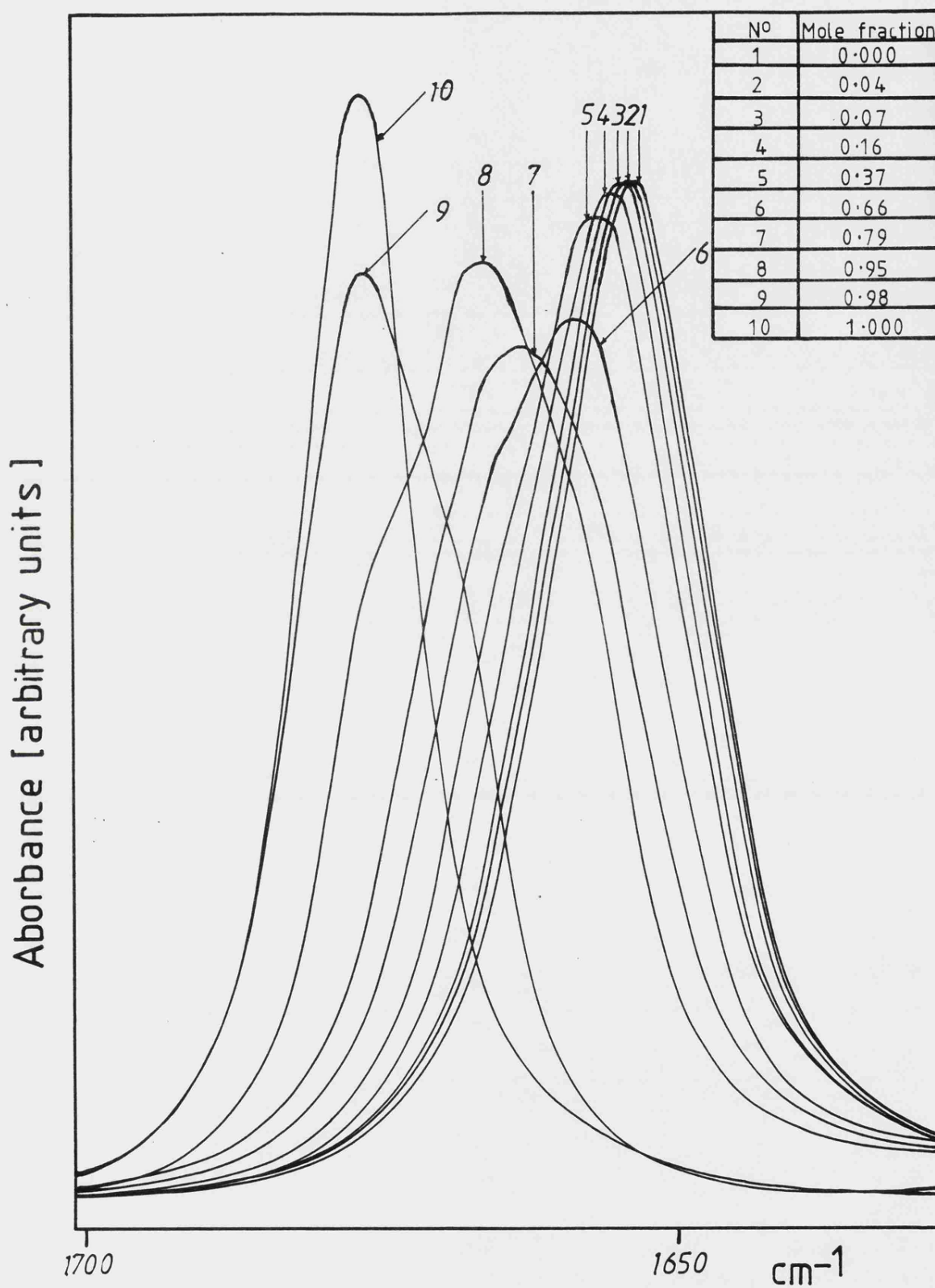
Spectra showing the change in the C=O stretch of $d_1$
N-Methyl Acetamide in a mixture, Water ($D_2O$) to Cyano-
methane.

# Figure    5.13



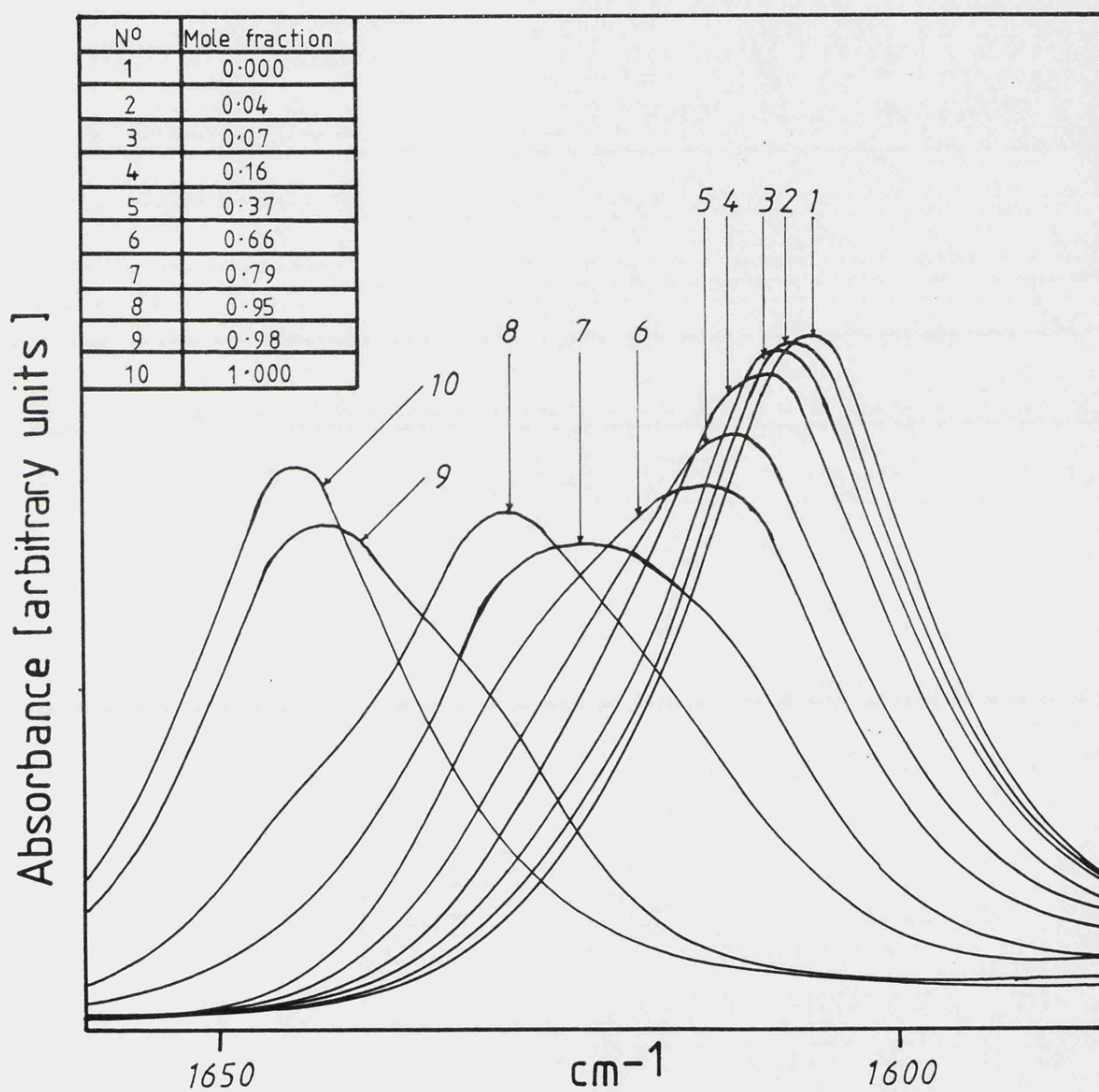| Nº | Mole fraction |
|----|---------------|
| 1  | 0·000         |
| 2  | 0·04          |
| 3  | 0·07          |
| 4  | 0·16          |
| 5  | 0·37          |
| 6  | 0·66          |
| 7  | 0·79          |
| 8  | 0·95          |
| 9  | 0·98          |
| 10 | 1·000         |

Spectra showing the change in C=O stretch of N,N'-
Dimethyl Formamide in a mixture, Water (D₂O) to
Cyanomethane.

# Figure     5.14



Spectra showing change in the C=O stretch of N,N'-Dimethyl Acetamide in a mixture, Water (D₂O) to Cyanomethane.

that three main bands are predominant throughout the mole fraction range, these can be interpreted as 'di-bound', 'mono-bound' and 'free'. This is caused by the '$(lp)_{free}$' production on adding base to water and has been described in previous chapters. However, on close examination of the various spectra sets, a very interesting effect is observed for N-methyl acetamide (NMA) probe. A fourth band appears during the initial mole fraction mixtures, a fairly distinct isosbestic point distinguishes it from the initial di-solvate state of the carbonyl. This effect is echoed by N-methyl formamide (NMF) probe to a much less well defined degree but not at all by the fully substituted di-methyl amides (DMA and DMF).

As this new band is so well defined it is difficult to assign it to secondary solvent effects such as the loss of water further into the bulk water structure, an explanation used for the small gradual shifts observed in most of our probe work (see Chapter 4). However, there is much evidence to suggest that these amides have a planar structure [10] and at least in the solid state exist in a preferred cyclic hydrogen bonded aqueous structure [11]. If this is the case, then an initial attack by the base at the relatively weakly hydrogen bonded N-H----- site would produce '$(lp)_{free}$' and N-H----- base. This then would break the cyclic nature of the system, possibly with a change in conformation about the C-N bond. Whether the shift in band position (approx. 5 $cm^{-1}$) is due to the loss of the cyclic structure, a change in conformation or a combination of both is open for discussion. However, the shift measured is almost exactly that observed for the difference in band position from a hexane solution to a water solution for NMA relative to that for the fully substituted DMA, between the same solvent solutions. A similar comparison is also valid for NMF probe relative to DMF probe with a shift

difference of approx. 3 cm$^{-1}$.  This extra band for NMA probe is
illustrated further in Figures 15 and 16.

Returning now to a typical system of 'Di-bound' to 'Mono-bound' to
'Free' these when deconvoluted and plotted in the usual manner are
shown by Figures 17 to 19, using DMA probe.  These plots are entirely
consistent with previous aqueous base systems studied via other probes
(see Chapters 3 and 4).
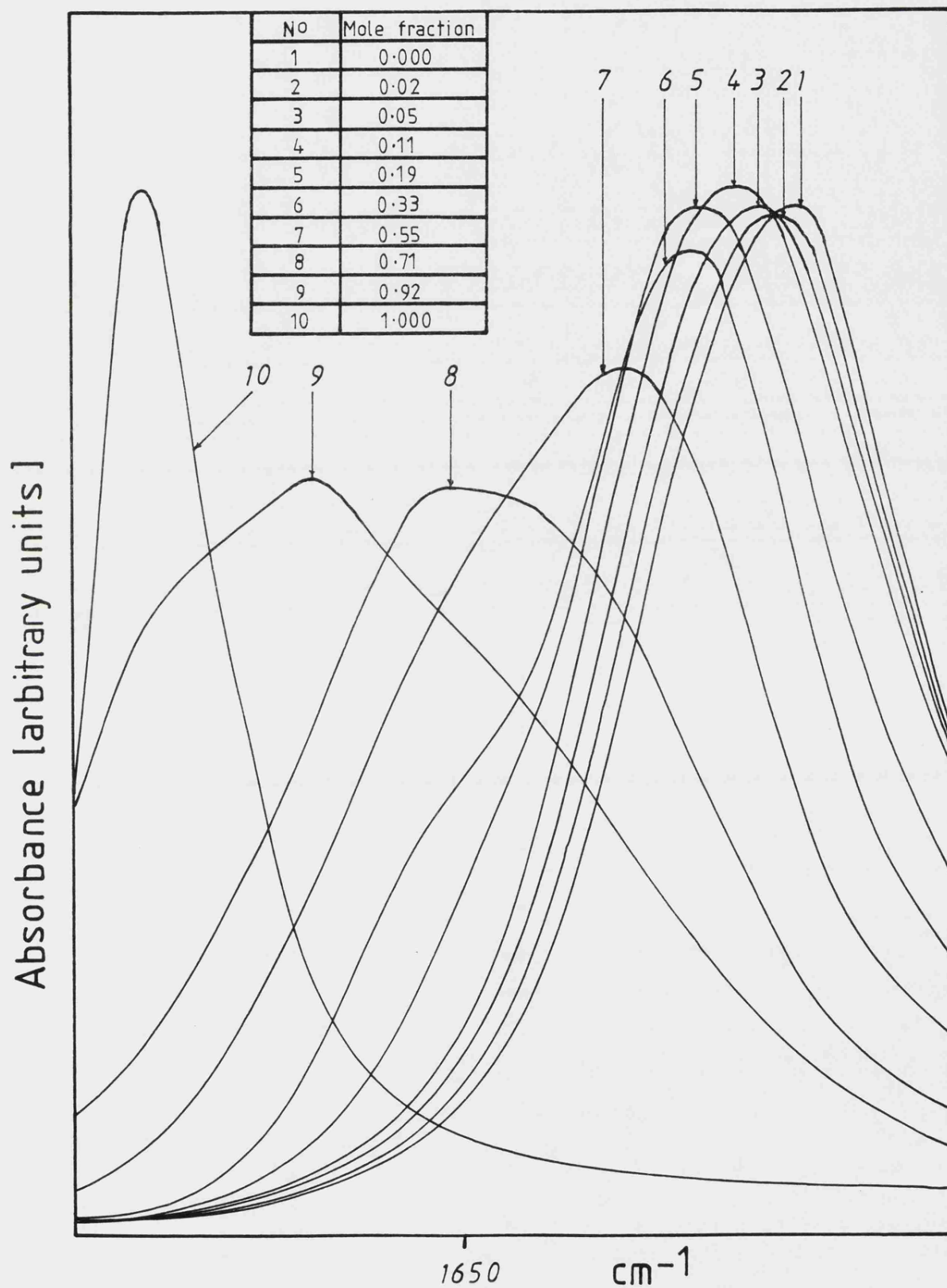
## D  The N-H------ Hydrogen Bonding System

As seen from the previous study the carbonyl stretch of the amides is
fairly insensitive to any hydrogen bonding at the N-H proton.  There are
two more infrared group frequencies that can be used to good effect,
namely the N-H stretch (approx. 3400 cm$^{-1}$) and the C-$\widehat{N}$-H bend (Amide II
band approx. 1600 cm$^{-1}$).

We used the N-H stretch only as a proof that any N-H was totally
bound when the amide was in solution in aprotic bases.  The free N-H
stretch is a sharp narrow band at 3460 cm$^{-1}$ with any bound bands being
much broader and at lower wavenumbers depending upon base strength.

The amide II band was relatively easy to observe along with the
carbonyl stretch for the secondary amide probes in various systems.
Figure 20 shows the band positions in various solvents for NMA.  The
positions given for unassociated NMA, i.e. in Tetrachloromethane and
Hexane are found only in extreme dilution, any significant increase in
the NMA concentration giving rise to bands at higher wavenumbers due to
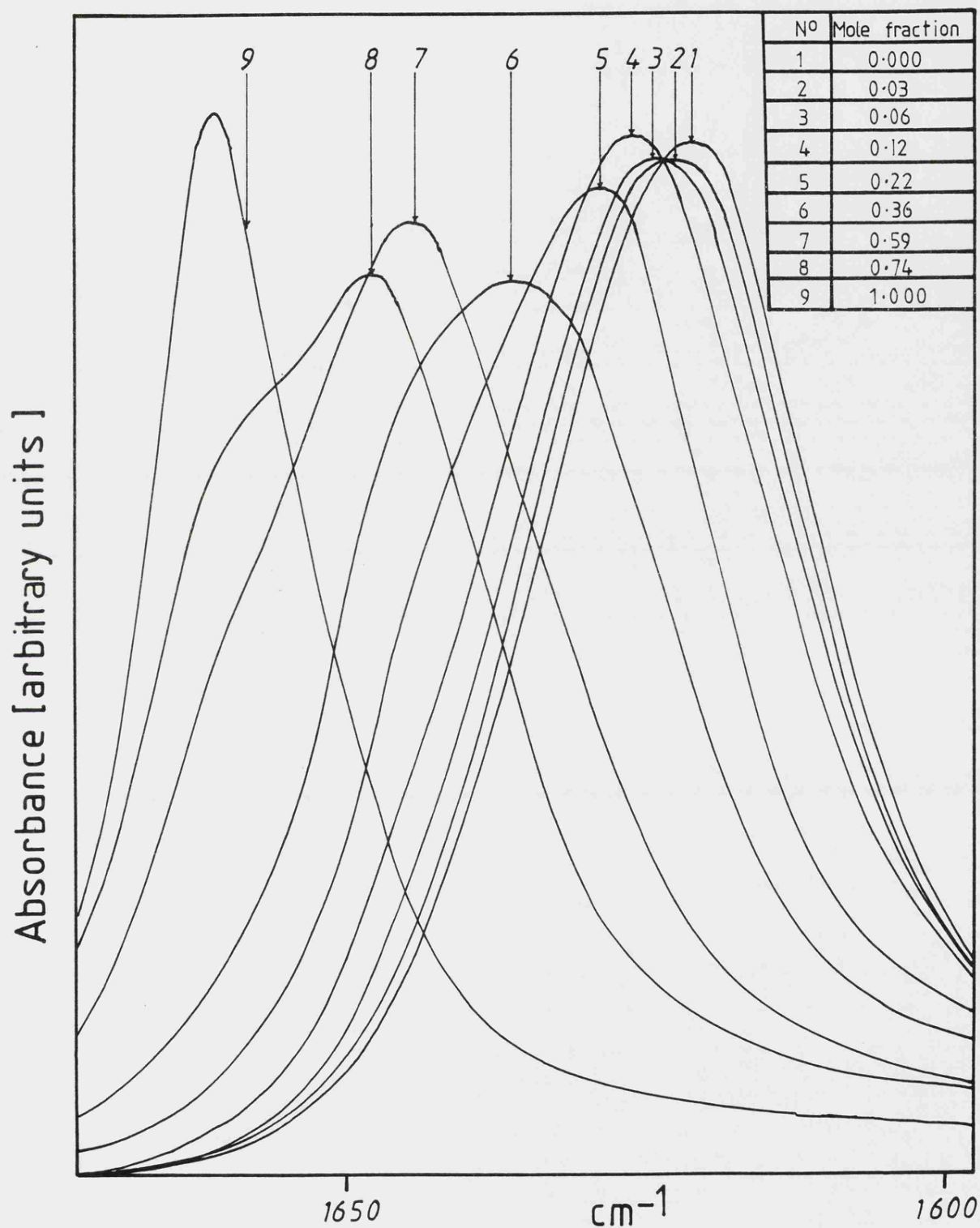various self-associated polymers being formed.

Two major considerations must be observed for the amide II band study.
Firstly, the planar nature of the probe with delocalisation of the $\pi$
electron system over O$\overline{-}$C$\overline{-}$N [10].  Secondly, the amide II band is a
strongly coupled band comprising the C-$\widehat{N}$-H bend (in plane) and the C-N

# Figure 5.15



| No | Mole fraction |
|----|---------------|
| 1 | 0·000 |
| 2 | 0·02 |
| 3 | 0·05 |
| 4 | 0·11 |
| 5 | 0·19 |
| 6 | 0·33 |
| 7 | 0·55 |
| 8 | 0·71 |
| 9 | 0·92 |
| 10 | 1·000 |

Spectra showing the change of the C=O stretch of $d_1$ N-Methyl Acetamide in a mixture, Water ($D_2O$) to Tetrahydrofuran.

# Figure   5.16



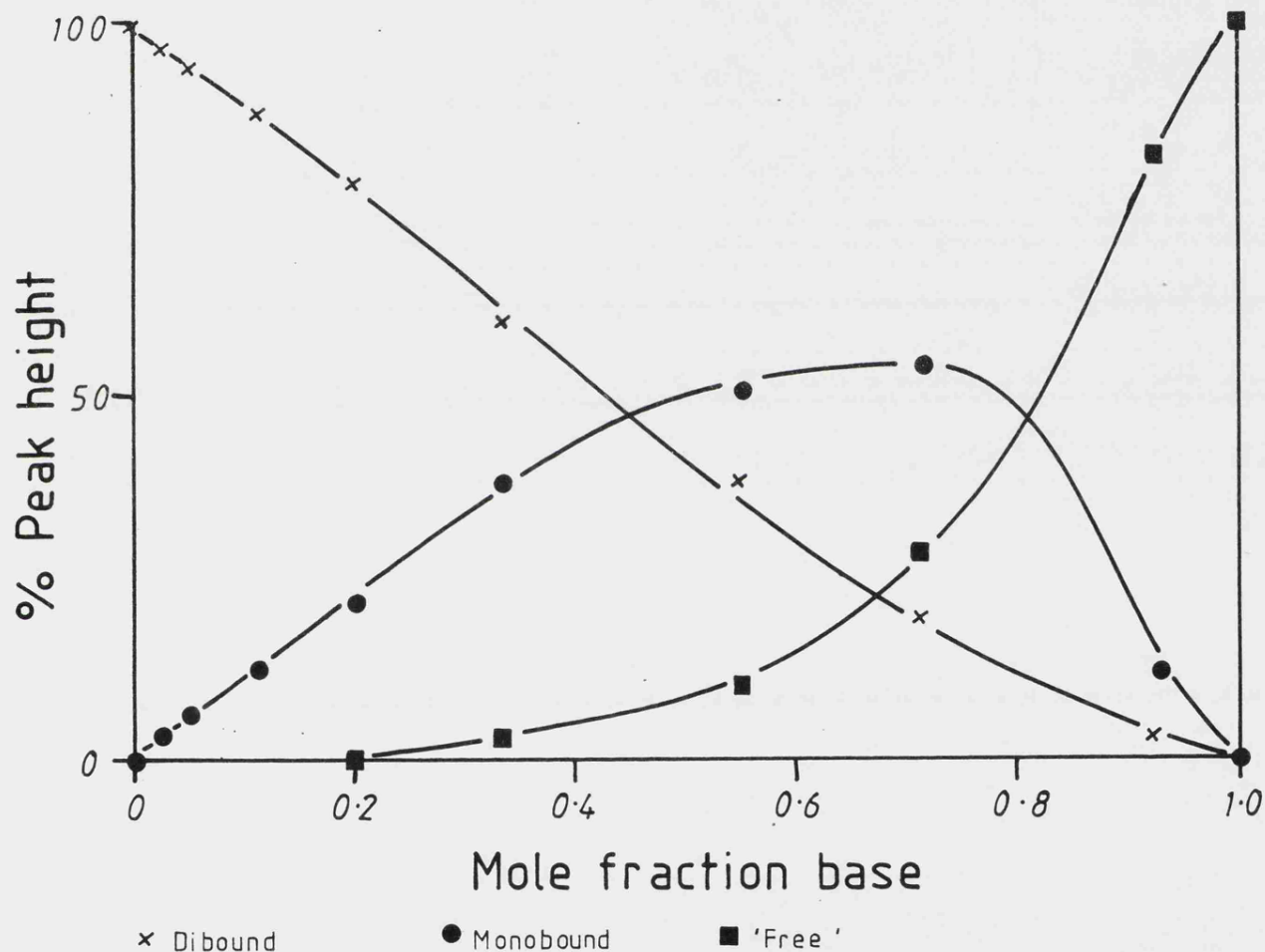| No | Mole fraction |
|----|---------------|
| 1  | 0·000         |
| 2  | 0·03          |
| 3  | 0·06          |
| 4  | 0·12          |
| 5  | 0·22          |
| 6  | 0·36          |
| 7  | 0·59          |
| 8  | 0·74          |
| 9  | 1·000         |

Spectra showing the change of the C=O stretch of $d_1$ N-Methyl
Acetamide in a mixture, Water ($D_2O$) to Dimethyl Sulphoxide.
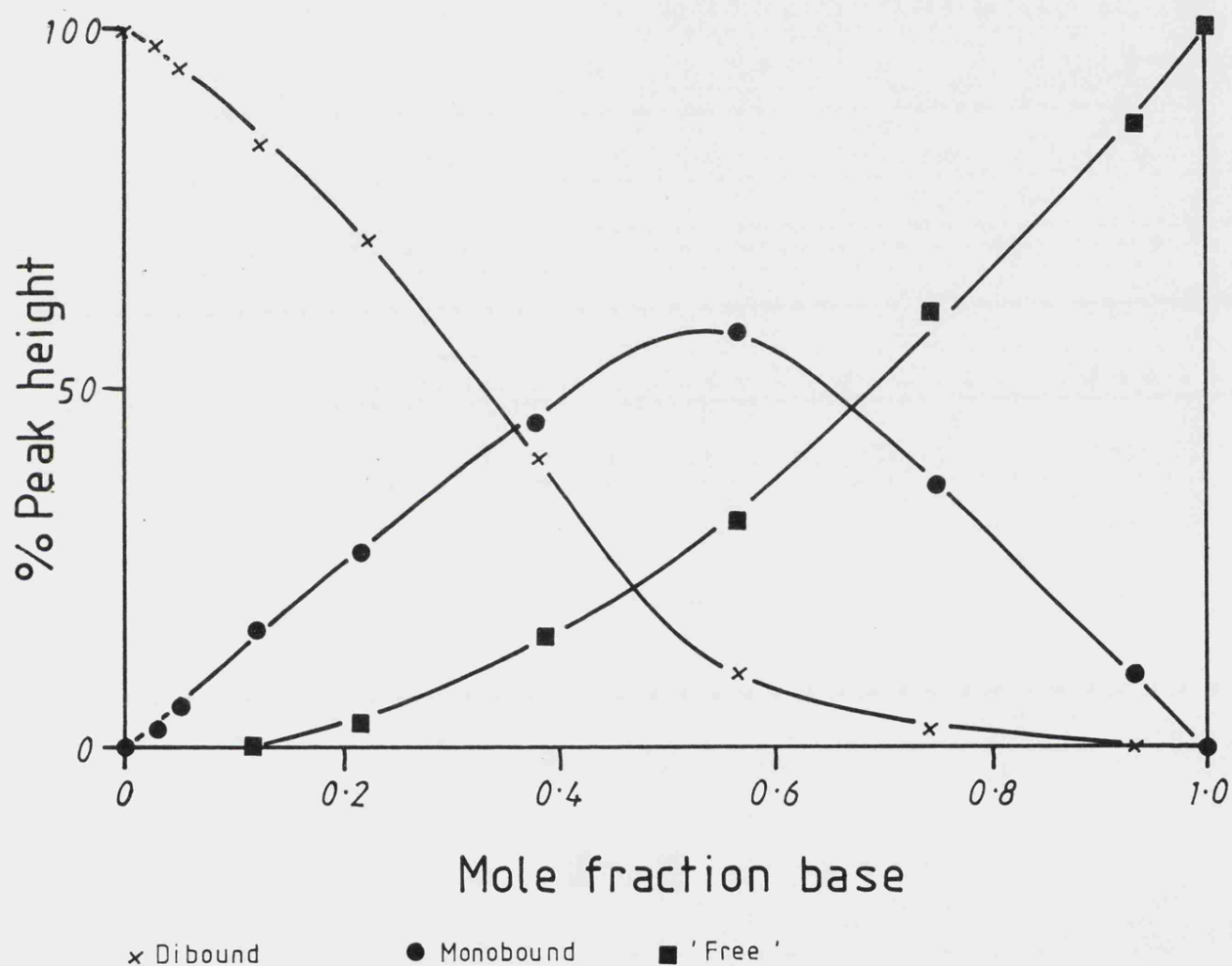
# Figure    5.17
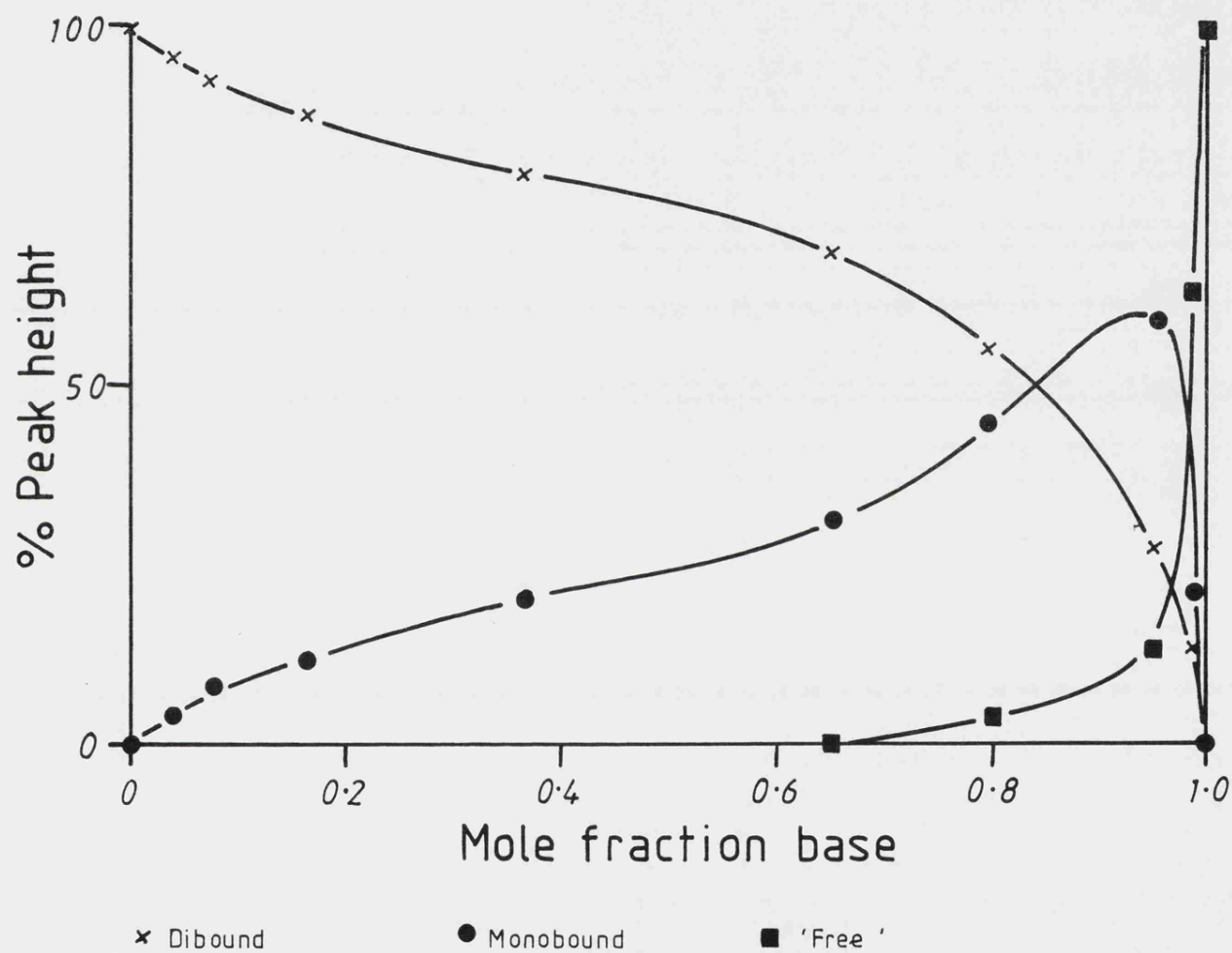
Deconvoluted bands shown as a percentage peak height
of maximum value.  N,N'-Dimethyl Acetamide probe in
mixture Water to Cyanomethane.

Figure 5.18

Deconvoluted bands shown as a percentage peak height
of maximum value.  N,N'-Dimethyl Acetamide probe in
mixture Water to Tetrahydrofuran.

# Figure 5.19



Deconvoluted bands shown as a percentage peak height
of maximum value.  N,N'-Dimethyl Acetamide probe in
mixture Water to Dimethyl Sulphoxide.

stretch, for NMA this has been calculated as approximately 60:40 respectively [1]. The non-associated bands occur at lowest frequency with the various aprotic bases interacting according to base strength to give bands at higher frequencies. Methanol and water at first appear to give exceptional shifts, however these protic solvents also strongly hydrogen bonded to the carbonyl group as described earlier in this chapter. Due to the delocalisation of the carbonyl $\pi$ system through to the nitrogen, along with the coupled nature of the amide II band, any strong interaction at the oxygen would produce a strong change in the amide II band frequency. In addition there is also the possibility of a cyclic form in aqueous solution as postulated earlier for NMA and NMF.

When observed for the mixed solvent systems methanol to base, the amide II band can be observed and follows a simple loss/gain two band sequence. This is illustrated in Figure 21. The effect of going from methanol to several bases is illustrated in Figures 22 to 24 in the form of deconvolution data versus mole fraction. Base strength appears to be the deciding factor in the rate of exchange from protic to aprotic bound systems.

5.3  CONCLUDING REMARKS

The carbonyl stretching frequency of amides is a useful tool in the study of amide solvation. As probes the amides follow the general pattern observed for other carbonyl compounds. The use of the amide II band is obviously complicated, however, some useful information can be gleaned as to the solvation of the N-H protons.
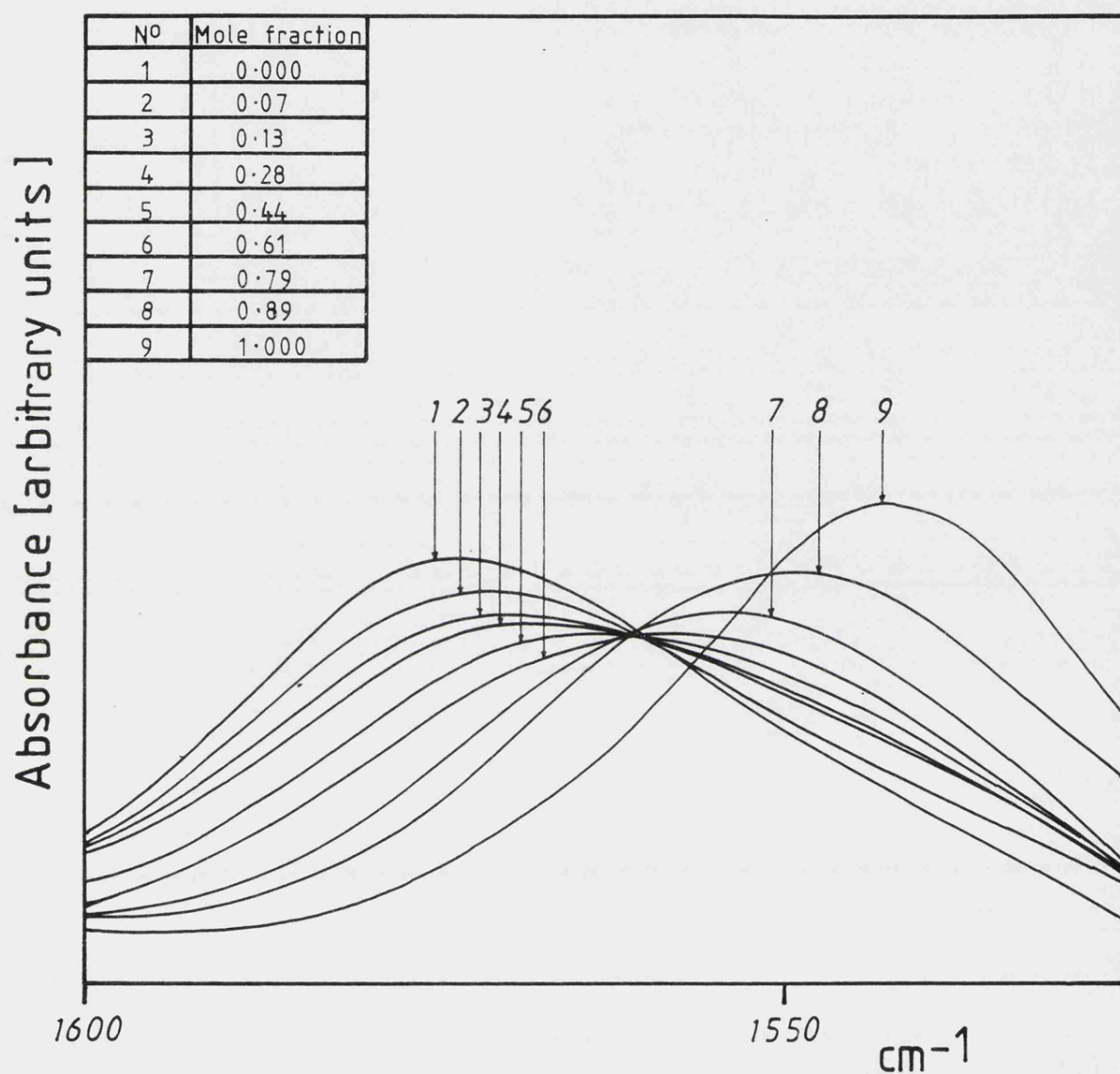
# Figure    5.20

Amide II band positions for N-Methyl Acetamide in various solvents.
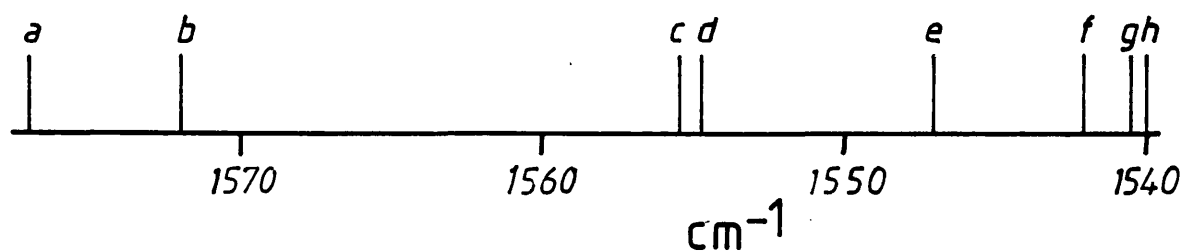


| KEY | |
|-----|-----|
| a | Water |
| b | Methanol |
| c | Triethylamine |
| d | Dimethylsulphoxide |
| e | Tetrahydrofuran |
| f | Cyanomethane |
| g | Tetrachloromethane |
| h | Cyclohexane |

# Figure 5.21



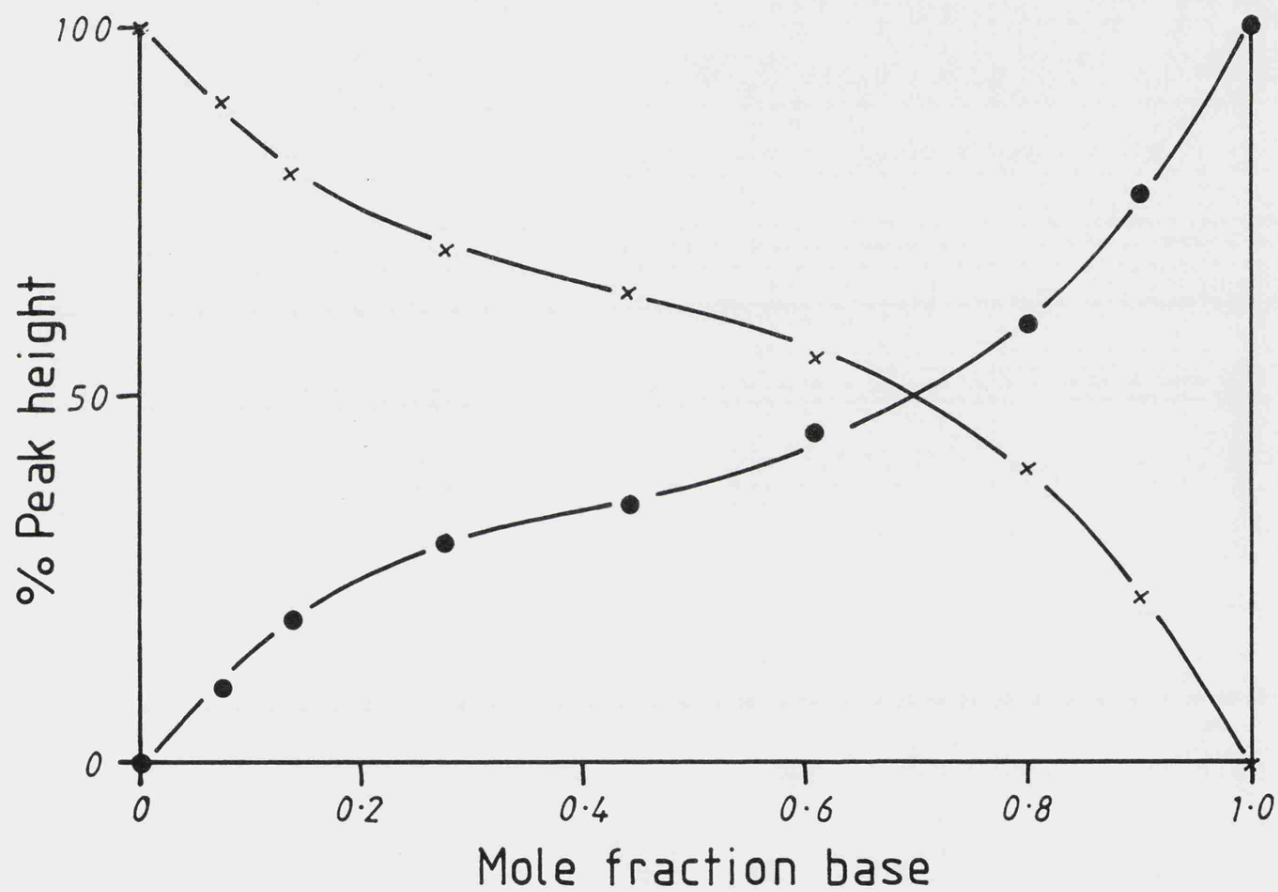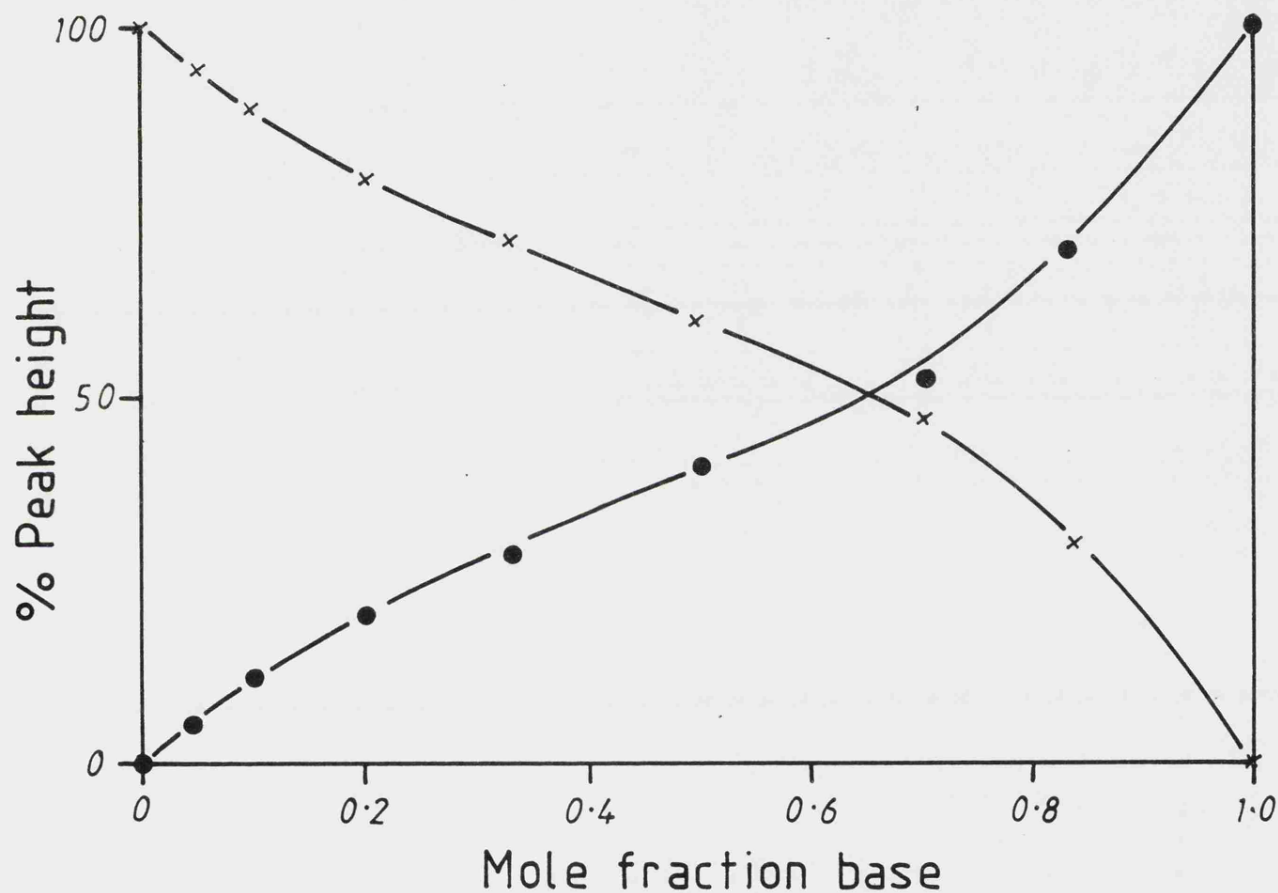| Nº | Mole fraction |
|---|---|
| 1 | 0·000 |
| 2 | 0·07 |
| 3 | 0·13 |
| 4 | 0·28 |
| 5 | 0·44 |
| 6 | 0·61 |
| 7 | 0·79 |
| 8 | 0·89 |
| 9 | 1·000 |

Spectra showing change in Amide II band in mixture,
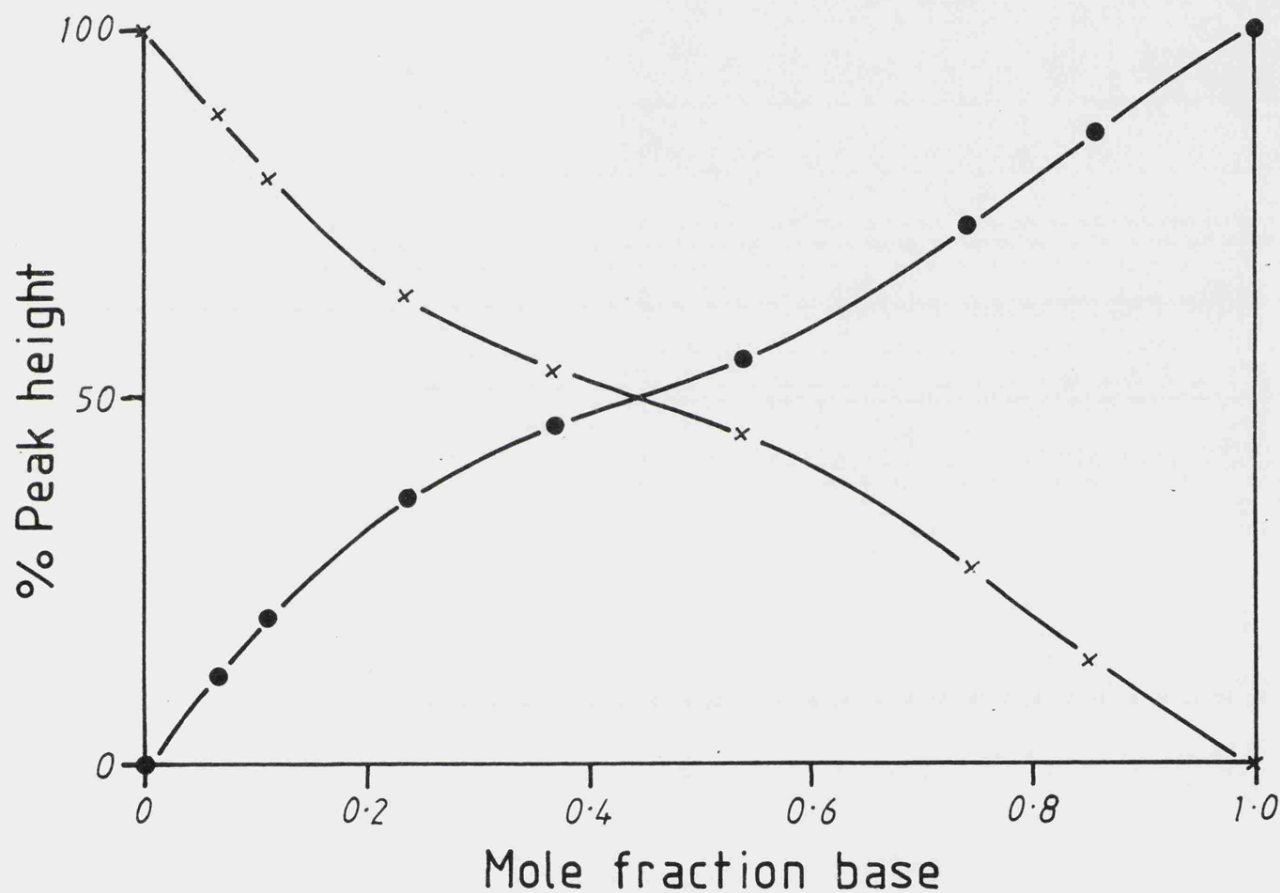Methanol to Cyanomethane.  N-Methyl Acetamide.

Figure 5.22

Deconvoluted bands shown as a percentage peak height
of maximum value. N-Methyl Acetamide probe, Amide II
band in mixture, Methanol to Cyanomethane.

# Figure    5.23



Deconvoluted bands shown as percentage peak height
of maximum value.  N-Methyl Acetamide probe, Amide
II band in mixture, Methanol to Tetrahydrofuran.

# Figure    5.24



Deconvoluted bands shown as percentage peak height
of maximum value.   N-Methyl Acetamide probe, Amide
II band in mixture, Methanol to Dimethyl Sulphoxide.

REFERENCES FOR CHAPTER 5

1.  L. J. Bellamy, 'The Infrared Spectra of Complex Molecules',
    Vol. II, (1980), Chapman & Hall.

2.  A. V. Iogansen, G. A. Kurkchi and L. A. Dement'eva, Zh. Strukt.
    Khim., 18, (1977) 743.

3.  F. Fillaux and M. H. Baron, J. Chem. Phys., 62, (1981) 275.

4.  A. Pullman, H. Berthod, C. Geissner-Prettre, J. F. Hinton and
    D. Harpool, J. Am. Chem. Soc., 100:13, (1978) 3991.

5.  J. F. Hinton and K. H. Ladner, Spectrochim. Acta, 28A, (1972)
    1731.

6.  O. D. Bonner and Y. S. Choi, Spectrochim. Acta, 31A, (1975) 1975.

7.  E. S. Amis and J. F. Hinton, 'Solvent Effects on Chemical
    Phenomena', Vol. 1, Academic Press, (1973).

8.  M. C. R. Symons, T. A. Shippey and P. P. Rastogi, J. Chem. Soc.,
    Faraday Trans. 1, 76, (1980) 2251.

9.  N. G. M. Pay, Ph.D. Thesis, Leicester University, (1981).

10. L. Leiserowitz and M. Tuval, Acta Crystallogr., Sect. B, 34:7,
    (1978) 1230.

11. L. Leiserowitz and G. M. J. Shmidt, J. Chem. Soc. A, (1969) 2372.

# CHAPTER 6

## MISCELLANEOUS PROBE STUDIES

## 6.1  INTRODUCTION

Many compounds are suitable candidates for use in probe studies. They may have particularly useful infrared frequencies, ultraviolet/visible bands, unpaired electrons or a suitable nuclear spin for n.m.r. measurements. On the other hand, they may have unusual solvation states, or structural peculiarities making their study of particular importance. During the course of this work many such compounds were investigated, the more important and informative have been discussed in their relevant chapters. However, mention must be made of those others that promise to provide more detailed information after further study. To this end each will be discussed under its individual heading with a resumé of the experimental results obtained.

## 6.2  DIMETHYL SULPHOXIDE (DMSO)

The apparent similarity of DMSO to acetone suggested it as a suitable probe molecule. It is a strong aprotic base and has an S-O stretching frequency that is easily detected by infrared or Raman studies. A useful outline on the infrared of sulphoxides in general is given by Bellamy [1]. He describes the S-O bond as a mixture of a strong σ bond plus weak interactions between the oxygen p-orbitals and the sulphur d-orbitals. This gives rise to a strongly dipolar bond but slightly less basic at the oxygen than would be expected on purely charge separation terms.

The structure of DMSO is pyramidal with sulphur at the apex and oxygen and the two methyl groups occupying the three other corners of a triangular-based pyramid [2]. This means that the S-O dipole is very exposed allowing strong dipolar interactions in addition to hydrogen bonding effects. [See Chapter 3.] The DMSO-Water system has been studied by a wide variety of techniques including infrared [3], Raman [4]
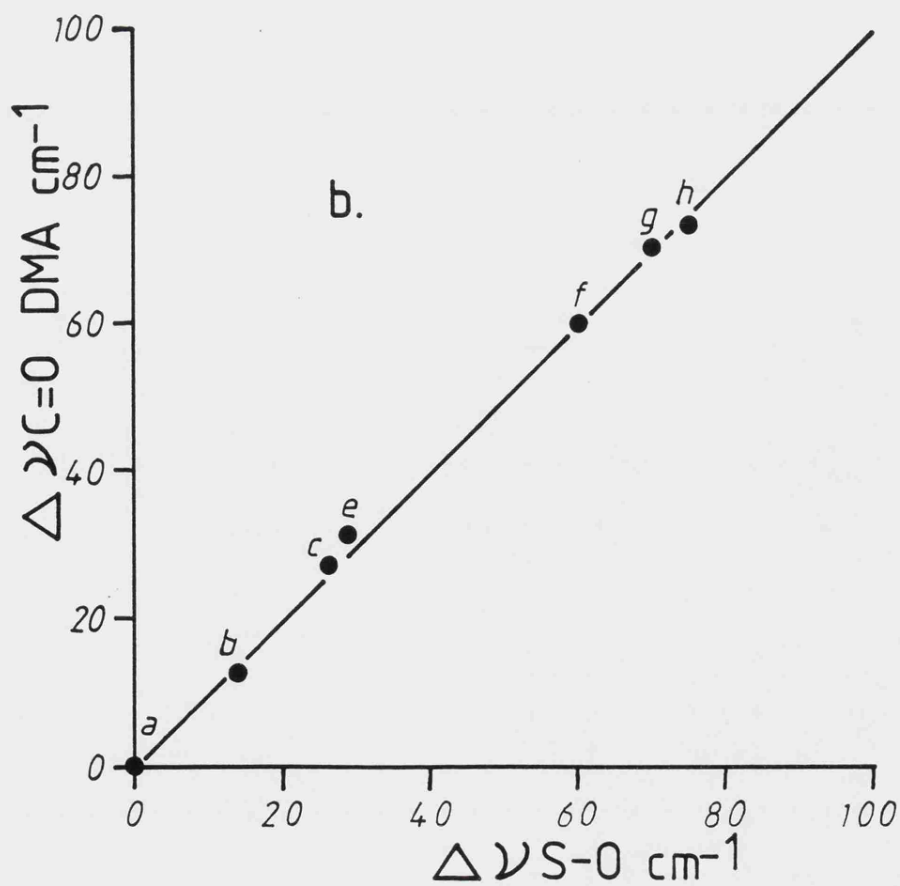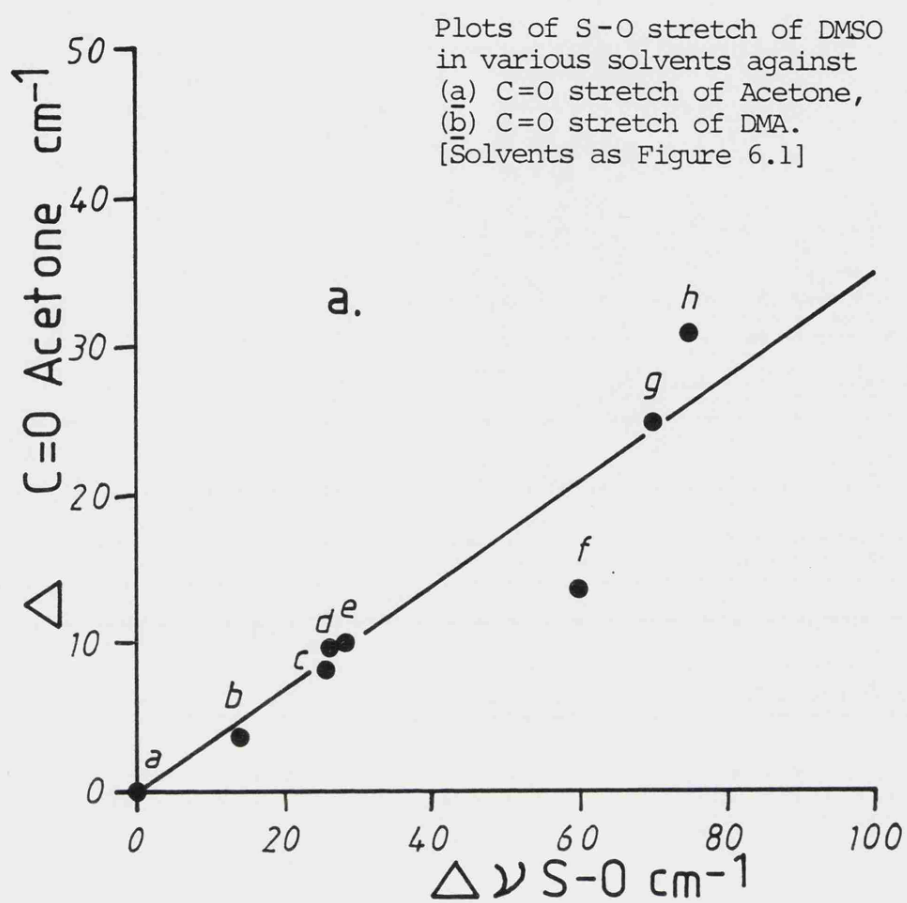
# Figure    6.1
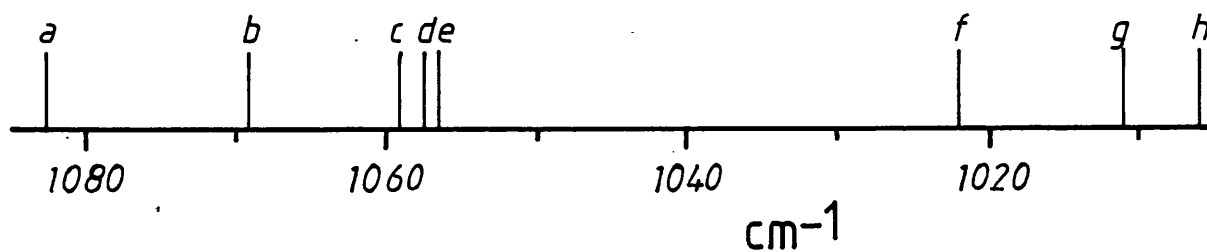


| KEY | |
|---|---|
| a | Hexane |
| b | Tetrachloromethane |
| c | Cyanomethane |
| d | Dichloromethane |
| e | Dimethylsulphoxide |
| f | Methanol (d$_4$) |
| g | Water |
| h | Perfluoro-t-butanol |

Band positions of S-O stretch of DMSO in various solvents.

# Figure 6.2



Plots of S-O stretch of DMSO
in various solvents against
(a) C=O stretch of Acetone,
(b) C=O stretch of DMA.
[Solvents as Figure 6.1]

and neutron inelastic scattering [5]. There is, however, considerable disagreement on the type of interactions deduced from the experimental results, with some workers arguing for purely dipolar interactions and others for fully hydrogen bonded systems. Work in this laboratory, however, supports the view of DMSO being dibasic and doubly hydrogen bonded when dilute in aqueous solution [6].

If we consider Figure 1 this shows the band positions for S-O stretch in different solvents. Plotting these positions against those for the C=O stretch of acetone probe produces a linear relationship but with methanol significantly off the line. However, a similar plot against the C=O stretch of N,N'-Dimethyl Acetamide probe shows that di-bound probe in methanol is consistent with the linearity. These plots are shown in Figure 2. The suggested interpretation is, therefore, that dilute DMSO in water and in methanol exists as a di-bound hydrogen bonded species.

There are, however, severe limitations on the use of sulphoxides as probes when using Raman or infrared S-O stretch. The band position occurs in a region of the spectrum where many other bands from solvents, such as C-H bending modes, interfere very strongly. Consequently, future work will require a large portion of care and luck in order to utilise this potentially useful probe.
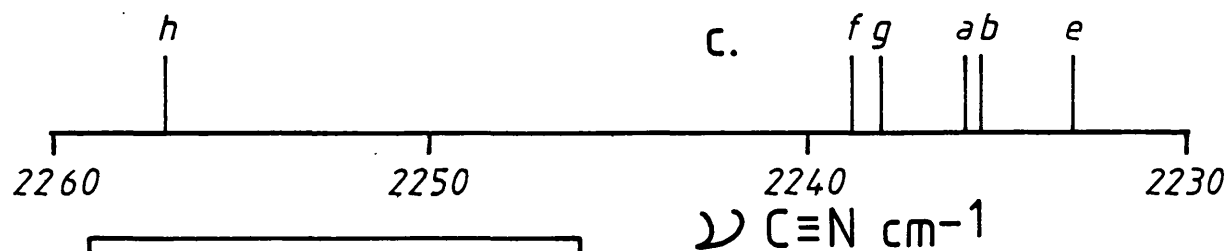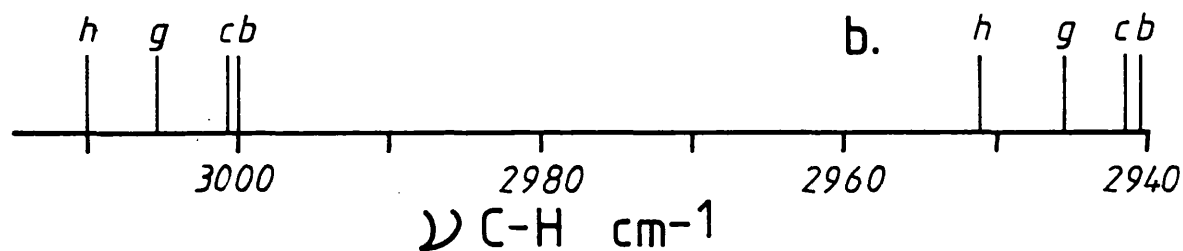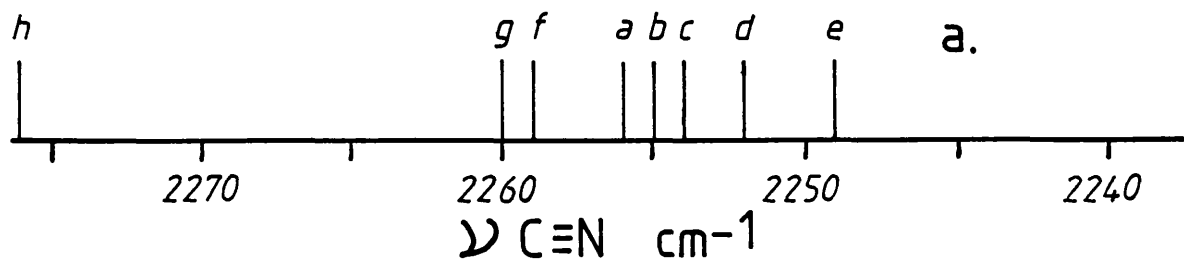
## 6.3 CYANOMETHANE (MeCN)

The $-C \equiv N$ stretching frequency of various nitriles occurs in an otherwise very clear area of the infrared spectrum. This makes such compounds obvious candidates as probes for solvation studies. Cyanomethane is a small linear molecule, weakly basic and with a strong dipole. The general infrared frequencies associated with nitriles are discussed by Bellamy [1] who demonstrates that there is seemingly little relationship

between bond length and force constant. Cyanomethane is an important solvent, particularly for ionic species and has been studied in its interactions with water, alcohols and salts [7,8,9]. From one of these studies [9] there is evidence that whilst a strong interaction can be observed between cyanomethane and cations _via_ the nitrogen there is also an interaction with anions through the methyl C-H's.

Figure 3 shows the positions for (a) C≡N stretch of cyanomethane, (b) C-H stretch of cyanomethane,(c)C≡N stretch of t-Butyl nitrile, in dilute solution in various solvents. It can be observed that there is a solvent dependence of the C-H stretch which indicates some interaction between solvent and the methyl group, possibly dipolar. This supports the anion interaction work. The dependence of the C≡N stretch is seen to behave differently to previous probes studied. In fact, the strong dipolar aprotic solvents produce a low frequency shift whereas the protic solvents produce a high frequency shift, from the value obtained in an inert medium. Methanol and water produce very similar shifts suggesting that their interaction is very similar, possibly singly hydrogen bonded to the C≡N nitrogen. The reason for the unusual shifts are unclear, it may be a purely mechanical restriction of the C≡N stretch by 'end-on' hydrogen bonding. Alternatively, there may be some change in the bonding character of the C≡N bond produced by hydrogen bonding through the nitrogen lone pair. However, this effect is not restricted to cyanomethane, all alkyl nitriles show similar trends. If we use MeCN as a probe between water and DMSO, a simple two-band system is observed, Figure 4. This is further evidence for a singly hydrogen bonded species in water.

Nitriles are obviously useful probes, however a greater understanding of the C≡N bond is needed in order to realise the full potential of such
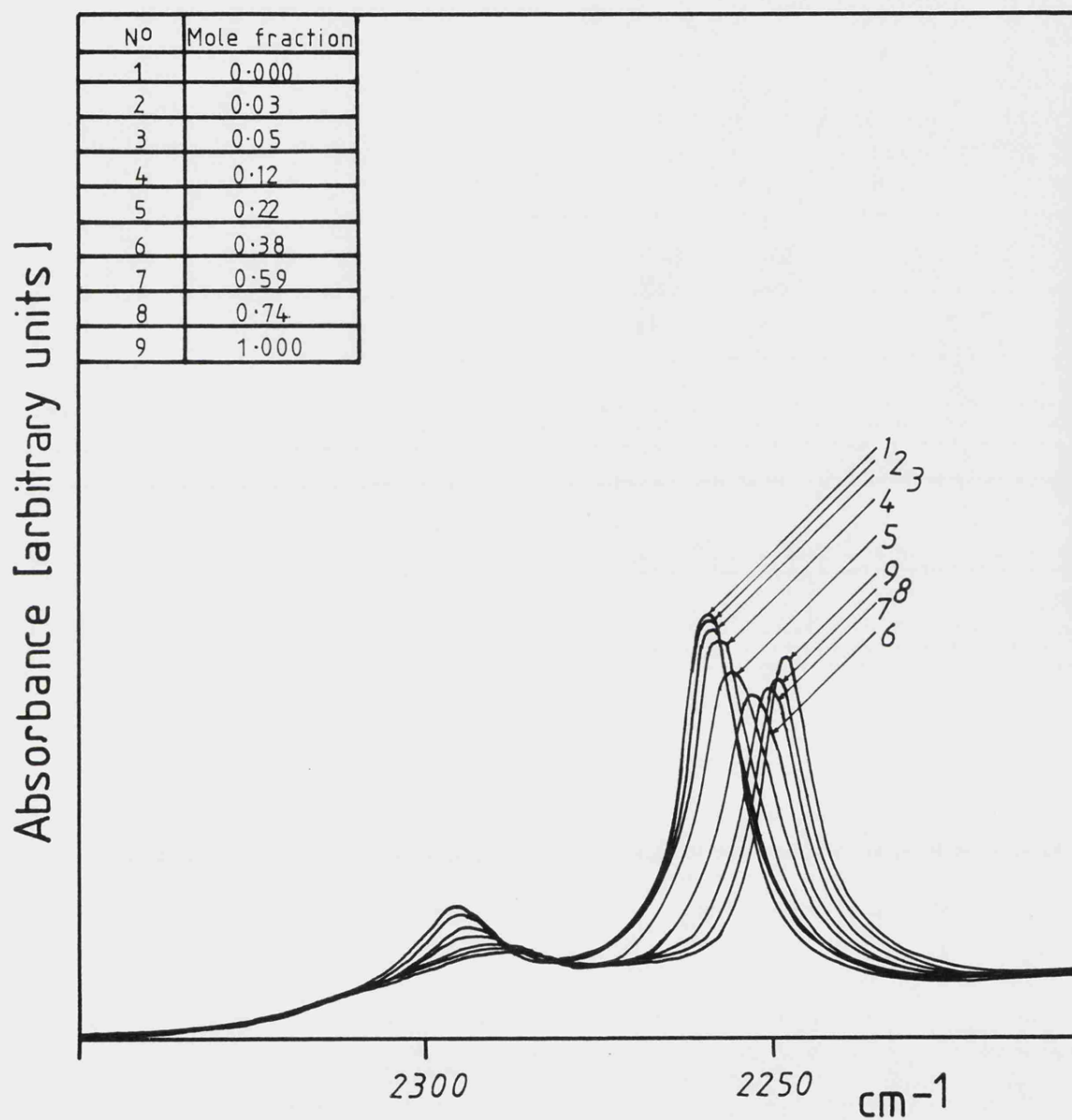
Figure 6.3

Band positions of (a) C≡N stretch of MeCN, (b) C-H stretch of MeCN and (c) C≡N stretch of t-Butyl.CN in various solvents.

KEY

a Hexane
b Tetrachloromethane
c Cyanomethane
d Tetrahydrofuran
e Dimethylsulphoxide
f Methanol
g Water
h Hexafluoroisopropanol

# Figure    6.4

| Nº | Mole fraction |
|----|---------------|
| 1  | 0·000         |
| 2  | 0·03          |
| 3  | 0·05          |
| 4  | 0·12          |
| 5  | 0·22          |
| 6  | 0·38          |
| 7  | 0·59          |
| 8  | 0·74          |
| 9  | 1·000         |

Spectra showing change in C≡N stretch of MeCN in
mixed solvents, Water to Dimethyl Sulphoxide.

as cyanomethane.

## 6.4 HEXAMETHYLPHOSPHORAMIDE (HMPA)

The success of the Triethyl Phosphine Oxide probe work prompted an
investigation into other phosphoryl group containing compounds. One
such was HMPA, which when used as a strong base during various studies
at this laboratory [10-12] had lead to some fairly unusual results. As
with $Et_3PO$ both the infrared $P{=}O$ stretch and $^{31}P$ n.m.r. techniques were
used for the study. Figure 5 shows the linear relationship between the
two measurements. On the other hand, a plot of $^{31}P$ shift against
Gutmann's Acceptor Numbers [13] shows a marked deviation from linearity
(Figure 6). In order to produce a linear plot estimated acceptor numbers
for water and methanol must be used which correspond to a five-bound
solvent state for water and a tri-bound state for methanolic solutions.
This, however, is in agreement with Smith [12] who from water second
overtone OH studies estimated HMPA to be 5 basic. Also during the $Et_3PO$
probe work (Chapter 4) the rate of initial loss of $Et_3PO$ $3.H_2O$ on the
addition of HMPA to an aqueous solution of $Et_3PO$, observed by following
$^{31}P$ shift, occurs at about $2\frac{1}{2}$ times the rate for the addition of DMSO.
If DMSO is taken as a di-base, HMPA then is estimated at 5 basic.

The $P{=}O$ stretching region of HMPA is however complicated by several
bands of uncertain origin, allowing a detailed study in mixed solvents
only when a greater understanding of the nature of this region has been
reached.

## 6.5 UREA

During the work on Amides (Chapter 5) various amides were utilised,
having 0, 1 or 2 exchangeable protons. Urea having four such protons was,

# Figure     6.5

Plot showing relationship between $^{31}$P shift and
P$=$O stretch of HMPA in various solvents.
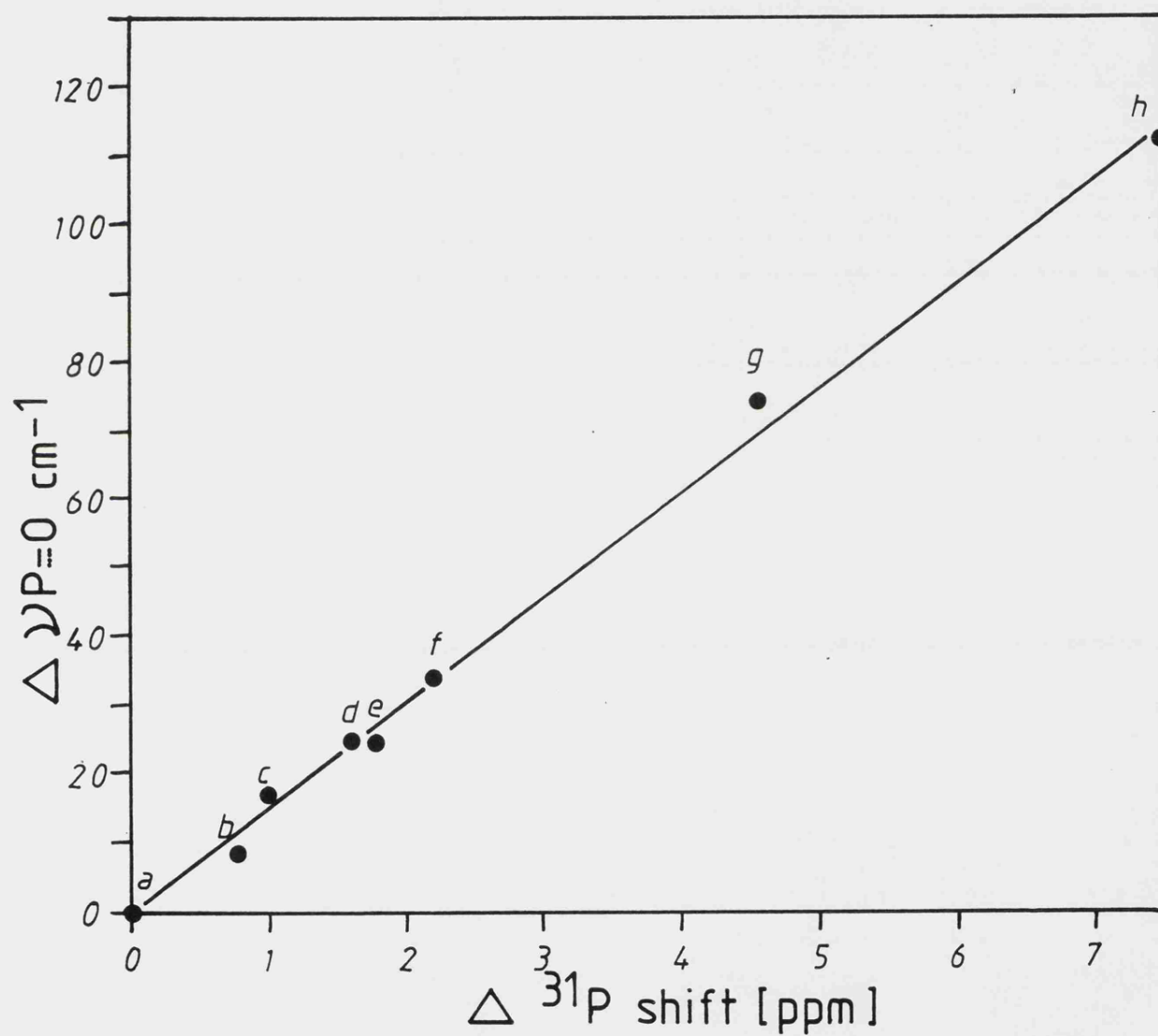


| | KEY | |
|---|---|---|
| a | Hexane | |
| b | Triethylamine | |
| c | Tetrahydrofuran | |
| d | Cyanomethane | |
| e | Dimethylsulphoxide | |
| f | Dichloromethane | |
| g | Methanol | |
| h | Water | |

# Figure 6.6

Plot of $^{31}$P shift against Gutmann's Acceptor
number showing effect of assuming higher
basicities, of HMPA.  [Solvents as Figure 6.5]
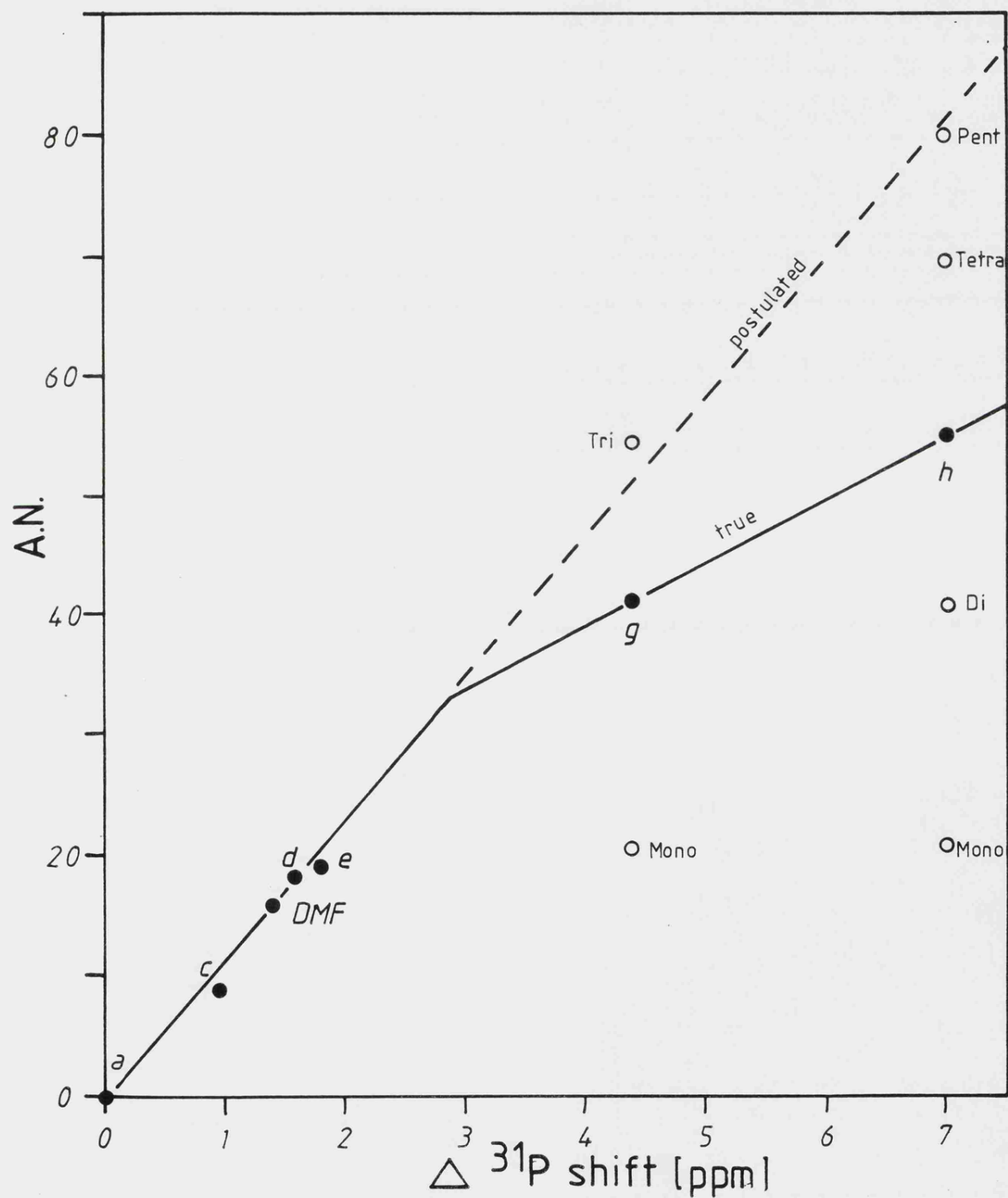
therefore, an obvious extension to that study. The possibility that this compound would produce the same effect on our water model, i.e.

$$H_2O_{bulk} \rightleftharpoons OH_{free} + lp_{free} \qquad \dots \ (1)$$
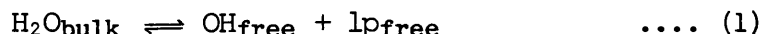
as a di-acid by scavenging $2 \times OH_{free}$ and $4 \times lp_{free}$ with a net increase of $2\ OH_{free}$ has been studied by Jackson [14] and other workers at this laboratory. The results from this work suggest that urea is still acting as a base in water with only a minor $lp_{free}$ 'scavenging' effect by the protons. As for the previously studied amides a linear relationship was observed for the carbonyl band positions in various solvents against those for a fully substituted amide, shown in Figure 7. However, several problems arise, namely (a) urea is not very soluble in many inert solvents, (b) for urea in water the carbonyl spectrum is complex, the main band laying on the line but with a shoulder at higher frequency, (c) the carbonyl band for urea in methanol is also a doublet, with a similar (but slightly larger) separation than that in water, the high frequency band is the one on the line this time. No suitable explanation is available, however the carbonyl bands observed for urea are probably not pure C=O stretch and may well be coupled strongly to C-N stretch or H-N̂-C bending. Any effect such as hydrogen bonding with a cyclic structure utilising both the C=O oxygen and the N-H proton may well lead to new bands. It is interesting to note that for the deuterated compound in deuterated solvents this complexity does not arise, single carbonyl bands are observed in both cases, giving also a linear plot against DMA.


## 6.6  DI-TERT-BUTYL NITROXIDE (DTBN)

This stable radical has been extensively studied by e.s.r. techniques both as a spin label in biological systems [15,16] and as a probe for solvation studies [17,18]. The usual quantity measured for solvent
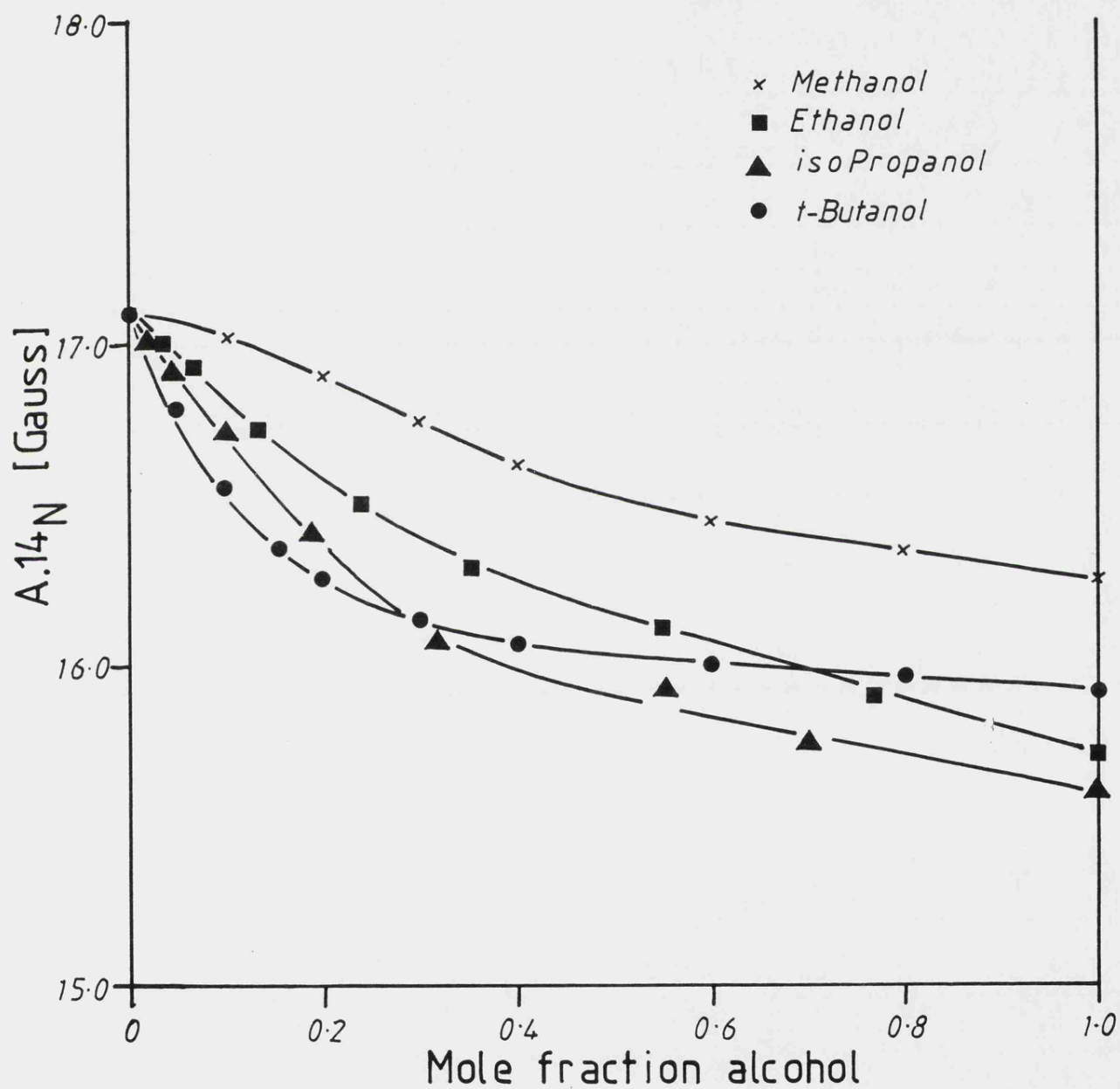
Figure 6.7
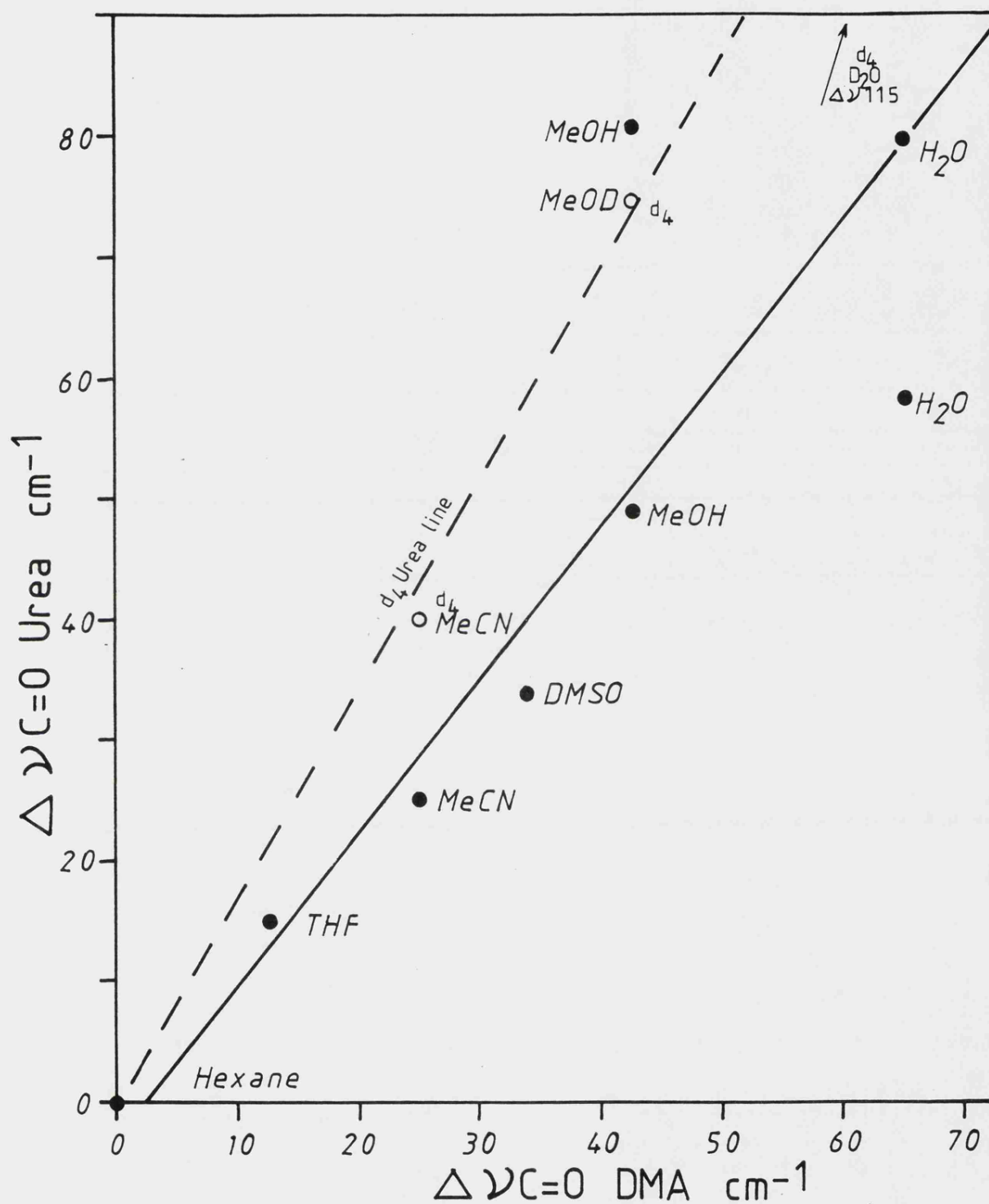
Plot of the C=O stretch of Urea against C=O stretch
of N,N'-Dimethyl Acetamide in various solvents.

studies is the nitrogen hyperfine coupling constant $A(^{14}N)$. This was studied by Smith [18] for many pure solvent systems, and in many mixed solvent systems, however during the $Et_3PO$ probe work on alcohol-water mixed solvent systems it was considered useful to have further information drawn from other established probes. To this end several mixed solvent systems, involving DTBN as probe, for alcohol/water mixtures were studied by e.s.r. The resulting plots of $A(^{14}N)$ versus mole fraction of alcohol are shown in Figure 8, with a typical spectrum shown in Figure 9. It is observed that the initial gradients are very much of the same order relative to each other as those found in the $^{31}P$ n.m.r. studies of Chapter 4 (Figure 4.23) and, therefore, adds support to the arguments presented therein. The main problem associated with the use of such probes is that the e.s.r. technique as for n.m.r. suffers from time-averaged signals. Individual solvated states are rarely seen and most arguments are thus based on assumptions about the various structures involved.

## 6.7 CONCLUDING REMARKS

It is obvious from these previous examples that there is a vast number of possible probe molecules. The main limitations are lack of a suitable observation technique and/or lack of imagination by the worker. Much information about the probe itself and about its environment can be obtained by this type of study, although care must be exercised when dealing with time-averaged quantities.
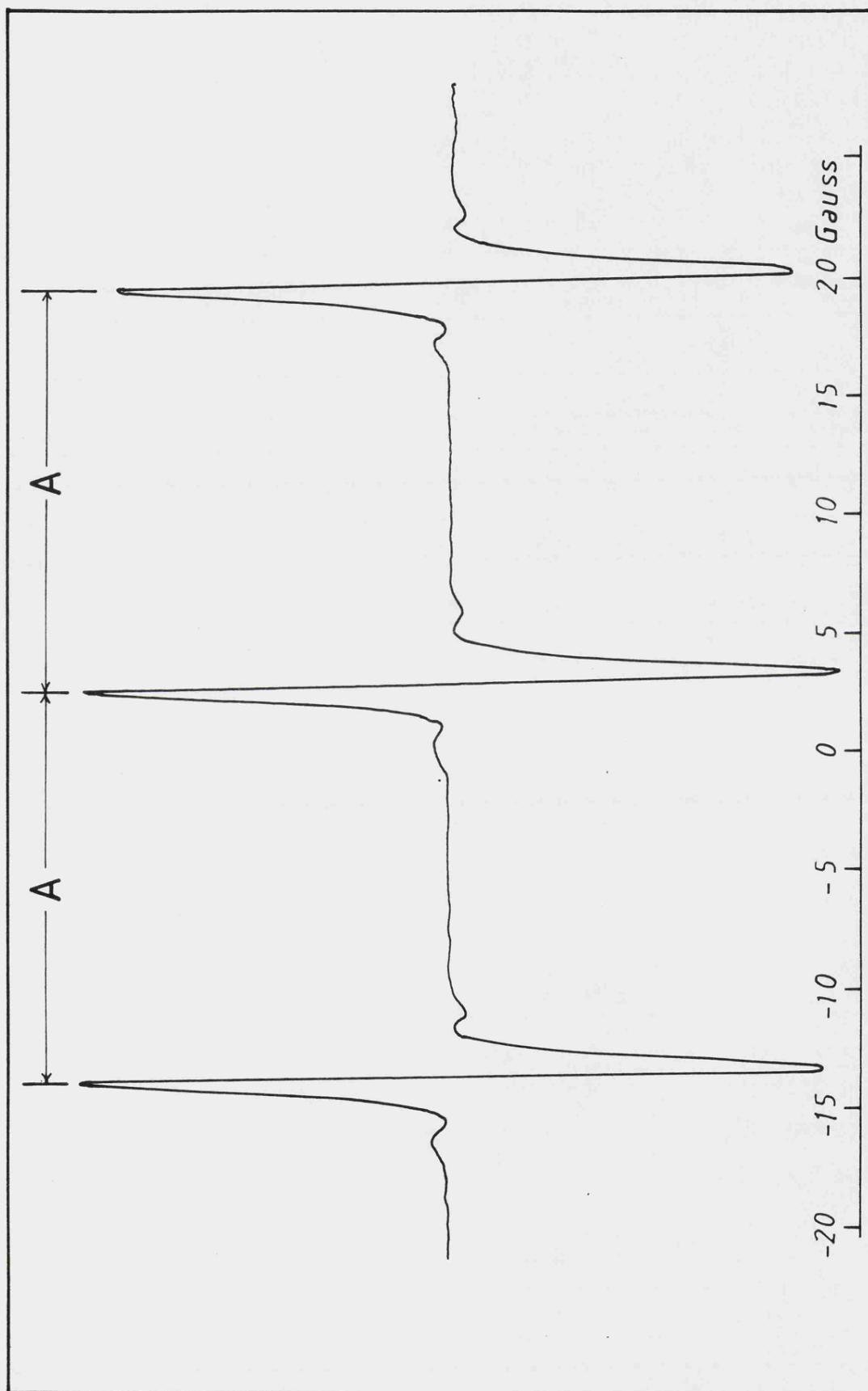
# Figure   6.8



Plot showing change of A($^{14}$N) of DTBN on adding alcohol
to aqueous solution of DTBN.

Figure 6.9

Typical e.s.r. spectrum of Di-tert-Butyl Nitroxide

# REFERENCES FOR CHAPTER 6

1.  L. J. Bellamy, "The Infrared Spectra of Complex Molecules", Vol. 2, Chapman & Hall, (1980).

2.  W. D. Horrocks, Jr. and F. A. Cotton, Spectrochim. Acta, 17, (1961) 134.

3.  J. J. Lindberg and C. Majani, Acta Chem. Scand., 17.5, (1963).

4.  H. Kelm, J. Klosowski and E. Steger, J. Mol. Struct., 28(1), (1975).

5.  G. J. Stafford, P. C. Schaffer, P. S. Leung, G. F. Doebbler, G. W. Brady and E. F. X. Lyden, J. Chem. Phys., 50, (1969) 5.

6.  A. S. Harvey and J. M. Harvey, unpublished results.

7.  D. A. Armitage, M. J. Blandamer, M. J. Foster, N. J. Hidden, K. W. Morcom, M. C. R. Symons and M. J. Wootton, Trans. Faraday Soc., 64, (1968) 5.

8.  A. I. Sidorova, I. N. Kochnev, L. V. Moiseeva and B. N. Narziev, from Zhurnal Strukturnoi Khimii, 9, (1968) 4.

9.  I. S. Perelygin, Optika i Spektroskopiya, 13, (1962) 360.

10. V. K. Thomas, Ph.D. Thesis, Leicester University, (1980).

11. N. J. Fletcher, Ph.D. Thesis, Leicester University, (1981).

12. G. P. Smith, Ph.D. Thesis, Leicester University, (1982).

13. V. Gutmann, "The Donor-Acceptor Approach to Molecular Interactions", Plenum Press, (1978).

14. S. E. Jackson, Ph.D. Thesis, Leicester University, (1980).

15. T. J. Stone, T. Buckman, P. L. Nordio and H. M. McConnell, Proc. Natl. Acad. Sci. USA, 54, (1965) 1010.

16. P. Jost, A. S. Waggoner and O. H. Griffith, in Structure and Function of Biological Membranes, Academic Press, (1971).

17. Y. Y. Lim, E. A. Smith and M. C. R. Symons, J. Chem. Soc., Faraday Trans. 1, 72, (1976) 2876.

18. E. A. Smith, Ph.D. Thesis, Leicester University, (1979).

# CHAPTER 7

## SOLVENT SCALES

## 7.1  INTRODUCTION

The fact that chemical reactions are significantly affected by the solvent in which they take place has been realised for over 100 years [1]. It would therefore seem desirable to be able to predict these effects and to this end many investigations have been undertaken [2-5].

Most studies have been designed to measure some experimental quantity and hence to produce empirical scales of solvent behaviour. Theoretical calculations involving molecular electrostatic interaction models or quantum mechanical methods have generally proved to be unsuccessful.

The classically measured quantities for solvents such as dipole moment $\mu$, dielectric constant $\varepsilon$, only appear to apply to the behaviour of selected groups of solvents. Some correlation between these parameters and other measured quantities that have a wider application appears to exist [6] but must be treated with caution when specific interactions occur.

Because of the difficulties involved with classical and theoretical quantities many workers have turned to the more empirical approach of measuring solvent behaviour as a function of such parameters as rate constants for a known reaction, electronic transitions or infrared band shifts for reference compounds, etc.

Many of the parameters measured during the probe studies covered in this thesis fall into the empirical categories mentioned above. It was therefore considered a useful exercise to compare these measured quantities with the scales of other authors and to try and throw some light on the applicability of these scales to mixed solvent systems.


## 7.2  MAJOR SCALES OF SOLVENT BEHAVIOUR
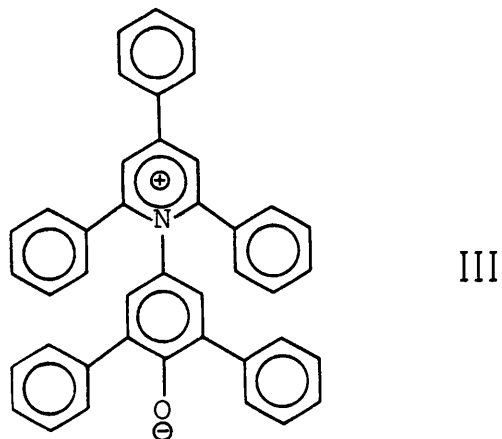
(i)  Z-values

-134-

Kosower proposed a scale of 'solvent polarity' [7] based on the UV
spectrum of 1-ethyl-4-carbomethoxypyridinium iodide.
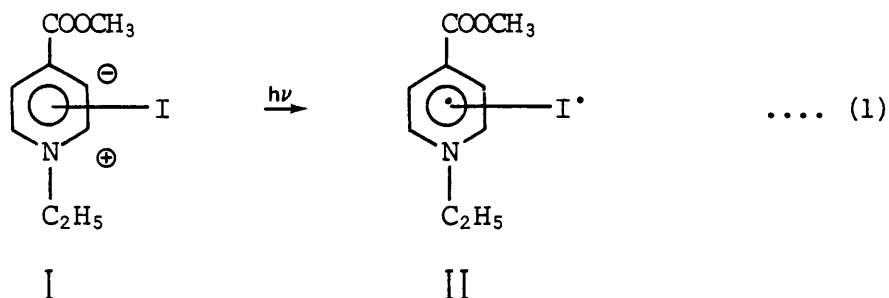


The solvent induced changes in the charge transfer energy are considered
to be an empirical measure of the electrophilic properties of the
solvent, since interaction occurs via electrophilic bonding to the
iodide ion of the ion pair (I). For values see Table 1.

(ii) $E_T$-values

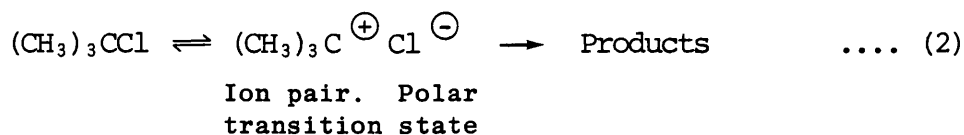A very similar scale to that of Kosower was proposed by Dimroth and
Reichardt [8]. This was based on the energy of the lowest electronic
transition of pyridinium-N-phenol betain III.



This has a large π electron system and although neutral overall has a
highly basic oxygen site. This allows electrophilic attachment by
solvent with the UV spectrum sensitive to this attack. For $E_T$ values
see Table 1.

(iii) <u>Y-values</u>

An earlier system devised for following the electrophilic properties

of solvents was given by Winstein and Grunwald [9]. They considered the

solvolysis of t-butyl chloride.

$$(CH_3)_3CCl \rightleftharpoons (CH_3)_3C^{\oplus} Cl^{\ominus} \longrightarrow Products \qquad \dots (2)$$

**Ion pair. Polar**
**transition state**

The stabilisation of the transition state will essentially depend upon

electrophilic interaction of solvent with the halide ion. The 'Y' value

was defined by an equation relating the first order rate constants in a

solvent S to a standard solvent $S^\circ$:-

$$Y = \log \frac{k^S}{k^{S^\circ}} \qquad \dots (3)$$

The standard solvent chosen was ethanol : water 4:1 by volume. Some Y

values can be found in Table 1.


(iv) <u>G-values</u>

Allerhand and Schleyer [10] noted that the X-H stretching frequency

for the infrared spectra of X—H----A complexes was solvent sensitive and

correlated linearly with stretch (for probes in the same solvents). The

more usual measure is one of solvent nucleophilicity and results in a

shift of X-H stretch (vapour or totally inert solvent) to the X—H----B

complex, i.e. free → bound [11]. The shifts reported by Allerhand and

Schleyer should, however, be independent of specific interactions and be

a measure of bulk and/or dipolar effects.

$$aG = \frac{(\nu^\circ - \nu^S)}{\nu^S} \qquad \dots (4)$$

with $\nu^\circ$ - the X-H stretching frequency of the complex in the
vapour

$\nu^s$ - the X-H stretching frequency of the complex in the solvent

a - a function of the infrared oscillator

G-values were then calculated using shift of the methanol-ether and phenol-ether complexes (O-H····ether stretch) and $>C=O$ stretch of benzophenone and dimethylformamide with also $>S-O$ stretch of dimethyl-sulphoxide, in various solvents. See Table 1 for quoted G-values.

(v) α and β - scales

Taft and co-workers [12-15] used what they called a "solvatochromic comparison method" in order to produce scales of hydrogen-bonding capability of solvents. In essence this is based on the idea that a plot of spectral shifts for an electrophilic probe against those for a nucleophilic probe in non-hydrogen bonding solvents should result in a linear regression. All hydrogen bonded solvents will lie off the line, the magnitude of their deviation from the line being a measure of their hydrogen bonding capability either as a donor or acceptor.

The direction of deviation from the regression line would depend upon whether the hydrogen bond former is an electron donor or acceptor. For most applications it is easier to use the plot of an ampiphilic probe against that of either the electrophilic or nucleophilic probe. Thus a single deviation is observed for hydrogen bonding due to the electron donating or accepting properties of the solvent respectively.

For the β-scale of solvent basicity, i.e. electron donating capability, Taft measured the shifts of the electronic transition for 4-nitroaniline (eqn. 5) against that of the N,N-diethyl-4-nitroaniline. The former compound is both electrophilic and nucleophilic whereas the diethyl compound is only nucleophilic. The plot correlating the two for various non-hydrogen bonding solvents is linear with the hydrogen bonding solvents

.... (5)
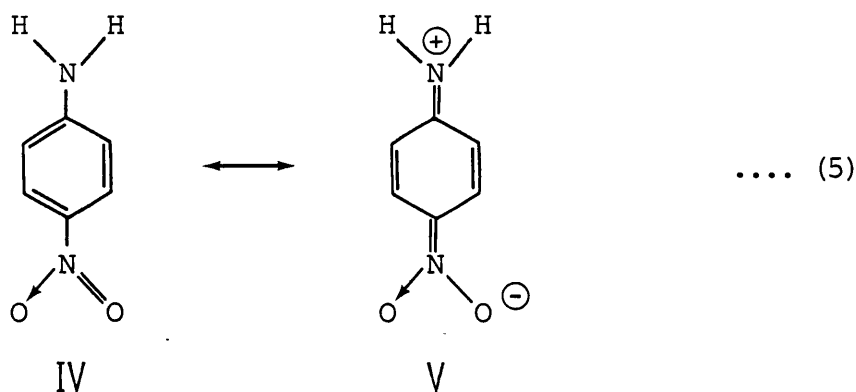
displaced down the nitroaniline axis. This displacement is then used to calculate the relative basic strengths of the various solvents, denoted as β-values. See Table 1 for values.

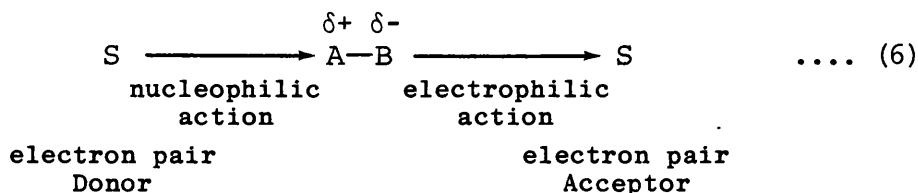Several compounds were used to construct a corresponding scale of α-values, i.e. the electron acceptor capability of the solvents. Some of the main compounds chosen were those used by other workers such as Dimroth [8], Kosower [7], Brooker [16], etc.. The shifts of the various electronic transitions of these compounds were correlated with the shifts for the electronic transitions of 4-nitroanisole (VI).
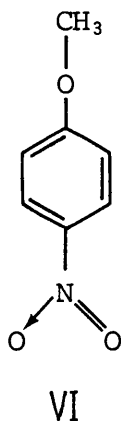


The deviations of the various hydrogen-bonding solvents are along the various compound axes rather than the 4-nitroanisole axes indicating the electrophilic character of the solvents, i.e. their relative acidities. These relative acid strengths were denoted as α-values, a selection of which are seen in Table 1.

(vi) <u>Donor Numbers (DN) and Acceptor Numbers (AN)</u>

The concept that solvent interactions are akin to the classical Lewis acid-base situation was proposed by Gutmann and co-workers [5,17,18]. They suggested that solvent attack on a solute could be described by the scheme:-

$$S \xrightarrow[\substack{\text{nucleophilic}\\\text{action}\\\text{electron pair}\\\text{Donor}}]{} \overset{\delta+ \;\; \delta-}{A—B} \xrightarrow[\substack{\text{electrophilic}\\\text{action}\\\text{electron pair}\\\text{Acceptor}}]{} S \qquad \dots\text{(6)}$$

A suitable measure of the electron donor strength of a solvent was suggested as, "The molar enthalpy value for the reaction of the donor with antimony pentachloride $SbCl_5$ as a reference acceptor in a $10^{-3}$ M solution of dichloroethane".

$$D + SbCl_5 \rightleftharpoons D.SbCl_5 \qquad (-\Delta H_{D.SbCl_5} \equiv DN) \qquad \dots\text{(7)}$$

It was also found that there was a linear relationship between these donor numbers and $^{23}Na$ n.m.r. shifts of $NaClO_4$ in various solvents [19] and $^{19}F$ n.m.r. shifts of $CF_3I$ in various solvents [20] and also $^{29}Si$ n.m.r. shifts of silanols in various solvents. This has enabled the range of donor numbers to be extended.

The measure of the electron acceptor strength of various solvents was pursued using a probe that should only act as an electron donor. The compound chosen was triethylphosphine oxide $Et_3PO$. The bulky alkane groups prevent nucleophilic attachment at the phosphorus but allow electrophilic attachment at the oxygen. The effect was followed by $^{31}P$ n.m.r. and a solvent acceptor number (AN) defined by:-

$$AN = \frac{\delta_{corr}}{\delta_{corr} \; (SbCl_5.Et_3PO)} \times 100 \qquad \dots\text{(7)}$$

$$AN = \delta_{corr} \times 2.348 \qquad \dots\text{(8)}$$

$\delta_{corr}$ values are chemical shifts of the $^{31}P$ of $Et_3PO$ extrapolated to infinite dilution and measured relative to hexane solution.

$\delta_{corr}$ ($SbCl_5.Et_3PO$) is the shift of the antimony pentachloride adduct in dichloroethane at $10^{-3}$ M.

The AN for this adduct was arbitrarily assigned a value of 100 and the other AN values scaled accordingly. Donor numbers and acceptor numbers can be found in Table 1.

## 7.3  RESULTS AND DISCUSSION

Triethyl phosphine oxide was chosen by Gutmann [5] as a good n.m.r. probe on which to base a scale of solvent acceptor numbers. This compound was also studied in our work as an infrared and n.m.r. probe. The linear correlation between infrared and n.m.r. was demonstrated in Chapter 4. It would therefore be expected that AN would correlate with the infrared shift of the P===O stretching frequency (Fig. 1a) and this indeed is found to be the case.

However, if a similar plot is constructed for the infrared shift of the C=O stretching frequency against AN (Fig. 1b), it is immediately obvious that significant deviations occur from linearity. These deviations occur primarily for the protic solvents and can be explained by considering the solvent-probe interactions. The AN scale is based on $Et_3PO$ as probe and as we have already seen in Chapter 4 when in an aqueous environment this is a 'tri-bound' situation, i.e. 3 hydrogen bonds to the probe. However for acetone as probe in an aqueous system only a 'di-bound' situation is observed (see Chapter 3). For alcoholic systems $Et_3PO$ is mostly 'di-bound' and acetone 'mono-bound'. By correlating these various states observed in the infrared P===O stretch (see Chapter 4) region, with the $^{31}P$ shift or AN, an approximate AN for

TABLE 7.1

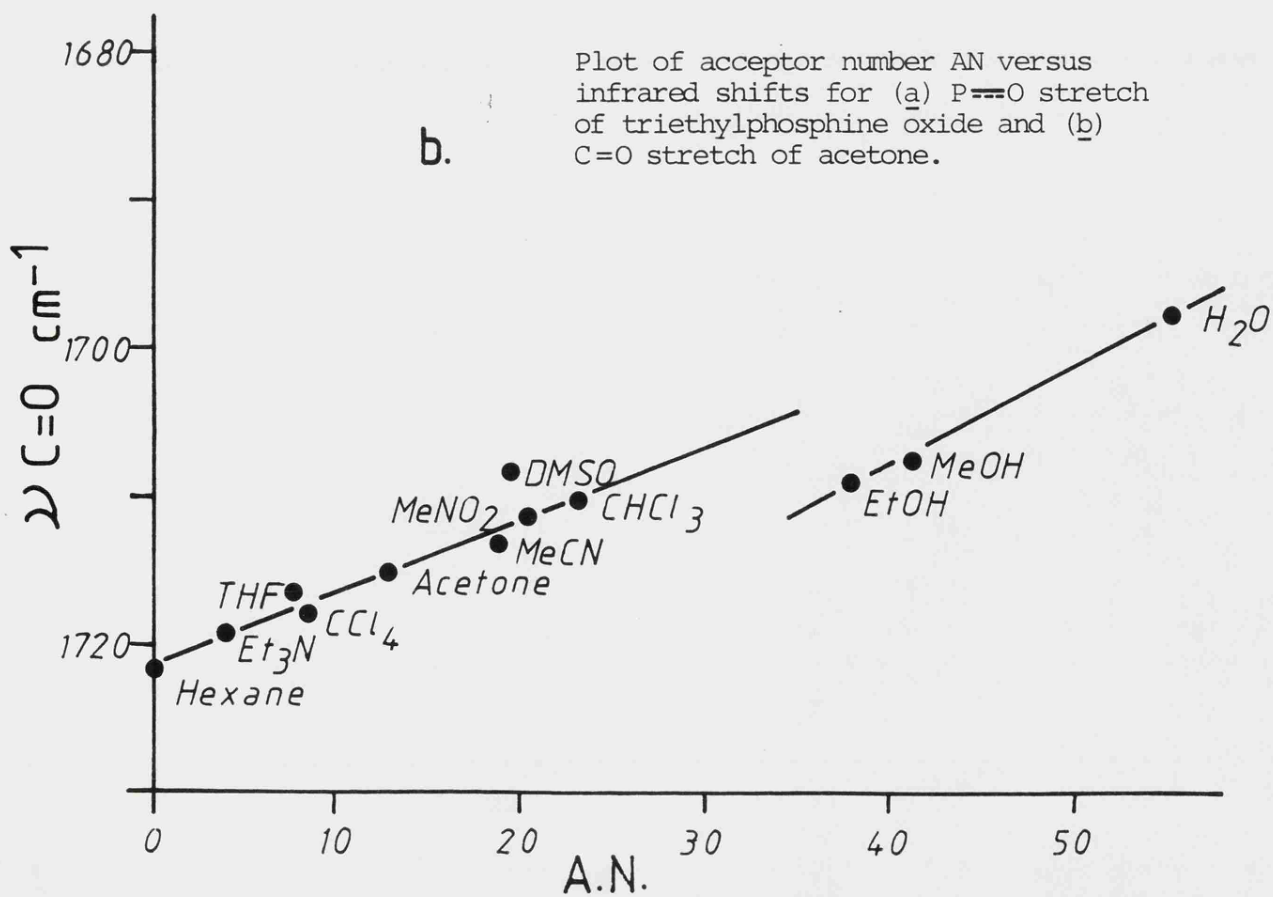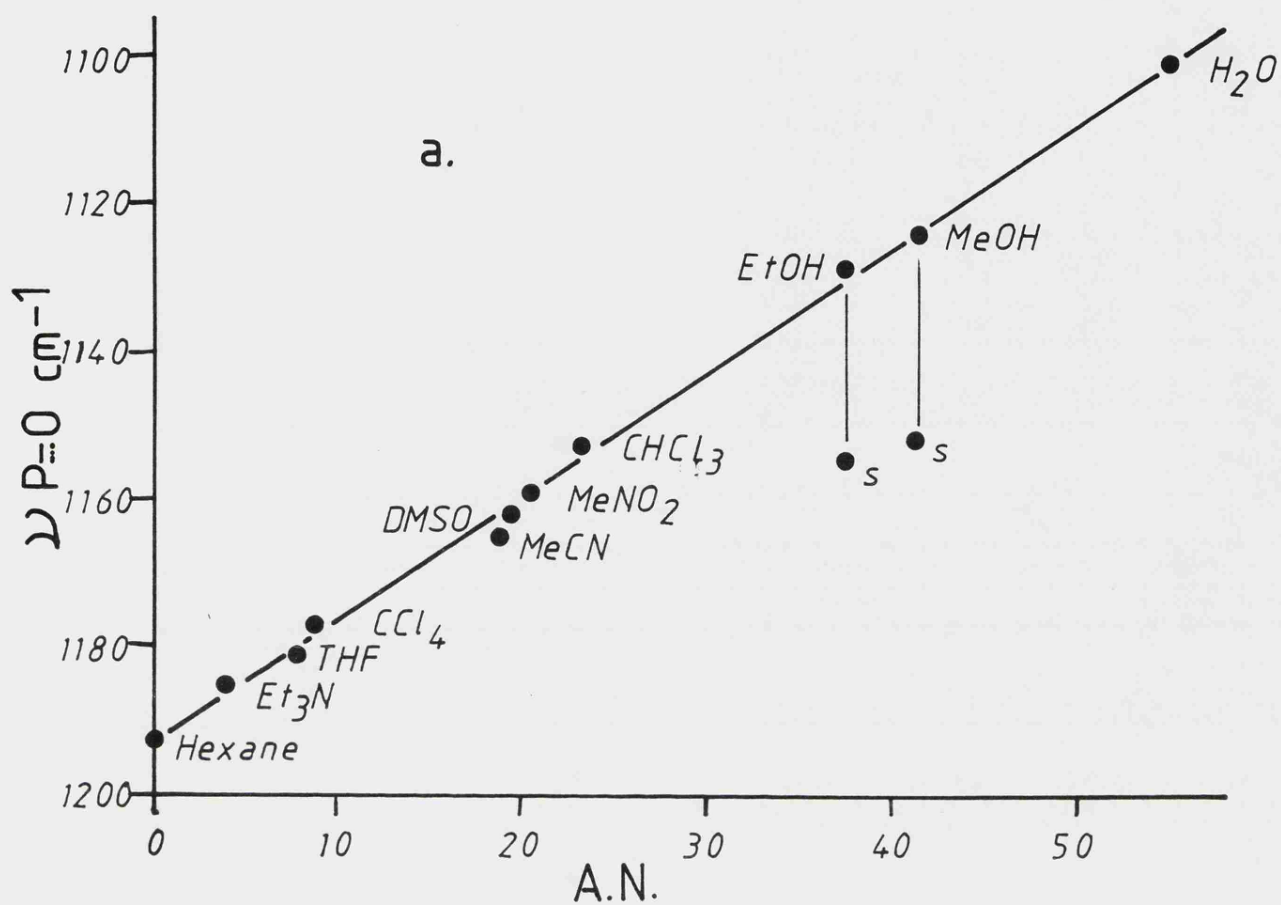Various solvent scale values

| Solvent | AN | DN | Z k·cal mol⁻¹ | E_T k·cal mol⁻¹ | Y | G | α | β | ε | μ Debye |
|---|---|---|---|---|---|---|---|---|---|---|
| Hexane | 0.0 | – | – | 30.9 | – | 44 | 0.0 | 0.0 | 1.9 | 0.0 |
| Triethylamine | 4.2 | 61/30.7* | – | – | – | 62 | 0.0 | 0.70 | 2.4 | 0.9 |
| Tetrahydrofuran | 8.0 | 20 | 58.8 | 37.4 | – | – | 0.0 | 0.55 | 7.4 | 1.7 |
| Tetrachloromethane | 8.6 | – | – | 32.5 | – | 69 | 0.0 | – | 2.2 | 0.0 |
| Acetone | 12.5 | 17.0 | 65.6 | 42.2 | – | – | 0.1 | 0.51 | 20.7 | 2.9 |
| Dimethylacetamide | 13.6 | 27.8 | 66.9 | 43.7 | – | – | 0.0 | 0.73 | 37.8 | 3.8 |
| Cyanomethane | 18.9 | 14.1 | 71.3 | 46.0 | – | 93 | 0.29 | – | 36.0 | 3.4 |
| Dimethylsulphoxide | 19.3 | 29.8 | 71.1 | 45.0 | – | – | 0.0 | 0.74 | 46.7 | 3.9 |
| Nitromethane | 20.5 | 2.7 | 71.2 | 46.3 | – | 99 | 0.29 | – | 36.7 | 3.6 |
| Trichloromethane | 23.1 | – | 63.2 | 39.1 | – | 106 | – | – | 4.7 | 1.1 |
| i.Propanol | 33.5 | – | 76.3 | 48.6 | -2.73 | – | 0.69 | 0.92 | 18.3 | 1.7 |
| Ethanol | 37.1 | 20.0 | 79.6 | 51.9 | -2.03 | – | 0.85 | 0.77 | 24.3 | 1.7 |
| Methanol | 41.3 | 19.0 | 83.6 | 55.5 | -1.09 | – | 0.99 | 0.62 | 32.6 | 1.7 |
| Water | 54.8 | 18.0 | 96.6 | 63.1 | -3.49 | – | 1.02 | 0.14 | 78.5 | 1.8 |

* 61 from Gutmann [5]
  30.7 from Taft [15]

# Figure 7.1



a.

Plot of acceptor number AN versus
infrared shifts for (a) P=O stretch
of triethylphosphine oxide and (b)
C=O stretch of acetone.

b.

the di-bound and mono-bound species can be obtained. Plotting these
values against infrared C=O stretch gives a good linear relationship
(Fig. 2). This example illustrates the danger of applying such solvent
parameters without considering the solvation differences between
differing solutes. Other probe studies lend further weight to this
argument (Figs. 3 and 4).

Donor numbers, on the other hand, appear to be more generally
applicable. For simple acceptor solutes such as alcohols a linear
relationship is found between the infrared OH stretch and DN (Fig. 5).

Many of the other solvent scales result in very inconclusive
correlations when plotted against the various infrared and n.m.r. shifts
observed during the probe studies, a selection of plots illustrates this
point (Figs. 6 to 9). This lack of overall agreement is probably due to
many different factors. The 'bulk' effect scales can generally be seen
to be applicable to only certain groups of compounds. The spectroscopic
scales appear to be very dependent upon the type of probe and type of
transition being observed which makes interrelation very difficult. Two
types of scales stand out as having a reasonable degree of correlation
with the type of work included in this thesis, namely 'Gutmann's'
Acceptor and Donor numbers and 'Taft's' $\alpha$ and $\beta$ numbers where attempts
have been made to separate the nucleophilic and electrophilic solvent
effects.

Mixed solvent systems present a somewhat different situation. Whilst
various solvent parameters for the pure solvents may be irregular, one
may expect a fairly uniform change occurring upon mixing through a mole
fraction range. This may well be the case for a bulk property of a
mixture of two dipolar aprotic solvents. However, where specific inter-
actions occur such as hydrogen bonding, marked deviations from linearity
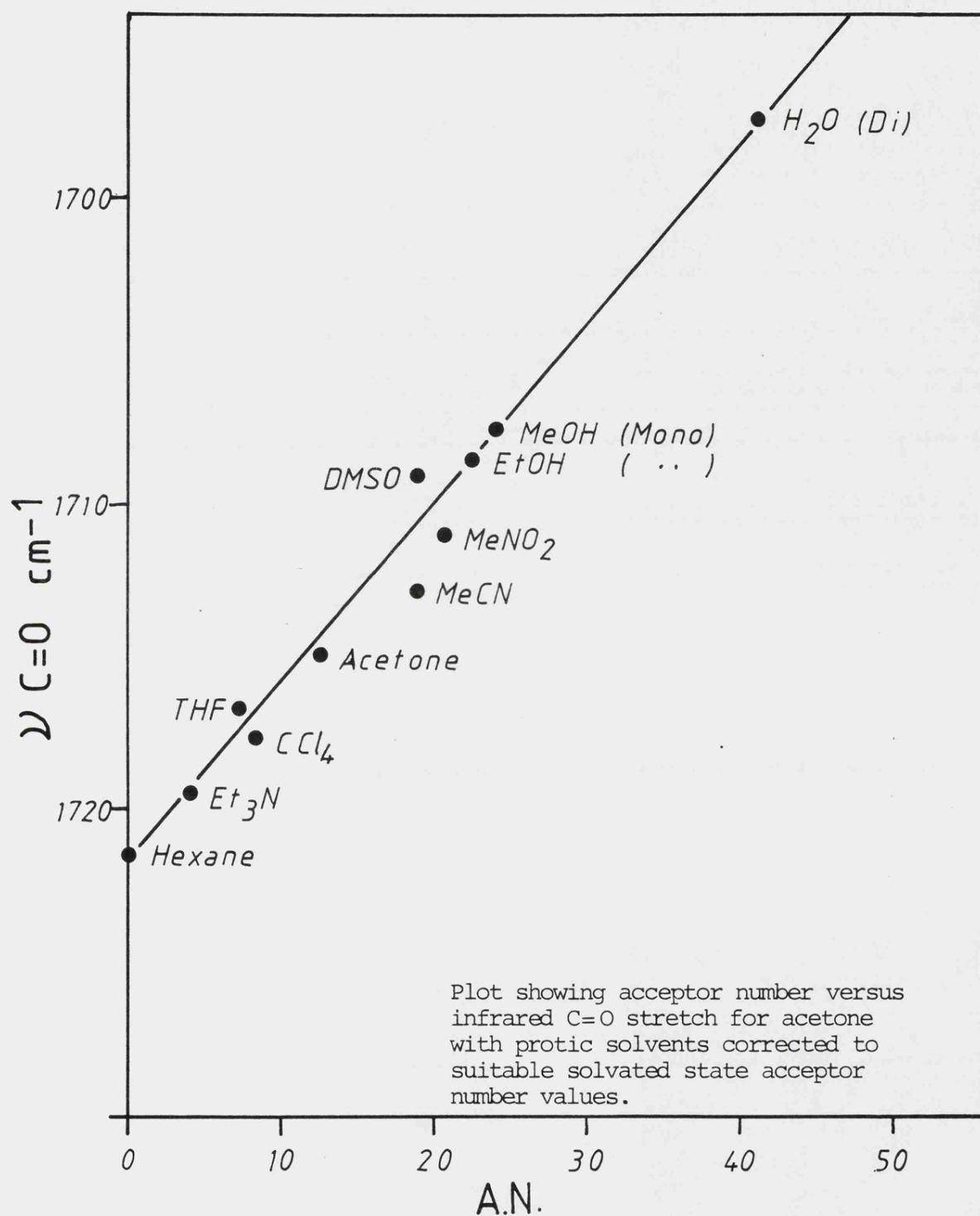
# Figure    7.2



Plot showing acceptor number versus
infrared C=O stretch for acetone
with protic solvents corrected to
suitable solvated state acceptor
number values.

# Figure   7.3

Plot showing acceptor number versus infrared C=O
stretch for Dimethyl acetamide (DMA) and N-Methyl
acetamide (NMA).

# Figure 7.4
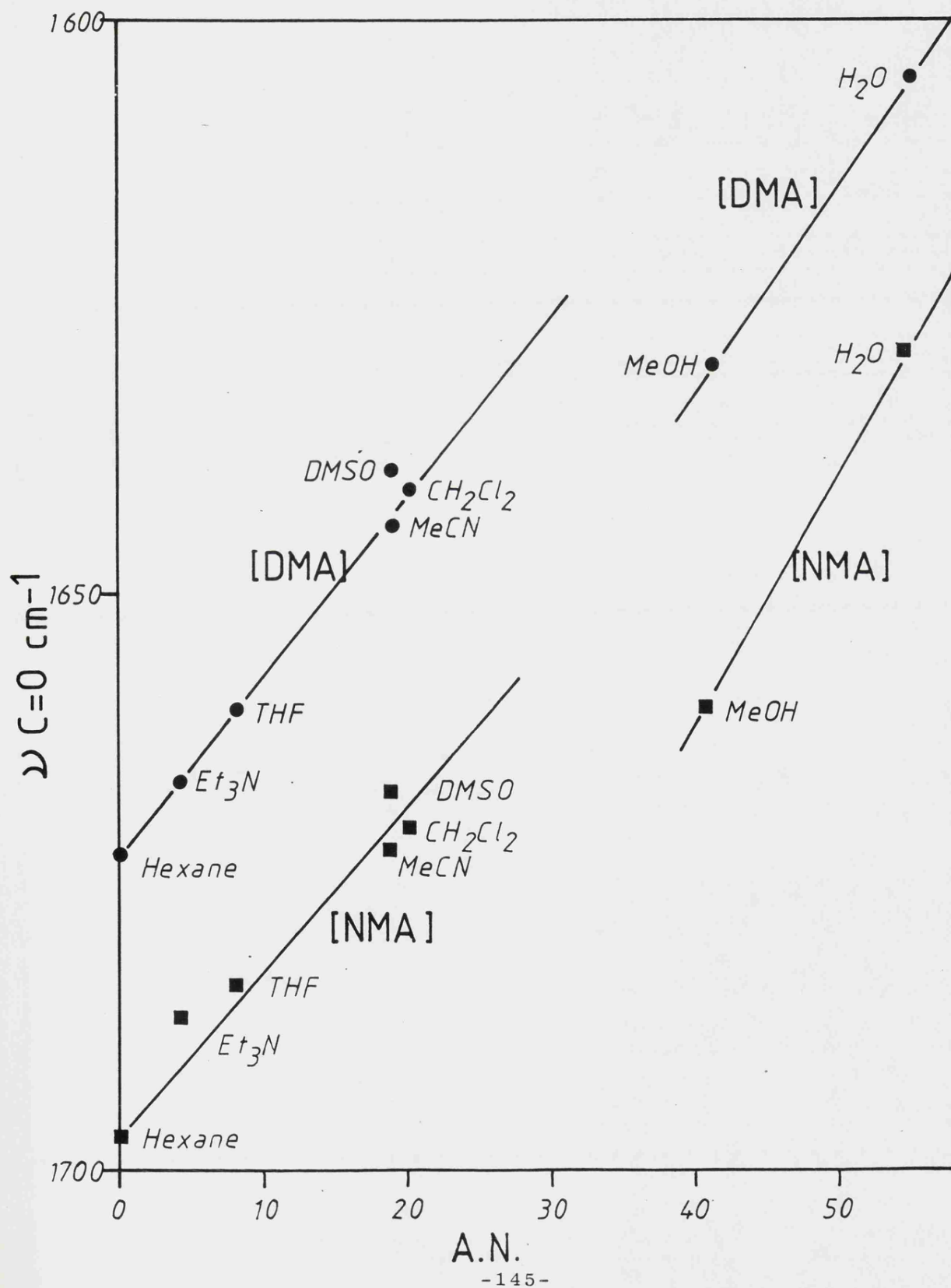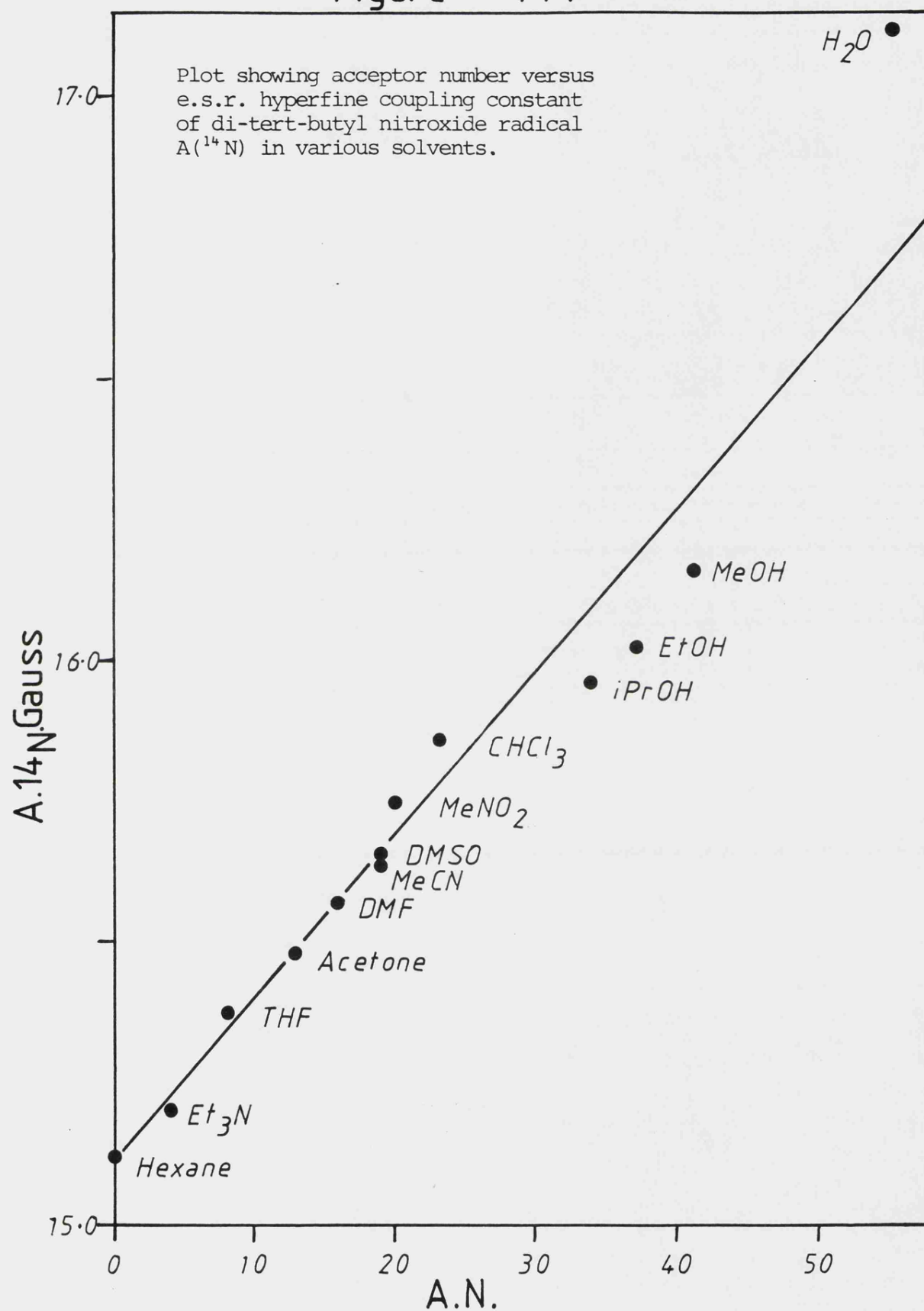


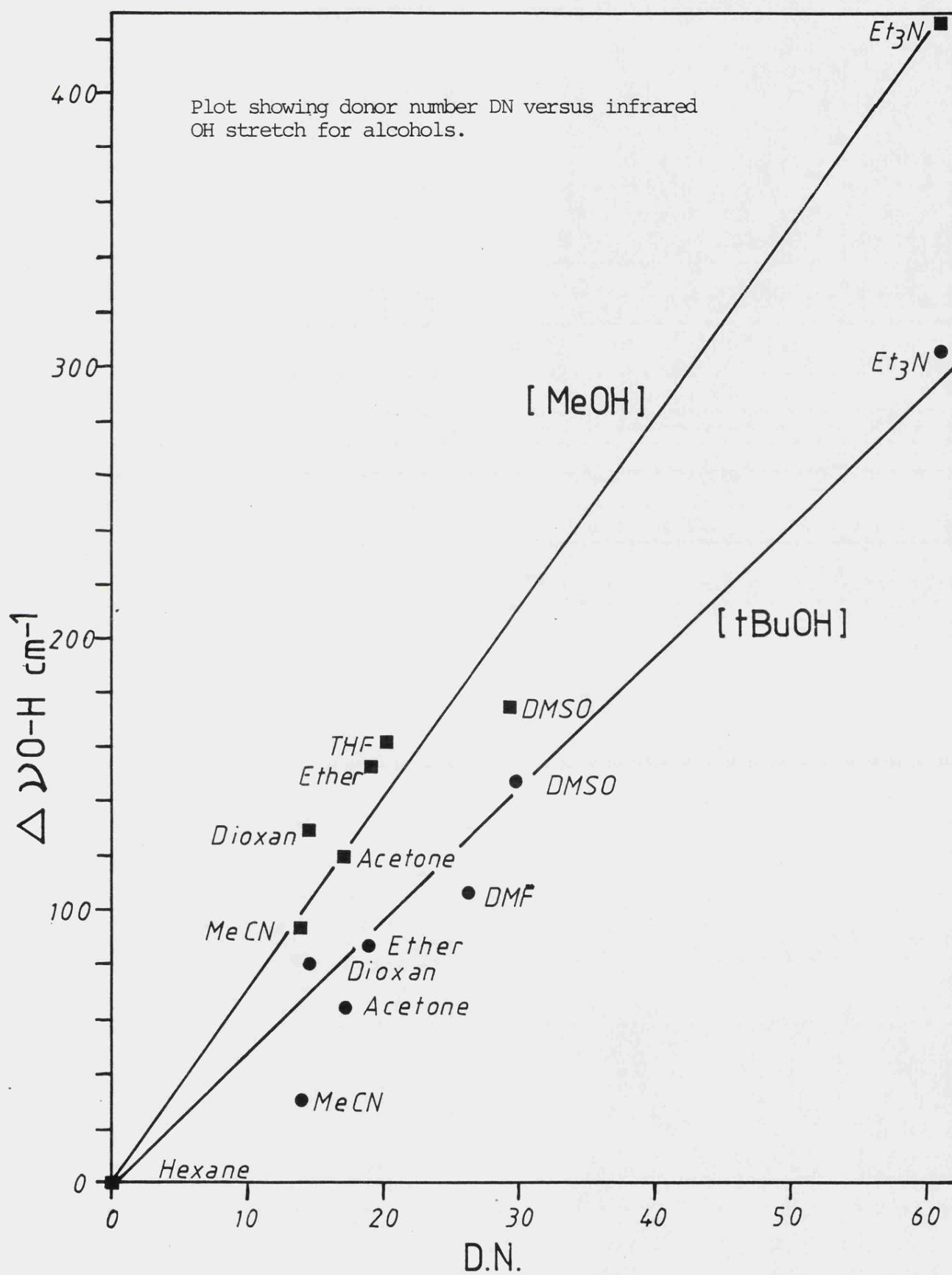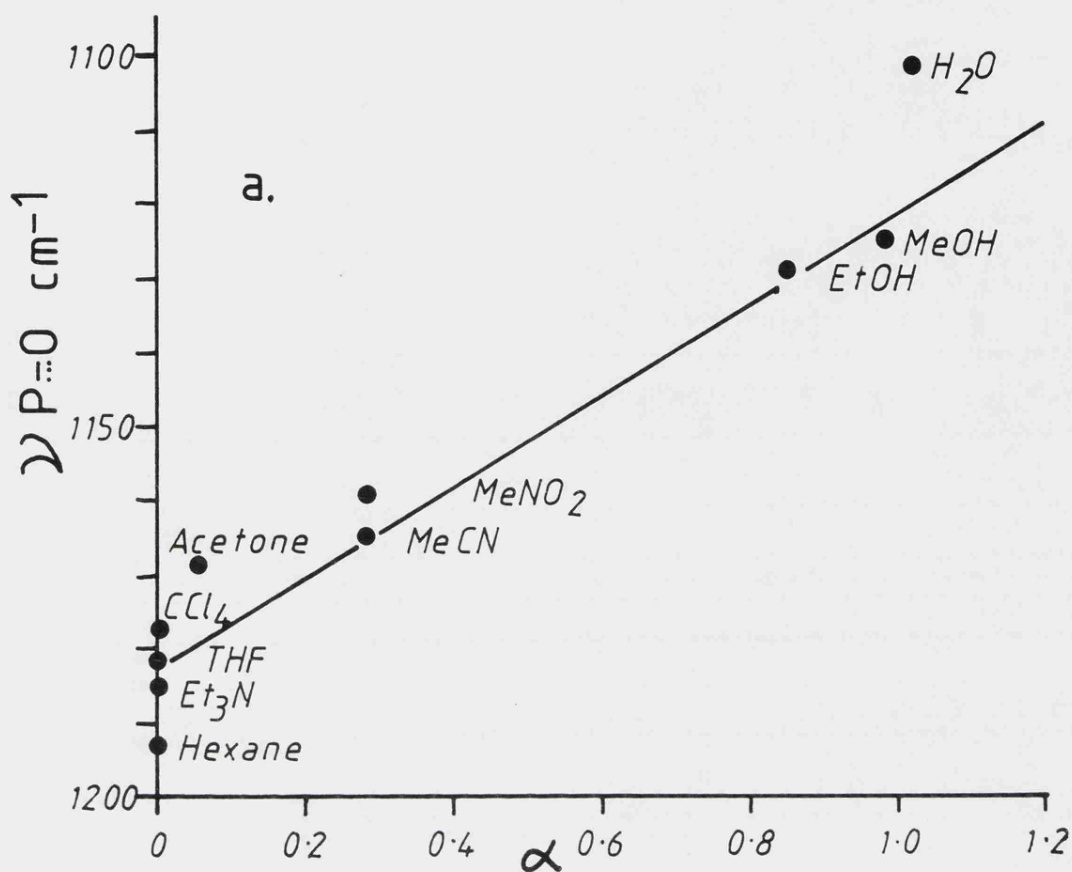Plot showing acceptor number versus
e.s.r. hyperfine coupling constant
of di-tert-butyl nitroxide radical
$A(^{14}N)$ in various solvents.

# Figure 7.5



Plot showing donor number DN versus infrared OH stretch for alcohols.

Figure    7.6

Plot of α values versus infrared for
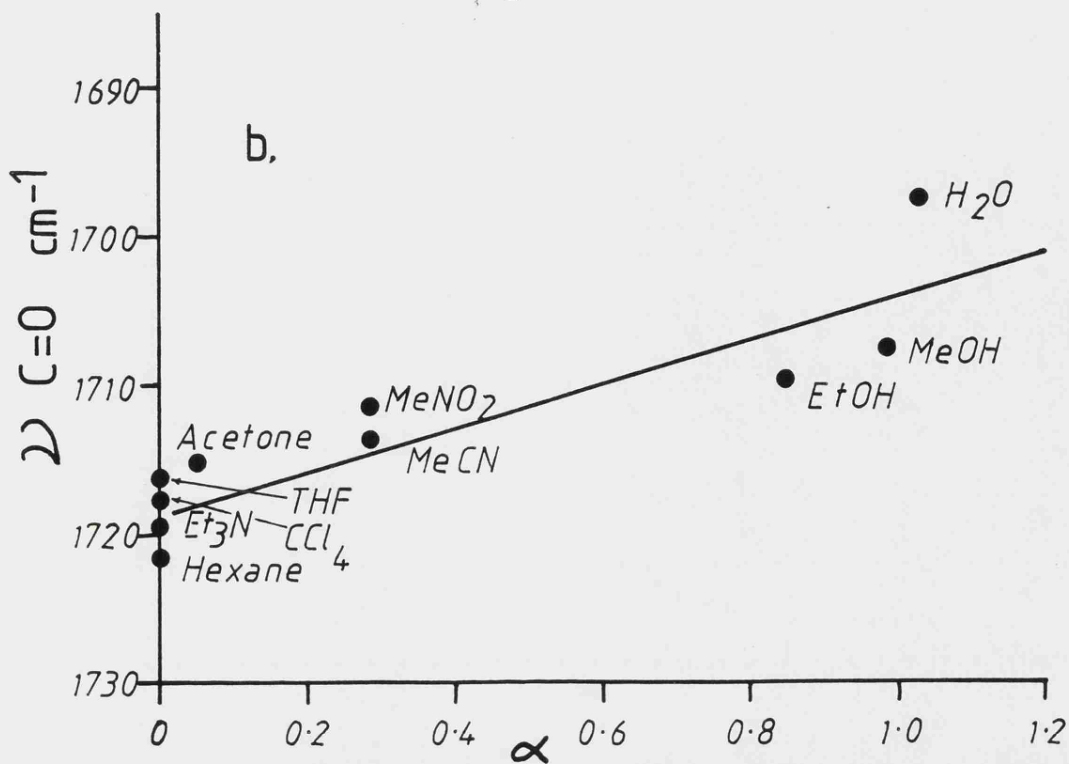(a) P═O stretch of triethylphosphine
oxide and (b) C=O stretch of acetone.

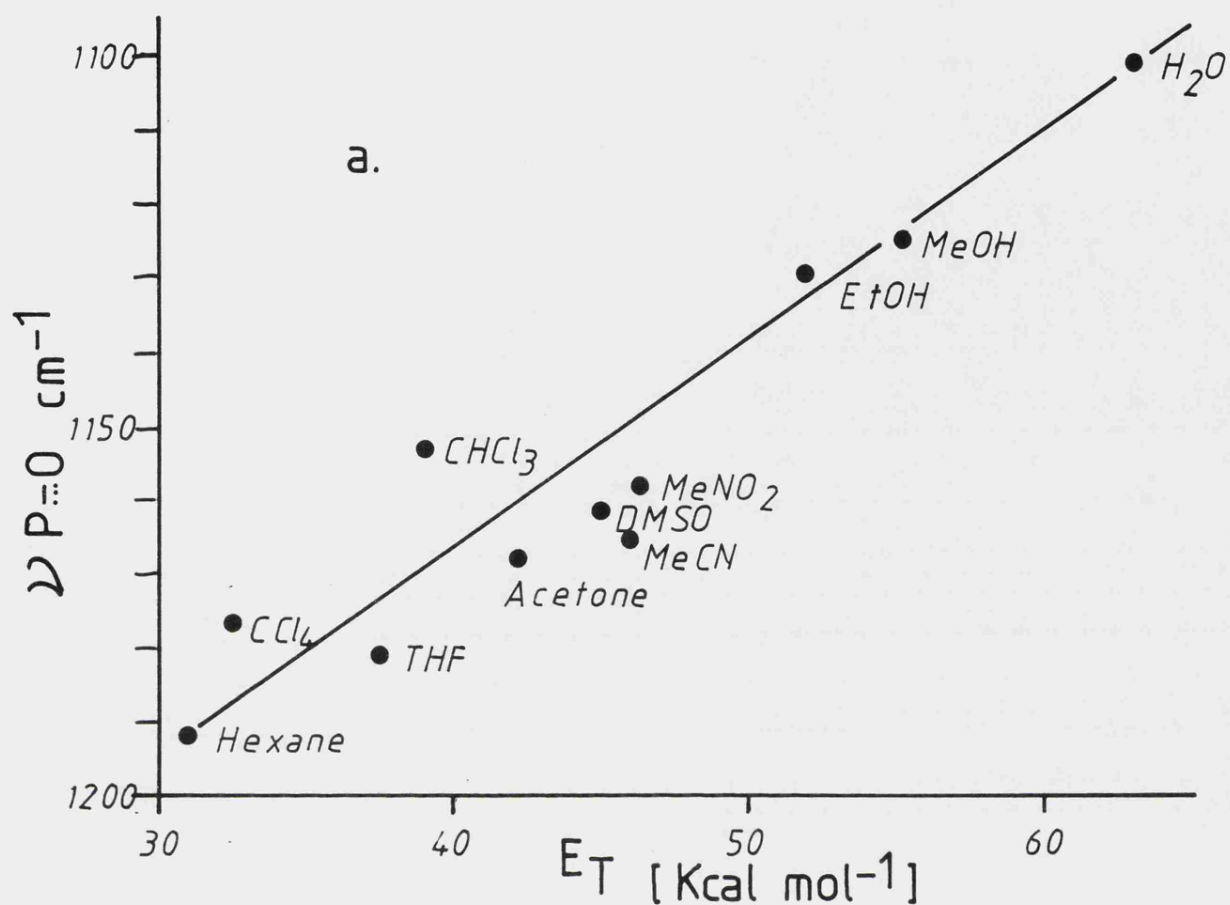# Figure 7.7



Plot showing $E_T$ values versus infrared (a) P≡O stretch of triethylphosphine oxide and (b) C=O stretch of acetone.

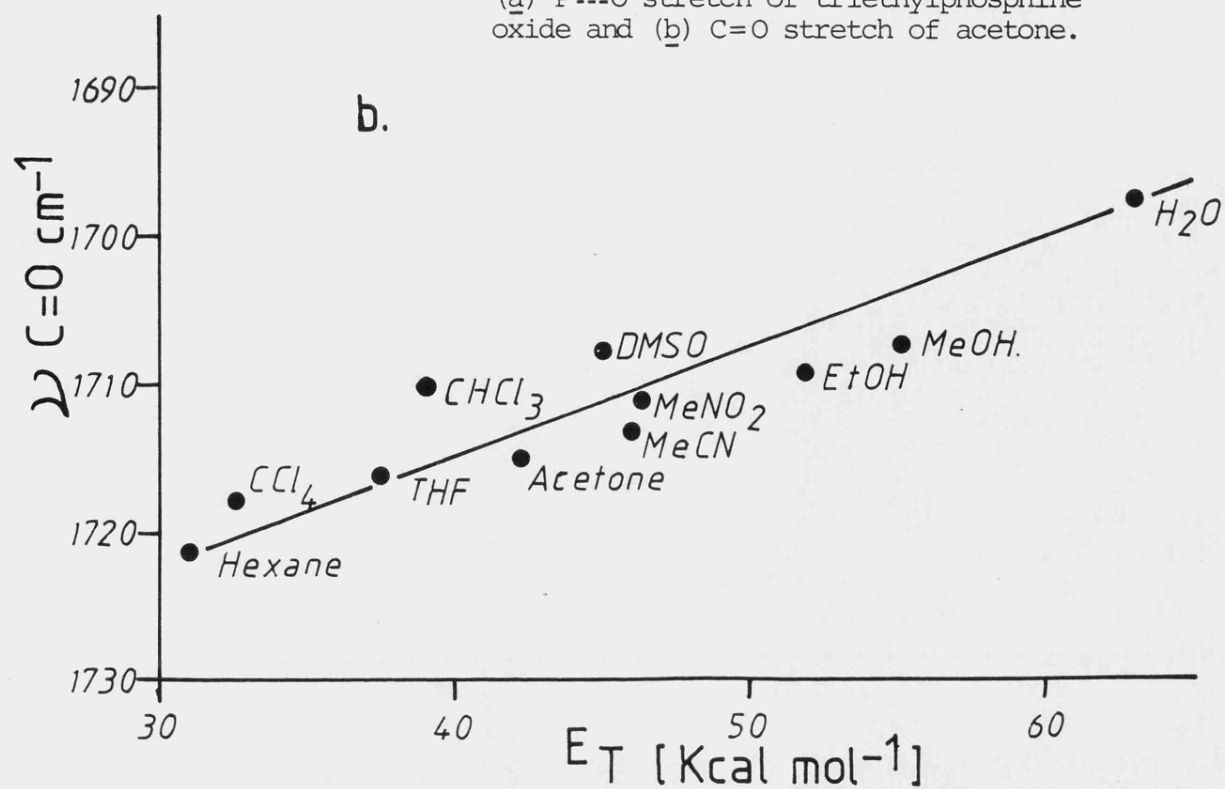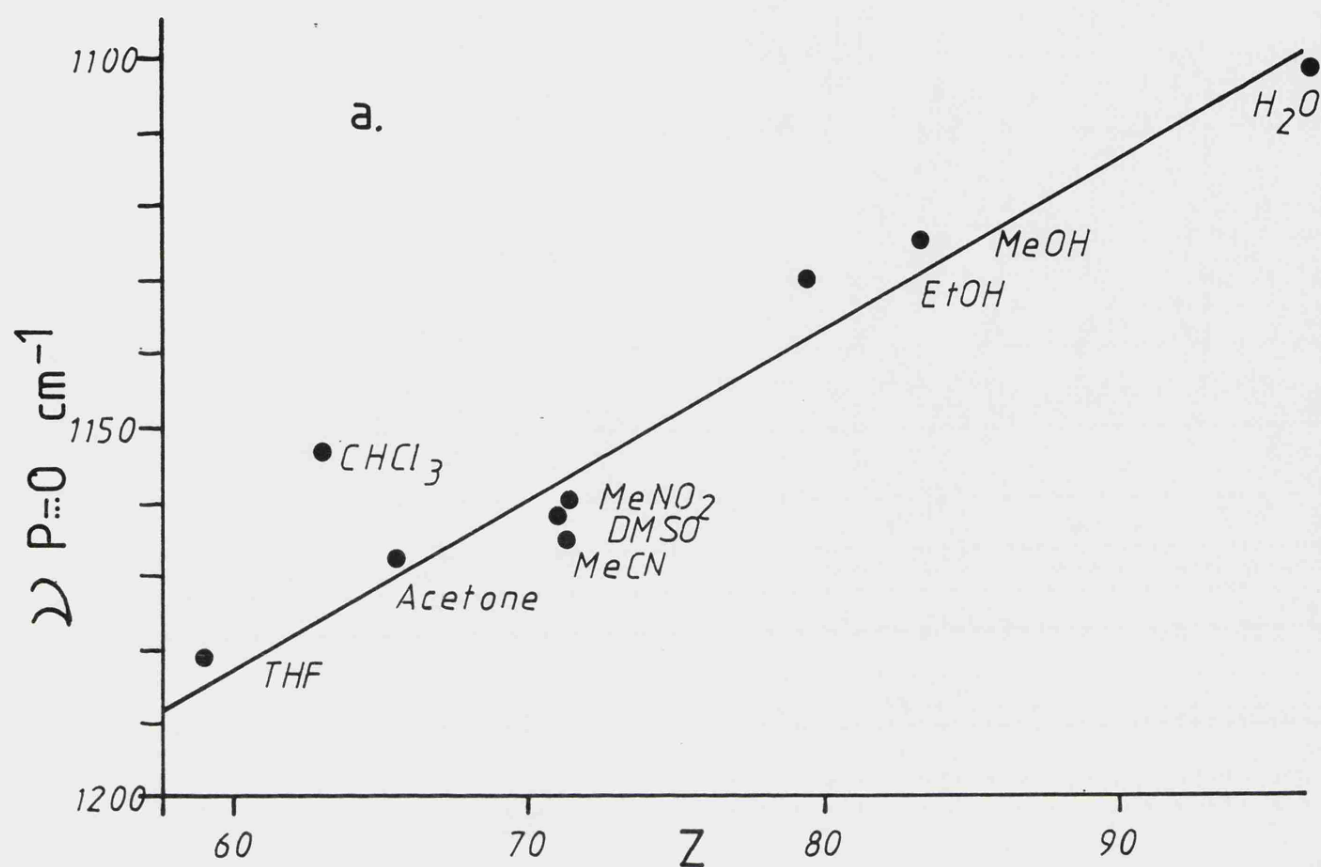# Figure    7.8



Plot of Z values versus infrared shift
(a) P=O stretch of triethylphosphine
oxide and (b) C=O stretch of acetone.

Figure 7.9

Plot showing dielectric constant versus infrared (a) P≡O stretch of triethyl phosphine oxide and (b) C=O stretch of acetone.

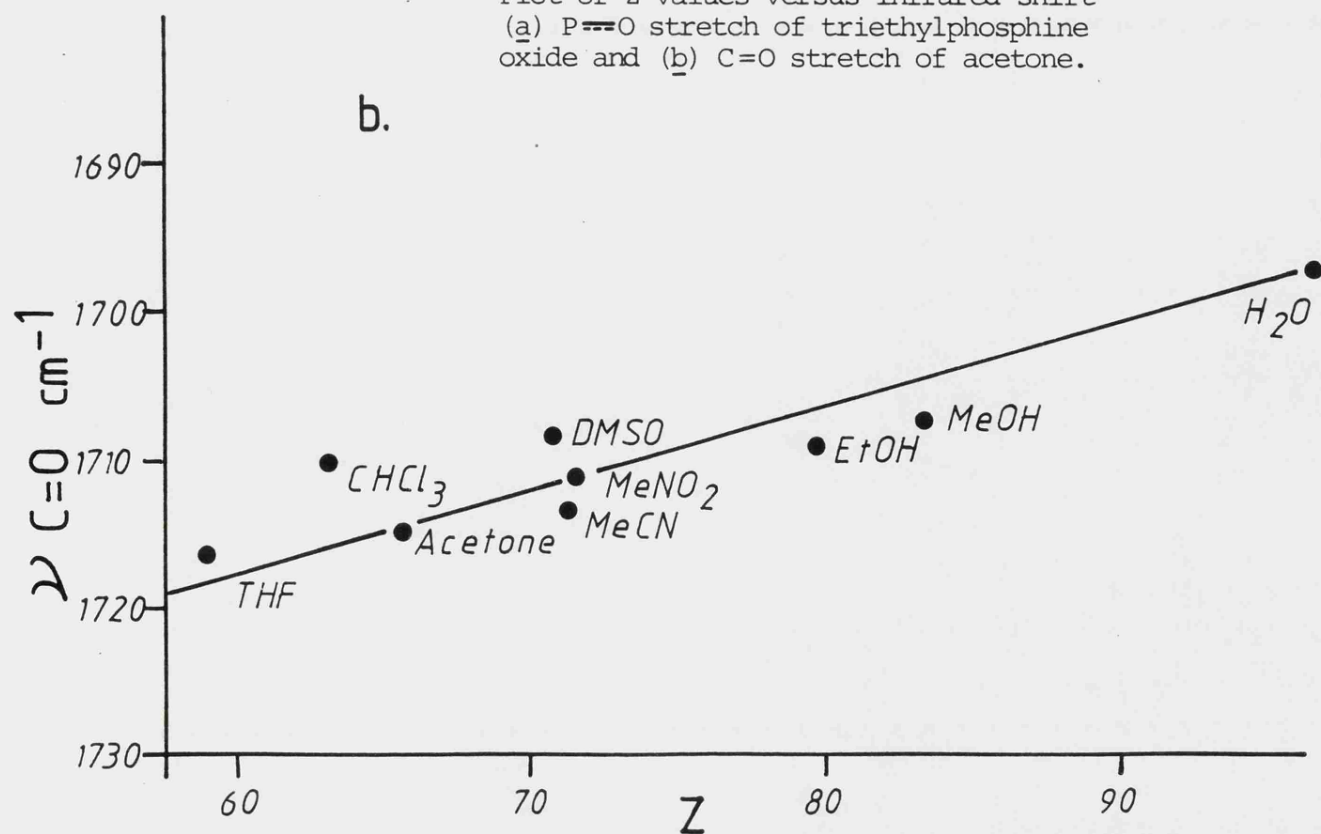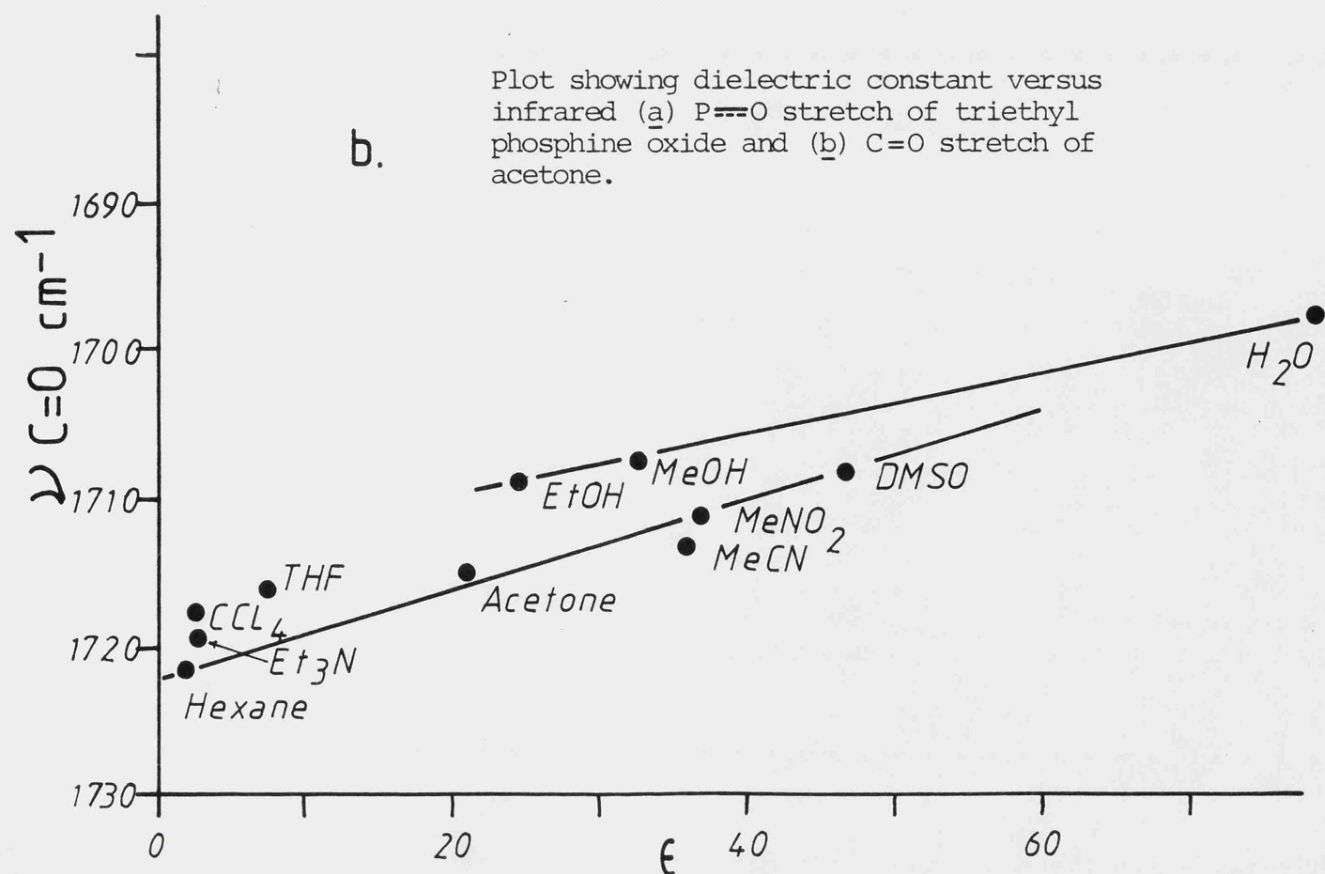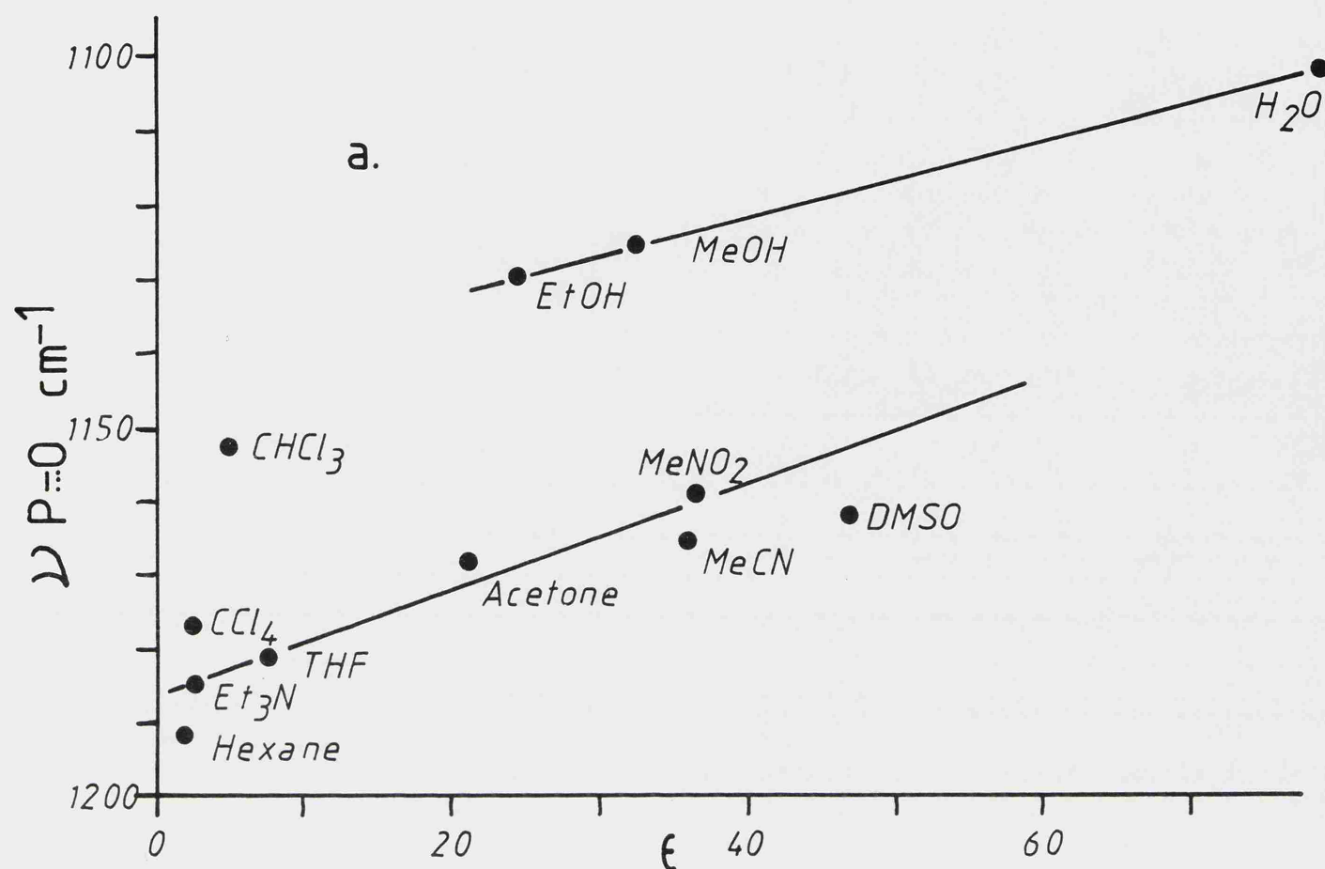# Figure    7 .10

Plot showing change of acceptor number for mixed
solvent systems, Water to Base.
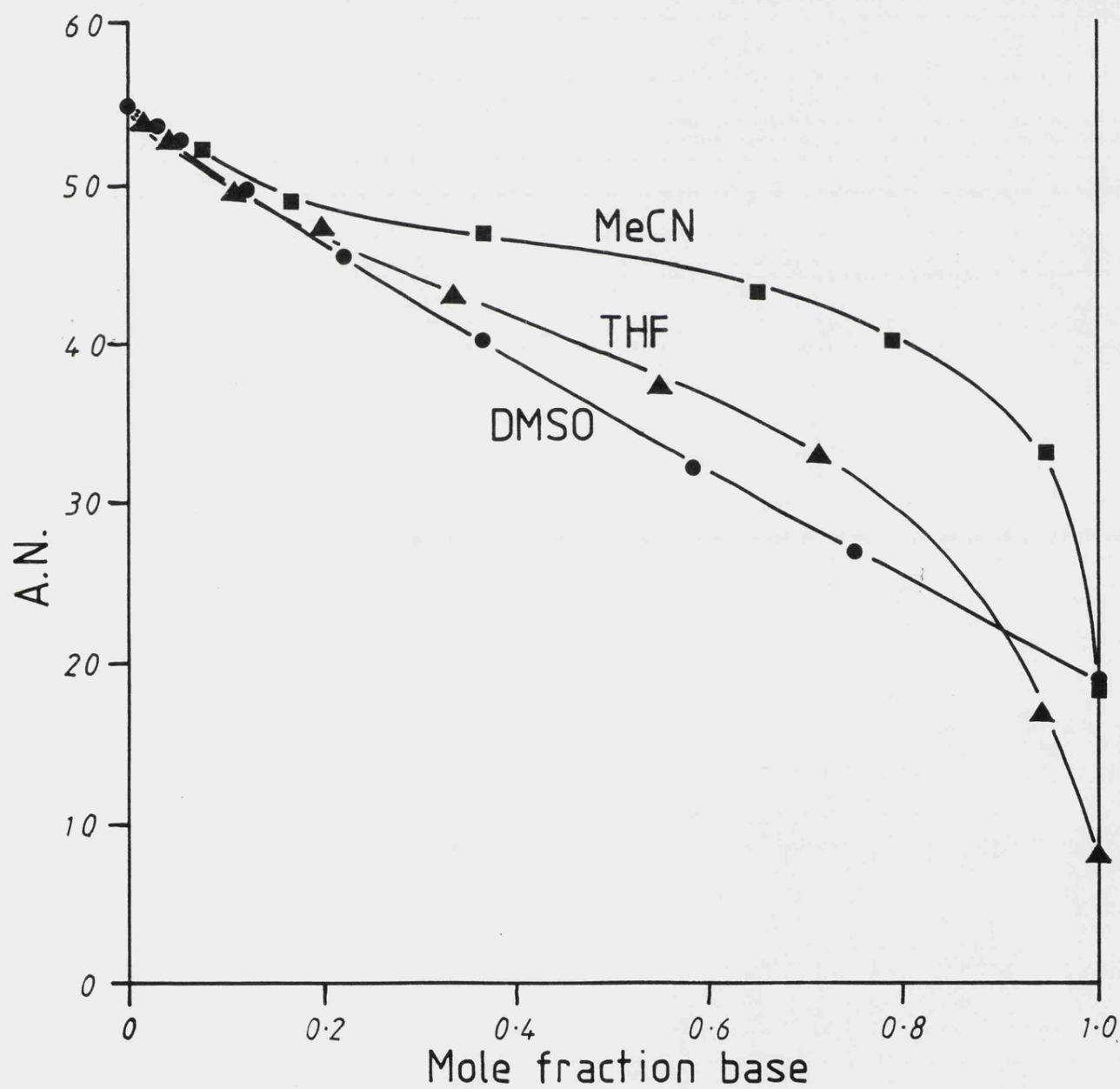
are observed.  A prime example of this is the change in AN for a mixture
of water to aprotic base (Fig. 10).  Obviously this plot is akin to those
of $^{31}$P shift versus mole fraction of base for water/base systems in
Chapter 4 with partial linearity only occurring fortuitously for the case
of water/DMSO.

7.4  CONCLUDING REMARKS

It has been shown that no one scale is generally applicable to all
solvents.  Certain carefully prepared scales, however, are very useful
pointers to solvent behaviour with a particular solute.  It must also be
appreciated that whilst these scales appear to be very comprehensive they
must be used with extreme caution especially where specific interactions
are known to occur.

REFERENCES FOR CHAPTER 7

1.  N. Menschutkin, Z. Physik Chem., 1, (1887) 611.

2.  M. Born, Z. Physik, 1, (1920) 45.

3.  J. G. Kirkwood, J. Chem. Phys., 2, (1934) 351.

4.  C. Reichardt, 'Lösungsmittel - Effekte in der Organischen Chemie',
    Verlag Chemie, Weinheim, (1969).

5.  V. Gutmann, 'The Donor-Acceptor approach to Molecular Interactions',
    Plenum Press, New York, (1978).

6.  A. H. Reddoch and S. Konishi, J. Chem. Phys., 70.5, (1979) 2121.

7.  E. M. Kosower, J. Am. Chem. Soc., 80, (1958) 3253.

8.  K. Dimroth, C. Reichardt, T. Siepmann and F. Bohlmann, Justus
    Liebigs. Ann. Chem., 661.1, (1963).

9.  E. Grunwald and S. Winstein, J. Am. Chem. Soc., 70, (1948) 846.

10. A. Allerhand and P. von R. Schleyer, J. Am. Chem. Soc., 85, (1963)
    371.

11. L. J. Bellamy and R. J. Pace, Spectrochimica Acta, 25A, (1969) 319.

12. R. W. Taft and M. J. Kamlet, J. Am. Chem. Soc., 98, (1976) 2886.

13. M. J. Kamlet and R. W. Taft, J. Am. Chem. Soc., 98, (1976) 377.

14. M. J. Kamlet, A. Solomonovici and R. W. Taft, J. Am. Chem. Soc.,
    101, (1979) 3734.

15. R. W. Taft, N. J. Pienta, M. J. Kamlet and E. M. Arnett, J. Org.
    Chem., 46, (1981) 661.

16. L. G. S. Brooker, A. C. Craig, D. W. Heseltine, P. W. Jenkins and
    L. L. Lincoln, J. Am. Chem. Soc., 87, (1965) 2443.

17. V. Gutmann and E. Wychera, Inorg. Nucl. Chem. Lett., 2, (1966) 257.

18. U. Mayer, V. Gutmann and W. Gerger, Monatshefte für Chemie, 106,
    (1975) 1235.

19. R. H. Erlich and A. I. Popov, J. Am. Chem. Soc., 93, (1971) 5620.

20. P. Spaziante and V. Gutmann, Inorg. Chim. Acta, 5, (1971) 273.

# CHAPTER 8

ACETONE CLATHRATE HYDRATE STUDIES

## 8.1 INTRODUCTION

The propensity for water to form 'cages' of fully hydrogen bonded molecules around inert solutes in the solid state has been well known for many years [1]. A hypothesis invoking similar 'cage' like structures has been suggested in order to explain many experimental results from liquid phase studies. For example, the intense ultrasonic relaxation effects measured for water and tert-butanol mixtures [2] were explained by 'cage' formation. Studies of solutions of m-Dinitrobenzene anion using e.s.r. [3] have shown that in aprotic solvents both nitro groups are equivalent. However, in aqueous solution an asymmetric situation arises which can easily be understood in terms of partial 'cage' formation around one nitro group and hydrogen bonding to the other (Figure 1). This 'cage' structure slows down the rate of charge transfer between the nitro groups, observed from the e.s.r. linewidths. Other e.s.r. studies involving di-t-butyl nitroxide radicals in aqueous solutions gave results that can be interpreted in terms of 'cage' structure around the bulky alkyl groups [4,5].

Acetone forms a well-defined clathrate hydrate [6] in the solid state. The similarity already demonstrated between acetone and di-t-butyl nitroxide solvation (see Chapter 3) and the explanation of some acetone results in terms of 'cage' formation [7] indicated that an infrared study may prove to be a useful probe of the fluid and solid systems.

## 8.2 RESULTS AND DISCUSSION

Two experimental routines were found to be successful in forming the acetone clathrate.

Firstly the classical method involved lowering the temperature of a suitable acetone/water mixture and holding that temperature (-30°C) for

# Figure 8.1



a.

$$\psi_S(2)$$
$$\psi_{As}(1) \qquad \psi_{As}(2)$$
$$\psi_S(1)$$

b.
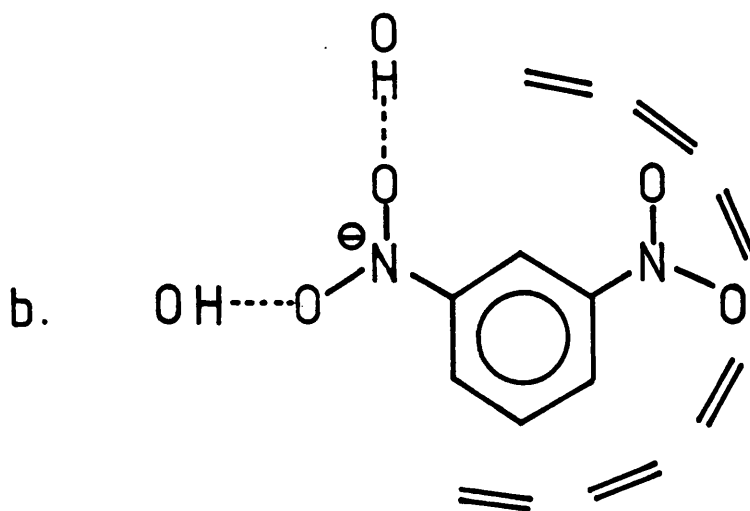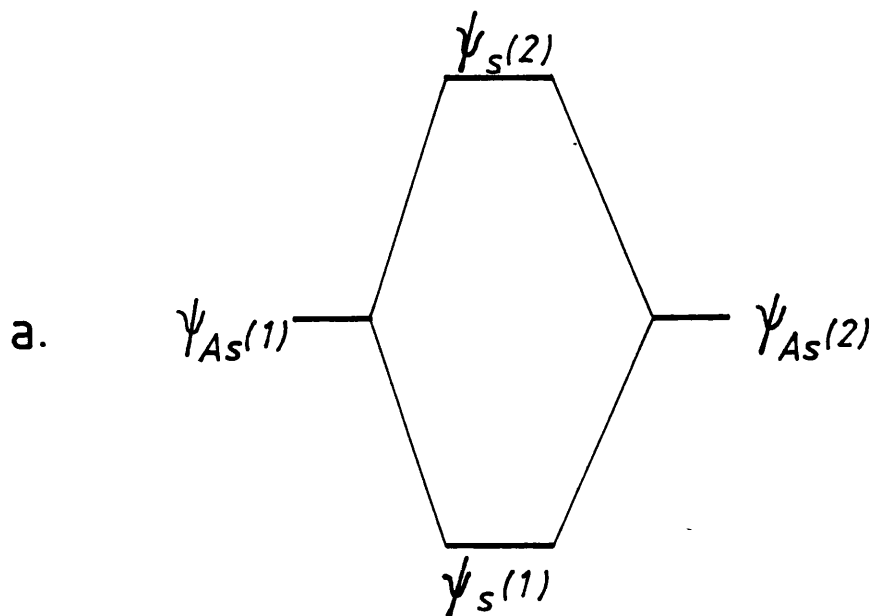
a) Combination of the ground state $\psi_S(1)$ and a low-lying
   excited state $\psi_S(2)$ for m-dinitrobenzene anions to
   give two asymmetric levels $\psi_{As}(1)$ and $\psi_{As}(2)$. These
   can be thought of as being primarily located on one
   or other nitro group. The asymmetric wavefunction
   being stabilised by asymmetric hydration – hydrogen
   bonding and partial cage formation shown by b).

several hours. The clathrate slowly formed over this time (Fig. 2).

Secondly a slightly more involved but faster procedure involved lowering the temperature of a suitable acetone/water mixture to around -100°C and then slowly warming at a constant rate $(1° min^{-1})$. The clathrate was seen to form rapidly on attaining the lower stable temperature (-40°C). On continued warming a sudden dramatic loss of the clathrate was observed at the upper stable temperature (-19°C) (Fig. 3). Holding between these temperatures, or freezing from this range to lower temperatures retained the clathrate. The temperatures quoted agree excellently with those in the literature [1].

A study of the infrared band positions and shapes for the various observed states (Fig. 4) is extremely informative. It is noted that the band for the fluid aqueous acetone (1697 cm $^1$) is completely separate and distinct from that for the clathrate. This indicates that little or no true clathrate is present in the fluid state. On cooling the band broadens and shifts to higher wavenumber $(1705 cm^{-1} \rightarrow 1712 cm^{-1})$; this is indicative of a loss of some hydrogen bonding to the acetone. It has already been shown that in water the acetone is di-bound, the new band on cooling covers a region assigned to bulk (self-associating) acetone $(1715 cm^{-1})$, mono-bound $(1708 cm^{-1})$ acetone and di-bound $(1697 cm^{-1})$ acetone. This broad feature is probably a result of partial phase separation with ice forming and an enriched fluid region of acetone and water.

When the clathrate forms, it shows a clean and total transition to the new band centred at a position $(1722 cm^{-1})$ almost identical to that of acetone in a totally inert medium such as n-hexane. This indicates that the acetone is in a 'free' state with no hydrogen bonds and even no self-interactions, i.e. dipole-dipole interactions.

# Figure 8.2
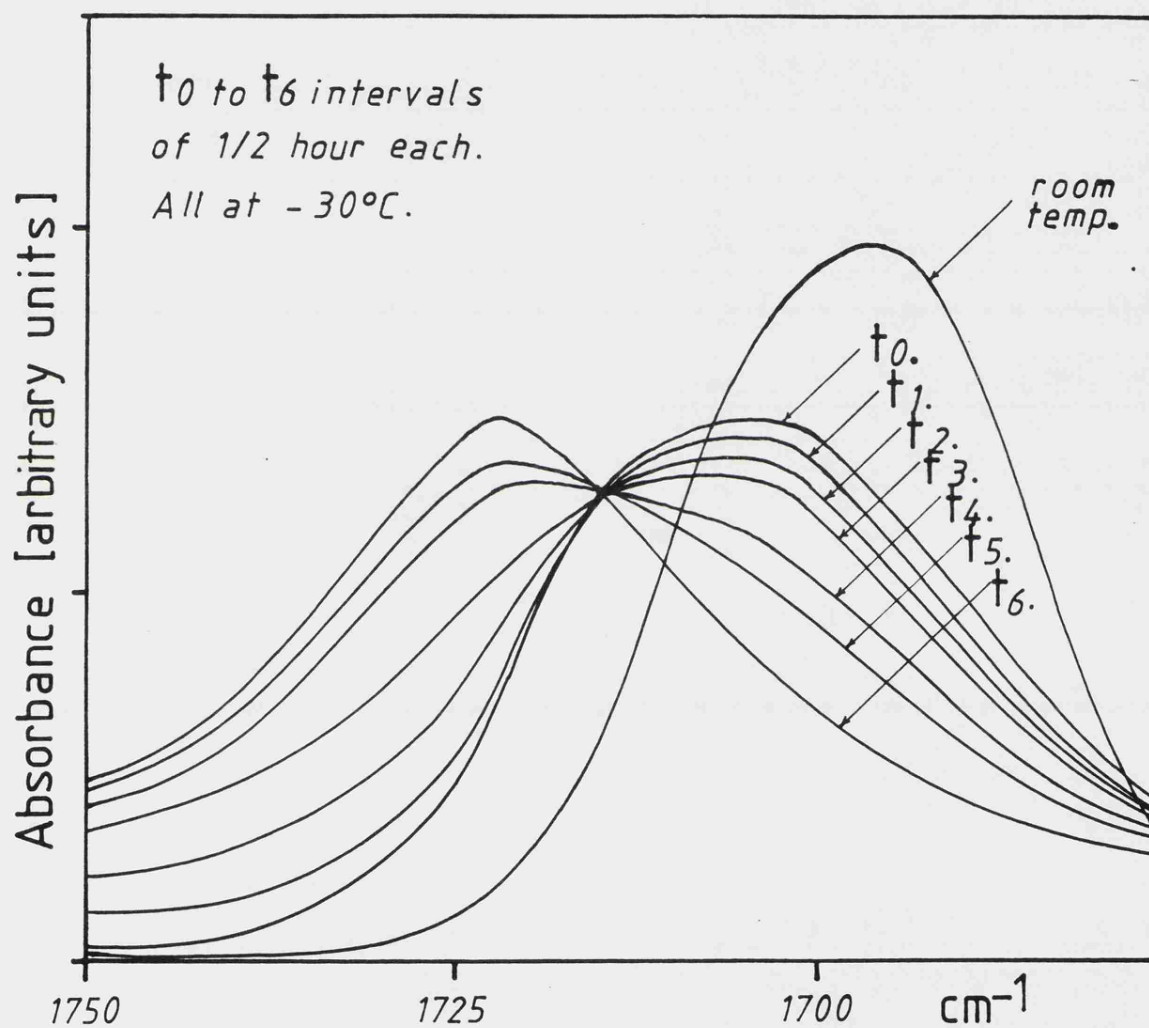


Spectra showing change in $\nu$ C=O stretch of aqueous
acetone on lowering temperature and holding.
Classical procedure for formation of clathrate.

Figure 8.3
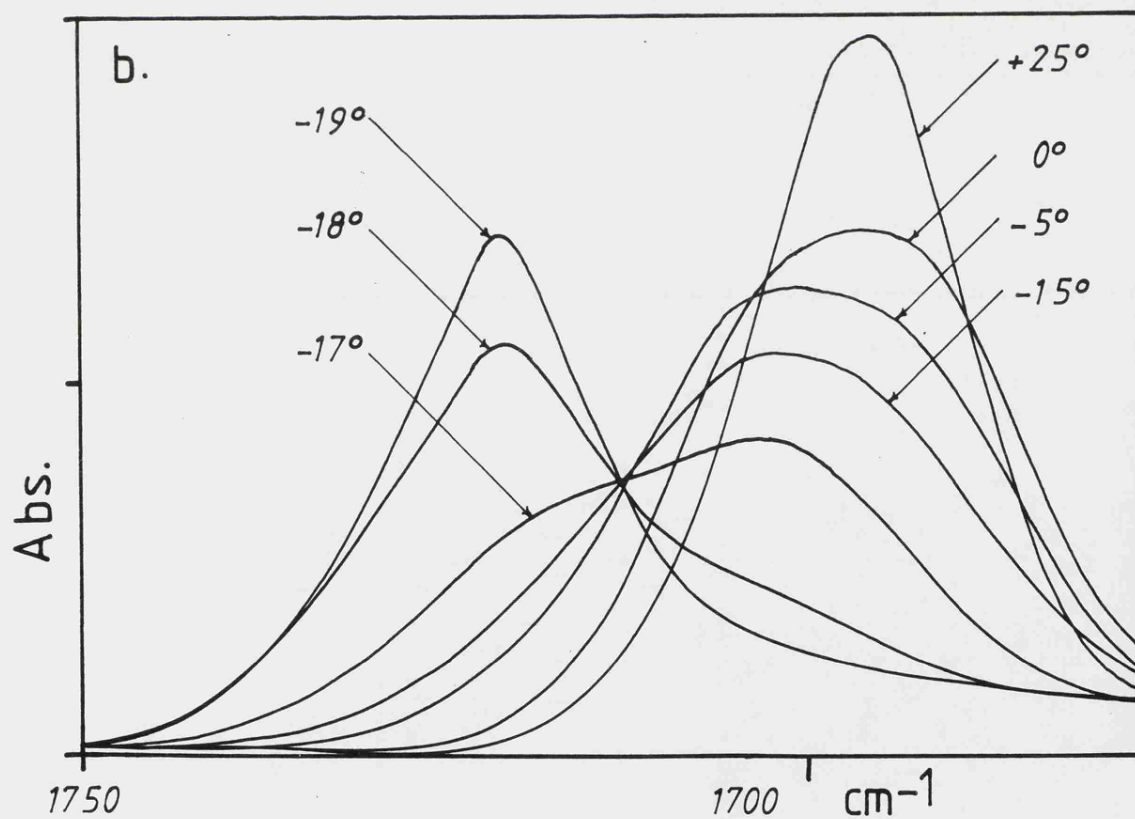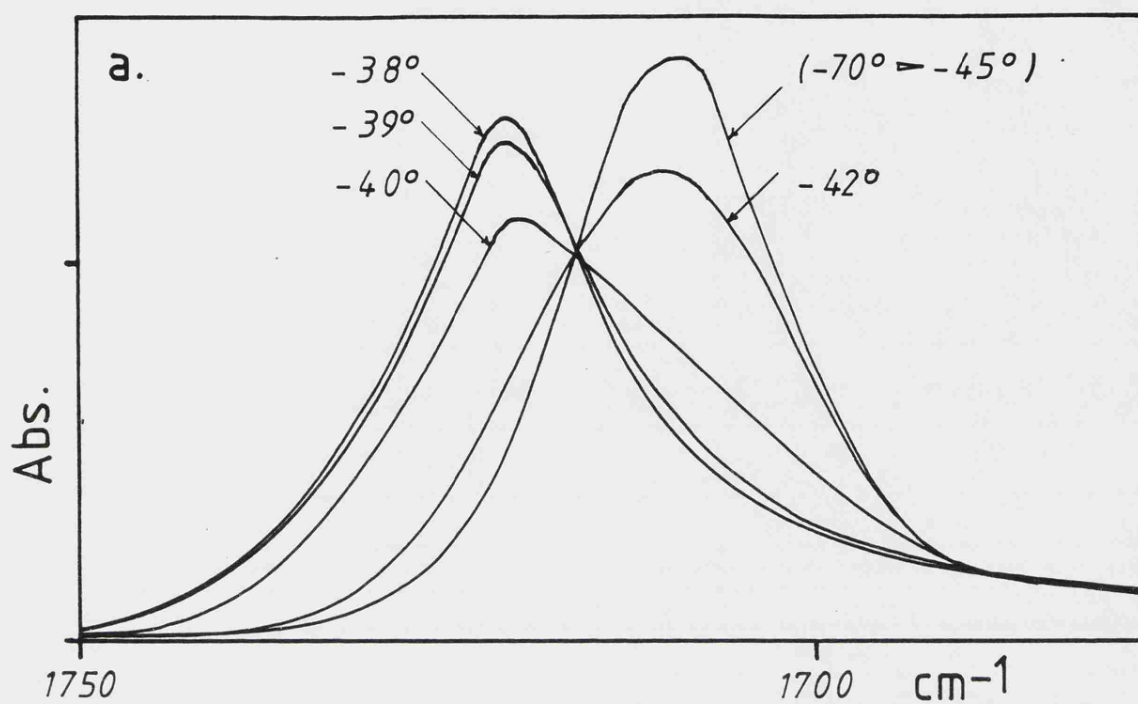
Spectra showing typical warming cycle
a) -70° → -38°C - formation of clathrate
b) -19° → +25°C - 'melting' of clathrate.

# Figure 8.4
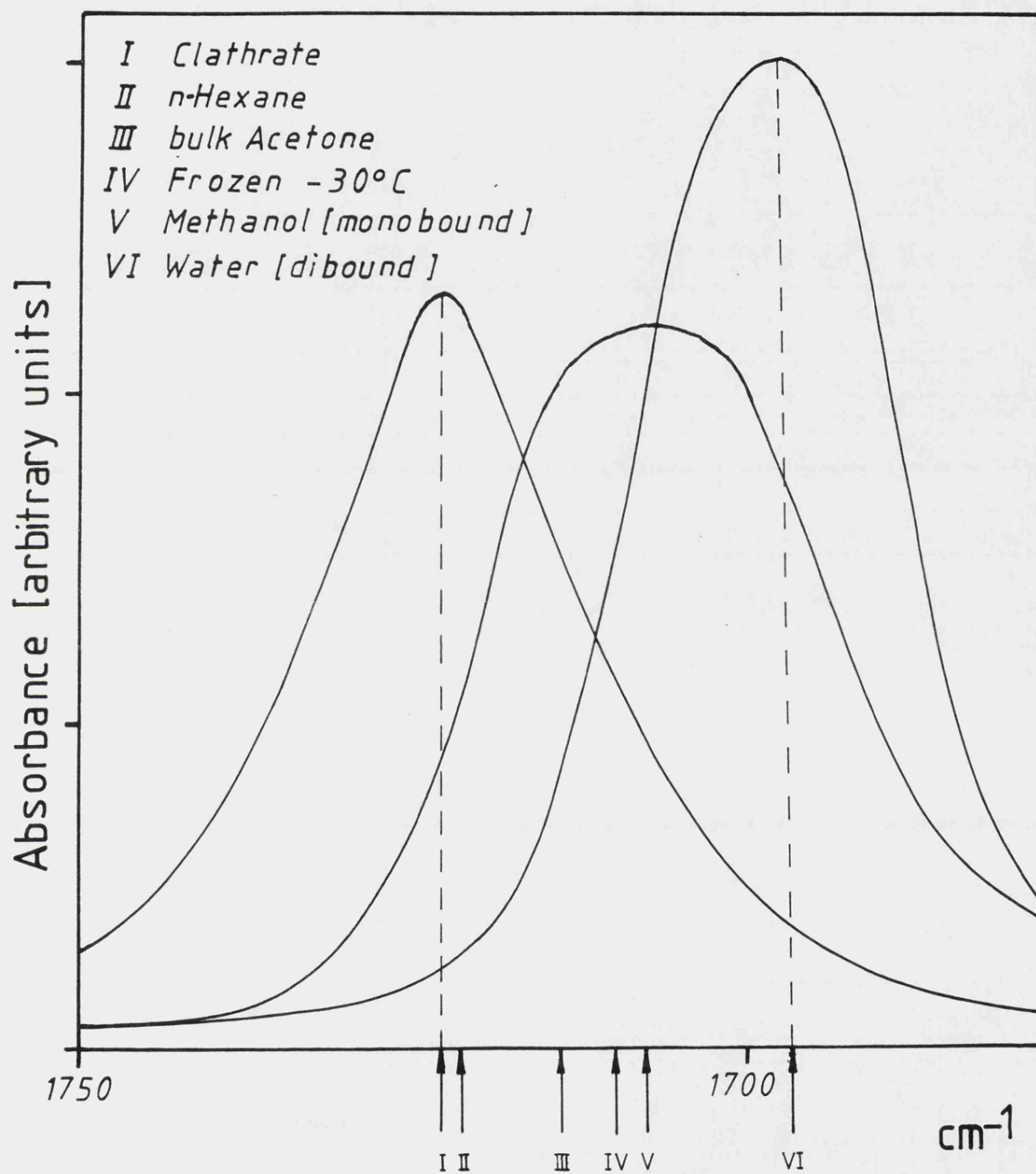
Spectra showing lineshapes and positions of C=O
stretch of aqueous acetone solutions with n-hexane
and methanolic solution positions for comparison.

The line-shape of the clathrate band is also different from that of the cooled bulk and liquid aqueous systems. The C=O stretch band for acetone in the liquid aqueous system is Gaussian, indicating a range of different structures for the hydrogen bonded system, i.e. long bonds, short bonds, some bent bonds, etc. The clathrate band, however, is Lorentzian, suggesting a high degree of rotational freedom for the oscillator. This degree of freedom would only be available if there were no hydrogen bonding to the acetone, the clathrate formed having a true clathrate structure, with one guest molecule per 'cage'.

Together with the infrared, $^{13}C$ and $^{17}O$ n.m.r. studies were undertaken. As shown previously (Chapters 3 and 4) infrared and n.m.r. data follow a linear correlation for $^{13}C$ and $^{17}O$ with C=O stretch. For $^{13}C$ studies of the clathrate system distinct n.m.r. signals were obtained for the di-bound, mono-bound and pure bulk acetone. However, due to very long accumulation times, low signal-to-noise and the expected broadening of any clathrate band, no such separate band was observed.

The $^{17}O$ on the other hand, provided signals identifiable with all the above species plus a distinct band for the clathrate. The fact that the $^{17}O$ clathrate band was no broader than the liquid state bands confirmed the high degree of rotational freedom of the acetone in the cage.

The correlation of n.m.r. and infrared data for the aqueous acetone system is shown in Fig. 5 where the room temperature mono-bound methanol system is also included. Allied to the theory of clathrate formation in the solid or liquid is the idea that 'cages breed cages' [8]. The behaviour of t-Butanol in aqueous solution has often been explained using a cage model [2]. It was, therefore, interesting to examine the effect that this had on the formation of the acetone clathrate. As a comparison methanol was also used as this normally shows no tendency to participate

# Figure 8.5
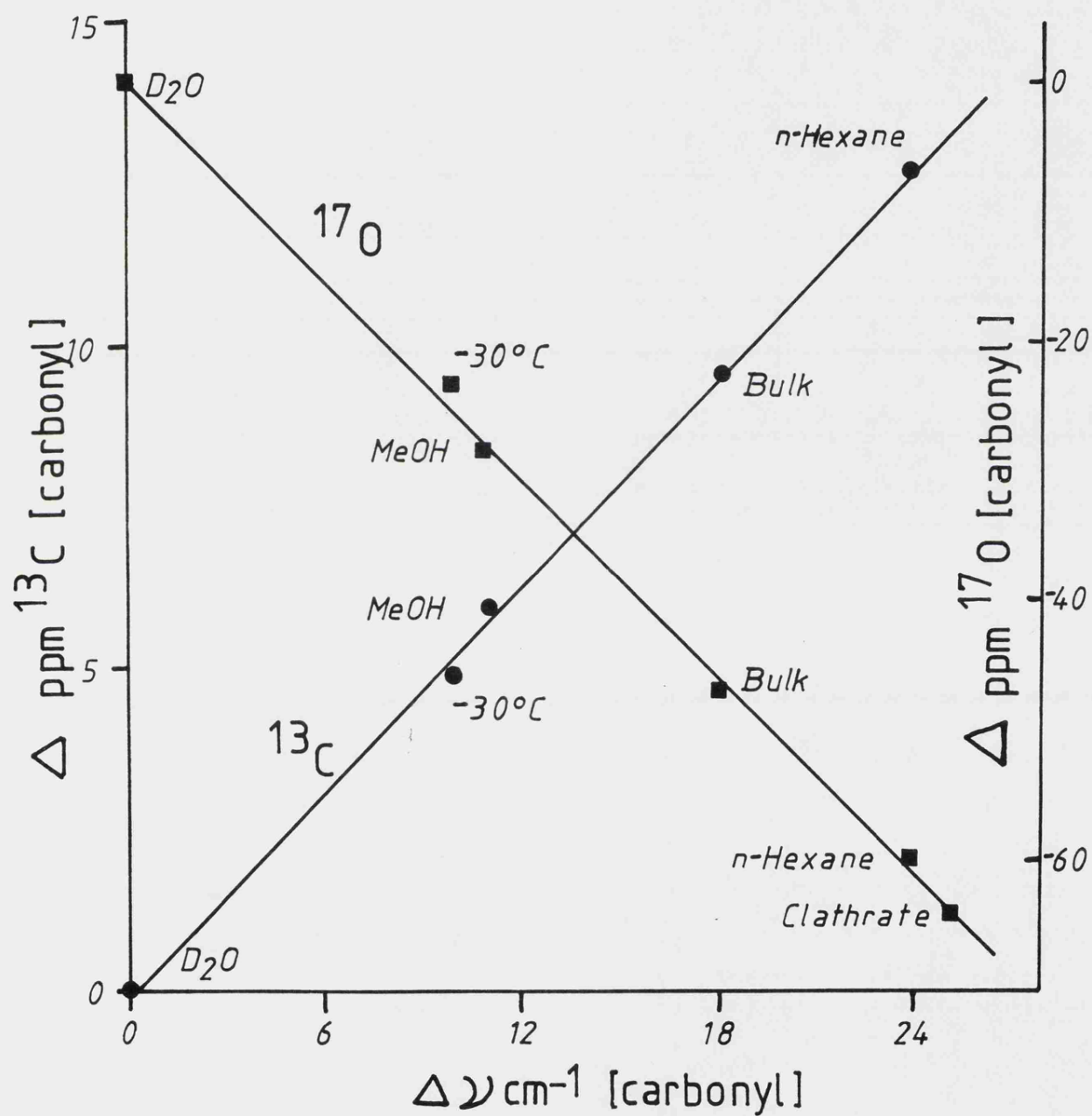


Relationship between n.m.r. and infrared data for
the carbonyl group of acetone in various states.

in cage formation.

The method employed was that using the formation of the clathrate during the warming cycle. At a constant rate of temperature rise the spectra were monitored for mixtures containing known mole fractions of alcohol with the same mole ratio of water to acetone. Figures 6 and 7 show the effect of t-Butanol and Methanol respectively.

At first glance the results appear to be opposite to those expected, with t-Butanol seemingly destroying the stability of the acetone clathrate and Methanol enhancing it. However, the lowering of the temperature at which the clathrate begins to form, by methanol and the raising of the temperature by t-Butanol is probably due simply to the increase and decrease in fluidity, at low temperatures, of the mixtures by the respective alcohols. Both alcohols appear to have a similar overall effect on the formation of the clathrate in that at concentrations above $22 \times 10^{-3}$ mole fraction no clathrate was observed during the warming cycle for either alcohol. The observation that t-Butanol does not seem to enhance the formation of the acetone clathrate may provide some evidence against the 'cage' idea for the solvation of t-Butanol although this is slender. A possible true clathrate of t-Butanol has been reported [9] where the alcohol is totally 'free' in its cage. The formation of this should enhance the formation of cages suitable for the acetone clathrate. If, however, hydrogen bonding effects predominate, it is probable that the 'structuring' of water into true cages suitable for the acetone clathrate to form is not possible with the alcohols present, any alcohol having a generally similar effect. This does not, however, rule out the partial cage structure of water around the t-Butyl groups in fluid aqueous t-Butanol solutions.

# Figure 8.6



Effect of added tBuOH to aqueous acetone system during warming cycle. Clathrate formation observed by growth of $\nu$ C=O band at 1722 cm$^{-1}$.
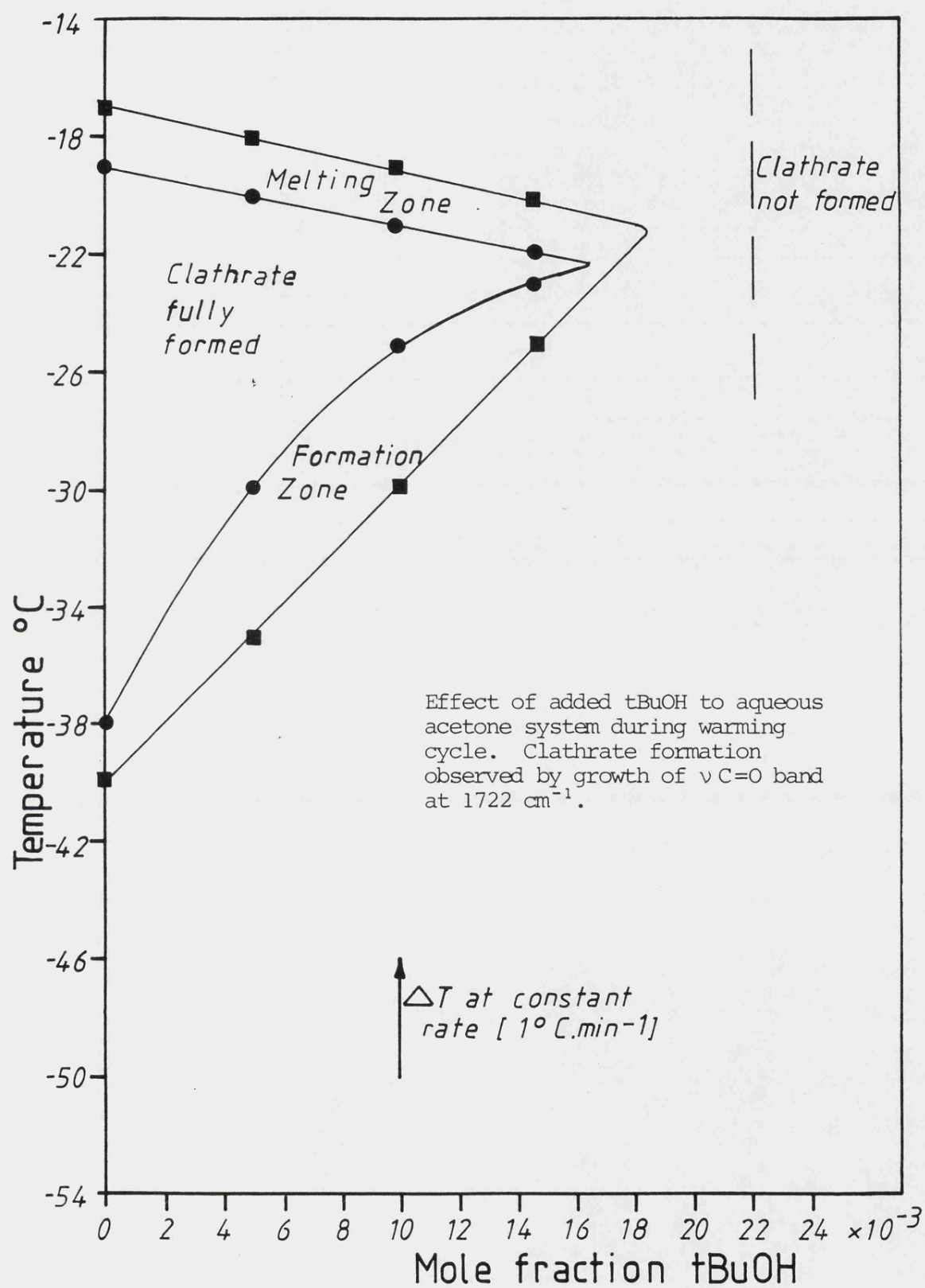
# Figure 8.7
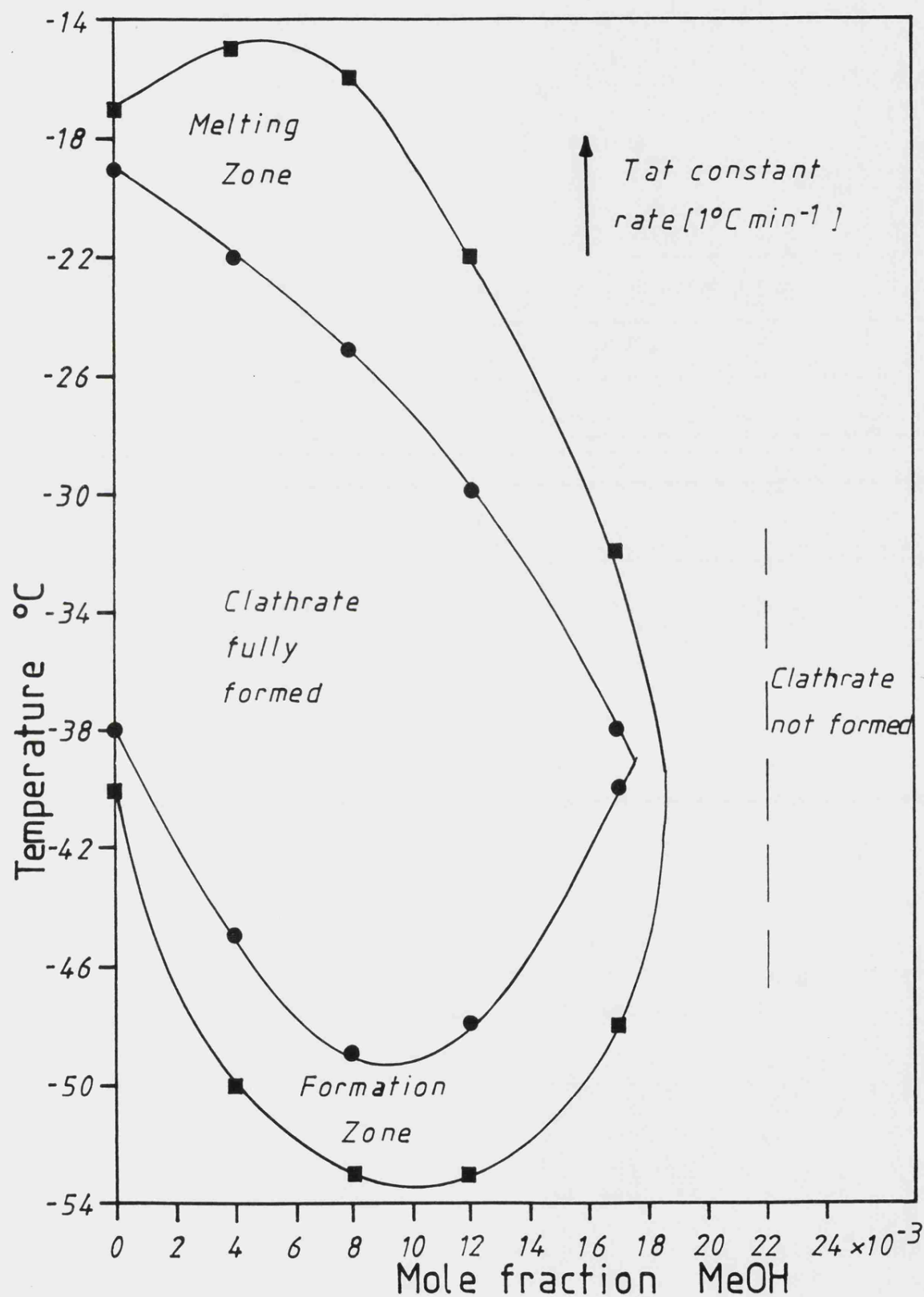


Effect of adding MeOH to aqueous acetone system
during warming cycle.  Clathrate formation observed
by growth of $\nu$ C=O band at 1722 $cm^{-1}$.

## 8.3 CONCLUDING REMARKS

The main result of this work indicates that the solid clathrate structures have no foundation spectroscopically in the liquid phase. The predominant effect upon liquid structure of aqueous systems appears to be hydrogen bonding. However, some partial 'structuring' may still be invoked to explain solutions of bulky hydrophobic molecules.

REFERENCES FOR CHAPTER 8

1.  D. W. Davidson in 'Water - A Comprehensive Treatise', Vol. 2,
    Ch. 3, ed. F. Franks, Plenum Press, (1973).

2.  M. C. R. Symons and M. J. Blandamer in 'Hydrogen-Bonded Solvent
    Systems', ed. A. K. Covington and P. Jones, Taylor & Francis,
    London, (1968).

3.  D. Jones and M. C. R. Symons, Trans. Faraday Soc., 67, (1971) 961.

4.  S. E. Jackson, E. A. Smith and M. C. R. Symons, Faraday Discuss.
    Chem. Soc., 64, (1977) 173.

5.  C. Jolicoeur and H. L. Friedman, Ber. Bunsenges. Phys. Chem., 76,
    (1971) 248.

6.  A. S. Quisk and H. S. Frank, J. Phys. Chem., 65, (1961) 560.

7.  E. V. Goldammer and H. G. Hertz, J. Phys. Chem., 74, (1970) 3734.

8.  M. C. R. Symons and G. Eaton, Faraday Symposium 17, 17/5, (1982).

9.  B. Z. Gorbunov and Yu. I. Naberukhin, Chem. Phys. Letters, 19,
    (1973) 2.

# CHAPTER 9

SOLVOLYSIS OF MONOHALOALKANES

## 9.1  INTRODUCTION

The solvolysis of monohaloalkanes has been the subject of several

investigations [1-4]. Many mechanisms have been suggested generally of

the $S_N1$ or $S_N2$ type, depending upon the monohaloalkane under review.

For the bulky t-butyl halides the $S_N1$ type mechanism is generally

accepted as being a fair approximation. There are, however, several

questions arising from this mechanism that required further investigation.

This was undertaken by Blandamer et al. [5] in order to explain the non-

linearity of the Arrhenius plots.

$$R\text{-}X \xrightleftharpoons[k_{-2}]{k_1} \quad R^+ X^- \xrightarrow{k_3} \quad products \qquad \dots (1)$$

with rate constant

$$k_{(obs)} = \frac{k_1}{1 + k_2/k_3} \qquad \dots (2)$$

The initial part of the mechanism requires the formation of ions from

the pure haloalkane and the existence of a 'transition state' in which

the ion pairs become solvated and thence separated. The lifetime of

this transition state, however, is exceedingly short ($\sim 10^{-12}$ sec) and

for solvation to take place within this time span would require very

rapid rearrangement of solvent molecules.

An alternative approach, invoking attack by $(OH)_{free}$ in aqueous

systems is outlined below:-

$$R\text{-}X + (OH)_{free} \rightleftharpoons RX\text{-----}HO \qquad \dots (3)$$

$$R\text{-}X\text{----}H\text{-}O + (OH)_{free} \rightleftharpoons RX \begin{smallmatrix} \text{----}HO \\ \\ \text{----}HO \end{smallmatrix} \qquad \dots (4)$$

$$R\text{-}X \xrightleftharpoons{R.D.S.} R^+ + X^-_{solvated} \qquad \dots (5)$$
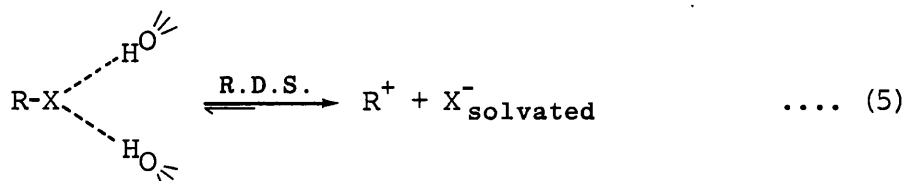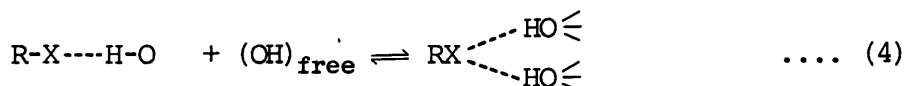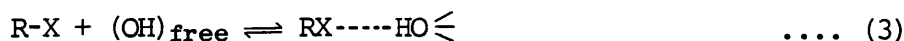
where X is halogen and stage (5) is the rate determining step. Stage
(3) is the formation of a hydrogen bond with the monohaloalkane and,
spectroscopically, such bonds should be capable of observation.

The favoured method for the study of hydrogen bonds is by observing
the OH stretching frequency of dilute alcohol or water in various
solvents and solvent mixtures [6-8]. In fact, the protic component can
be viewed in a similar way to the aprotic probe studies of previous
chapters.

The relationship between infrared spectral shifts and energy of
interaction was described by Badger and Bauer [9] and is known as their
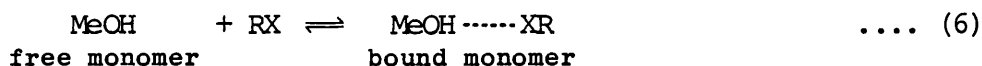rule. This requires a linear relationship however, but much evidence
supports a non-linear dependence for very weak interactions [10,11].
The Badger-Bauer rule was applied to the results of this work as further
proof towards the existence of hydrogen bonds in the monohaloalkane-
protic systems.

## 9.2  BASIS OF CALCULATIONS

Most of the calculations of equilibrium constants (K) and subsequently
free energy of interaction ($\Delta$G) were undertaken on methanolic systems.
Very dilute methanol in aprotic solvents exists as the monomer and a
plot of absorbance against concentration is linear for the OH oscillator,
both for fundamental infrared and for first overtone near infrared.
This shows observance of the Beer-Lambert law and provides a rapid method
for the determination of concentrations of methanol in mixed, interacting
solvent systems.

If we write the equilibrium in a mixed system such as tetrachloro-
methane and monohaloalkane:-

$$\text{MeOH} \quad + \text{RX} \rightleftharpoons \quad \text{MeOH} \cdots \cdots \text{XR} \qquad \cdots \cdots \text{(6)}$$
$$\text{free monomer} \qquad\qquad \text{bound monomer}$$

we can determine the equilibrium constant as

$$K = \frac{[\text{MeOH} \cdots \cdots \text{XR}]}{[\text{MeOH}][\text{RX}]} \qquad \cdots \cdots \text{(7)}$$

However, if we use this equation there are systematic variations in the values of K as the concentration of RX changes. The probability is that interactions are occurring between the methanol and either the $CCl_4$ or itself. As the Beer-Lambert law is obeyed and very dilute solutions were used, the possibility of self-association is eliminated. However, there is evidence that methanol is hydrogen-bonded with $CCl_4$ albeit very weakly [12,13]. The equilibrium then becomes:-

$$\text{MeOH} \cdots \cdots CCl_4 + \text{RX} \rightleftharpoons \text{MeOH} \cdots \cdots \text{XR} + CCl_4 \qquad \cdots \cdots \text{(8)}$$
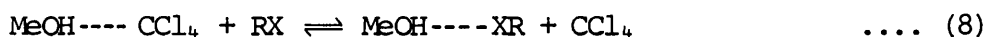
and K determined from

$$K = \frac{[\text{MeOH} \cdots \cdots \text{XR}][CCl_4]}{[\text{MeOH} \cdots \cdots CCl_4][\text{RX}]} \qquad \cdots \cdots \text{(9)}$$

We can determine [MeOH-----XR] and [MeOH-----$CCl_4$] from the Beer-Lambert law:-

$$A = \varepsilon C L \qquad \cdots \text{(10)}$$

where A is absorbance at $\nu_{max}$, $\varepsilon$ is the molar absorptivity and constant, L is the path length of the cell, also constant and C the molarity.

From the absorbance values for $\nu_{OH}$ in $CCl_4$ using the Beer-Lambert plot we get [MeOH-----$CCl_4$] for any addition of RX. The difference between these values ($A_2$) and the initial absorbance for methanol in pure $CCl_4$ ($A_1$) will be proportional to the amount of bound methanol, hence

$$[\text{MeOH} \cdots \cdots CCl_4] = \frac{A_2}{\varepsilon L} \qquad \cdots \text{(11)}$$

$$[\text{MeOH} \cdots \cdots \text{XR}] = \frac{A_1 - A_2}{\varepsilon L} = \frac{\Delta A}{\varepsilon L} \qquad \cdots \text{(12)}$$

Combining (11) and (12) with equation (9) we get:-

$$K = \frac{\Delta A}{A_2} \times \frac{[CCl_4]}{[RX]} \qquad \qquad \cdots \cdots (13)$$

$[CCl_4]$ and $[RX]$ are directly measured quantities. This equation (13) was used throughout the work and gave consistent results.


## 9.3   RESULTS AND DISCUSSION

Figure 9.1 shows the position of the OH stretching frequency for methanol and water in different solvents. The inert very weakly interacting solvents give the highest frequency absorption whereas the stronger basic solvents shift the absorption to lower frequency. An almost identical picture emerges if we plot the first overtone values in the same manner. Two points are apparent from these frequency shifts:-

a) Tetrachloromethane shows a substantial shift from the more inert
   solvents such as cyclohexane. This supports the idea of a
   methanol $CCl_4$ interaction proposed by Mizugai et al. [12].

b) The monohaloalkanes all shift the OH peak substantially and there
   appears to be an order of interaction, i.e. RI > RBr > RCl.

It is possible to suggest two major types of interaction that would account for the shifts as observed, either dipole-dipole interactions or hydrogen bonding. If the former were operating then for a mixed solvent system a gradual shift of band maximum would be expected. For the hydrogen-bonded system only two states would be observed with a loss of one band and a simultaneous gain of the new band. Fig. 9.2 illustrates this point with the tetrachloromethane -iodomethane system. A distinct isosbestic point is observed, with only two bands. This is also observed for the same system in the overtone region (Fig. 9.3), and all

## Figure 9.1
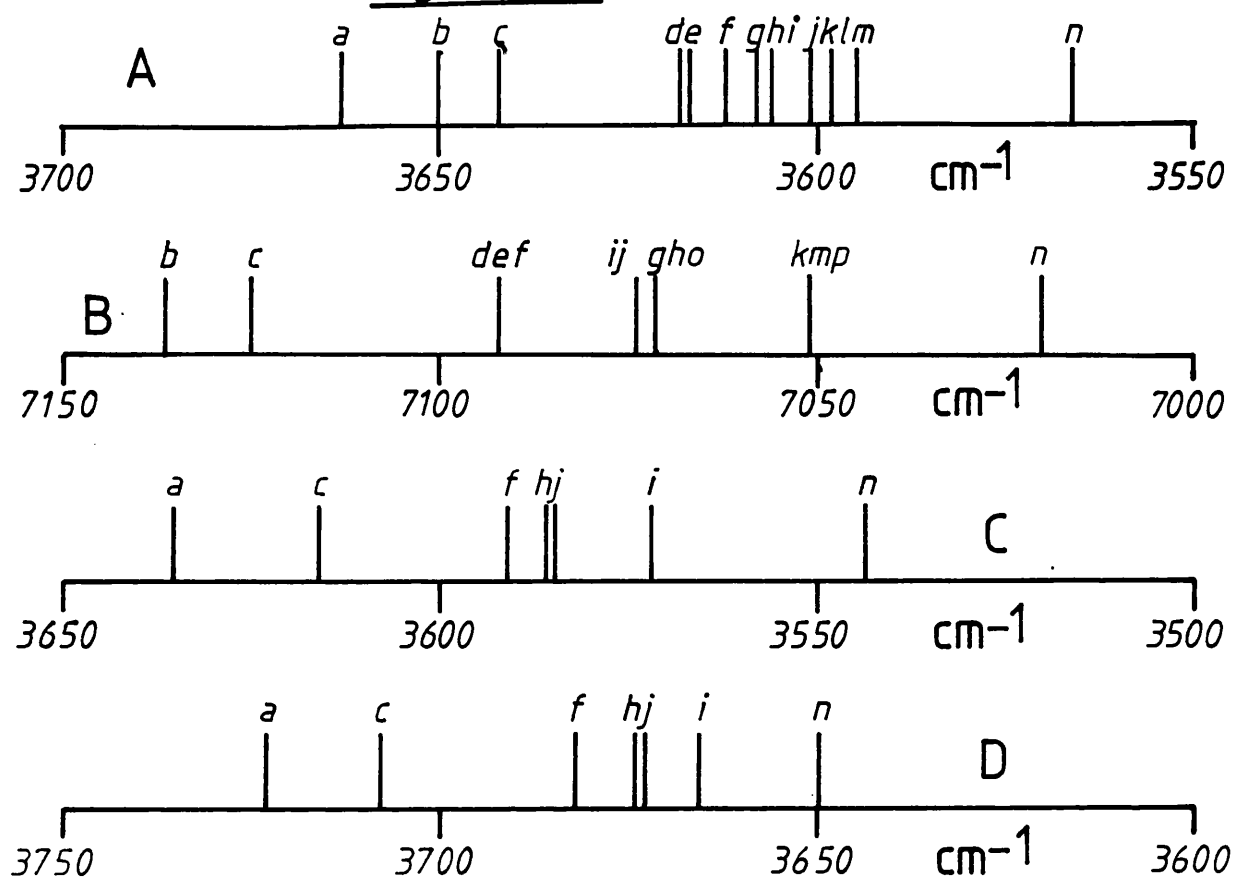


a  Hexafluorobenzene
b  Cyclohexane
c  Tetrachloromethane
d  2-Chloropropane
e  1-Chloropropane
f  t-Butyl chloride
g  Bromoethane
h  2-Bromopropane
i  Nitromethane
j  t Butylbromide
k  Iodomethane

l  Iodoethane
m  2-Iodopropane
n  Cyanomethane
o  1-Bromopropane
p  1-Iodopropane

A  $\nu$ OH Methanol
B  $\nu$ OH 1st overtone Methanol
C  $\nu_1$ OH  Water
D  $\nu_3$ OH  Water

Plot showing relative $\nu_{max}$ OH stretch for dilute methanol and water in various solvents.

# Figure 9.2



| N° | Mole fraction |
|----|---------------|
| 1  | 0·00          |
| 2  | 0·13          |
| 3  | 0·24          |
| 4  | 0·44          |
| 5  | 0·61          |
| 6  | 0·76          |
| 7  | 0·89          |
| 8  | 0·94          |
| 9  | 1·00          |
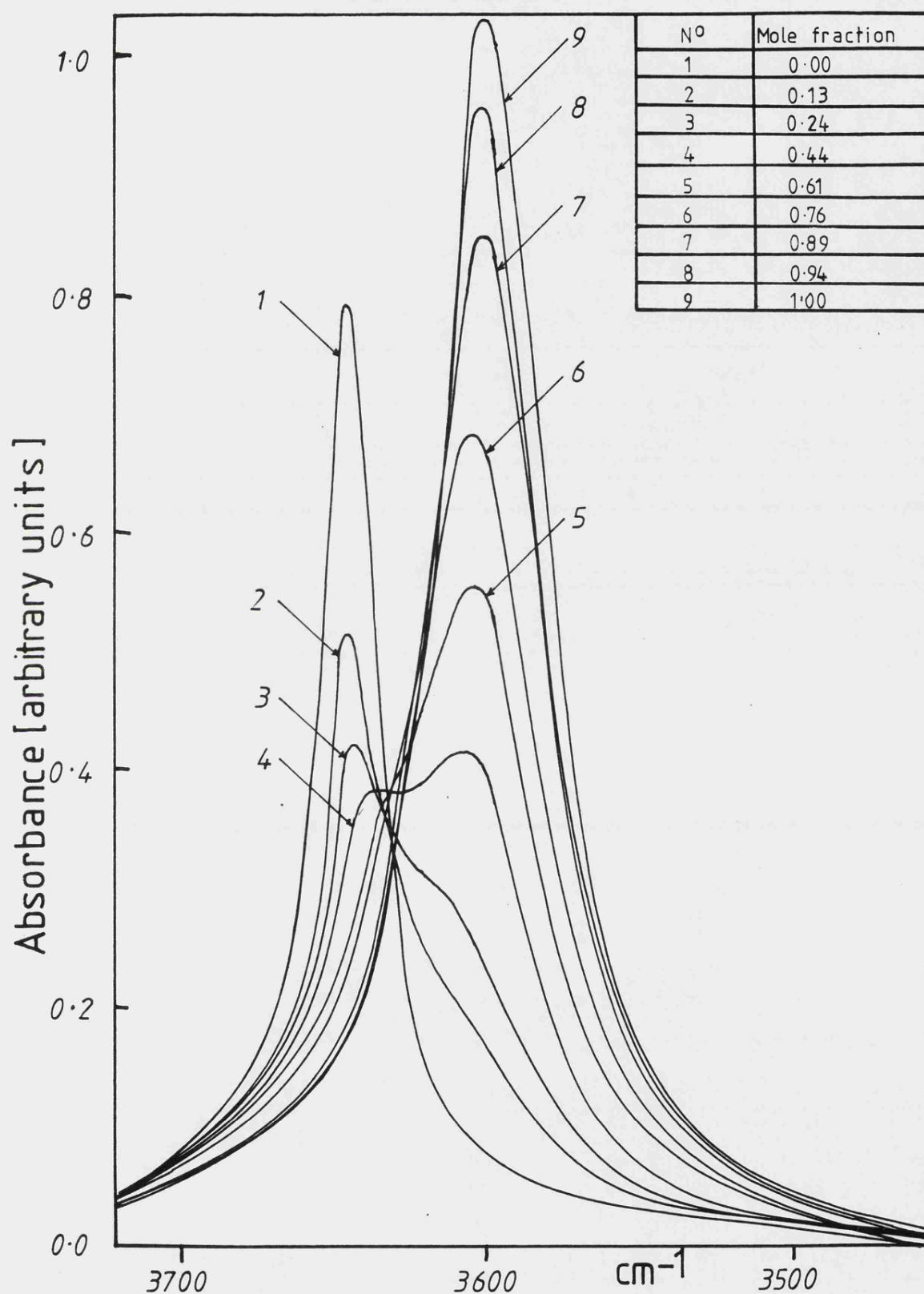
Change of $\nu$ OH band of methanol in range of mixtures,
tetrachloromethane – iodomethane.

# Figure 9.3



| Nº | Mole fraction |
|----|---------------|
| 1  | 0·00          |
| 2  | 0·44          |
| 3  | 0·61          |
| 4  | 0·89          |
| 5  | 1·00          |
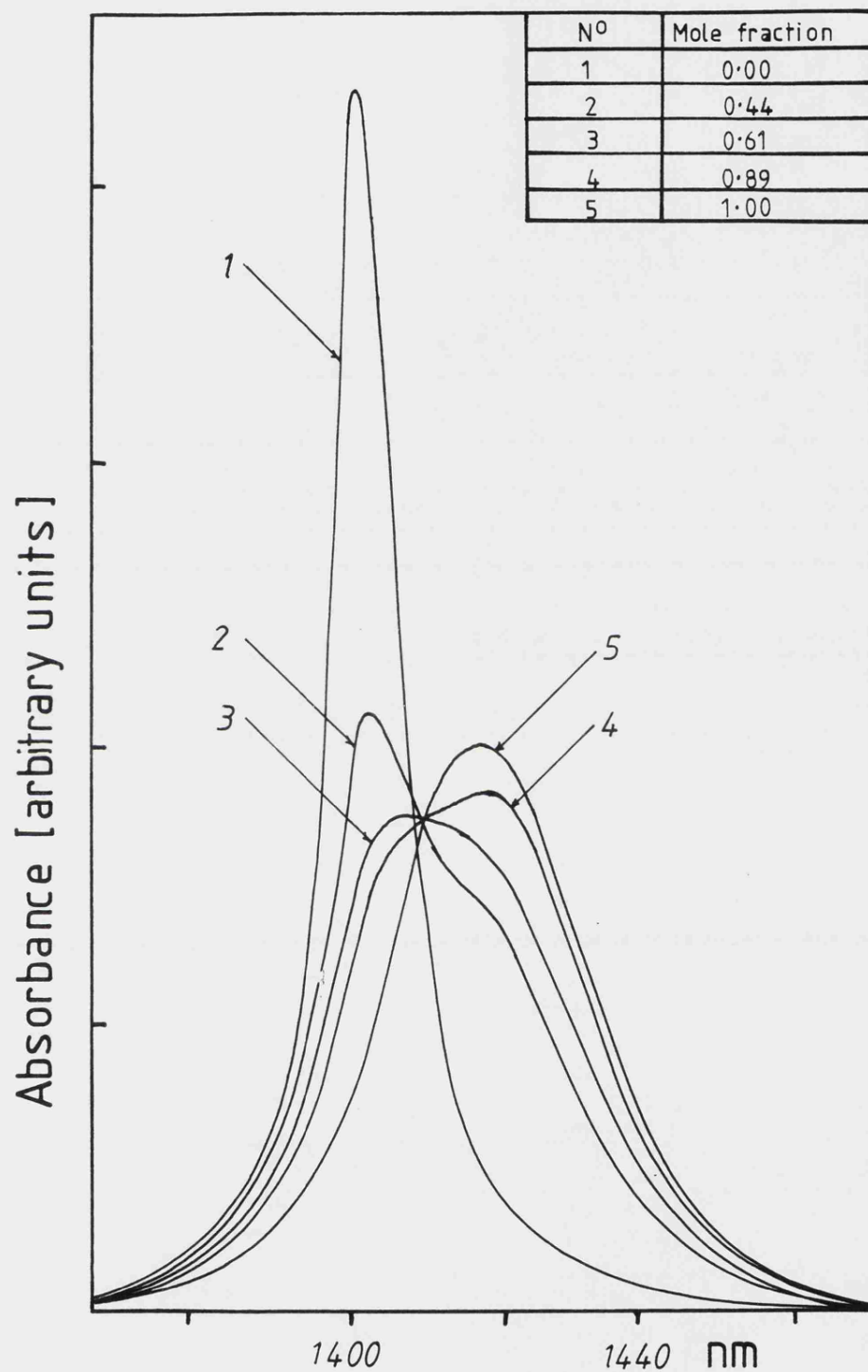
Change of first overtone $\nu$ OH band of methanol
in range of mixtures, tetrachloromethane –
iodomethane.

of the other mixed solvent systems studied.

The reason for using methanol as a simpler system than water is illustrated in Figure 9.4 where water OH bands are resolved for the corresponding mixed solvent system. The water spectrum is, however, more complex, having two coupled bands - the $\nu_1$ symmetric stretch and $\nu_3$ asymmetric stretch. There is also the possibility of two different species being formed on going from a weakly interacting solvent to a stronger interaction, namely B----H-O-H and B----H-O-H----B units. This accounts for the different shifts observed for $\nu_1$ and $\nu_3$ bands, and is in agreement with expectation, and with the results of Bonner and Choi [13] who indicate that H-O-H----B is a stronger interaction than B----H-O-H----B. The latter is only likely, therefore, to be formed in very dilute solutions of water in a moderate to strong base.

The equilibrium constant K was determined for a series of monohalo-alkanes. Figures 9.5, 9.6 and 9.7 show the experimental fundamental infrared curves used for this. For comparison, cyanomethane and nitro-methane were also used as these are accepted as weak hydrogen bond formers. The results are summarised in Table 9.1, including the corresponding results from the overtone study. As the new band being formed is often overlapping the initial band, deconvolution was used to obtain accurate absorbance values. Figure 9.8 shows a plot of equilibrium constant against spectral shift of the new band. Two different curves are seen for infrared fundamental and overtone. The reason for this is not entirely understood but is believed to be mainly due to anharmonicity. The theory behind this has been discussed in Chapter 1. As neither the fundamental infrared band shape nor the overtone band shape follow the true energy distribution profile for the OH oscillator, (the fundamental favours the stronger bonds whereas the overtone favours the weaker bonds)

# Figure 9. 4
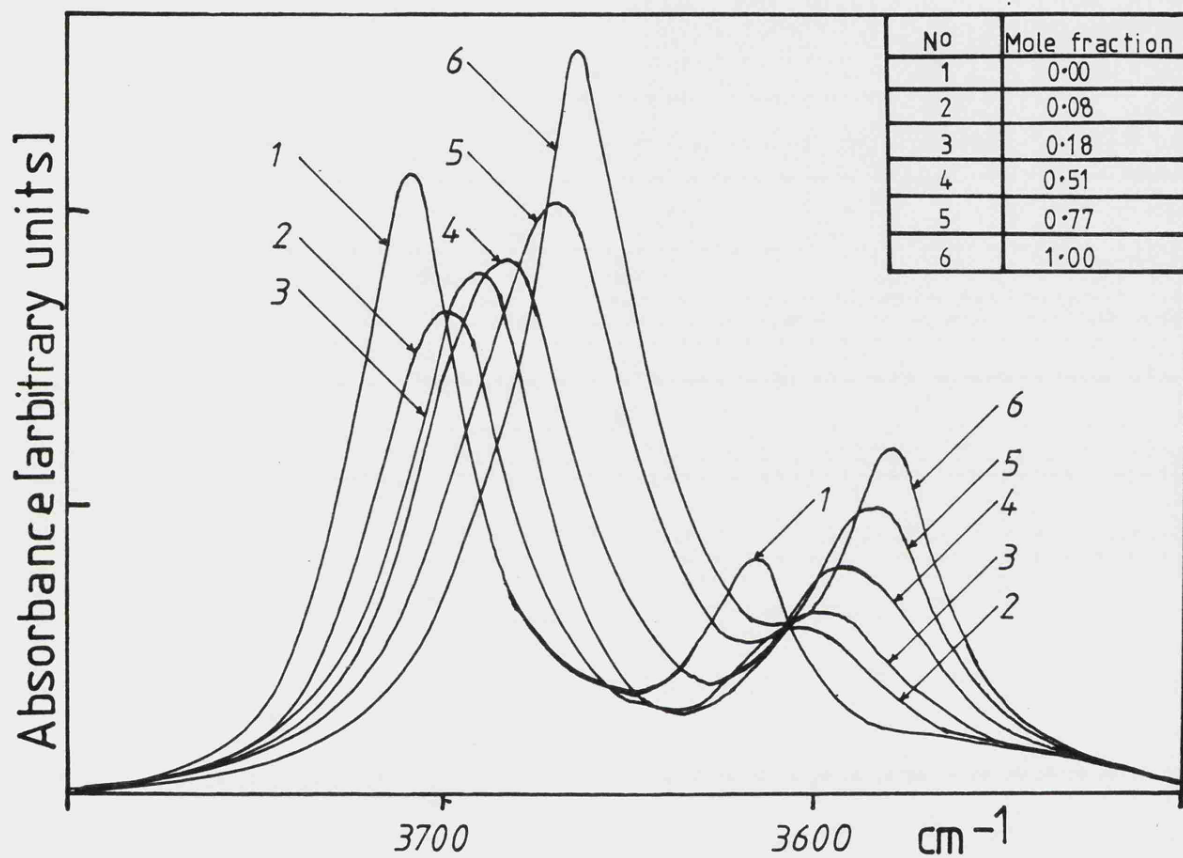


Change of $\nu_1$ and $\nu_3$ bands of water in a range of
mixtures, tetrachloromethane - iodomethane.

# Figure 9. 5
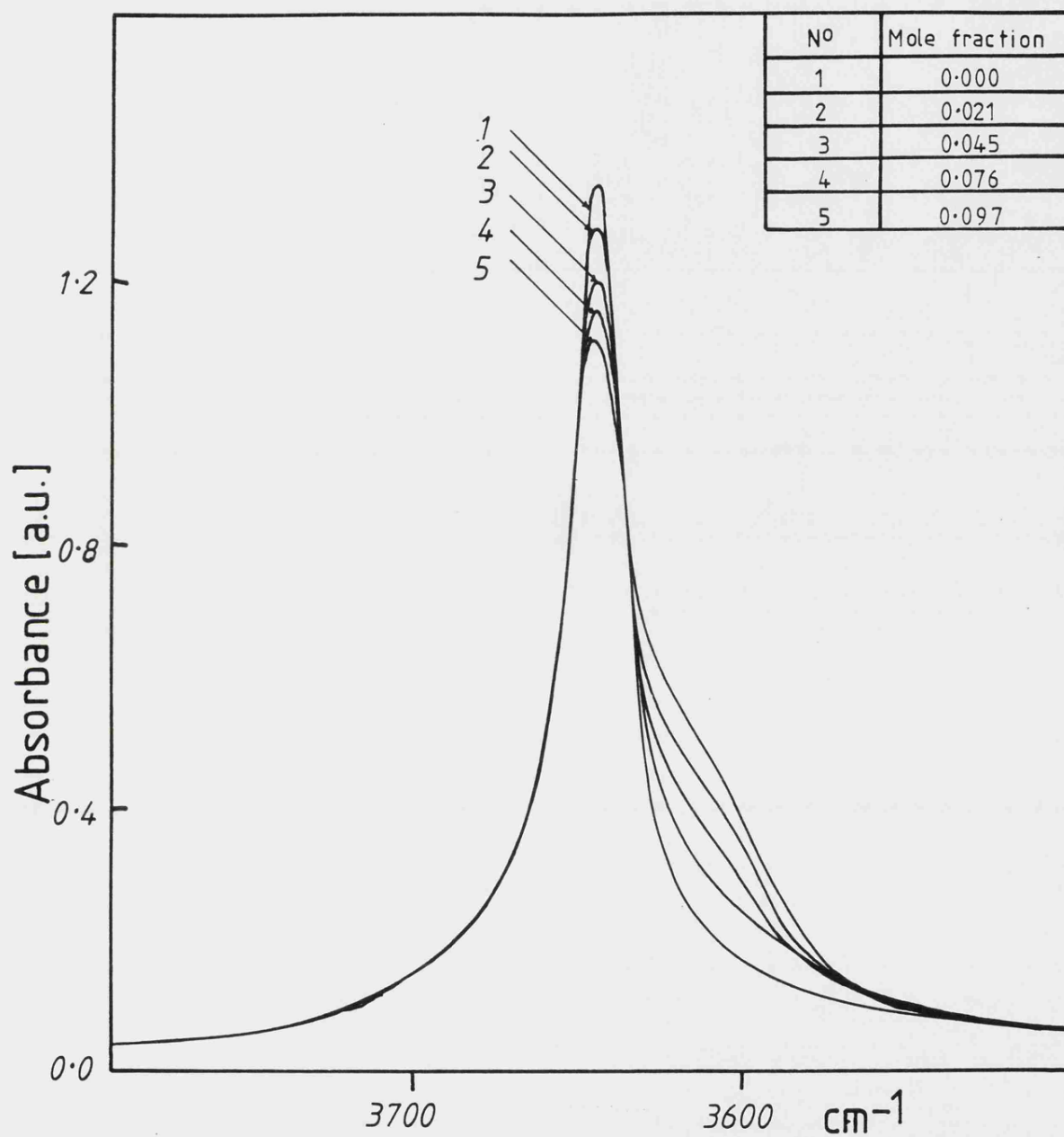
| Nº | Mole fraction |
|----|---------------|
| 1  | 0·000         |
| 2  | 0·021         |
| 3  | 0·045         |
| 4  | 0·076         |
| 5  | 0·097         |

Spectra showing fall in absorbance of OH str Methanol in mixtures of tetrachloromethane and small aliquots of 2-chloropropane.

# Figure 9.6
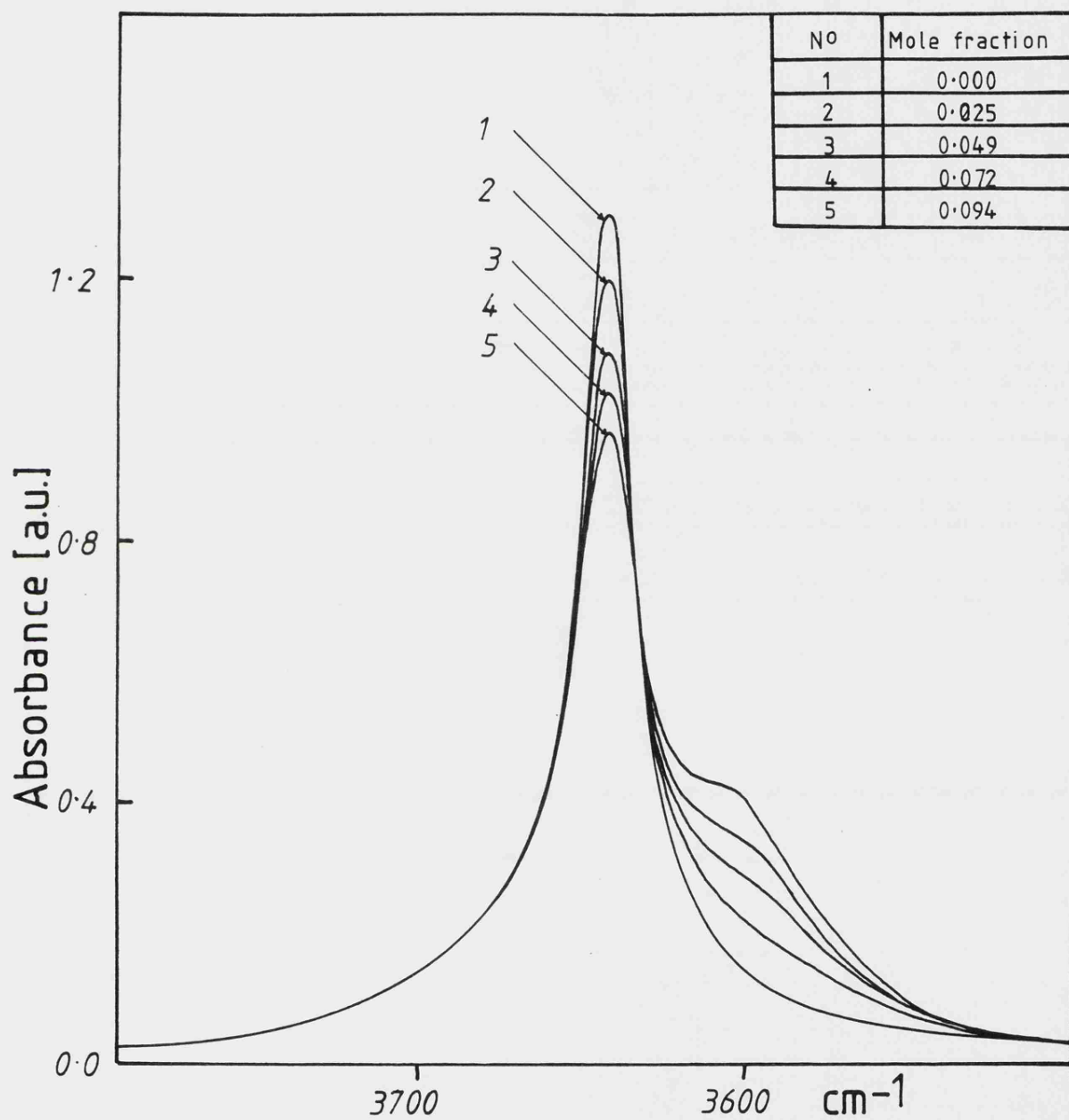


| No | Mole fraction |
|----|---------------|
| 1  | 0·000         |
| 2  | 0·025         |
| 3  | 0·049         |
| 4  | 0·072         |
| 5  | 0·094         |

Spectra showing fall in absorbance of OH str Methanol in mixtures of tetrachloromethane and small aliquots of 2-bromopropane.

# Figure 9.7



| No | Mole fraction |
|----|---------------|
| 1  | 0·000         |
| 2  | 0·024         |
| 3  | 0·042         |
| 4  | 0·063         |
| 5  | 0·088         |

Spectra showing fall in absorbance of OH str Methanol
in mixtures of tetrachloromethane and small aliquots
of 2-iodopropane.

# Table 9.1

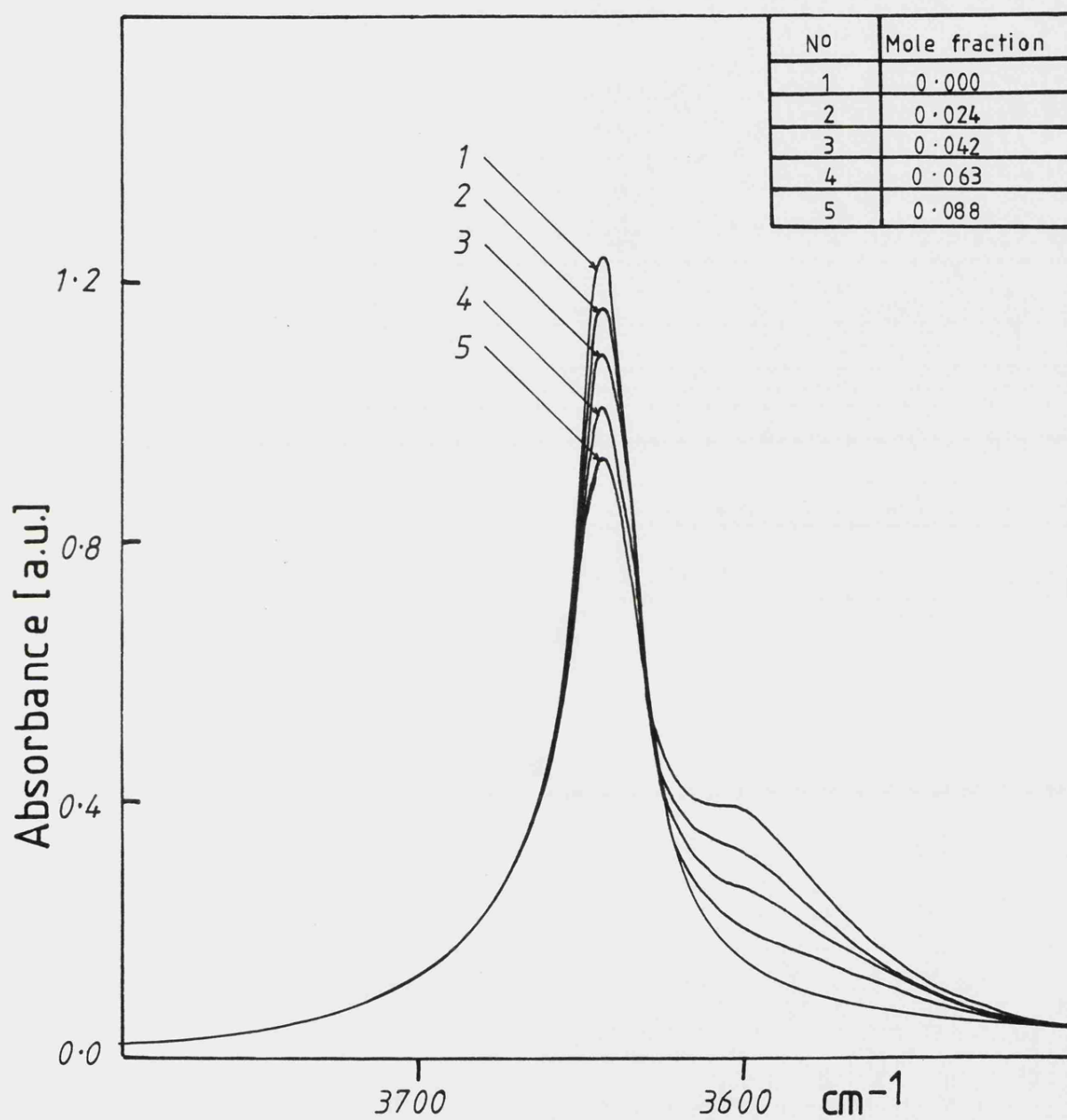| Cosolvent | FUNDAMENTAL | | OVERTONE | |
|---|---|---|---|---|
| | K | ± error | K | ± error |
| 2-Chloropropane | 1·7 | 0·7 | 0·95 | 0·6 |
| | 1·9 | 0·5 | 1·25 | 0·3 |
| | 2·0 | 0·4 | 1·21 | 0·2 |
| 2-Bromopropane | 3·7 | 0·8 | 2·2 | 0·2 |
| | 3·1 | 0·6 | 1·9 | 0·3 |
| | 3·1 | 0·5 | 1·9 | 0·3 |
| 2-Iodopropane | 4·5 | 0·9 | 3·7 | 0·3 |
| | 4·0 | 0·7 | 3·6 | 0·5 |
| | 3·9 | 0·6 | 3·5 | 0·3 |
| Cyanomethane | 6·8 | 0·9 | 6·5 | 0·4 |
| | 7·2 | 0·9 | 7·1 | 0·5 |
| | 7·5 | 0·9 | 6·9 | 0·5 |
| Nitromethane | 2·9 | 0·7 | 3·1 | 0·4 |
| | 2·7 | 0·7 | 3·1 | 0·4 |
| | 2·8 | 0·8 | 3·0 | 0·3 |

Calculated equilibrium constants for the
2-halopropane series plus cyanomethane and
nitromethane.

# Figure 9.8
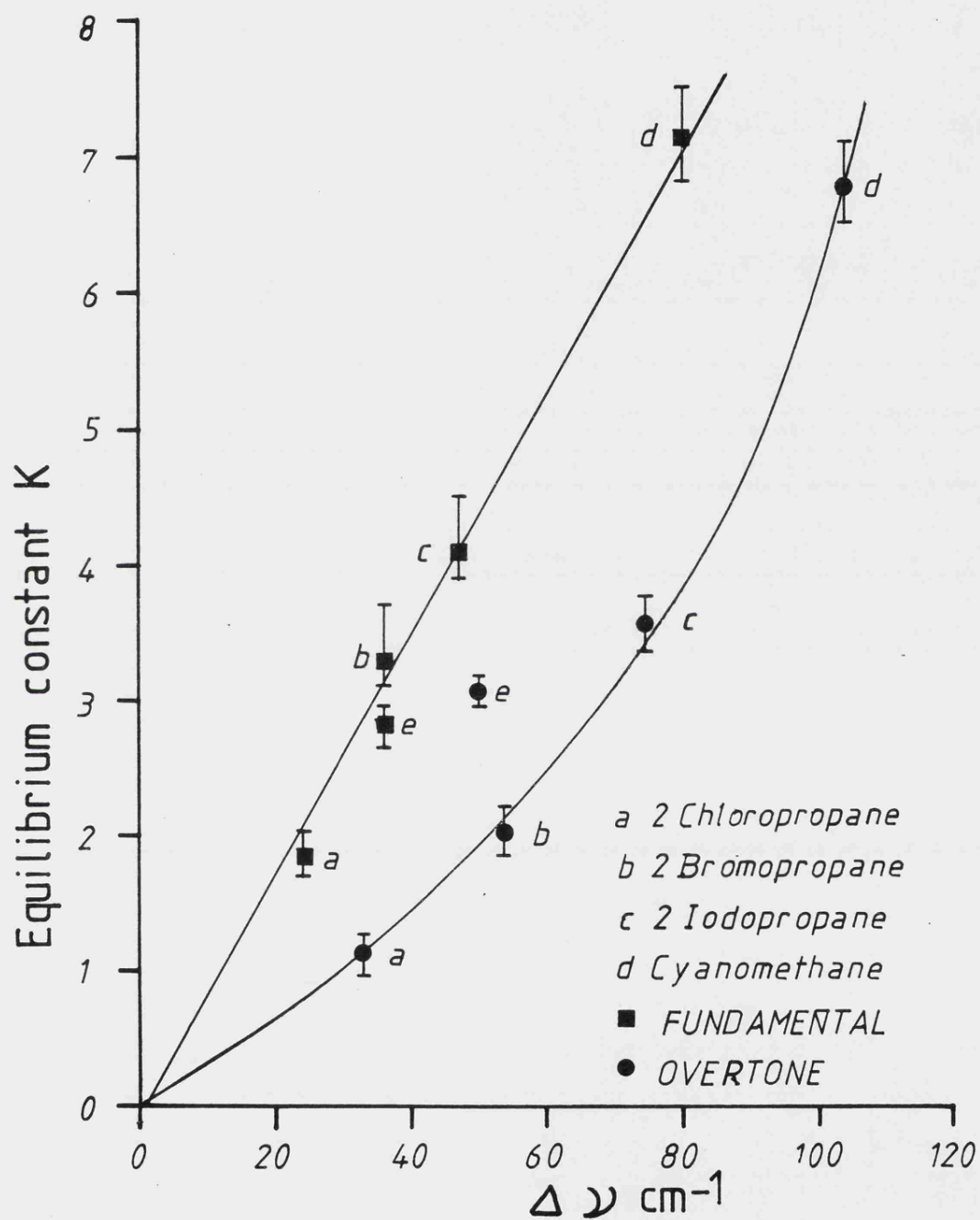


The correlation between equilibrium constant and spectral shift for the 2-halopropane series plus cyanomethane and nitromethane.

a larger shift in frequency might be expected to occur for weakly interacting species in the overtone region.

An analogous plot to the Badger-Bauer rule can be obtained by converting K into $-\Delta G^{\ominus}$, the free energy of interaction (Fig. 9.9). It can be seen that there is a relationship, albeit non-linear, between $-\Delta G^{\ominus}$ and shift indicating the validity of the scale of interaction RI > RBr > RCl. This scale is at first surprising as for the case of the halide ions the reverse holds true [14], i.e. $Cl^- > Br^- > I^-$. However, two factors can be used to explain this effect. Firstly, we are dealing with covalent neutral molecules and the bond strengths C-X decrease along the series C-Cl > C-Br > C-I. Secondly, the ability of the C-X bond to polarise increases along the series C-Cl < C-Br < C-I allowing the halogen site a partial charge and hence making any hydrogen bonding stronger along the series.

Further support for hydrogen bonding comes also from the spectral shifts observed for the $\gtrless$C-Cl stretching mode in the infrared on going from cyclohexane solutions to methanolic solutions, (Figure 9.10). Although the shifts are small (approximately 10 $cm^{-1}$) they are deemed significant. They correspond to ca. 2% change which is approximately twice that for the relative OH stretching change. The shifts observed are towards lower frequency indicating weaker bonding and hence that the system is moving towards heterolytic cleavage (stage 2 of the proposed initial sequence for the $S_N1$ mechanism).


9.4  CONCLUDING REMARKS


The data produced from this work gives strong support for the initial state solvation theory of the $S_N1$ type mechanism for the solvolysis of

# Figure 9. 9
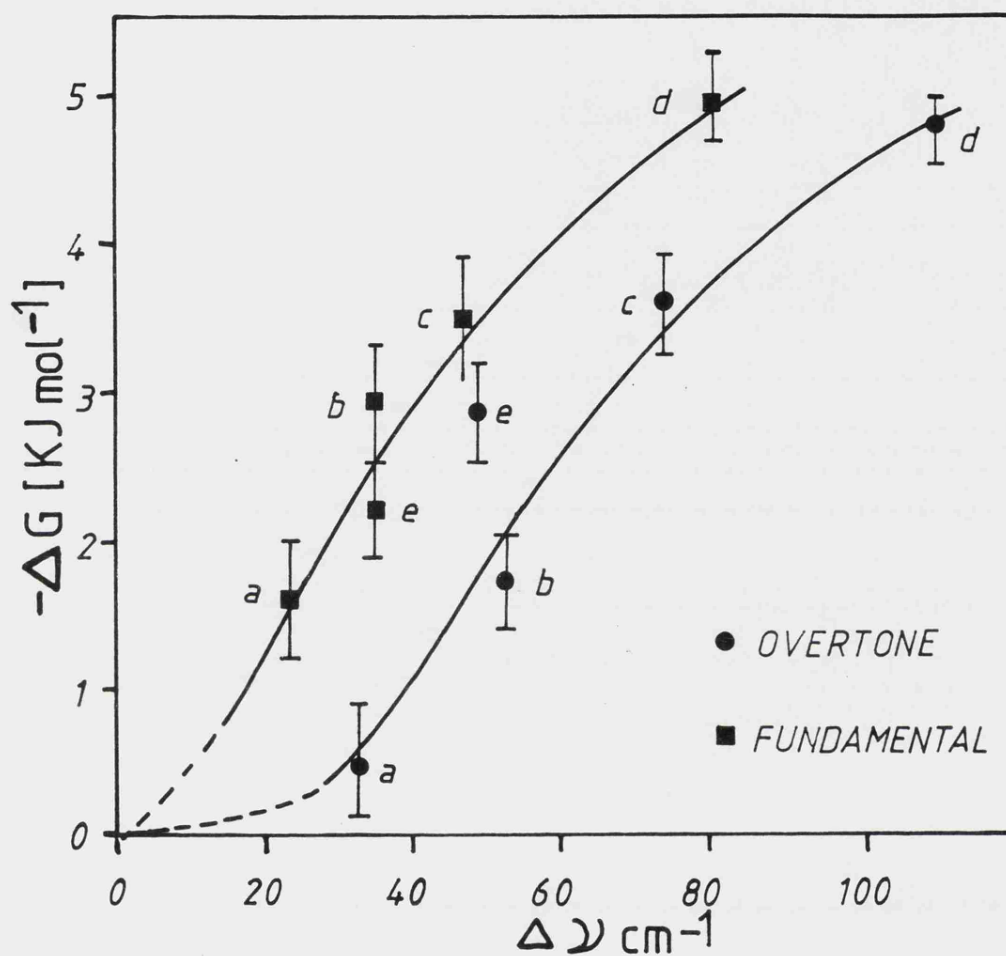


The correlation between free energy of interaction $-\Delta G^{\ominus}$ and spectral shift for the 2-halopropane series plus cyanomethane and nitromethane. [Cosolvents as Figure 9.8]

# Figure 9. 10



a 1-Chloropropane
b 2-Chloropropane
c t-Butyl chloride

―――― in Hexane
- - - - in Methanol
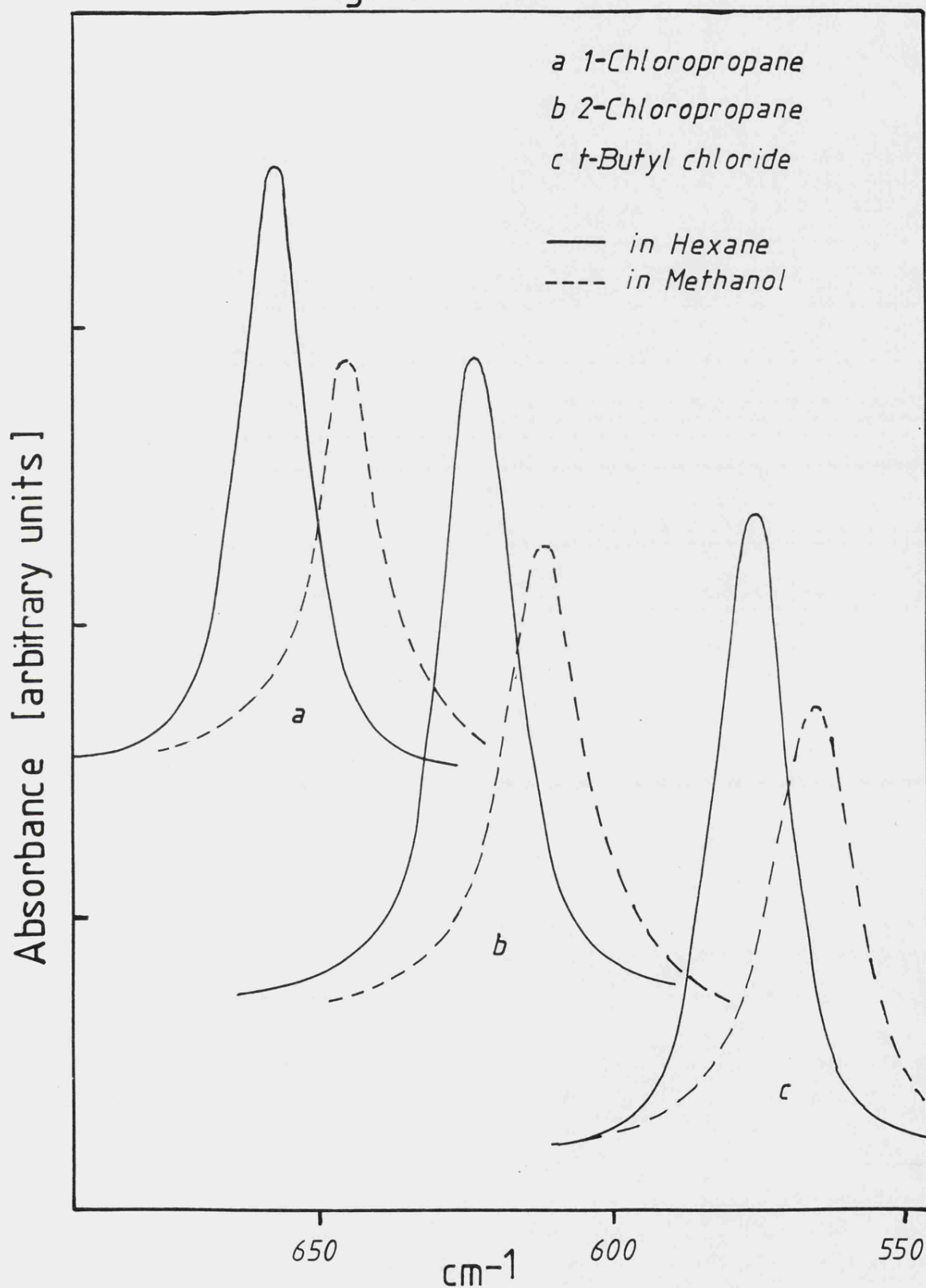
Spectra demonstrating shift of C-Cl band on changing
solvent from cyclohexane to methanol.

monohaloalkanes. The concept of hydrogen bonding to these haloalkanes has been demonstrated.

It must also be borne in mind that the interactions shown here are between monomer alcohol or water and the haloalkane. Any interaction between bulk alcohol or water and the haloalkane will be ca. twice as strong and this is the situation for the $S_N1$ process described.

REFERENCES FOR CHAPTER 9

1.  C. K. Ingold, 'Structure and Mechanism in Organic Chemistry',
    G. Bell & Sons, London (1953).

2.  D. J. Raber, J. M. Harris, R. E. Hall and R. von Schleyer,
    J. Am. Chem. Soc., 93, (1971) 4821.

3.  J. M. Harris, A. Becker, F. A. Fagan and F. A. Walden, J. Am. Chem.
    Soc., 96, (1974) 4484.

4.  T. W. Bentley and R. von Schleyer, 'Advances in Physical Organic
    Chemistry', ed. V. Gold and D. Bethall, Academic Press, London
    (1977).

5.  M. J. Blandamer, J. Burgess, P. P. Duce, R. E. Robertson and
    J. M. W. Scott, J. Chem. Soc., Chem. Commun., 13, (1981).

6.  R. Mecke, Discussions Faraday Soc., 9, (1950) 161.

7.  M. C. R. Symons, T. A. Shippey and P. P. Rastogi, J. Chem. Soc.,
    Faraday Trans. I, 76, (1980) 2251.

8.  S. C. Mohr, W. D. Wilk and G. M. Barrow, J. Am. Chem. Soc., 87,
    (1965) 3048.

9.  R. M. Badger and S. H. Bauer, J. Chem. Phys., 5, (1939) 839.

10. S. Singh, A. S. N. Muothy and C. N. R. Rao, Trans. Faraday Soc.,
    62, (1966) 1056.

11. C. N. R. Rao, P. C. Dwivedi, P. C. Ratajczak and W. J. Orville-
    Thomas, J.C.S. Faraday Trans. II, 71, (1975) 955.

12. Y. Mizugai, F. Takimoto and M. Katayama, J. Chem. Phys. Letters,
    76:3, (1980) 615.

13. O. D. Bonner and Y. S. Choi, J. Phys. Chem., 78, (1974) 1723.

14. R. R. Ryall, H. A. Strobel and M. C. R. Symons, J. Phys. Chem.,
    81, (1977) 253.

# APPENDICES

## Introduction

Most types of absorption spectra contain regions where several bands overlap. This is particularly true where the same transition is being observed for different solvation states. In order to compare individual bands some method of analysing the overall envelope into its components is necessary.

Many methods are available which are applicable to all types of absorption spectra [1]. These can be categorised:-

a  Visual Inspection
b  Analogue curve fitting
c  Digital curve fitting
d  Computer methods involving mathematical convergence.

Visual inspection is effectively only another term for guesswork, however with experience and a knowledge of the system it can give a useful starting point to the curve fitting techniques.

The analogue method is that used by the 'Du Pont' curve resolver [2]. Several function generator channels are used together, each producing a single distribution function (Gaussian, Lorentzian, etc.) and jointly capable of reproducing the experimental curve profile. The individual channels can then be inspected and plotted as necessary.

The synthesised curves are produced on a cathode ray tube and compared via a series of mirrors with the original spectrum. This can lead to errors due to different viewing positions. There is also no direct check on the validity of the 'fit' between the experimental and synthetic curves, this relies entirely on the skill of the operator.

Digital curve fitting techniques operate along similar lines to the analogue methods. Curves are synthesised by summing mathematical band functions. Display of the various bands and curves is usually on a

'refresh graphics' screen and the fit achieved by trial and error. Most of the main disadvantages of the analogue method are eliminated by the digital technique, but a certain amount of operator subjectivity is still apparent.

For good curve fitting several rules need to be observed:-

a̲  Use the minimum number of bands possible.

b̲  The bands used must correspond to the model for the system.

Pure computer methods of curve analysis are also available. These eliminate operator subjectivity but can lead to other errors such as too many or too few bands. In general, the curve to be analysed is fitted to some polynomial function which is then reconstructed using the sum or product of various band functions. The computer converges on the line-shape by a series of steps, each new set of parameters being calculated from the previous set. There are several methods of convergence in use and a good example of their various applicabilities is given by Pitha and Jones [3].

Visually Displayed Curve Analysis - VIDCA

The VIDCA program was written by N. G. M. Pay [4] for the analysis of overlapping absorption bands. This is a digital curve fitting technique with some refinements.

The absorption profile, usually in the form of a pen trace on a sheet of chart paper, is turned into digital form using a computer controlled digitising table. The program VIDCA when activated first displays this curve profile with axes and defined baseline. Band functions are then defined by the operator according to requirements by means of band height, width at half height, position on abscissa and composition. The composition of the band is on a scale from pure Lorentzian to pure Gaussian function as 0 ⟶ 100% Gaussian. When several of these bands are displayed

and combined the required 'fit' can be achieved by adjusting all the respective parameters. Various 'error' procedures are available in VIDCA, this enables the operator to apply his or her own adjustments in order to 'converge' on a 'fit' within pre-set error limits over the whole or part curve.

When a suitable fit has been achieved the various bands with their respective parameters and overall envelope can be plotted onto a sheet of paper for inspection.

An example of this is shown in Fig. 1.

General Comments

Throughout the work of this thesis the VIDCA system was used for most of the curve deconvolution. Where only a rough idea of bands was required the Du Pont curve resolver was used.

REFERENCES FOR APPENDIX 1

V.I.D.C.A. V1-S.02 N.G.M.PAY - PARAMETERS

| BAND | HEIGHT | POSITION | %AGE | HALF BAND WIDTH |
|------|--------|----------|------|-----------------|
| 1 | .110 | 1675.500 | 35.000 | 6.000 |
| 2 | .690 | 1658.000 | 20.000 | 10.000 |
| 3 | .185 | 1638.000 | 35.000 | 13.000 |

COLOUR KEY :-

BLACK - OBSERVED SPECTRUM
RED - COMPONENT BANDS
GREEN - TOTAL ORDINATE
BLUE - BASELINE/HEADINGS/
GRATICULE

BASELINE - LHS    .110
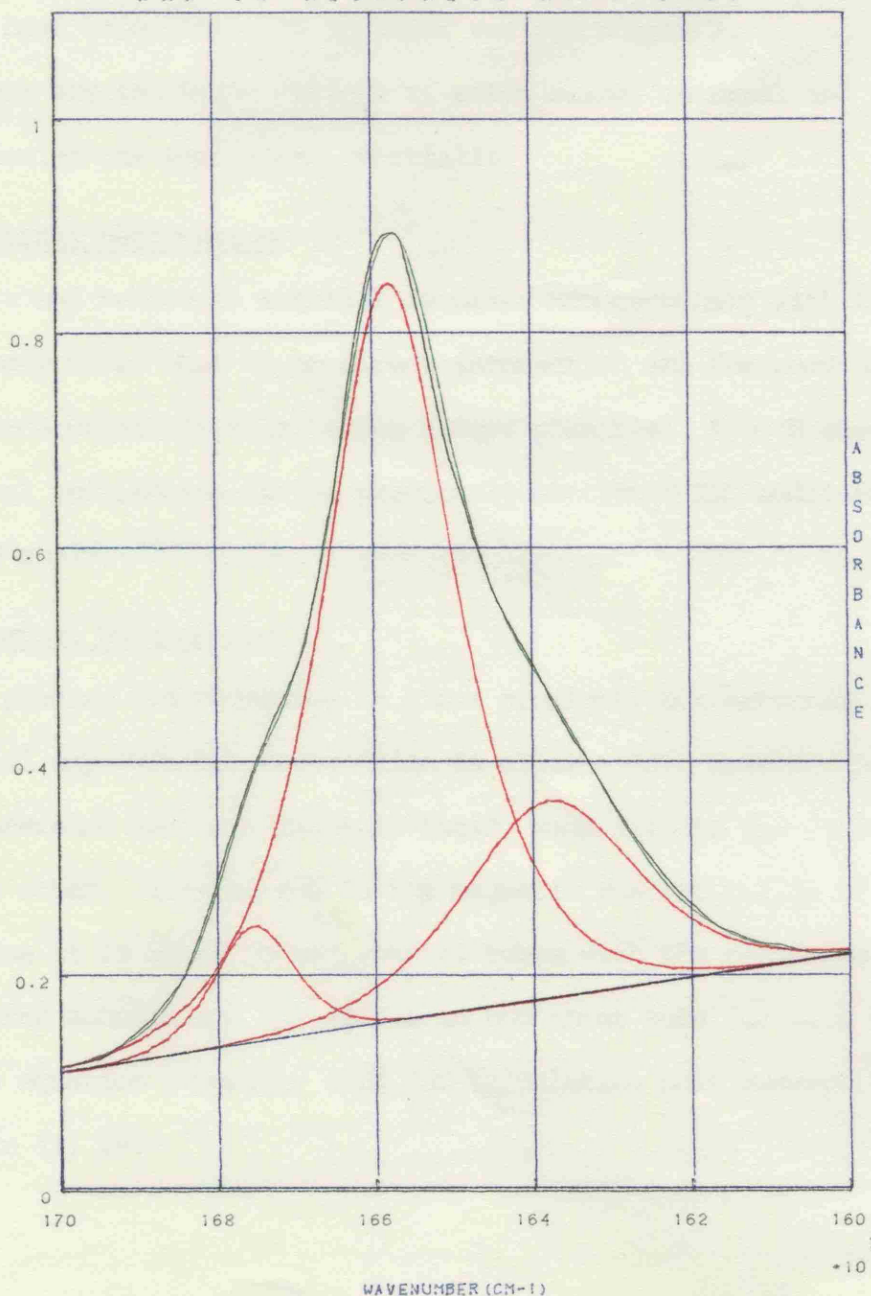         - RHS    .220

# USER:- G.EATON

# Figure    A.1



NMA IN MEOH/MECN M.F.=0.61

ABSORBANCE

WAVENUMBER(CM-1)

*10

## REFERENCES FOR APPENDIX I

1.  B. E. Barker and M. F. Fox, Chem. Soc. Reviews, 9, (1980) 2.

2.  Instruction Manual 310 Curve Resolver, EI Du Pont (Inc), (1970).

3.  J. Pitha and R. N. Jones, Can. J. Chem., 44, (1966) 3031.

4.  N. G. M. Pay, Ph.D. Thesis, Leicester University, (1981).

As for most spectroscopic techniques it is desirable to measure signal positions with a high degree of accuracy. Absolute positions of nuclear resonances are difficult to determine and so some reference signal must be used and signals measured relative to those of the reference. For standard $^1$H n.m.r. work the most common reference signal is that from the protons of tetramethylsilane (TMS). This is a single sharp line at a field usually higher than most observed signals and often is given an arbitrary position of 0 ppm. However for other nuclei and for aqueous solutions TMS is unsuitable and other reference materials are used - these have been mentioned in their various chapters.

There are two basic methods of referencing, internal and external, each having its merits and shortfalls.

### a Internal Referencing

Here the reference material is mixed homogeneously with the sample. Obviously there must be no direct interaction and for some samples and reference materials this is not always possible. A good example of internal referencing is the previously mentioned TMS addition to samples for $^1$H n.m.r.

### b External Referencing

By placing the reference in close proximity but external to the sample material any chemical interaction is eliminated. However, because sample and reference are in a magnetic field, each affects the field experienced by the other. This is due to the magnetic susceptibility of each. In practice it is usual to use coaxial tubes with the reference material in the outer annulus and the sample in the inner tube (or vice versa).

The equation generally used for calculating bulk susceptibility effects [1] is:-

$$\delta_{true} = \delta_{obs} + \frac{2\pi}{3} (X_v R - X_v S) \qquad \dots \ (1)$$

This assumes a cylindrical tube arrangement with length $\gg$ diameter. $X_v$ is the volume susceptibility and is related to the mass susceptibility $(X_m)$ by:-

$$X_v = X_m \rho \qquad \dots \ (2)$$

$\rho$ is the density and $X_m$ is either a literature value or measured by use of a Gouy balance. It must be noted also that $\delta$ values are measured in arbitrary units of ppm but the $\frac{2\pi}{3} (X_v R - X_v S)$ term is not and must therefore be modified by $10^6$ in order to turn it into the same units. The factor $\frac{2\pi}{3}$ is related to the tube shape, i.e. a cylinder, in fact if perfectly coaxial spheres are utilised the factor becomes zero and susceptibility corrections are unnecessary [2].

---

The above examples apply primarily to the measurement between signals from the same nuclei. However most modern Fourier Transform instruments use a reference nucleus as a lock signal that is different from the nucleus being observed. This heteronuclear lock is usually a deuterium nucleus. As with the previously mentioned referencing it may be external, i.e. in a coaxial tube or a separate probe, or it may be internal and mixed with the sample. If it is external then the usual susceptibility corrections using equation (1) apply but if it is internal other factors need to be considered [3]. In order to maintain a lock signal a second field (as a radio frequency) is applied and, as this is not at the resonance frequency of the nucleus under observation, this nucleus experiences a slightly different magnetic field; hence it has a slightly different resonant position. Also the lock nucleus will experience a different field due to the radio frequency applied to the observed nucleus. These effects are in addition to the susceptibility effects

which are now seen as different shifts of the two different nuclei. The equation then takes the form:-

$$\delta_{correct} = \delta_{obs} + C + \frac{2\pi}{3} \left( X_R - X_S \right) \qquad \dots \quad (3)$$

where C is a value derived from field changes and screening constant differences between lock and observed nuclei.

C is best determined experimentally using a second externally situated lock nucleus. It has been found that, for some cases, C may be greater than the general susceptibility corrections and is therefore not to be ignored if using this method.

REFERENCES FOR APPENDIX II

1.  J. A. Pople, W. G. Schneider and H. J. Bernstein, 'High Resolution
    Nuclear Magnetic Resonance', McGraw-Hill, 1959.

2.  D. J. Frost and G. E. Hall, Mol. Phys., 10, (1966) 191.

3.  J. Homer, private communication 1982.